Behaviour of Shallow Strip Foundation on Granular Soil under Eccentrically Inclined Load

A THESIS SUBMITTED

FOR THE AWARD OF THE DEGREE

OF

DOCTOR OF PHILOSOPHY

IN

CIVIL ENGINEERING

BY

RABI NARAYAN BEHERA

(ROLL NO. 50701002)

NATIONAL INSTITUTE OF TECHNOLOGY
ROURKELA - 769008, INDIA
July – 2013

CERTIFICATE

This to certify that the thesis entitled "**Behaviour of Shallow Strip Foundation on Granular Soil under Eccentrically Inclined Load**" being submitted by **Mr. Rabi Narayan Behera** for the award of the degree of Doctor of Philosophy (Civil Engineering) of NIT Rourkela, is a record of bonafide research work carried out by him under my supervision and guidance. Mr. Rabi Narayan Behera has worked for more than five years on the above problem in the Department of Civil Engineering, National Institute of Technology Rourkela and this has reached the standard for fulfilling the requirements and the regulation relating to the degree. The contents of this thesis, in full or part, have not been submitted to any other university or institution for the award of any degree or diploma.

Dr. Chittaranjan Patra
Professor
Department of Civil Engineering
NIT Rourkela

Place: Rourkela

Date:

Dedicated To

My Parents

ACKNOWLEDGEMENT

This thesis is a result of the research that has been carried out at National Institute of Technology Rourkela. During this period, I came across with a great number of people whose contributions in various ways helped my field of research and they deserve special thanks. It is a pleasure to convey my gratitude to all of them.

In the first place, I would like to express my deep sense of gratitude and indebtedness to my supervisor Prof. Chittaranjan Patra for his invaluable advice, and guidance from the formative stage of this research and providing me extraordinary experiences throughout the work. Above all, he provided me unflinching encouragement and support in various ways which inspired and enriched my sphere of knowledge. It is a great honour to have him as my supervisor. I am also thankful to his family for the hospitality I was rendered.

I wish to express my sincere thanks to Prof. N. Roy, Chairman of doctoral committee and the doctoral committee members Prof. M. Panda and Prof. S. K. Sahoo, for their suggestions and interest in my work.

I would like to express my gratitude to all the faculty and staff members of the Department of Civil Engineering, National Institute of Technology, Rourkela for their continuous support and moral encouragement.

The suggestions and comments of Dr. S. K. Chand, Professor, IGIT Sarang during the preparation of thesis is gratefully acknowledged.

I am also thankful to M/s N K Instruments and M/s Rourkela Fabrication Works for their timely and effective services towards smooth running of the experimental setup as and when needed.

Financial support extended for experimentation by MHRD sponsored project (CE-GRS), DST sponsored project (CE-BGR) as well as Authority of NIT Rourkela is highly appreciated.

My sincere thanks to Mr. Kalakar Tanty, Mr. Chamru Suniani, Mr. Harihar Garnayak and Mr. Debnath Tanty, for their cooperation during exhaustive experiments in the laboratory.

I am indebted to my lab mates Pratap, Shuvranshu, Alok, Roma and Rupashree for their help and support during my stay in laboratory and making it a memorable experience in my life.

A special word of thanks is due to Mr. S K Nayak, Ph. D. Scholar of Civil Engineering Department, for his moral support and encouragements which at times rejuvenated my vigor for research.

I would like to thank senior Ph. D. students Mr. P K Muduli, Mr. P K Mohanty, Mr. P K Parida, and Mr. K C Bhuyan for their love, affection, and companionship. The pleasure of their company and the cheerful moments I had in their company is gratefully acknowledged.

I would like to keep in record the incredible moments I spent with some special friends in Biswajit, Nihar, Sarat, Satish, and Bibhuti. Those extraordinary lighter moments were not only enjoyable but also helped me reinvigorate the academic prowess to start things afresh. I am also thankful to my undergraduate friends Amit and Gokul for their friendship and constant help throughout my doctoral programme.

Last but not the least; I would like to express my gratitude to my parents and family members for their unwavering support and invariable source of motivation.

Rabi Narayan Behera

Abstract

Since the publication of Terzaghi's theory on the ultimate bearing capacity of shallow foundations in 1943, results of numerous studies—both theoretical and experimental—by various investigators have been published. Most of the studies relate to the case of a vertical load applied centrally to the foundation. Meyerhof (1953) developed empirical procedures for estimating the ultimate bearing capacity of foundations subjected to eccentric and inclined loads. Based on the review of the existing literature on the bearing capacity of shallow foundations, it appears that limited attention has been paid to estimate the ultimate bearing capacity when the foundation is subjected to both eccentric and inclined load and the objective of present study stems from this paucity. Besides, only a few studies have been made to estimate the average settlement of embedded footings when subjected to eccentric load.

In order to arrive at the objective and to quantify certain parameters, extensive laboratory model tests have been conducted to determine the ultimate bearing capacity of shallow strip foundation resting over sand bed and subjected to eccentric and inclined loads. The tests have been conducted on two types of sand i.e. dense sand and medium dense sand. The load inclination has been varied from 0^0 to 20^0 whereas the eccentricity varies from 0 to $0.15B$ (B = width of footing). Depth of the footing is varied from 0 to B. Traditionally, in all analysis of such problems; the line of load application is towards the center line of the footing. However, in this thesis, it is investigated for the two possible ways of load application i.e. (i) towards and (ii) away from the center line of the footing.

Based on the model test results, an empirical non-dimensional reduction factor has been developed for each mode of load application. This reduction factor will compute the ultimate bearing capacity of footing subjected to eccentric and inclined load by knowing the ultimate bearing capacity of footings under centric vertical load at the same depth of footing. Similarly, neural network models have been developed under each mode of load application and combined mode of load application to compute reduction factor as described above. Finally, the developed equations are compared with the existing theories.

In addition to bearing capacity, the settlement of eccentrically loaded embedded footings is investigated. Based on some of those laboratory test results as discussed above, an empirical procedure has been developed to estimate the average settlement of the foundation subjected to an average allowable eccentric load per unit area, where the applied load is vertical.

Table of Contents

List of Tables

List of Figures

List of Abbreviations and Symbols

Abbreviations

RF	Reduction Factor
ubc	Ultimate bearing capacity
MSE	Mean Square Error
LA	Load Arrangement

Symbols

B	Width of foundation
L	Length of foundation
t	Thickness of foundation
e	Load eccentricity
α	Load inclination with the vertical
Q_u	Ultimate load per unit length of the foundation
D_f	Depth of embedment
γ	Unit weight of sand
γ_d	Dry unit weight of sand
$\gamma_{d(max)}$	Maximum dry unit weight of sand
$\gamma_{d(min)}$	Minimum dry unit weight of sand
ϕ	Friction angle of sand
ϕ'	Effective friction angle of sand
q_u	Ultimate bearing capacity
q	Surface surcharge
N_c, N_q, N_γ	Bearing capacity factors

s_c, s_q, s_γ	Shape factors
d_c, d_q, d_γ	Depth factors
s	Settlement
s_u	Ultimate settlement
B'	Effective width of foundation
A'	Effective area of foundation
i_c, i_q, i_γ	Inclination factors
w_l	Liquid limit
w_p	Plastic limit
w	Average water content
c_u	Undrained shear strength
I_L	Liquidity index
C_u	Coefficient of uniformity
C_c	Coefficient of curvature
c	Cohesion
V_L	(Vertical) limit load
G	Specific gravity
D_{10}	Effecive particle size
D_{50}	Mean particle size
f_{ie}	Combined inclination-eccentricity factor
D_r	Relative Density
r	Correlation coefficient
R^2	Coefficient of efficiency
e_r	Residual

1. INTRODUCTION

Every civil engineering structure, whether it is a building, bridge, highway pavement or railway track, will in general have a superstructure and a foundation. The function of the foundation is to receive the loads from the superstructure and transmit safely them to the soil or rock below as the case may be. The design of shallow foundation (i.e. the plan dimensions of the foundation) is accomplished by satisfying two requirements: (1) bearing capacity and (2) settlement. Bearing capacity refers to the ultimate, i.e., the maximum load the soil can bear or sustain under given circumstances.

Engineers need to be able to calculate the capacity of foundations subject to; at least, central vertical loads. This need has led to the development of the theories of bearing capacity, notably Terzaghi's method. Bearing capacity predictions based on Terzaghi's (1943) superposition method are partly theoretical and partly empirical in which the contribution of different loading and soil strength parameters (cohesion, friction angle, surface surcharge and self-weight) expressed in the form of non-dimensional bearing capacity factors N_c, N_q, and N_γ are summed. Several analytical solutions have been proposed for computing these factors. The literature contains many theoretical derivations, as well as experimental results from model tests and prototype footings.

All the bearing capacity estimation methods may be classified into the following four categories: (1) the limit equilibrium method; (2) the method of characteristics; (3) the upper-bound plastic limit analysis and (4) the numerical methods based on either the finite-element method or finite-difference method. The problems can be solved by two different approaches: experimentally, by conducting model and full-scale tests; or, by

using numerical methods such as finite element analyses. Full-scale tests are the ideal method for obtaining data, however, practical difficulties and economic considerations either eliminate or considerably restrict the possibility of full-scale testing. As an alternative model tests may be employed, but they have disadvantages. The results of these model tests are usually affected by the boundary conditions of the test box, the size of the footing, the sample disturbance, the test setup and procedure. It is advantageous to use the techniques of numerical methods to simulate the conditions of model tests to verify the theoretical models.

Most of the studies for bearing capacity calculation are based on the foundation under vertical and central load. However in some cases due to bending moments and horizontal thrusts transferred from the superstructure, shallow foundations of structures like retaining walls, abutments, waterfront structures, oil/gas platforms in offshore area, industrial machines, and portal framed buildings are very often subjected to eccentric and inclined loads. This may be due to (a) moments with or without axial forces (b) the oblique loading (c) their location near the property line (d) wind force and (e) earth pressure and water pressure. They can be analyzed as eccentrically inclined loaded strip footings, with eccentricity of e and load inclination of α to the vertical. Due to load eccentricity and inclination, the overall stability of foundation decreases along with differential settlement and tilting of the foundation which reduces the bearing capacity.

The increase of stress in soil layers due to the load imposed by various structures at the foundation level will always be accompanied by some strain, which will result in the settlement of the structures. The estimation of settlements of shallow foundations in cohesionless soils is still considered as a serious geotechnical problem, both from

practical and theoretical point of view. In general, settlement of a foundation consists of two major components - elastic settlement (S_e) and consolidation settlement (S_c). For a foundation supported by granular soil, the elastic settlement is the only component that needs consideration. Different methods are available for the determination of settlement of shallow foundation on cohesionless soil. But, most of the available methods fail to achieve consistent performance in predicting accurate settlement and most of them are based on foundations subjected to central vertical load.

The estimation of bearing capacity and settlement of foundations under eccentric and inclined loads is of considerable importance in geotechnical engineering. In order to study further in this area, extensive literature review is made to narrow down the objective of the present investigation. Detailed investigation and analyses are presented in the subsequent chapters for both bearing capacity and settlement aspects. A procedure for estimation of settlement of footing under eccentric load is proposed.

2. LITERATURE REVIEW

2.1 Introduction

The lowest part of a structure which transfers its load to the underlying soil or rock is known as foundation. Foundations can be of shallow or deep depending on the depth of embedment. Very often foundations of structures like earth retaining structures, abutments, waterfront structures, industrial machines, oil/gas platform in offshore area may be subjected to eccentric and/or inclined loading. This may be due to (i) moments with or without axial forces (ii) the oblique loading (iii) their location near the property line (iv) wind force and (v) earth pressure and water pressure. Due to eccentric and/or inclined loading, the footing tilts and the pressure below the footing does not remain uniform. The tilt of footing increases with an increase in the eccentricity and inclination and the bearing capacity reduces considerably and undergoes differential settlements.

2.2 Bearing Capacity of Shallow Foundations on granular soil

The stability of a structure depends upon the stability of the supporting soil. For that the foundation must be stable against shear failure of the supporting soil and must not settle beyond a tolerable limit to avoid damage to the structure. For a given foundation to perform its optimum capacity, one must be ensured that it does not exceed its safe bearing capacity. The ultimate bearing capacity (q_u) is defined as the pressure at which shear failure occurs in the supporting soil immediately below and adjacent to the foundation.

Since the publications of Terzaghi's theory on the bearing capacity of shallow foundations in 1943, numerous studies (both experimental and theoretical) have been made by various investigators. Most of these studies are related to footings subjected to vertical and central loads. Meyerhof (1953) developed empirical procedures for estimating the ultimate bearing capacity of foundations subjected to eccentric vertical loads. Researchers like Prakash and Saran (1971) and Purkayastha and Char (1977) also studied the behavior of eccentrically loaded footings. Similarly, the effect of inclined load on the foundation has been investigated by few investigators (Meyerhof 1953; Muhs and Weiss 1973; Hanna and Meyerhof 1981; Sastry and Meyerhof 1987). However a few works have been done by Meyerhof 1963, Saran and Agarwal (1991) and Loukidis et al. (2008) towards the bearing capacity of footings subjected to combined action of eccentric and inclined load which is the subject of the thesis. An extensive review of literature based on bearing capacity of shallow foundations under different loading conditions is presented below.

2.2.1 Central Vertical Loading

Terzaghi (1943) proposed that the ultimate bearing capacity of a strip foundation subjected to a vertical central load [Figure 2.1] over a homogenous soil can be expressed as

$$q_u = cN_c + qN_q + \frac{1}{2}\gamma B N_\gamma \qquad (2.1)$$

For granular soil the above equation is reduced to the form as expressed by:

$$q_u = qN_q + \frac{1}{2}\gamma BN_\gamma \tag{2.2}$$

Similarly, Meyerhof (1951) proposed a generalized equation for centrally vertical loaded foundations as

$$q_u = cN_c s_c d_c + qN_q s_q d_q + \frac{1}{2}\gamma BN_\gamma s_\gamma d_\gamma \tag{2.3}$$

For granular soil the above equation (2.3) can be reduced to the form as:

$$q_u = qN_q s_q d_q + \frac{1}{2}\gamma BN_\gamma s_\gamma d_\gamma \tag{2.4}$$

where q_u = ultimate bearing capacity; q = surcharge pressure at footing level = γD_f; D_f = depth of foundation; γ = unit weight of soil; B = width of foundation; N_c, N_q , N_γ = bearing capacity factors; s_c, s_q, s_γ = shape factors; d_c, d_q, d_γ = depth factors.

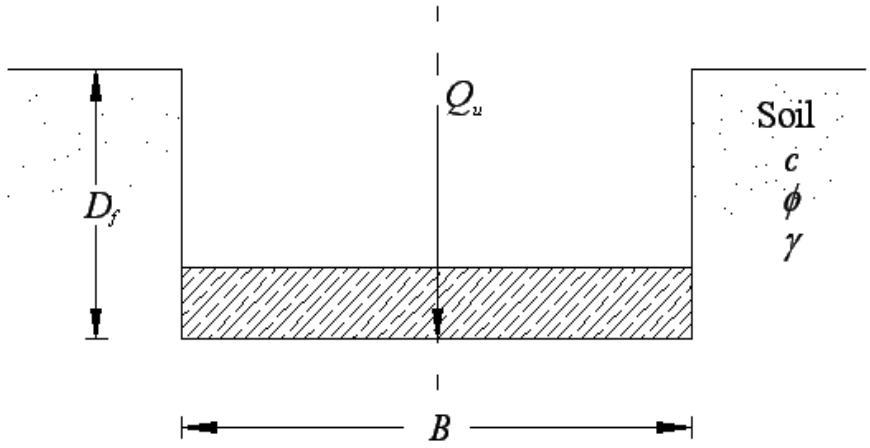

Figure 2.1: Ultimate load per unit length Q_u on a strip foundation for centric vertical load

In the past, many investigators have proposed bearing capacity factors as well as shape and depth factors for estimating the bearing capacity of footings in above conditions. These factors are summarized in Table 2.1 and Table 2.2.

Table 2.1: Summary of Bearing Capacity factors

Bearing Capacity Factors	Equation	Investigator
N_c	$N_c = (N_q - 1)\cot\phi$	Prandtl (1921), Reissner (1924), Terzaghi (1943), Meyerhof (1963)
N_c	$N_c = \frac{228 + 4.3\phi}{40 - \phi}$	Krizek (1965)
N_q	$N_q = \tan^2\left(45 + \frac{\phi}{2}\right) e^{\pi \tan\phi}$	Prandtl (1921), Reissner (1924), Meyerhof (1963)
N_q	$N_q = \frac{e^{2\left(\frac{3\pi}{4} - \frac{\phi}{2}\right)\tan\phi}}{2\cos\left(45 + \frac{\phi}{2}\right)^2}$	Terzaghi (1943)
N_q	$N_q = \frac{40 + 5\phi}{40 - \phi}$	Krizek (1965)
N_γ	$N_\gamma \approx 1.8(N_q - 1)\cot\phi(\tan\phi)^2$	Terzaghi (1943)
N_γ	$N_\gamma = 1.5(N_q - 1)\tan\phi$	Lundgren and Mortensen (1953) and Hansen (1970)
N_γ	$N_\gamma = 1.8(N_q - 1)\tan\phi$	Biarez et al. (1961)
N_γ	$N_\gamma = 0.01 e^{0.25\phi}$	Feda (1961)
N_γ	$N_\gamma = (N_q - 1)\tan(1.4\phi)$	Meyerhof (1963)
N_γ	$N_\gamma = \frac{6\phi}{40 - \phi}$	Krizek (1965)
N_γ	$N_\gamma = 1.5\, N_c (\tan\phi)^2$	Hansen (1970)
N_γ	$N_\gamma = 2(N_q + 1)\tan\phi$	Vesic (1973)
N_γ	$N_\gamma = 1.1(N_q - 1)\tan(1.3\phi)$	Spangler and Handy (1982)
N_γ	$N_\gamma = e^{(-1.646 + 0.173\phi)}$	Ingra and Baecher (1983)

Bearing Capacity Factors	Equation	Investigator
N_γ	$N_\gamma = e^{(0.66+5.1\tan\phi)}\tan\phi$	Michalowski (1997)
N_γ	$N_\gamma \approx 0.1045 e^{9.6\phi}$ ϕ is in radians	Poulos et al. (2001)
N_γ	$N_\gamma = e^{\frac{1}{6}\left(\pi+3\pi^2\tan\varphi\right)}\left(\tan\phi\right)^{\frac{2\pi}{5}}$	Hjiaj et al. (2005)
N_γ	$N_\gamma = \left(N_q - 1\right)\tan\left(1.32\phi\right)$	Salgado (2008)

Table 2.2: Summary of Shape and Depth factors

Factors	Equation	Investigator
Shape	For $\phi = 0^0$: $s_c = 1+0.2\left(\frac{B}{L}\right)$ $s_q = s_\gamma = 1$ For $\phi \geq 10^0$: $s_c = 1+0.2\left(\frac{B}{L}\right)\tan\left(45+\frac{\phi}{2}\right)^2$ $s_q = s_\gamma = 1+0.1\left(\frac{B}{L}\right)\tan\left(45+\frac{\phi}{2}\right)^2$	Meyerhof (1963)
	$s_c = 1+\left(\frac{N_q}{N_c}\right)\left(\frac{B}{L}\right)$ [Use N_c and N_q given by Meyerhof (1963)] $s_q = 1+\left(\frac{B}{L}\right)\tan\phi$ $s_\gamma = 1-0.4\left(\frac{B}{L}\right)$	DeBeer (1970), Vesic (1975)
	$s_c = 1+\left(1.8\left(\tan\phi\right)^2+0.1\right)\left(\frac{B}{L}\right)^{0.5}$	Michalowski (1997)

Factors	Equation	Investigator
	$s_q = 1 + 1.9(\tan\phi)^2 \left(\frac{B}{L}\right)^{0.5}$ $s_\gamma = 1 + \left(0.6(\tan\phi)^2 - 0.25\right)\left(\frac{B}{L}\right) \quad (for\ \phi \le 30^0)$ $s_\gamma = 1 + \left(1.3(\tan\phi)^2 - 0.5\right)\left(\frac{L}{B}\right)^{1.5} e^{-\left(\frac{L}{B}\right)} \quad (for\ \phi > 30^0)$	
	$s_c = 1 + C_1\left(\frac{B}{L}\right) + C_2\left(\frac{D_f}{B}\right)^{0.5} \quad (for\ \phi = 0)$ *B/L* — *C1* — *C2* Circle — 0.163 — 0.21 1.0 — 0.125 — 0.219 0.5 — 0.156 — 0.173 0.33 — 0.159 — 0.137 0.25 — 0.172 — 0.11 0.2 — 0.19 — 0.09	Salgado et al. (2004)
Depth	For $\phi = 0^0$: $d_c = 1 + 0.2\left(\frac{D_f}{B}\right)$ $d_q = d_\gamma = 1$ For $\phi \ge 10^0$: $d_c = 1 + 0.2\left(\frac{D_f}{B}\right)\tan\left(45 + \frac{\phi}{2}\right)$ $d_q = d_\gamma = 1 + 0.1\left(\frac{D_f}{B}\right)\tan\left(45 + \frac{\phi}{2}\right)$	Meyerhof (1963)
	For $D_f/B \le 1$: $d_c = 1 + 0.4\left(\frac{D_f}{B}\right) \quad (for\ \phi = 0)$ $d_c = d_q - \frac{1 - d_q}{N_q \tan\phi}$ (for $\phi > 0$)	Hansen (1970), Vesic (1975)

Factors	Equation	Investigator
	$d_q = 1 + 2\ \tan\phi(1-\sin\phi)^2\left(\frac{D_f}{B}\right)$ $d_\gamma = 1$ For $D_f/B > 1$: $d_c = 1 + 0.4\tan^{-1}\left(\frac{D_f}{B}\right)$ $d_q = 1 + 2\ \tan\phi(1-\sin\phi)^2\ \tan^{-1}\left(\frac{D_f}{B}\right)$ where, $\tan^{-1}(D_f/B)$ is in radians $d_\gamma = 1$	
	$d_c = 1 + 0.27\left(\frac{D_f}{B}\right)^{0.5}$	Salgado et al. (2004)

The above section discusses about the bearing capacity of shallow foundations when the loads are applied vertically at the center. However, to account for the bearing capacity of the foundations when subjected to eccentric and inclined loads the extension of the above theory can be made in three possible ways i.e. eccentric vertical condition, centric inclined condition and eccentrically inclined condition. These there aspects are described below.

2.2.2 Eccentric Vertical Condition

Meyerhof (1953) proposed an effective width method for foundations subjected to an eccentric load. Due to an eccentric load on the foundation, the foundation tilts towards the side of the eccentricity and the contact pressure below the foundation does not remain uniform. Thus for a shallow horizontal strip foundation of width *B* and depth *D* carrying a

vertical load Q with an eccentricity e on the base as shown in Figure 2.2, the ultimate bearing capacity q can be expressed as

$$q = cN_{cq} + \frac{1}{2}\gamma B' N\gamma_q \tag{2.5}$$

where N_{cq}, $N\gamma_q$ = resultant bearing capacity factors for a central load and depend on ϕ and D/B' ; c = unit cohesion; γ = density of soil; B' = effective width $= B - 2e$

$$Q = qA' \tag{2.6}$$

where A' = *effective area* = B' x *1* (for strip footing)

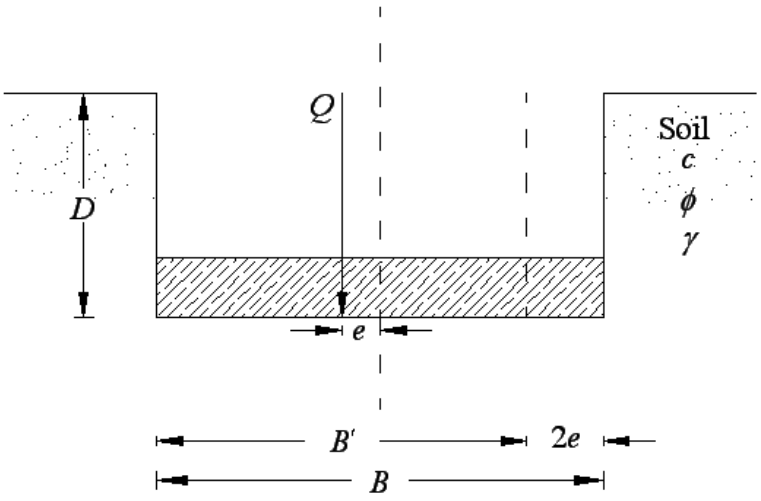

Figure 2.2: Eccentrically loaded footing (Meyerhof, 1953)

Prakash and Saran (1971) suggested a comprehensive mathematical formulation to estimate the ultimate bearing capacity of a rough strip foundation under eccentric load. The failure surface as assumed in a c–ϕ soil under a continuous foundation subjected to a load with eccentricity e is shown in Figure 2.3(a).

The contact width of the foundation with the soil is equal to Bx_1 (Figure 2.3b).

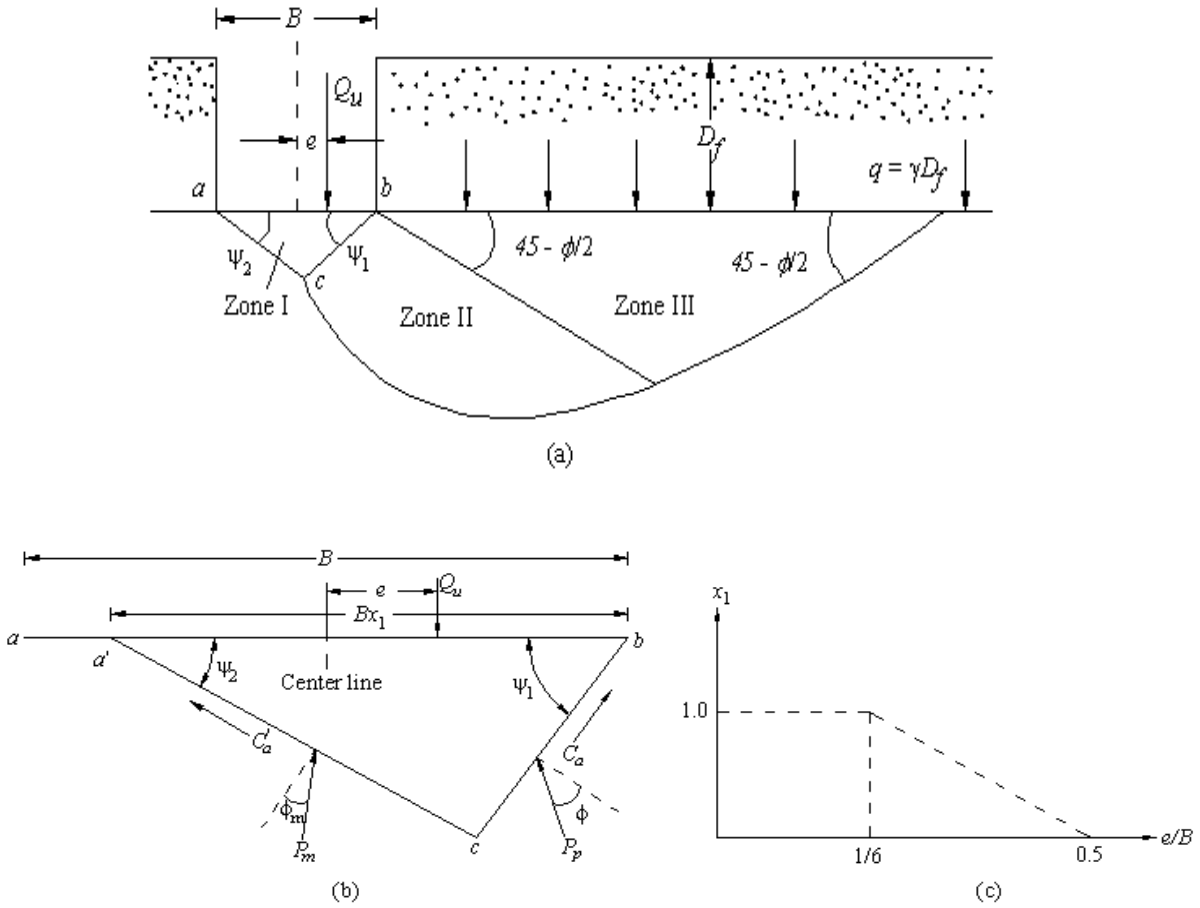

Figure 2.3: Derivation of the bearing capacity theory by Prakash and Saran (1971)

According to this theory, for a strip foundation on a *c*-ϕ soil the ultimate bearing capacity can be expressed as,

$$q_u = \frac{Q_u}{(B \times 1)} = cN_{c(e)} + \gamma D_f N_{q(e)} + \frac{1}{2}\gamma B N_{\gamma(e)} \qquad (2.7)$$

where $N_{c(e)}$, $N_{q(e)}$, $N_{\gamma(e)}$ are the bearing capacity factors for an eccentrically loaded strip foundation. The bearing capacity factors are functions of *e/B*, ϕ and foundation contact factor x_1. The variation of x_1 with *e/B* is shown in Figure 2.3(c). The bearing capacity factors are presented in the form of figure for different *e/B* and ϕ.

Purkayastha and Char (1977) performed stability analysis of an eccentrically loaded strip foundation on sand using the method of slices as proposed by Janbu (1957). Based on the analysis, they proposed that

$$R_k = 1 - \frac{q_{u(eccentric)}}{q_{u(centric)}} \tag{2.8}$$

where R_k = reduction factor; $q_{u(eccentric)}$ = ultimate bearing capacity of eccentrically loaded continuous foundations; $q_{u(centric)}$ = ultimate bearing capacity of centrally loaded continuous foundations.

The magnitude of R_k can be expressed as

$$R_k = a\left(\frac{e}{B}\right)^k \tag{2.9}$$

where a and k are functions of D_f/B

Combining Eqns. (2.8) and (2.9)

$$q_{u(eccentric)} = q_{u(centric)}\left(1 - R_k\right) = q_{u(centric)}\left(1 - a\left(\frac{e}{B}\right)^k\right) \tag{2.10}$$

where

$$q_{u(centric)} = qN_q d_q + \frac{1}{2}\gamma B N_\gamma d_\gamma \quad (c = 0) \tag{2.11}$$

The values of a and k are presented in Table 2.3 for different D_f/B.

Table 2.3: Values of a and k

D_f /B	a	k
0	1.862	0.73
0.25	1.811	0.785
0.5	1.754	0.8
1.0	1.820	0.888

From the analysis they found that the width of the footing and friction angle has no influence on the reduction factor.

Michalowski and You (1998) presented the bearing capacity of eccentrically loaded footings using the kinematic approach of limit analysis. They found that the effective width method given by Meyerhof (1953) leads to the same bearing capacity as the limit analysis solution for a smooth footing, and it underestimates the bearing capacity of footings on cohesive soils with frictional or adhesive soil-footing interfaces as shown in Figure 2.4. The effective width rule significantly underestimates the bearing capacity for clays ($\phi \approx 0$) only when the footing is bonded with the soil and the eccentricity is relatively large ($e/B > 0.25$) [Figure 2.4].

For cohesive-frictional soils this underestimation decreases with an increase in the internal friction angle. The rule of effective width gives very reasonable estimates of the bearing capacity of eccentrically loaded footings on cohesive or cohesive-frictional soils when the soil-footing interface is not bonded, and for any type of interface when the eccentricity is small ($e/B < 0.1$) as shown in Figure 2.5.

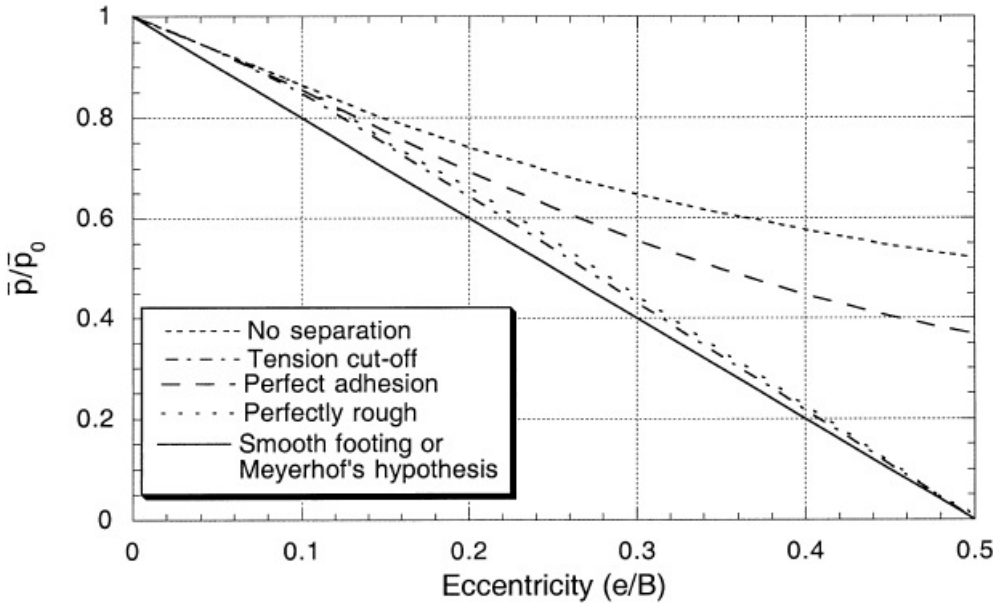

Figure 2.4: Solutions to bearing pressure $\bar{p}$ on cohesive soil for different soil-footing interface models (no surcharge)

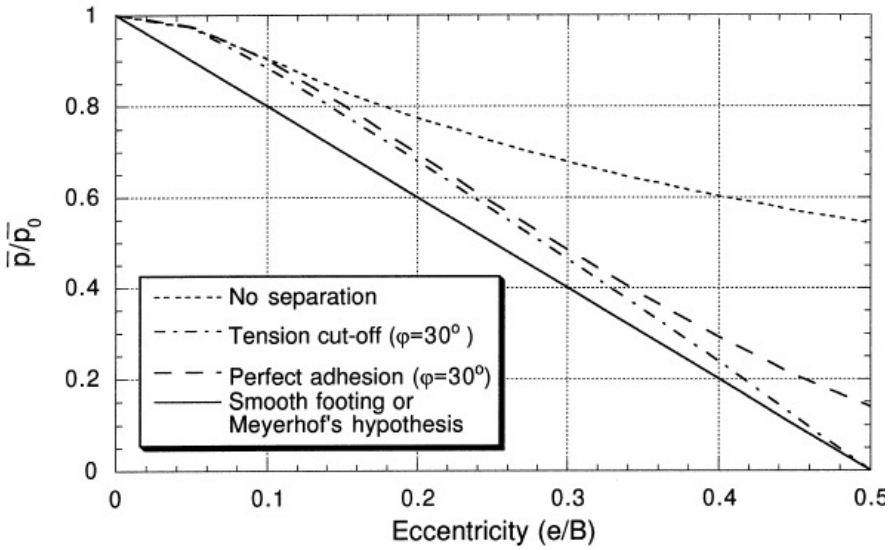

Figure 2.5: Solutions to bearing pressure $\bar{p}$ on cohesive-frictional soil for different soil-footing interface models (weightless soil, no surcharge)

The effective width rule also overestimates the bearing capacity for purely frictional soils when the surcharge load is relatively small. For cohesionless soils, however, the effective

width rule may overestimate the best upper bound and this overestimation increases with an increase in eccentricity [Figure 2.6].

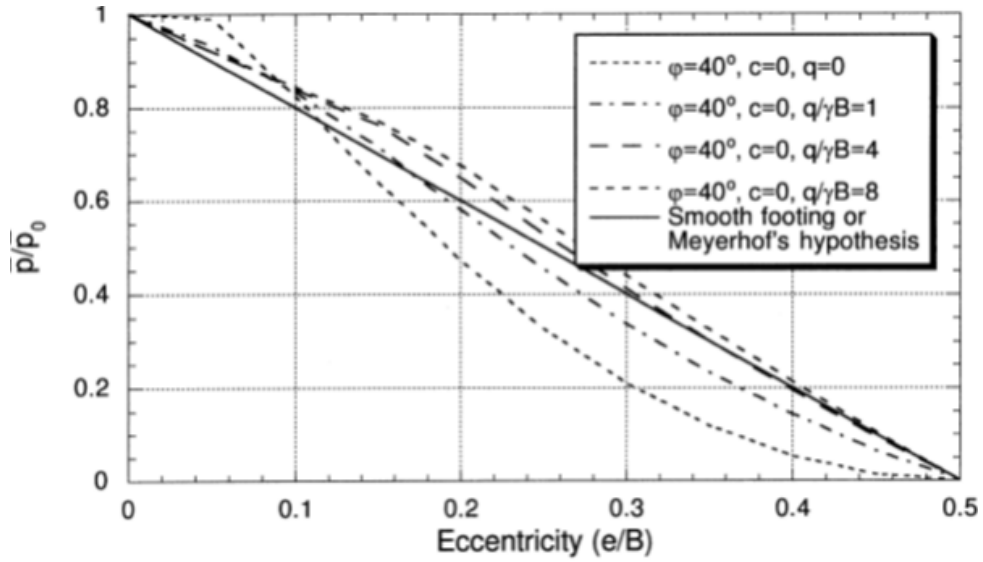

Figure 2.6: Numerical solutions to bearing pressure of eccentrically loaded footings (tension cut-off interface)

2.2.3 Central Inclined Condition

Meyerhof (1953) extended his theory for ultimate bearing capacity under vertical loading to the case with inclined load. They have considered two types of inclination, first one considering foundations with a horizontal base [Figure 2.7 (a) and (b)] and second one considering foundations with a base normal to the load (i.e. base inclined α to the horizontal) as shown in Figure 2.7 (c).

For foundations with a horizontal base, the ultimate bearing capacity, q is expressed as vertical component of the ultimate bearing capacity, i.e.

$$q_{(v)} = q\cos\alpha = cN_{cq} + \frac{1}{2}\gamma BN_{\gamma q} \tag{2.12}$$

where, $q_{(v)}$ = Vertical component of the ultimate bearing capacity; N_{cq}, $N_{\gamma q}$ = Bearing capacity factors which are functions of the soil friction angle, ϕ, depth of the foundation, D and load inclination α.

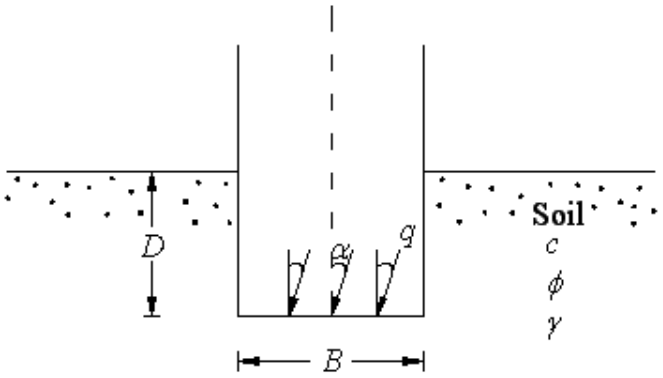

(a) Horizontal base with small inclination of load

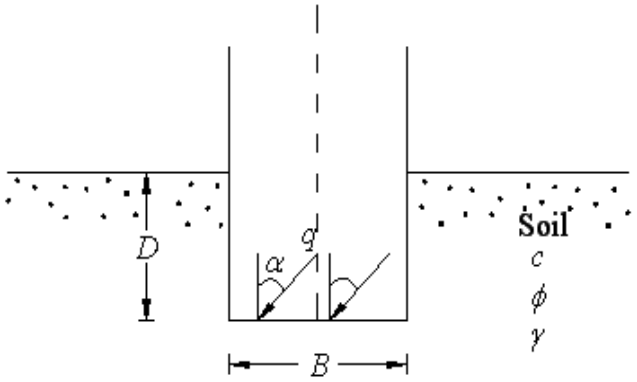

(b) Horizontal base with large inclination of load

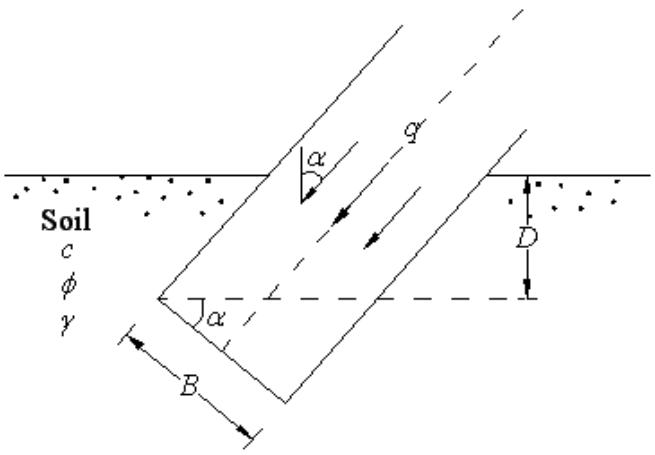

(c) Inclined base with normal load

Figure 2.7: Inclined load applied to a rough strip foundation [Meyerhof (1953)]

Likewise, for an inclined foundation with a base normal to the load [Figure 2.7 (c)] the ultimate bearing capacity can be expressed as

$$q = cN_{cq} + \frac{1}{2}\gamma BN_{\gamma q} \tag{2.13}$$

He presented the bearing capacity factors N_{cq}, $N_{\gamma q}$ in the form of chart for different values of α and ϕ. He also found that that for a given inclination α an inclined foundation can have a higher bearing capacity than a horizontal base.

Meyerhof (1963) proposed that for rough foundations the vertical component of the bearing capacity (q) under a load inclined at an angle of α with the vertical [Figure 2.8] can be expressed as

$$q = cN_c d_c i_c + \gamma DN_q d_q i_q + \frac{1}{2}\gamma BN_\gamma d_\gamma i_\gamma \tag{2.14}$$

where i_c, i_q, i_γ = inclination factors

d_c, d_q, d_γ = depth factors [as mentioned in Table 2.2]

$$i_c = i_q = \left(1 - \frac{\alpha}{90}\right)^2 \tag{2.15}$$

$$i_\gamma = \left(1 - \frac{\alpha}{\phi}\right)^2 \tag{2.16}$$

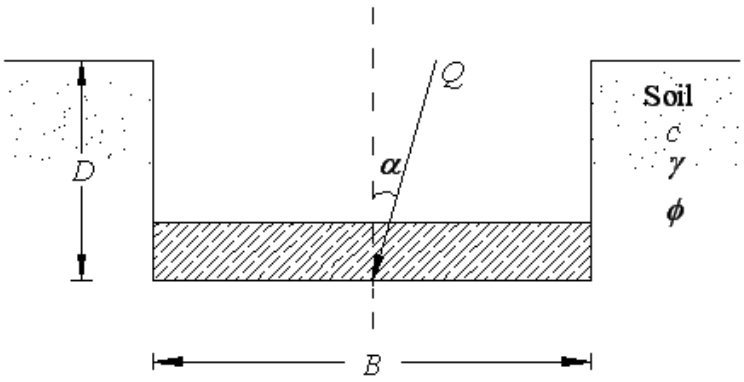

Figure 2.8: Ultimate load Q on a foundation for centric inclined load

Hansen (1970) proposed the relationships for inclination factors based on method of characteristics

$$\lambda_{qi} = \left(1 - \frac{0.5Q_u \sin\alpha}{Q_u \cos\alpha + BLc\cot\phi}\right)^5 \tag{2.17}$$

$$\lambda_{ci} = \lambda_{qi} - \left(\frac{1-\lambda_{qi}}{N_q - 1}\right) \tag{2.18}$$

$$\lambda_{\gamma i} = \left(1 - \frac{0.7Q_u \sin\alpha}{Q_u \cos\alpha + BLc\cot\phi}\right)^5 \tag{2.19}$$

where α = load inclination of foundation with the vertical; Q_u = Ultimate load on the foundation = $q_u BL$; B = width of the foundation; L = Length of the foundation.

Dubrova (1973) proposed a formulation for the ultimate bearing capacity of a continuous foundation with centric inclined load and is given by

$$q_u = c\left(N_q^* - 1\right)\cot\phi + 2qN_q^* + B\gamma N_\gamma^* \tag{2.20}$$

where, N_q^*, N_γ^* = bearing capacity factors; $q = \gamma D_f$

The value of N_q^*, N_γ^* are presented in the form of graph with different values of tanα and ϕ.

Muhs and Weiss (1973) conducted field tests and found that the ratio of the vertical component $Q_{u(v)}$ of the ultimate load with the inclination α with the vertical to the ultimate load Q_u, when the load is vertical (i.e. $\alpha = 0$) and is given by

$$\frac{Q_{u(v)}}{Q_{u(\alpha=0)}} = \left(1 - \tan\alpha\right)^2 \tag{2.21}$$

or

$$\frac{\dfrac{Q_{u(v)}}{BL}}{\dfrac{Q_{u(\alpha=0)}}{BL}} = \frac{q_{u(v)}}{q_{u(\alpha=0)}} = \left(1 - \tan\alpha\right)^2 \tag{2.22}$$

where B = width of the foundation; L = length of the foundation; $q_{u(v)}$ = vertical component of the ultimate bearing capacity when the load is inclined at an angle α with the vertical; $q_{u(\alpha=0)}$ = ultimate bearing capacity of the footing for central condition ($\alpha = 0$).

Vesic (1975) proposed equation for inclination factors based on method of characteristics

$$i_c = 1 - \frac{mH}{AcN_c} \quad for\ \phi = 0 \tag{2.23}$$

$$i_c = i_q - \frac{1 - i_q}{N_q - 1} \quad for\ \phi > 0 \tag{2.24}$$

$$i_q = \left(1 - \frac{H}{V + cBL\cot\phi}\right)^m \tag{2.25}$$

$$i_\gamma = \left(1 - \frac{H}{V + cBL\cot\phi}\right)^{m+1} \tag{2.26}$$

where $m = \dfrac{2 + \dfrac{B}{L}}{1 + \dfrac{B}{L}}$, for load inclined in in the direction parallel to the width of the footing

and $m = \dfrac{2 + \dfrac{L}{B}}{1 + \dfrac{L}{B}}$, for load inclined in in the direction parallel to the length of the footing; i_c, i_q, and i_γ are the inclination factors; c = cohesion; A = Area of the footing; H and V are the components of the load parallel and perpendicular to the base of the footing.

Sastry and Meyerhof (1987) carried out model tests to evaluate corresponding inclination factors for a surface strip footing on purely cohesive soil subjected to a central load at an inclination of α_L acting in the direction of the footing length [Figure 2.9 (a)]. Saturated clay of medium plasticity (liquid limit w_l = 43 %, plastic limit w_p = 21 %) was used with an average water content of w = 32 %. The average undrained shear strength c_u was 21 kN/m^2. The steel strip footing had a width B of 25.4 mm, length L of 127 mm (L/B = 5), and thickness of 9.5 mm with a rough base. The tests were carried out at load inclinations α of 0^0, 10^0, 15^0, 30^0, and 45^0.

The vertical component q_{uv} of the bearing capacity q_u of the surface strip footing supported by purely cohesive soil can be given by

$$q_{uv} = q_u \cos\alpha_B \tag{2.27}$$

$$q_{uv} = i_c c_u N_c \tag{2.28}$$

where i_c = inclination factor

The relationship between load inclination α_L along the direction of footing length and corresponding inclination factor i_c' can be given by

$$i_c^{'} = \left(1 - \frac{\alpha_L}{90}\right)^2 \tag{2.29}$$

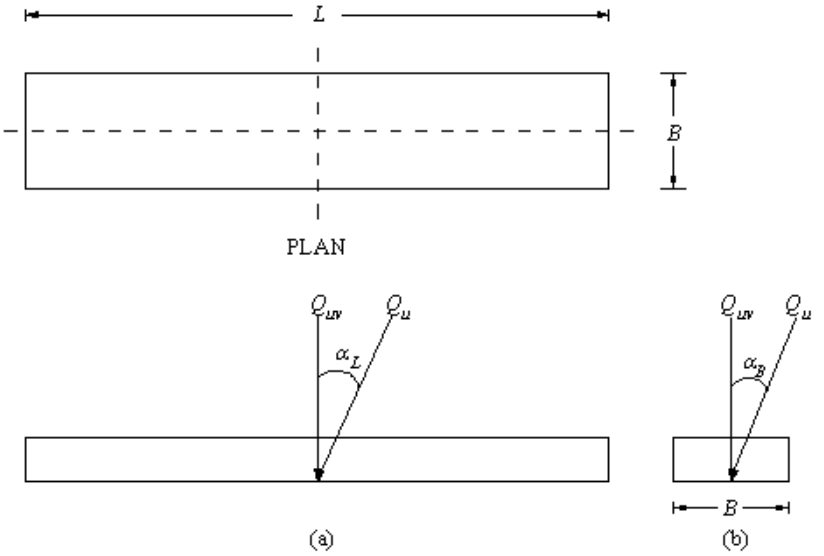

Figure 2.9: Strip footing under inclined load along (a) length and (b) breadth [Sastry and Meyerhof (1987)]

Similar tests were carried out on a shallow strip footing as shown in Figure 2.9 (a) supported by cohesionless soil with friction angle ϕ of 39^0 by Muhs and Weiss (1972). They found the relationship between α_L and corresponding inclination factor i_γ' as

$$i_\gamma^{'} = \left(1 - \frac{\alpha_L}{\phi}\right) \tag{2.30}$$

where, α_L = load inclination in the direction of footing length

i_c', i_γ' = inclination factors for load inclination in the direction of footing length

They found that for the same load inclination α, $i_c' \geq i_c$ and $i_\gamma' \geq i_\gamma$.

where i_c, i_γ = inclination factors for load inclination in the direction of footing width [Figure 2.9 (b)]

Meyerhof and Koumoto (1987) studied the ultimate bearing capacity of shallow strip footings under central load inclined in the direction of footing length to evaluate the inclination factors. The theoretical values of the present inclination factors were compared with some experimental results of model footings on clay and sand. They proposed the inclination factors as:

$$i_c' = \cos\alpha \left(1 - \left(1 - \frac{\frac{c_a}{c_u}}{\pi + 2} \right) \sin\alpha \right) \tag{2.31}$$

$$i_q' = \cos\alpha \left\{ 1 - \left[1 - \left(\frac{D}{B} \right)^2 \frac{\frac{B}{L} K_p \cos\phi + 2K_s \tan\phi}{N_{\gamma q}} \right] \sin\alpha \right\} \tag{2.32}$$

$$i_\gamma' = \cos\alpha \left(1 - \frac{\sin\alpha}{\cos\alpha} \right) \tag{2.33}$$

where, c_u and c_a = The undrained shear strength of clay and the adhesion of clay on the footing base; K_p and K_s = The average earth pressure coefficient on the footing front side and the footing side respectively.

From the theoretical analysis they concluded that the corresponding theoretical inclination factors are found to be generally larger than the previous factors for a load inclined in the direction of the footing width.

Hjiaj et al. (2004) investigated the ultimate bearing capacity of a rigid rough strip footing of width *B*, subjected to an inclined load *Q*, which was resting on a deep layer of homogeneous cohesive-frictional soil of unit weight γ and the centric force acting upon the foundation was inclined at an angle α with the vertical. The cohesive-frictional soil is assumed to be rigid perfectly plastic and modelled by a Mohr–Coulomb yield criterion with cohesion *c* and friction angle ϕ. Accurate lower and upper bounds are calculated rigorously using finite elements and nonlinear programming.

They concluded that, the Meyerhof inclination factors are deficient for centric inclined loading and that the Vesic's expression for N_γ slightly overestimates the influence of self-weight on the bearing capacity.

2.2.4 Eccentric Inclined Condition

Meyerhof (1963) extended the theory for shallow foundations subjected to centric vertical load (Meyerhof 1951) to incorporate load eccentricity and inclination as shown in Figure 2.10. He suggested that the vertical component of the bearing capacity in case of eccentric inclined loads can be given by

$$q = cN_c s_c d_c i_c + \gamma D N_q s_q d_q i_q + \frac{1}{2}\gamma B' N_\gamma s_\gamma d_\gamma i_\gamma \qquad (2.34)$$

where $B' = B - 2e$ = effective width; s_c, s_q , s_γ = shape factors [mentioned in Table 2.2], d_c, d_q , d_γ = depth factors [mentioned in Table 2.2], i_c, i_q , i_γ = inclination factors [mentioned in Eqs. (2.15) and (2.16)].

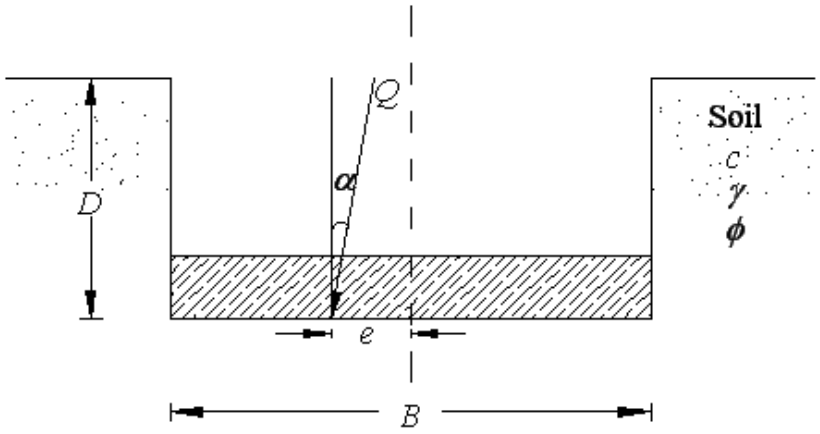

Figure 2.10: Eccentric inclined load on foundation [Meyerhof (1963)]

Saran and Agarwal (1991) used a similar technique to that of Prakash and Saran (1971) to theoretically evaluate the ultimate bearing capacity of a strip foundation subjected to eccentrically inclined load [Figure 2.10]. According to this analysis, the ultimate bearing capacity can be expressed as

$$q_u = \frac{Q_u}{B} = cN_c + \gamma D N_q + \frac{1}{2}\gamma B N_\gamma \tag{2.35}$$

For a foundation on granular soil, the above equation is reduced in the form as

$$q_u = \gamma D N_q + \frac{1}{2}\gamma B N_\gamma \tag{2.36}$$

where N_c, N_q and N_γ are the bearing capacity factors expressed in terms of load eccentricity e and inclined at an angle α to the vertical. They presented the bearing capacity factors in tabular and graphical forms.

Loukidis et al. (2008) performed finite element analysis to determine the collapse load of a rigid strip footing placed on a purely frictional soil subjected to eccentric and inclined loading. The analyses were conducted on the free surface of the soil mass. Associated flow rule and Nonassociated flow rule were adopted for the analysis. The equations which are well fit to the finite element results are

$$B' = B\left(1-2.273\frac{e}{B}\right)^{0.8} \tag{2.37}$$

$$H = 0.69V\left[1-\left(\frac{V}{V_{\max}}\right)^{0.5}\right] \tag{2.38}$$

$$M = 0.52V\left[1-\left(\frac{V}{V_{\max}}\right)^{0.5}\right] \tag{2.39}$$

$$i_\gamma = \left(1-0.94\frac{\tan\alpha}{\tan\phi}\right)^{(1.5\tan\phi+0.4)^2} \tag{2.40}$$

$$V_L = \frac{1}{2}\gamma B^2 N_\gamma f_{ie} \tag{2.41}$$

where, f_{ie}= combined inclination-eccentricity factor, expressed as

$$f_{ie} = \left[1-\sqrt{3.7\left(e/B\right)^2 + 2.1(\tan\alpha)^2 + 1.5\frac{e}{B}\tan\alpha}\right]^2 \tag{2.42}$$

B' = effective width of the footing; V_L = (Vertical) limit load; H = Horizontal load; M = Moment; V = Vertical load; V_{max} = Maximum vertical load; i_γ= inclination factor.

IS 6403: (1981) covers the procedure for determining the ultimate bearing capacity and allowable bearing pressure of shallow foundations based on shear and allowable settlement criteria.

For eccentrically loaded footing, eccentricity can be applied in two way i.e.

(i) Single Eccentricity — If the load has an eccentricity *e*, with respect to the centroid of the foundation in only one direction, then the dimension of the footing in the direction of eccentricity shall be reduced by a length equal to 2*e*. The modified dimension shall be used in the bearing capacity equation and in determining the effective area of the footing in resisting the load.

(ii) Double Eccentricity — If the load has double eccentricity (e_L and e_B) with respect to the centroid of the footing then the effective dimensions of the footing to be used in determining the bearing capacity as well as in computing the effective area of the footing in resisting the load shall be determined as given below:

$$L' = L - 2e_L \tag{2.43}$$

$$B' = B - 2e_B \tag{2.44}$$

$$A' = L' \times B' \tag{2.45}$$

For inclined footing, the inclination factors are expressed as follows:

$$i_c = i_q = \left(1 - \frac{\alpha}{90}\right)^2 \tag{2.46}$$

and

$$i_\gamma = \left(1 - \frac{\alpha}{\phi}\right)^2 \tag{2.47}$$

However, the code does not give any information to compute the bearing capacity of eccentrically inclined loaded footing.

Similarly, **IS 8009: (1976-Part I)** provides simple methods for the estimation of immediate and primary consolidation settlements of shallow foundations under symmetrical static vertical loads.

Settlement of cohesionless soil deposits may be estimated by a semi-empirical method based on the results of static cone or dynamic penetration test or plate load tests.

Based on standard cone penetration test, the settlement of each layer within the stressed zone due to the foundation loading, should be separately calculated using the equation below and the results added together to give the total settlement.

$$S_f = 2.303 \frac{H_t}{C} \log_{10} \left[\frac{\overline{p_0} + \Delta p}{\overline{p_0}} \right] \tag{2.48}$$

and $C = \frac{3}{2} \frac{C_{kd}}{\overline{p_0}}$

where S_f = settlement in each layer; H_t = Thickness of the layer; C= Compressibility coefficient; C_{kd} = static cone resistance; $\overline{p_0}$ = effective overburden pressure; Δp = increase in pressure

Based on Plate load test, the total settlement of the proposed foundation is given by

$$S_f = S_p \left[\frac{B(B_p + 30)}{B_p(B + 30)} \right]^2 \tag{2.49}$$

where S_p = Total settlement of test plate; B_p = width of square plate; B= width of square foundation

Similarly, based on dynamic penetration test, Settlement of a footing of width B under unit intensity of pressure resting on dry cohesionless deposit with known standard

penetration resistance value *N*, may be read from Figure 2.11 (b). The settlement under any other pressure may be computed by assuming that the settlement is proportional to the intensity of pressure. If the water table is at a shallow depth, the settlement read from Figure 2.11 (b) will be divided, by the correction factor *W′* read from Figure 2.11 (a).

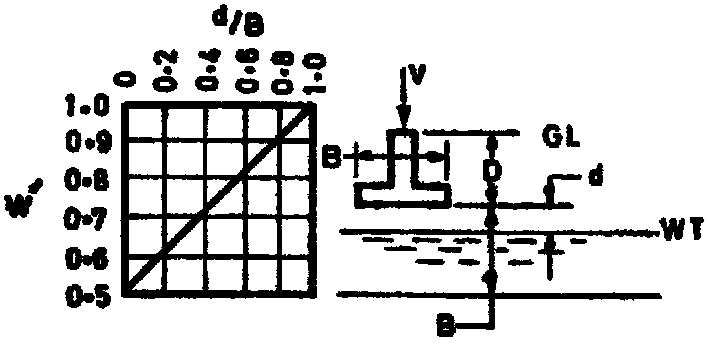

(a)

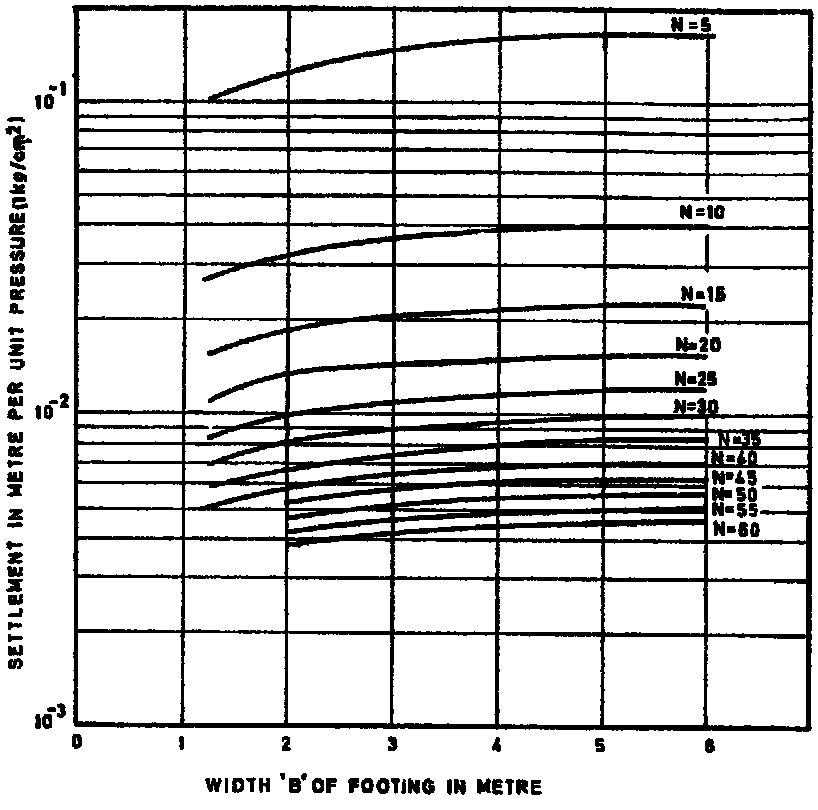

(b)

Figure 2.11: (a) Water table correction factor *W′* (b) Settlement per unit pressure from standard penetration resistance

where, GL=ground level; WT=water table

But the IS code does not provide any information to estimate the settlement of a footing on granular soil under the action of either eccentric load, inclined load or eccentrically inclined load.

2.3 Scope of the present study

Based on the review of the existing literature on the bearing capacity of shallow foundations, it appears that limited attention has been paid to estimate the ultimate bearing capacity when the foundation is subjected to an eccentrically inclined load. Most of these studies are based on theoretical analyses (limit equilibrium method) and numerical analyses (finite element method) supported by few number of model tests. So, the objective of the present thesis is to study the bearing capacity of eccentrically inclined loaded strip footing by conducting extensive laboratory model tests by varying eccentricity ratio (e/B), load inclination (α), depth of embedment ratio (D_f /B) and relative density (I_D) to quantify certain parameters. The effect of load application in two possible modes i.e. (i) towards and (ii) away from the center line of the footing [Figure 2.11] is investigated. Based on the laboratory model test results, empirical nondimensional equations have been developed by regression analysis to determine the ultimate bearing capacity of eccentrically inclined embedded strip footings for each mode of load application. Also, Neural network models are developed based on the present experimental results. Model equations are developed based on the trained weights and biases of the neural network model. The predicted equations obtained from regression analysis and neural network models have been compared with other available theories.

In addition to bearing capacity, based on the results of laboratory load tests, an empirical procedure is developed to estimate the average settlement of eccentrically loaded footings subjected to an average allowable load per unit area.

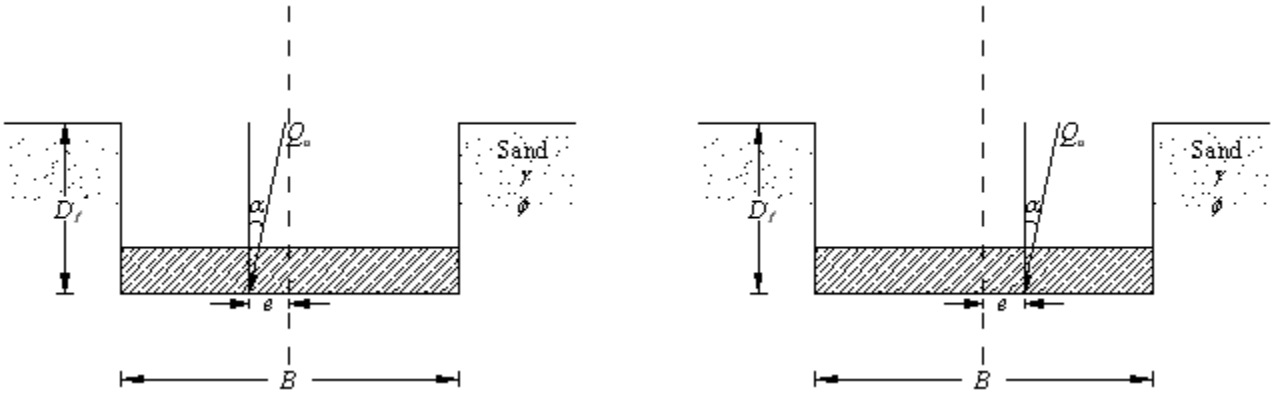

Figure 2.12: Eccentrically inclined load on a strip foundation: line of load application (a) towards the center line, and (b) away from the center line of the footing

The outlines of the analysis and results on the above aspects are discussed in subsequent chapters as mentioned below.

In Chapter 3, the test set up and procedure for experimentation has been discussed.

In Chapter 4, the details of tests sequence is reported when the line of load application is towards the center line of the footing [Figure 2.11 (a)]. Empirical model for prediction of ultimate bearing capacity has been developed using regression analysis. The results are compared with available theories.

In Chapter 5, the details of tests sequence for the case when the line of load application is away from the center line of the footing [Figure 2.11 (b)] is described. Based on the test results an empirical nondimensional equation for reduction factor has been developed to predict the ultimate bearing capacity. A comparison of the ultimate bearing capacity in both cases [Figure 2.11 (a) and (b)] has been discussed.

In Chapter 6, an artificial neural network model for estimating ultimate bearing capacity [Figure 2.11 (a)] is presented based on the test results as discussed in Chapter 4. The results from developed neural network model have been compared with developed empirical equation as reported in Chapter 4 and with other available theories.

In Chapter 7 an artificial neural network model for estimating ultimate bearing capacity [Figure 2.11 (b)] is presented based on the test results as discussed in Chapter 5. The predictions from ANN are compared with the results by using developed empirical equation mentioned in Chapter 5.

In Chapter 8 an ANN model has been developed by considering both mode of load application (i.e. towards and away from the center line of the footing) simultaneously. This model predicts the ultimate bearing capacity in either mode of load application on the footing. The obtained results are compared with the results as discussed in Chapters 4, 5, 6, and 7.

In Chapter 9 a relationship is developed between the average load per unit area and the average settlement of footing subjected to eccentric load. A step by step procedure is suggested to estimate the average settlement of the foundation while being subjected to an average allowable eccentric load per unit area.

Chapter 10 brings all the conclusions drawn from the above chapters and suggests for future research work.

3. MATERIALS USED AND EXPERIMENTAL PROCEDURE

3.1 Introduction

The experimental program was designed to study the bearing capacity of strip footings resting on granular soils and subjected to eccentric and inclined loading. For this purpose, the laboratory model tests were performed on strip footings resting on soil with two different densities. The load eccentricity e was varied from 0 to 0.15B (B = width of strip footing) with an increment of 0.05B, load inclination α was varied from 0° to 20° at an increment of 5° and the depth of embedment (D_f /B) was varied from 0 to 1.0 at an increment of 0.5. The ultimate bearing capacity was interpreted from each test and analysed.

3.2 Materials Used

3.2.1 Sand

The sand used in the experimental program was collected from the river bed of a nearby river. It is made free from roots, organic matters etc. by washing and cleaning. The above sample was then oven dried and sieved by passing through 710 micron and retained on 300 micron IS sieve to get the required grading. Dry sand is used as soil medium for the test as it does not include the effect of moisture and hence the apparent cohesion associated with it. The geotechnical properties of the sand used are given in Table 3.1. The grain size distribution curve is plotted in Figure 3.1. All the tests were conducted in two densities (dense and medium dense) with relative densities of 69% and 51% respectively. The respective average unit weights are 14.36 kN/m^3 and 13.97 kN/m^3. The

friction angle at these two relative densities are 40.8^0 and 37.5^0 respectively from direct shear tests. The tests were conducted in the pressure range of about 6-19kN/m^2.

Table 3.1. Geotechnical property of sand

Property	Value
Specific gravity (G)	2.61
Effective particle size (D_{10})	0.325mm
Mean particle size (D_{50})	0.46mm
Uniformity Coefficient (C_u)	1.45
Coefficient of Curvature (C_c)	1.15
Maximum unit weight ($\gamma_{d(max)}$)	15.1 kN/m^3
Minimum unit weight ($\gamma_{d(min)}$)	12.95 kN/m^3

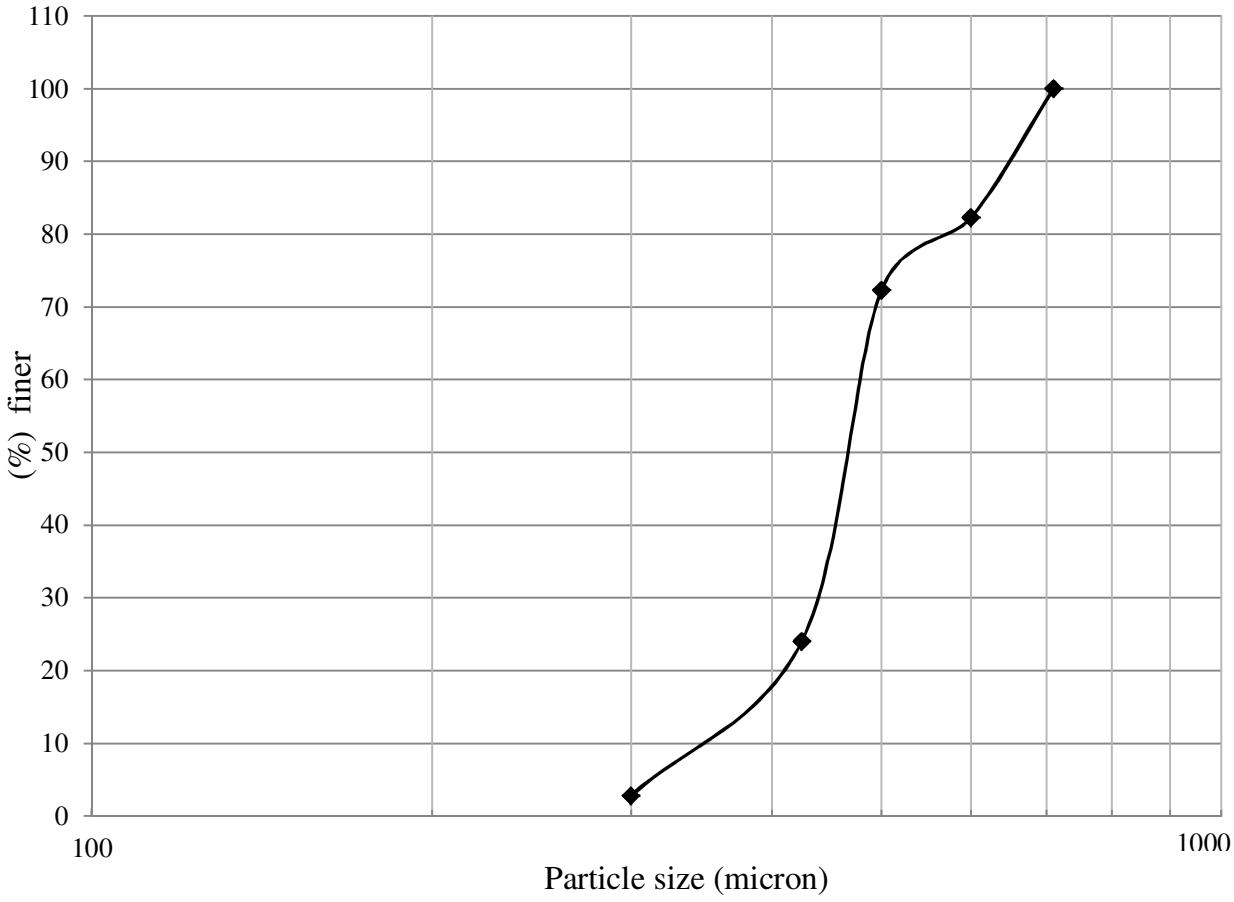

Figure 3.1: Grain-size distribution curve of sand

3.3 Experimental procedure

All the model tests were carried out in the Geotechnical Engineering Laboratory of NIT Rourkela, India. The model tests were conducted in a mild steel tank measuring 1.0m (length) × 0.504m (width) × 0.655m (height). The two length sides of the tank are made of 12mm thick high strength fiberglass. All four sides of the tank are braced to avoid bulging during testing. The size of the model foundation has been kept as 100mm (width B) × 500mm (length L) × 30mm (thickness t) and is made from a mild steel plate. The bottom of the footing was made rough by applying glue and then rolling the model footing over sand. Since the width of the test tank and the length of the model foundation are approximately the same and the length: width ratio of the model footing is 5:1, the plane strain condition exists during the tests.

Sand was poured into the test tank in layers of 25mm from a fixed height by raining technique to achieve the desired average unit weight. The height of fall was fixed by making several trials in the test tank to relate the height of fall and the density achieved. The model foundation was placed at a desired D_f/B ratio at the middle of the box. Load to the model foundation was applied by a loading assembly (shown in Figure 3.2). It consists of three units: (a) the electrical control panel, (b) hydraulic power pack and (c) loading device. The loading device is a combination of a beam, four cylinders, four supporting columns and a base. The hydraulic cylinder is the device that converts fluid power into linear mechanical force and motion. It converts fluid energy to an output force in a linear direction for executing different jobs. The capacity of the hydraulic cylinder in universal static loading setup is 100kN. The load can be applied to the model foundation

in the range of 0 to 100kN with an accuracy of 1N. The inclination of the load can be changed by forward and backward movement of the cylinder. The inclination of the load remains constant throughout the testing period by the provision of the check valve. The load applied to the model foundation is measured by proving ring. Settlement of the model foundation is measured by dial gauges placed on two edges along the width side of the model foundation. All the tests were conducted in stress controlled manner. Number of trials was made prior to the test to maintain uniform rate of load application. The rate of load application was 150N/min. For each sequence of test, approximate calculations for ultimate load were made and then this load is divided into about 12 equal increments to get well defined load-settlement curve. The loads are applied in increments and settlement is recorded through dial gauges placed on two edges along the width side of the model foundation. The next load of increment is applied when the rate of settlement dropped to less than 0.02mm/minute [IS 1888: 1982]. The above procedure is continued till the failure of footing. The accuracy of dial gauge is 0.01mm and the total range is 50mm. The load applied to the model foundation is measured by proving ring. Five numbers of proving ring were used with capacity of 50kN, 20kN, 10kN, 5kN, and 2.5kN and the respective least counts were 66.27N, 24.24N, 12.12N, 6.68N and 3.83N.

Figure 3.3 shows the photographic image of prepared sand sample for the test where the lines of colour sands are placed at a distance of 0.5*B* (*B*=width of the model footing) from the bottom of model footing up to a distance of 2*B* to observe the developed failure surface inside the soil mass. However, for the first 0.5*B* distance from the bottom of the footing, four lines of colour sand were drawn to observe the failure surface minutely.

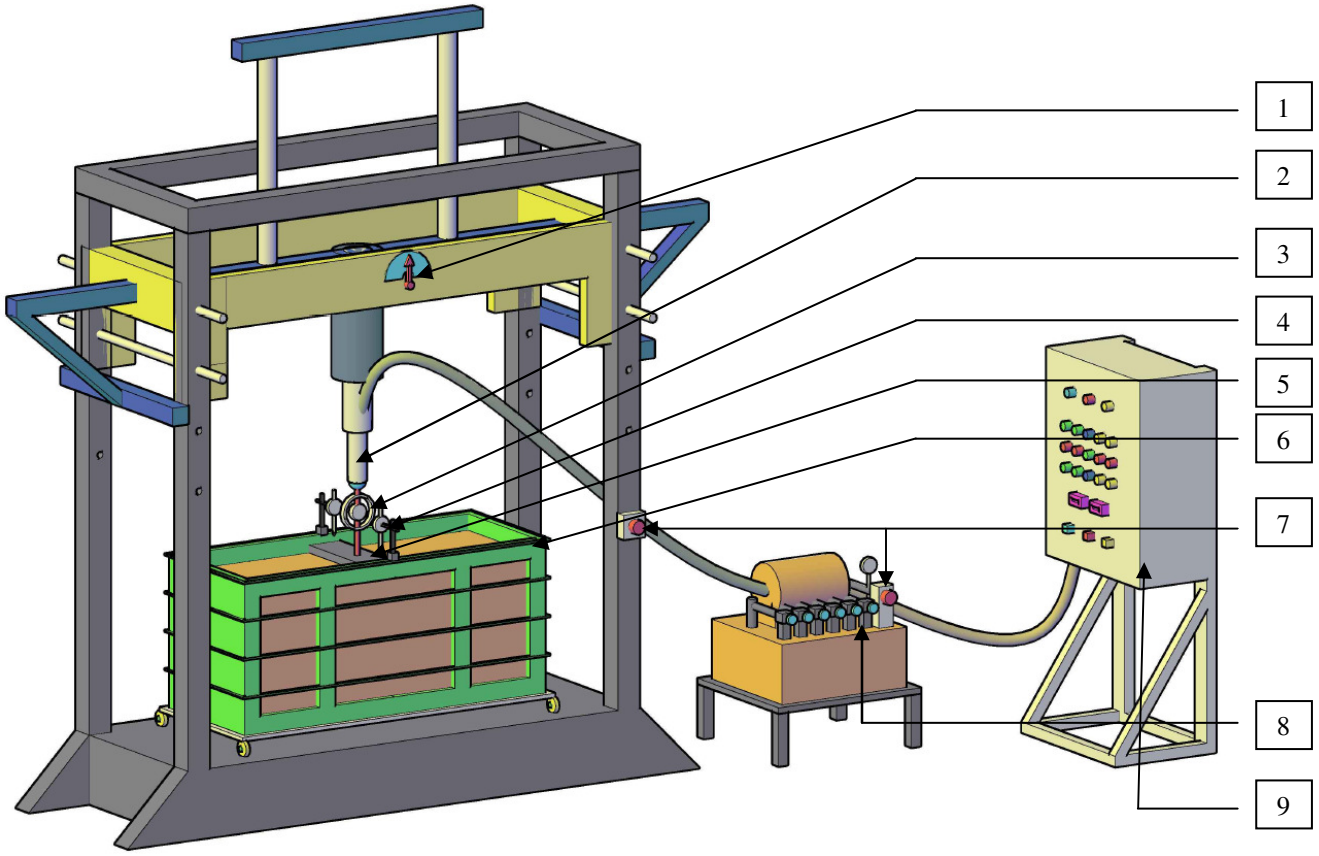

Legend	
1. Inclination Indicator	6. Test Tank (1.0m×0.504m×0.655m)
2. Hydraulic Cylinder	7. Pressure Adjustable Knob
3. Proving Ring	8. Hydraulic Power Pack
4. Dial Gauge	9. Electrical Control Panel
5. Model Footing (100mm×500mm×30mm)	

Figure 3.2: Three dimensional view of laboratory model experimental setup.

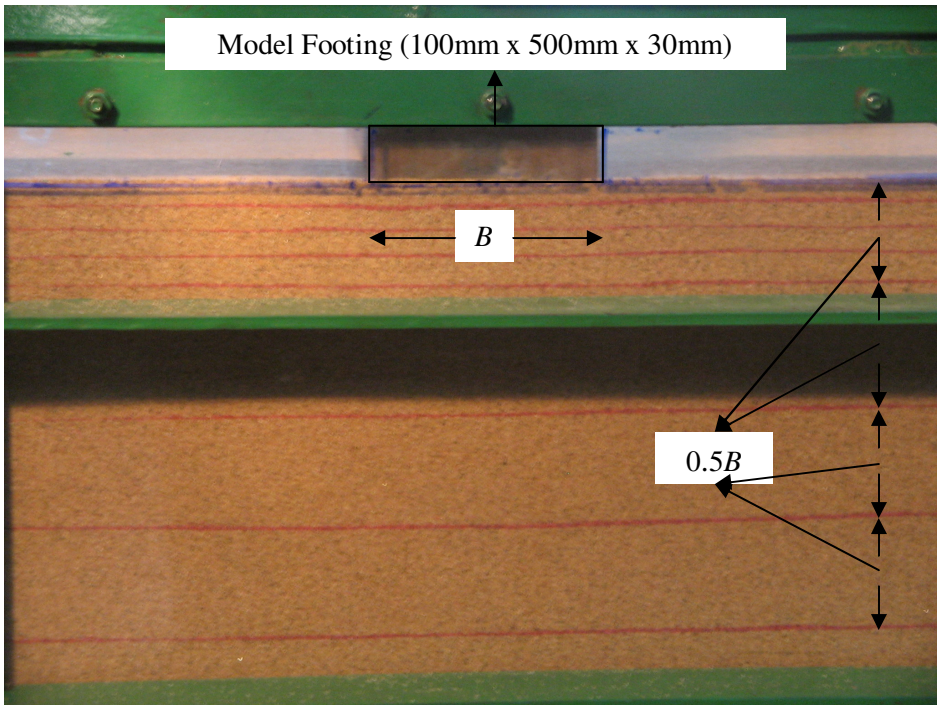

Figure 3.3: Photographic image of sand sample at the start of experiment

4. ULTIMATE BEARING CAPACITY OF ECCENTRICALLY INCLINED LOADED STRIP FOOTING WHEN THE LINE OF LOAD APPLICATION IS TOWARDS THE CENTER LINE OF THE FOOTING

4.1 Introduction

Eccentrically inclined load can be applied on the foundation in two ways. It can be referred to as *partially compensated* (Perloff and Baron, 1976) when the line of load application on the foundation is inclined towards the center line of the foundation [Figure 4.1]. In order to investigate the effect of load eccentricity and inclination, extensive laboratory model tests have been conducted on a strip footing supported by dry sand. The test results have been used to develop a nondimensional reduction factor which will be used for estimating the ultimate bearing capacity. The developed empirical equation is compared with the available theoretical and numerical approaches.

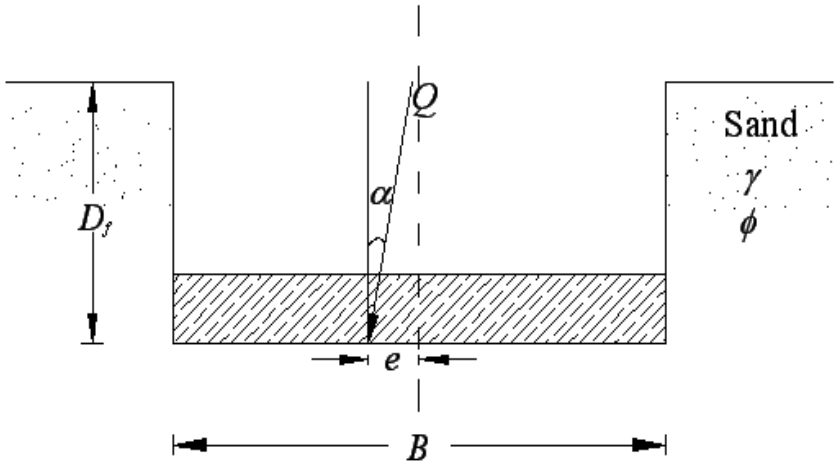

Figure 4.1: Eccentrically inclined load on strip foundation: line of load application towards the center line of the footing

Based on a review of published theoretical and experimental studies related to the estimation of ultimate bearing capacity of shallow strip foundation subjected to eccentric and inclined load, it is evident that further efforts are needed to quantify certain parameters.

Purkayastha and Char (1977) proposed the reduction factor for eccentricity for ultimate bearing capacity as follows:

$$R_k = 1 - \frac{q_{u(eccentric)}}{q_{u(centric)}} \tag{4.1}$$

where R_k = reduction factor; $q_{u(eccentric)}$ = ultimate bearing capacity of eccentrically loaded continuous foundations; $q_{u(centric)}$ = ultimate bearing capacity of centrally loaded continuous foundations.

Meyerhof (1963) proposed load inclination factors as follows:

$$i_c = i_q = \left(1 - \frac{\alpha}{90}\right)^2 \tag{4.2}$$

$$i_\gamma = \left(1 - \frac{\alpha}{\phi}\right)^2 \tag{4.3}$$

where i_c, i_q, i_γ = inclination factors

Therefore, it appears that, for a given value of D_f /B, a reduction factor RF can be developed based on the concept advanced in Eq. (4.1) for load eccentricity and the inclination factors similar to those given in Eqs. (4.2) and (4.3). Or,

$$RF = \frac{q_{u(D_f/B, e/B, \alpha/\phi)}}{q_{u(D_f/B, e/B=0, \alpha/\phi=0)}} \tag{4.4}$$

where $q_{u(D_f/B, e/B, \alpha/\phi)}$ = ultimate bearing capacity with eccentricity ratio e/B and inclination ratio α/ϕ at an embedment ratio D_f/B and $q_{u(D_f/B, e/B=0, \alpha/\phi=0)}$ = ultimate bearing capacity with central vertical loading (e/B = 0 and α/ϕ = 0) at the same embedment ratio D_f/B.

Thus it can initially be assumed that

$$RF = \left[1 - a\left(\frac{e}{B}\right)^m\right]\left(1 - \frac{\alpha}{\phi}\right)^n \tag{4.5}$$

where a, m, n = factors which are functions of D_f/B.

The purpose of this chapter is to discuss the results from several laboratory model tests on strip foundations with varying D_f/B, e/B and α and evaluate the coefficients a, m, and n as given in Eq. (4.5).

4.2 Experimental Module

One hundred and twenty numbers of laboratory model tests were conducted under the condition when the line of load application is towards the center line of the footing. The detail sequence of model tests in this condition are shown in Table 4.1 and Table 4.2 for dense sand and medium dense sand respectively.

Table 4.1. Sequence of model test for Dense sand in *Partially Compensated* condition

Test No.	*e/B*	*α*	D_f/B
1-5	0	0^0, 5^0, 10^0, 15^0, 20^0	0
6-10	0.05	0^0, 5^0, 10^0, 15^0, 20^0	0
11-15	0.1	0^0, 5^0, 10^0, 15^0, 20^0	0
16-20	0.15	0^0, 5^0, 10^0, 15^0, 20^0	0
21-25	0	0^0, 5^0, 10^0, 15^0, 20^0	0.5
26-30	0.05	0^0, 5^0, 10^0, 15^0, 20^0	0.5
31-35	0.1	0^0, 5^0, 10^0, 15^0, 20^0	0.5
36-40	0.15	0^0, 5^0, 10^0, 15^0, 20^0	0.5
41-45	0	0^0, 5^0, 10^0, 15^0, 20^0	1.0
46-50	0.05	0^0, 5^0, 10^0, 15^0, 20^0	1.0
51-55	0.1	0^0, 5^0, 10^0, 15^0, 20^0	1.0
56-60	0.15	0^0, 5^0, 10^0, 15^0, 20^0	1.0

Table 4.2. Sequence of model test for Medium Dense sand in *Partially Compensated* condition

Test No.	*e/B*	*α*	D_f/B
61-65	0	0^0, 5^0, 10^0, 15^0, 20^0	0
66-70	0.05	0^0, 5^0, 10^0, 15^0, 20^0	0
71-75	0.1	0^0, 5^0, 10^0, 15^0, 20^0	0
76-80	0.15	0^0, 5^0, 10^0, 15^0, 20^0	0
81-85	0	0^0, 5^0, 10^0, 15^0, 20^0	0.5
86-90	0.05	0^0, 5^0, 10^0, 15^0, 20^0	0.5
91-95	0.1	0^0, 5^0, 10^0, 15^0, 20^0	0.5

96-100	0.15	0^0, 5^0, 10^0, 15^0, 20^0	0.5
101-105	0	0^0, 5^0, 10^0, 15^0, 20^0	1.0
106-110	0.05	0^0, 5^0, 10^0, 15^0, 20^0	1.0
111-115	0.1	0^0, 5^0, 10^0, 15^0, 20^0	1.0
116-120	0.15	0^0, 5^0, 10^0, 15^0, 20^0	1.0

4.3 Model Test Results

4.3.1 Central Vertical Loading Conditions

Six number of model tests were performed (i.e. $e/B = 0$, $\alpha = 0^0$) in central vertical condition. The details of the test parameters are shown in Table 4.3. Basically there are five different methods to interpret the ultimate bearing capacity from the load-settlement curve namely Log-Log method (DeBeer 1970), Tangent Intersection method (Trautmann and Kulhawy 1988), 0.1B method (Briaud and Jeanjean 1994), Hyperbolic method (Cerato 2005), and Break Point method (Mosallanezhad et al. 2008). For the present test results, the ultimate bearing capacity is determined by Break Point method [Figure 4.2] as after the point of "failure load" with small increase in load significant increase in settlement occurs.

Table 4.3. Model test parameters for the case of Centric Vertical Loading condition

Sand type	Unit weight of compaction (kN/m³)	Relative density of sand (%)	Friction angle ϕ – direct shear test (degree)	$\frac{D_f}{B}$	$\frac{e}{B}$	Load Inclination, α (degree)
Dense	14.36	69	40.8	0 0.5 1.0	0	0
Medium dense	13.97	51	37.5	0 0.5 1.0	0	0

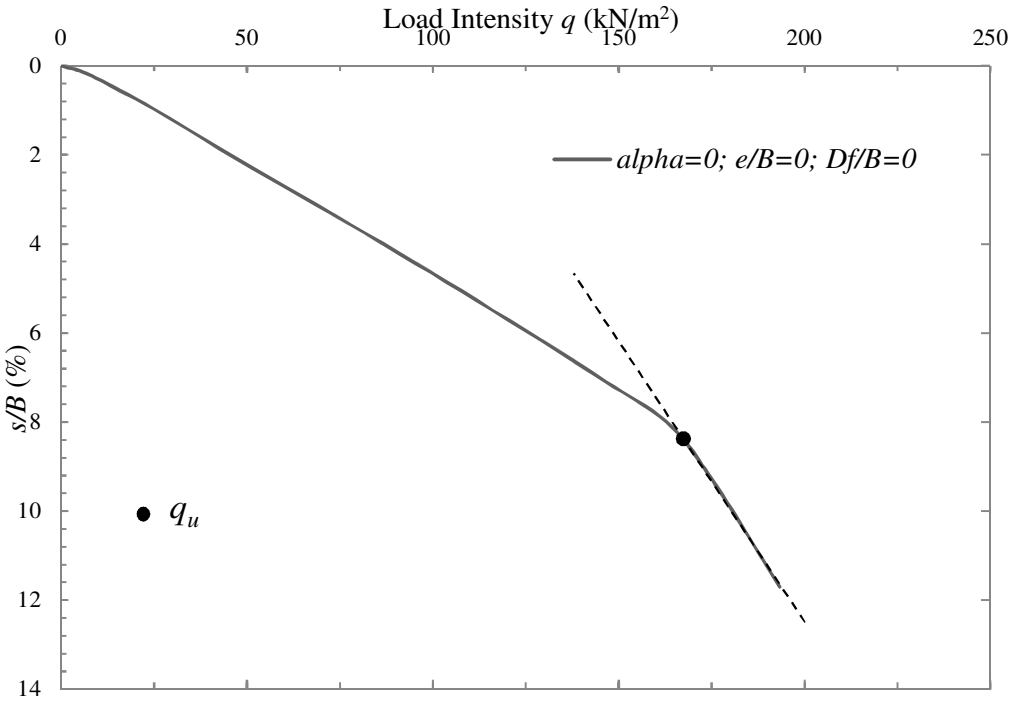

Figure 4.2: Interpretation of Ultimate bearing capacity q_u by Break Point method (Mosallanezhad et al. 2008)

Few number of load-settlement curves are shown in Figures 4.3 and 4.4 to realize the effect of depth of embedment and relative density of sand on ultimate bearing capacity. As seen in Figures 4.3 and 4.4, the bearing capacity of footing increases with the increase in depth of embedment as well as relative density of sand.

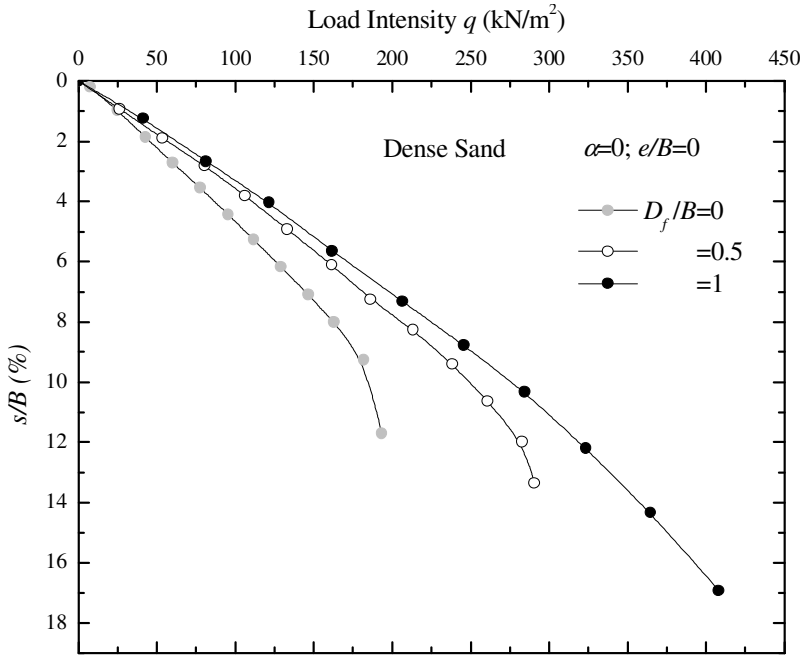

Figure 4.3: Variation of load-settlement curve with embedment ratio (D_f/B) at e/B=0 and α=0 in Dense sand

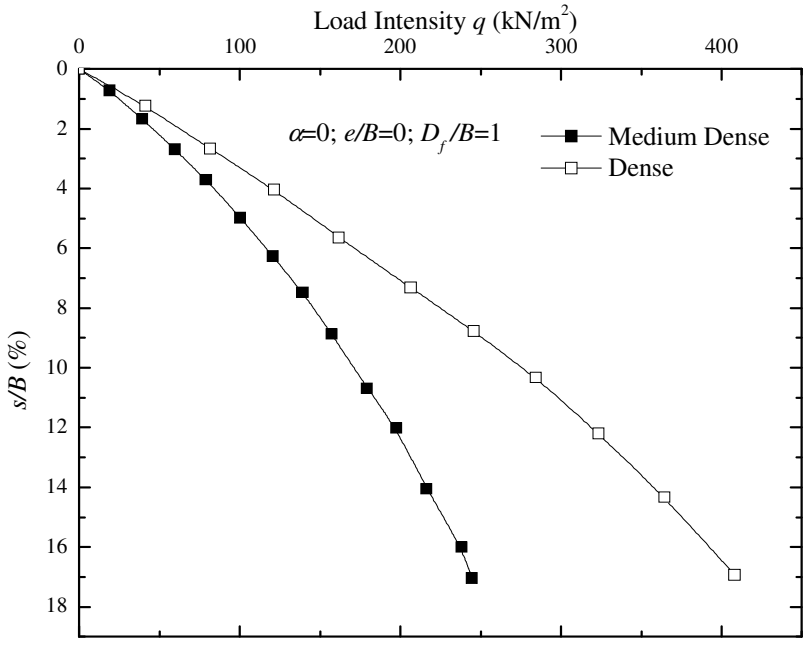

Figure 4.4: Variation of load-settlement curve with Relative Density (D_r) of sand at D_f/B=1, e/B=0 and α=0

The ultimate bearing capacities for centric vertical loading ($e/B = 0$, $\alpha = 0$) at $D_f/B = 0$, 0.5 and 1.0 for dense and medium dense sand obtained using the expressions mentioned in section 2.2.1. The values are plotted in Figure 4.5 and also presented in Table 4.4 and 4.5. It can be seen that experimental bearing capacities for a given D_f/B are significantly higher than those predicted by theory. Investigators like Balla 1962, Bolt 1982, Cichy et al. 1978, Ingra and Baecher 1983, Hartikainen and Zadroga 1994, Milovic 1965, Saran and Agarwal 1991, Shiraishi 1990, and Zadroga 1975 revealed that bearing-capacity model test results which are being carried out in various geotechnical laboratories of shallow footings and strip foundations are, in general, much higher than those calculated by traditional methods. There are several reasons for this, the most important of which is the unpredictability of N_γ and the scale effect associated with the model tests. DeBeer (1965) and Vesic (1973) have discussed this phenomenon at length. DeBeer (1965) compiled several bearing capacity test results which are shown in Figure 4.6 as a plot of N_γ vs. γB. The value of N_γ rapidly decreases with the increase in γB. In addition, DeBeer (1965) compared the variation of N_γ obtained from small scale laboratory and large scale field test results, and these are given in Figure 4.7. For loose sand, the N_γ value in the field is larger than it is in the laboratory. However, for medium dense and dense sands, it is the opposite. These results indicate that it is very difficult to isolate the discrepancies between laboratory test results and theory. In any case, it is reasonable to assume that the reduction factor *RF* as given in Eq. (4.4) is a ratio of two bearing capacities. Hence the scale effect and other unforeseen factors in laboratory model tests will cancel out or will be substantially minimized.

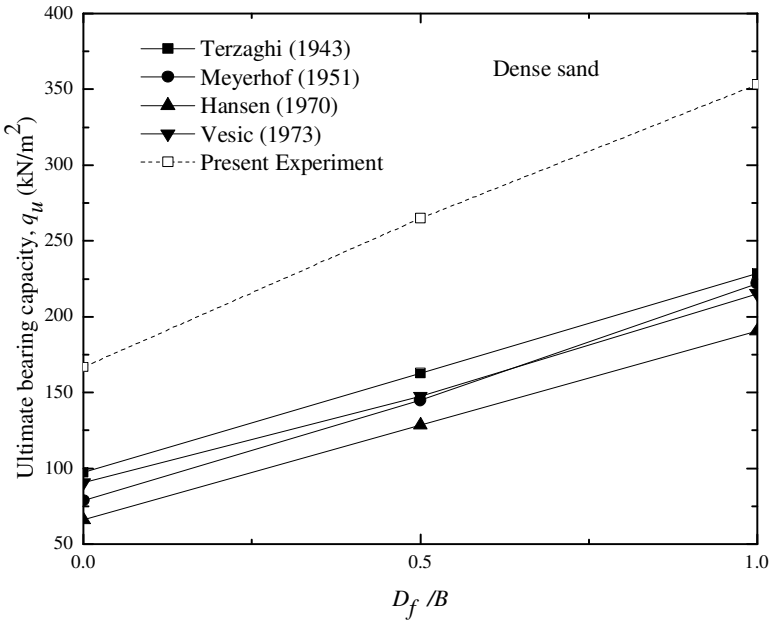

(a)

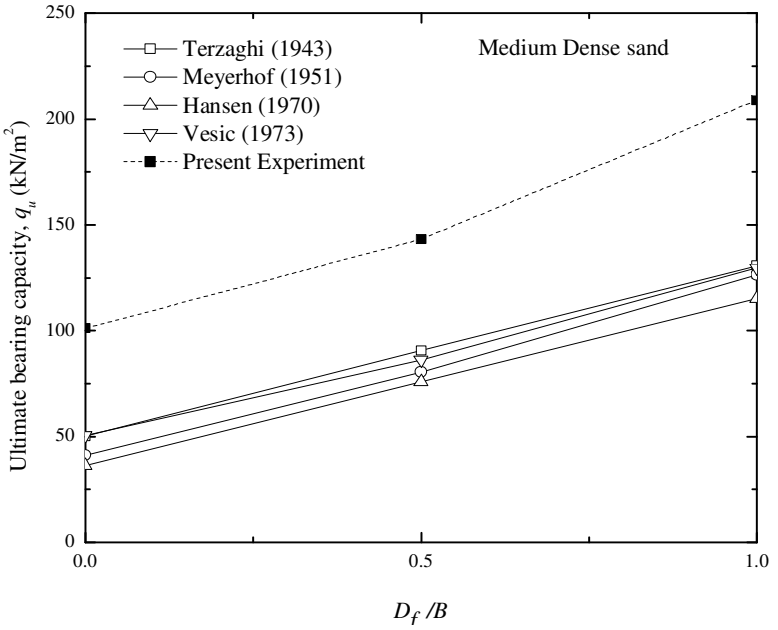

(b)

Figure 4.5: Variation of q_u with D_f/B for $\alpha = 0$ and $e/B = 0$ using formulae of existing theories along with present experimental values for (a) dense (b) medium dense sand

Table 4.4. Calculated values of ultimate bearing capacities q_u by Terzaghi (1943) and Meyerhof (1951) for centric vertical condition along with Present experimental values

Inclination (α)	e/B	D_f/B	Present Experiment; q_u (kN/m^2)		Terzaghi (1943); q_u (kN/m^2)		Meyerhof (1951); q_u (kN/m^2)	
			$\phi = 37.5^0$	$\phi = 40.8^0$	$\phi = 37.5^0$	$\phi = 40.8^0$	$\phi = 37.5^0$	$\phi = 40.8^0$
0	0	0	101.043	166.77	50.25	97.28	40.98	78.94
0	0	0.5	143.226	264.87	90.53	162.87	80.45	144.86
0	0	1	208.953	353.16	130.82	228.45	126.42	222.04

Table 4.5. Calculated values of ultimate bearing capacities q_u by Hansen (1970) and Vesic (1973) for centric vertical condition along with Present experimental values

Inclination (α)	e/B	D_f/B	Present Experiment; q_u (kN/m^2)		Hansen (1970); q_u (kN/m^2)		Vesic (1973); q_u (kN/m^2)	
			$\phi = 37.5^0$	$\phi = 40.8^0$	$\phi = 37.5^0$	$\phi = 40.8^0$	$\phi = 37.5^0$	$\phi = 40.8^0$
0	0	0	101.043	166.77	36.16	66.03	50.37	90.52
0	0	0.5	143.226	264.87	75.78	128.43	86.21	147.56
0	0	1	208.953	353.16	115.40	190.82	129.60	215.32

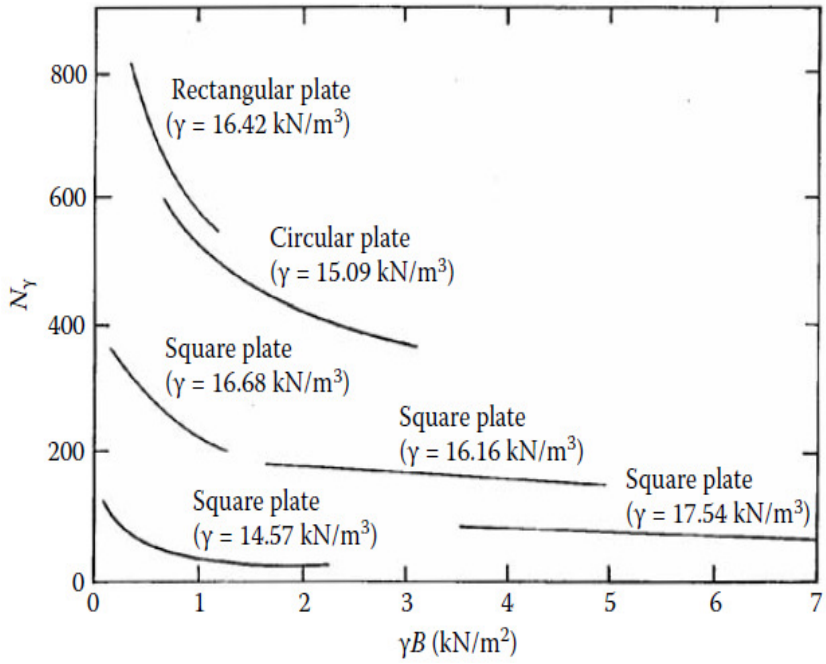

Figure 4.6: Variation of N_γ with γB (adapted after DeBeer, 1965)

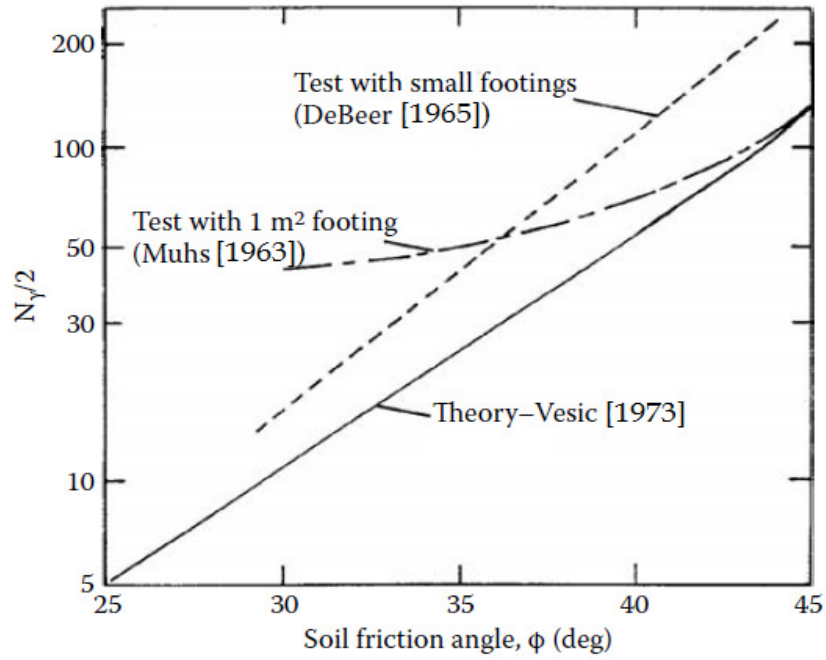

Figure 4.7: Comparison of N_γ obtained from tests with small footings and large footings of 1m² area on sand (adapted after DeBeer, 1965).

The observed failure surface for footing resting on dense sand in centric vertical condition (i.e. D_f/B=0, α=0, e/B=0) is shown in Figure 4.8. Up to a depth of B the effect of applied load is prominent beyond that it gradually decreases and at a depth of $2B$ it almost diminishes.

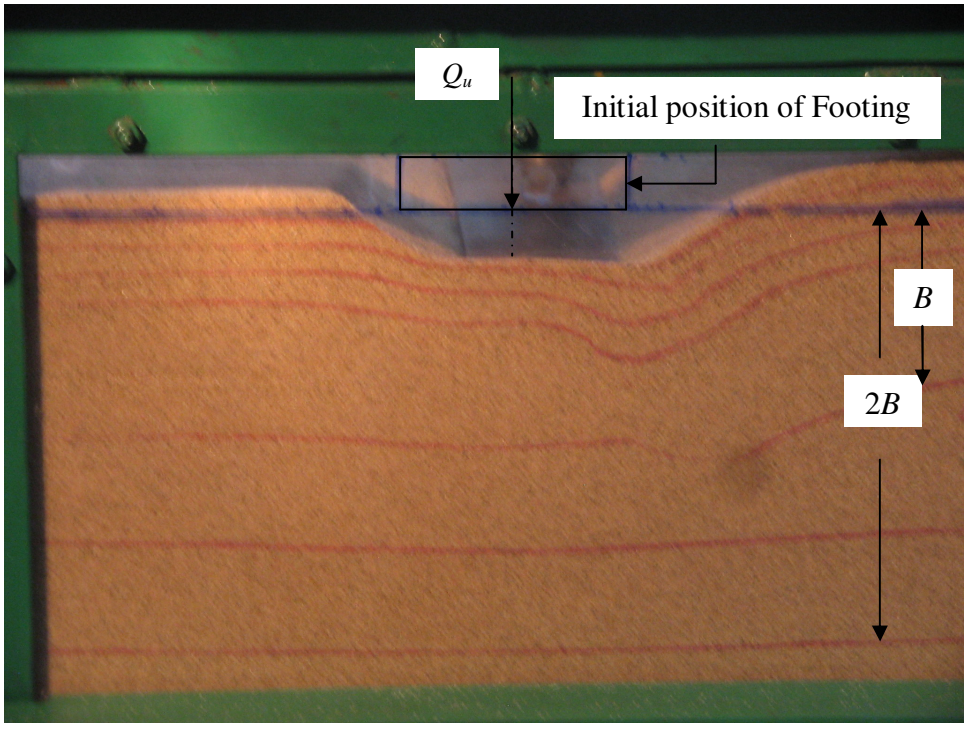

Figure 4.8: Photographic image of failure surface observed in dense sand in surface condition at $D_f/B = 0$, $\alpha = 0°$ and $e/B = 0$

4.3.2 Eccentric Vertical Loading Conditions

Twenty four numbers of model tests are conducted in eccentric vertical condition. The details of the test parameters are shown in Table 4.6. The load settlement curves of strip foundations ($\alpha = 0$ and e/B = 0, 0.05, 0.1 and 0.15) on dense sand in surface condition are plotted in Figure 4.9. The load carrying capacity decreases with increase in e/B ratio. Similarly, Figures 4.10 and 4.11 show the variation of load-settlement curve with depth of embedment (D_f/B) and relative density of sand respectively.

Table 4.6. Model test parameters for the case of Eccentric Vertical Loading condition

Sand type	Unit weight of compaction (kN/m³)	Relative density of sand (%)	Friction angle ϕ – direct shear test (degree)	$\frac{D_f}{B}$	$\frac{e}{B}$	Load Inclination, α (degree)
Dense	14.36	69	40.8	0 0.5 1.0	0 0.05 0.1 0.15	0
Medium dense	13.97	51	37.5	0 0.5 1.0	0 0.05 0.1 0.15	0

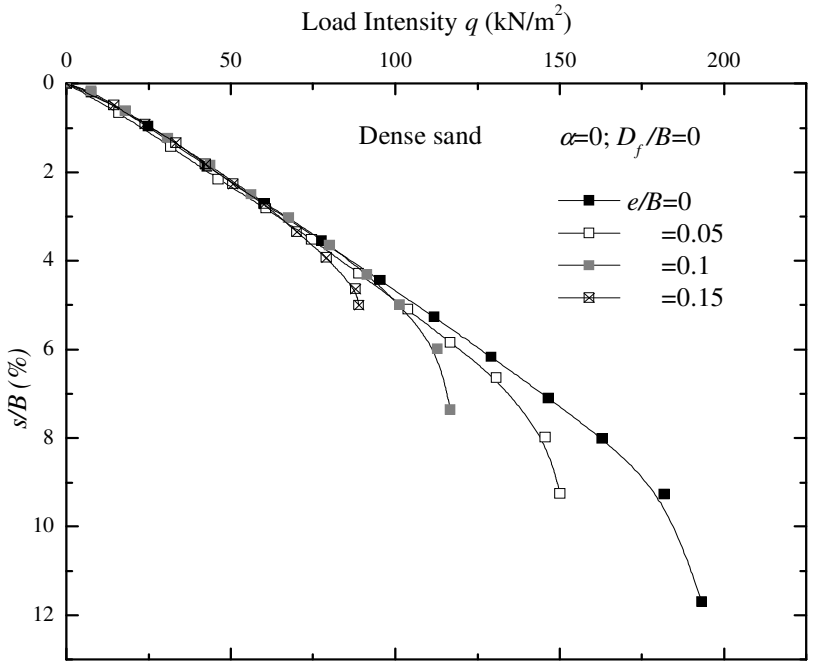

Figure 4.9: Variation of load-settlement curve with eccentricity in Dense sand in surface condition for α=0

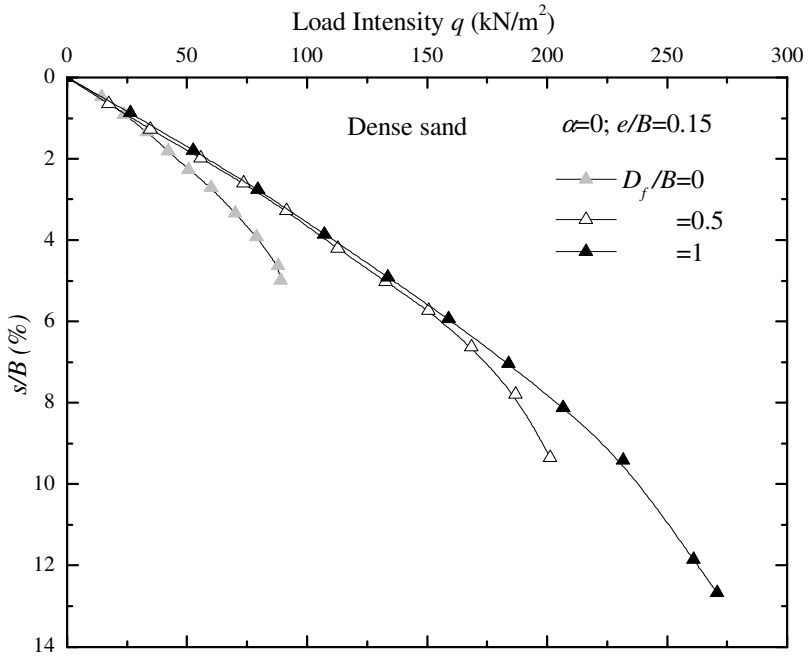

Figure 4.10: Effect of embedment on eccentricity in Dense sand for α=0, e/B=0.15

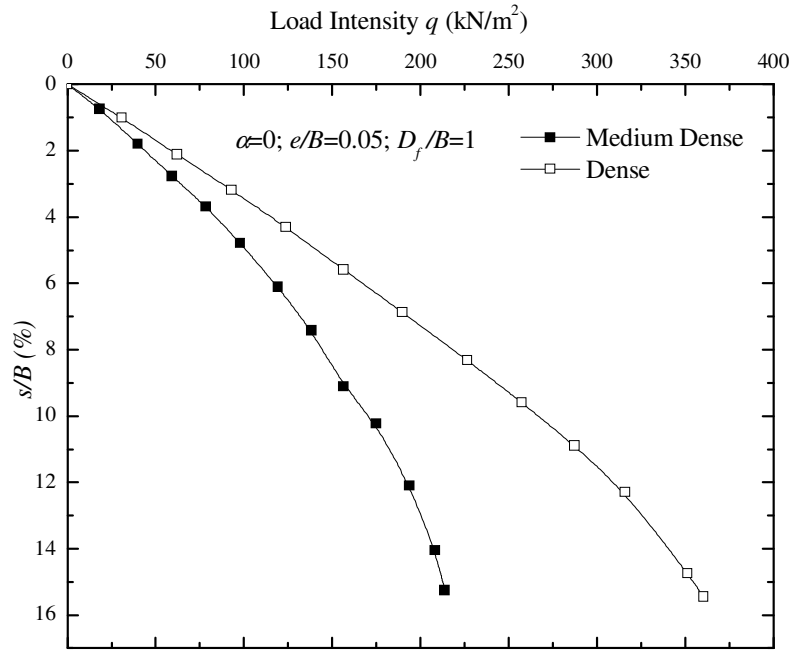

Figure 4.11: Variation of load settlement curve with relative density for α=0, e/B=0.05 and D_f/B=1

The experimental ultimate bearing capacities for eccentrically loaded foundations (e/B = 0, 0.05, 0.1 and 0.15, D_f/B = 0, 0.5 and 1, and D_r = 69%, 51%) are plotted along with the bearing capacities obtained by using Meyerhof's effective area method (Eq. 2.5). This is shown in Figure 4.12 and Table 4.7. The nature of decrease of bearing capacity with the increase in eccentricity as observed from experimental results are in good agreement with those using Meyerhof's method (1953).

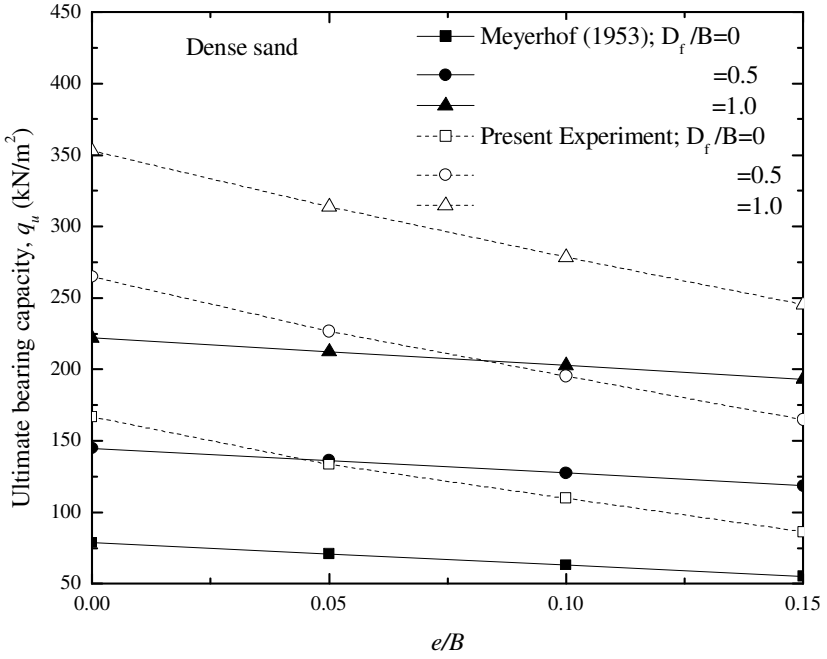

(a)

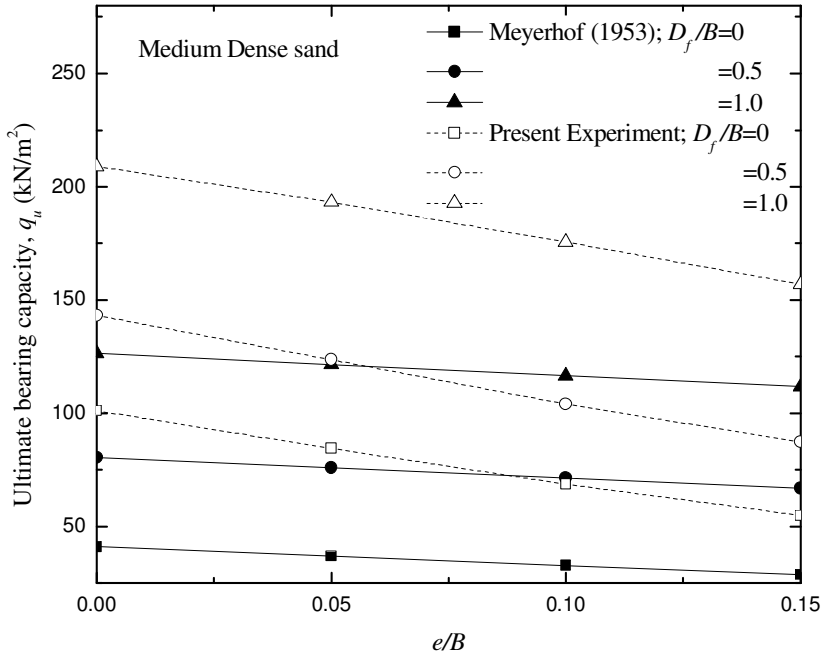

(b)

Figure 4.12: Comparison of ultimate bearing capacities of Present experimental results with Meyerhof's effective area method (1953) for (a) dense and (b) medium dense sand

Table 4.7. Calculated values of ultimate bearing capacities (q_u) by Meyerhof (1953) for eccentric vertical condition along with Present experimental values

Inclination (α)	e/B	D_f/B	Present Experiment; q_u (kN/m^2)		Meyerhof (1953); q_u (kN/m^2)		Variation (%)	
			ϕ =37.5^0	ϕ =40.8^0	ϕ =37.5^0	ϕ =40.8^0	ϕ =37.5^0	ϕ =40.8^0
0	0	0	101.043	166.77	40.98	78.94	-146.6	-111.3
0	0.05	0	84.366	133.416	36.88	71.05	-128.8	-87.8
0	0.1	0	68.67	109.872	32.78	63.15	-109.5	-74.0
0	0.15	0	54.936	86.328	28.69	55.26	-91.5	-56.2
0	0	0.5	143.226	264.87	80.45	144.86	-78.0	-82.8
0	0.05	0.5	123.606	226.611	75.94	136.10	-62.8	-66.5
0	0.1	0.5	103.986	195.219	71.43	127.35	-45.6	-53.3
0	0.15	0.5	87.309	164.808	66.91	118.59	-30.5	-39.0

Inclination (α)	e/B	D_f/B	Present Experiment; q_u (kN/m^2)		Meyerhof (1953); q_u (kN/m^2)		Variation (%)	
0	0	1	208.953	353.16	126.42	222.04	-65.3	-59.1
0	0.05	1	193.257	313.92	121.50	212.43	-59.1	-47.8
0	0.1	1	175.599	278.604	116.57	202.81	-50.6	-37.4
0	0.15	1	156.96	245.25	111.64	193.20	-40.6	-26.9

The ultimate bearing capacities (ubc) are obtained by using digitized values of $N_{q(e)}$ and $N_{\gamma(e)}$ *for* $\phi = 37.5^0$ as given by Prakash and Saran (1971). These ubc values have been compared with those obtained experimentally (Figure 4.13). The comparison is also shown in Table 4.8. From the figure it is found that the nature of variation of ubc with eccentricity is same as observed in experiment.

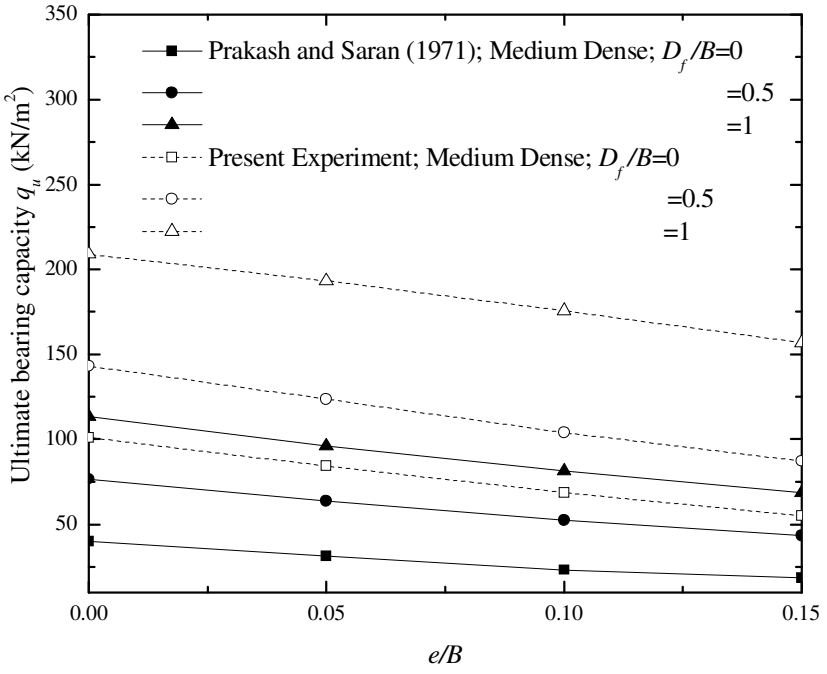

Figure 4.13: Comparison of Present experimental results with Prakash and Saran (1971) for medium dense sand

Table 4.8. Calculated values of ultimate bearing capacities (q_u) by Prakash and Saran (1971) for eccentric vertical condition along with Present experimental values for medium dense sand

Inclination (α)	e/B	D_f/B	Present Experiment; q_u (kN/m^2)	Prakash and Saran (1971); q_u (kN/m^2)	% Variation
			$\phi=37.5^0$	$\phi=37.5^0$	
0	0	0	101.043	39.88	60.5
0	0.05	0	84.366	31.29	62.9
0	0.1	0	68.67	23.26	66.1
0	0.15	0	54.936	18.44	66.4
0	0	0.5	143.226	76.69	46.5
0	0.05	0.5	123.606	63.63	48.5
0	0.1	0.5	103.986	52.32	49.7
0	0.15	0.5	87.309	43.44	50.2
0	0	1	208.953	113.50	45.7
0	0.05	1	193.257	95.97	50.3
0	0.1	1	175.599	81.37	53.7
0	0.15	1	156.96	68.45	56.4

Using Eqs. (2.8) and (2.9) and Table 2.3, the experimental reduction factor (*RF*) and theoretical reduction factor (*RF*) given by Purkayastha and Char (1977) are presented in Figure 4.14 and Table 4.9. The comparisons of reduction factor obtained from two approaches are reasonably good.

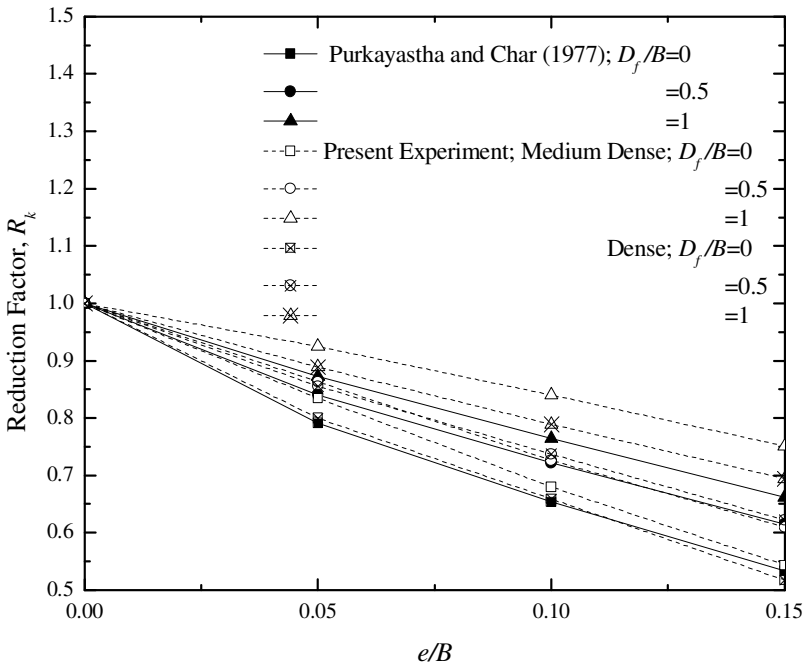

Figure 4.14: Comparison of Present experimental results with Purkayastha and Char (1977)

Table 4.9. Calculated values of R_k by Purkayastha and Char (1977) for eccentric vertical condition along with Present experimental values

Inclination (α)	e/B	D_f/B	Present Experiment; R_k		Purkayastha and Char (1977); R_k
			$\phi = 37.5^0$	$\phi = 40.8^0$	
0	0	0	1.00	1.00	1.00
0	0.05	0	0.83	0.80	0.79
0	0.1	0	0.68	0.66	0.65
0	0.15	0	0.54	0.52	0.53
0	0	0.5	1.00	1.00	1.00
0	0.05	0.5	0.86	0.86	0.84
0	0.1	0.5	0.73	0.74	0.72
0	0.15	0.5	0.61	0.62	0.62
0	0	1	1.00	1.00	1.00
0	0.05	1	0.92	0.89	0.87
0	0.1	1	0.84	0.79	0.76
0	0.15	1	0.75	0.69	0.66

Similarly, Loukidis et al. (2008) proposed an equation based on finite element method. The ultimate bearing capacities are calculated using Eq. 2.37 and plotted in Figure 4.15 along with present experimental values for surface condition. The comparisons have also been shown in Table 4.10.

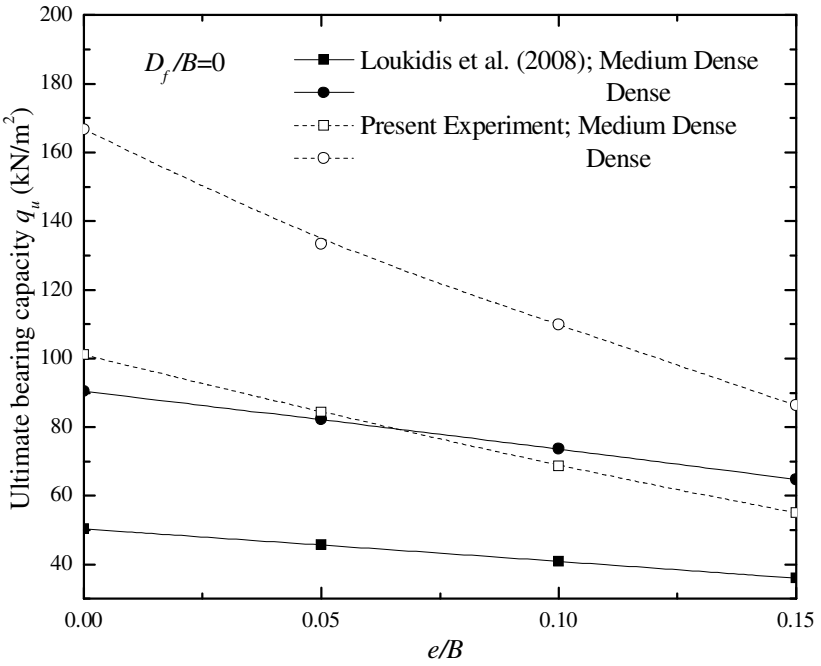

Figure 4.15: Comparison of Present experimental results with Loukidis et al. (2008)

Table 4.10. Calculated values of ultimate bearing capacities q_u by Loukidis et al. (2008) for eccentric vertical condition along with Present experimental values

Inclination (α)	e/B	D_f/B	Present Experiment; q_u (kN/m^2)		Loukidis et al. (2008); q_u (kN/m^2)	
			$\phi = 37.5^0$	$\phi = 40.8^0$	$\phi = 37.5^0$	$\phi = 40.8^0$
0	0	0	101.043	166.77	50.37	90.52
0	0.05	0	84.366	133.416	45.73	82.19
0	0.1	0	68.67	109.872	40.98	73.65
0	0.15	0	54.936	86.328	36.08	64.85

Figure 4.16 shows the observed failure surface for eccentrically loaded footing (i.e. D_f /B=0, α=0, e/B=0.15) where the tilting of the footing occurs at the time of failure which is due to load eccentricity.

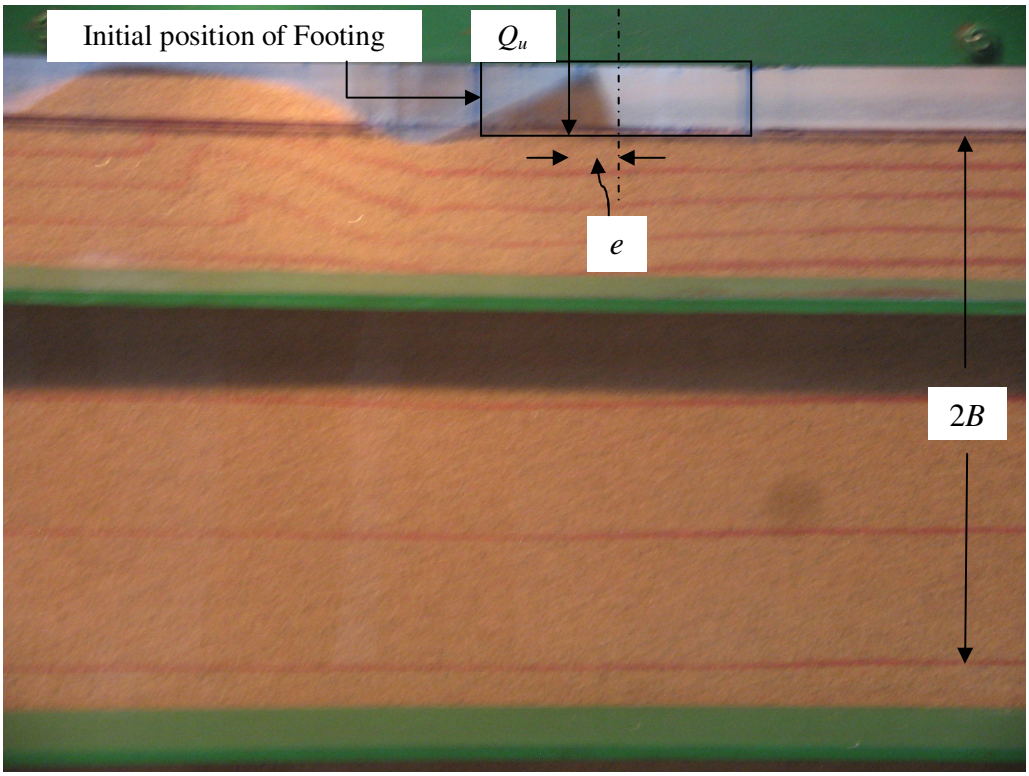

Figure 4.16: Photographic image of failure surface observed in medium dense sand in surface condition at $D_f/B = 0$, $\alpha = 0°$ and $e/B = 0.15$

4.3.3 Centric Inclined Loading Condition

Thirty numbers of model tests are conducted as per Figure 2.3. The detailed parameters are mentioned in Table 4.11. Figures 4.17 and 4.18 show the variation of load intensity vs. s/B at various load inclination in surface condition for both dense and medium dense sand respectively. Most of the curves appear to be local shear failure type as given by Vesic (1973). It is seen from graphs for both dense and medium dense sand that at any embedment ratio (D_f /B), the load carrying capacity decreases with increase in load

inclination. Similarly, Figures 4.19 and 4.20 show the variation of ubc with embedment ratio (D_f /B) and relative density (D_r) of sand respectively. As the embedment ratio (D_f /B) increases the load carrying capacity increases. Similarly, with increase in relative density of sand the ultimate bearing capacity increases.

Table 4.11. Model test parameters for the case of Centric Inclined Loading condition

Sand type	Unit weight of compaction (kN/m³)	Relative density of sand (%)	Friction angle ϕ – direct shear test (degree)	$\frac{D_f}{B}$	$\frac{e}{B}$	Load Inclination, α (degree)
Dense	14.36	69	40.8	0 0.5 1.0	0	0 5 10 15 20
Medium dense	13.97	51	37.5	0 0.5 1.0	0	0 5 10 15 20

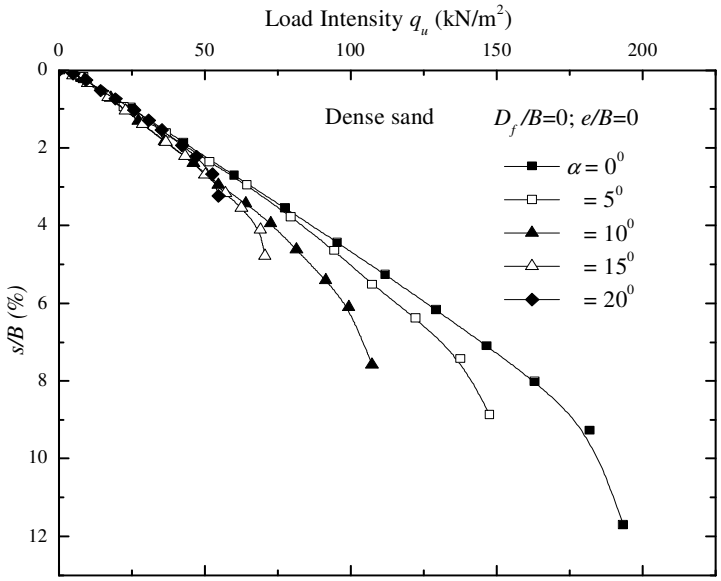

Figure 4.17: Variation of load settlement curve with load inclination (α) in dense sand for D_f /B=0 and e/B=0

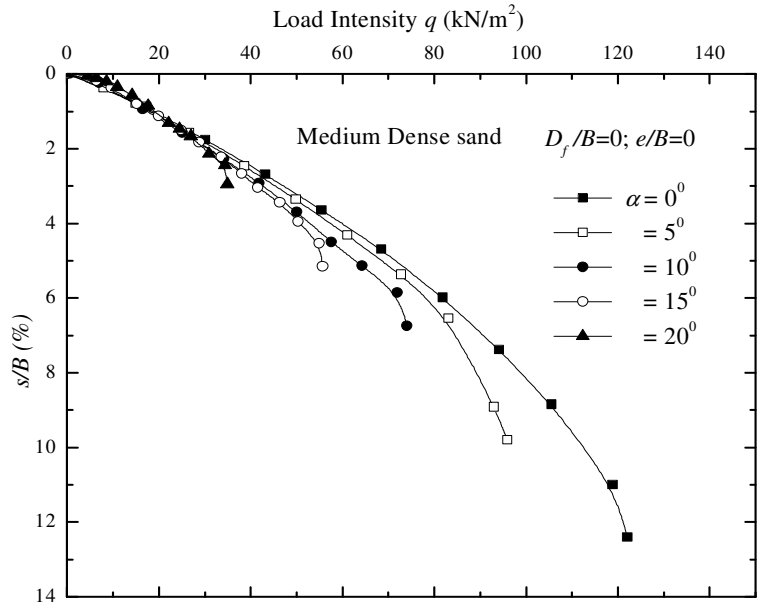

Figure 4.18: Variation of load-settlement curve with load inclination (α) in medium dense sand for D_f/B=0 and e/B=0

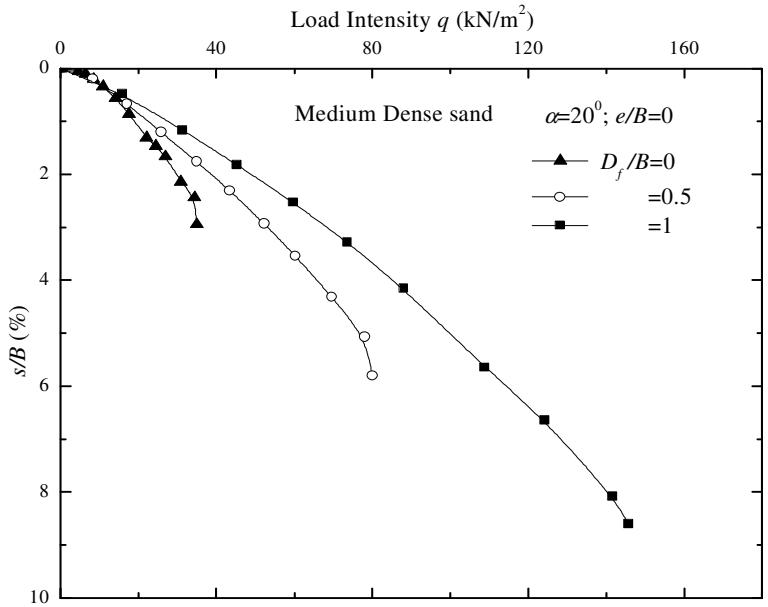

Figure 4.19: Variation of load-settlement curve with embedment ratio (D_f/B) in medium dense sand for α=20^0, e/B=0

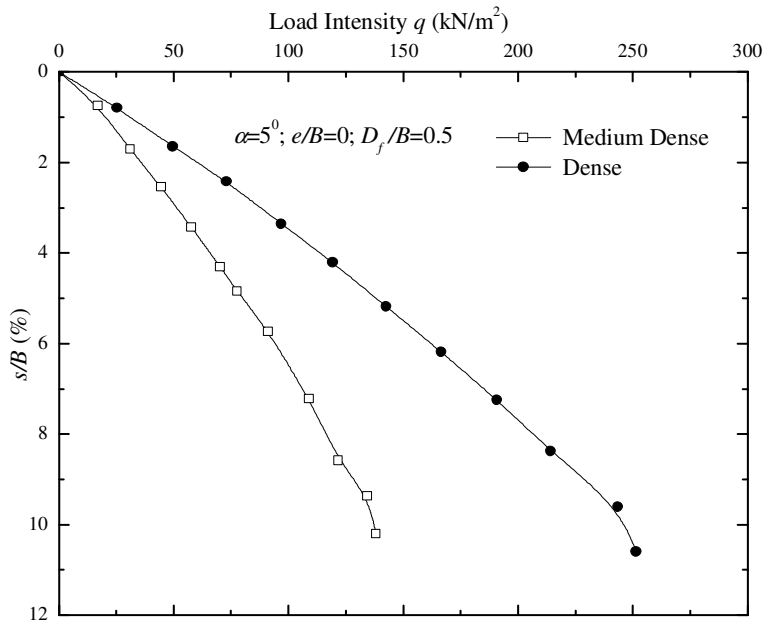

Figure 4.20: Variation of load-settlement curve with relative density of sand at $\alpha=5^0$, $e/B=0$ and $D_f/B=0.5$,

A comparison of the nature of variation of ultimate bearing capacities obtained from the experiment and those computed using various existing theories have been made and explained below. It is to be noted that in existing theories, q_u denotes the vertical component of the inclined load, whereas in the present experimentation, q_u is considered as inclined load. So, in order to compare experimental values with the values obtained using various theories present experimental value of q_u is multiplied with cosα (α is the load inclination with the vertical).

The ultimate bearing capacity values are calculated using Eqs. 2.14 through 2.16 as given by Meyerhof (1963) for centric inclined load and compared with experimental bearing capacities. The comparison is shown in Figure 4.21.

The bearing capacity values have been calculated using Eqs. 2.17 and 2.19 as proposed by Hansen (1970). As per Vesic (1975), the ubc have been calculated by using Eqs. 2.25

and 2.26. The calculated bearing capacity values as per Hansen (1970) and Vesic (1975) are shown in Figures 4.22 and 4.23 respectively along with experimental values. The above comparison is also shown in Table 4.12. The experimental values are higher than those obtained using equations proposed by Hansen (1970) and Vesic (1975). As has been pointed out by several investigators in the past, this is not very unusual primarily due to the inherent difficulty in establishing the proper magnitude of ϕ for bearing capacity calculations.

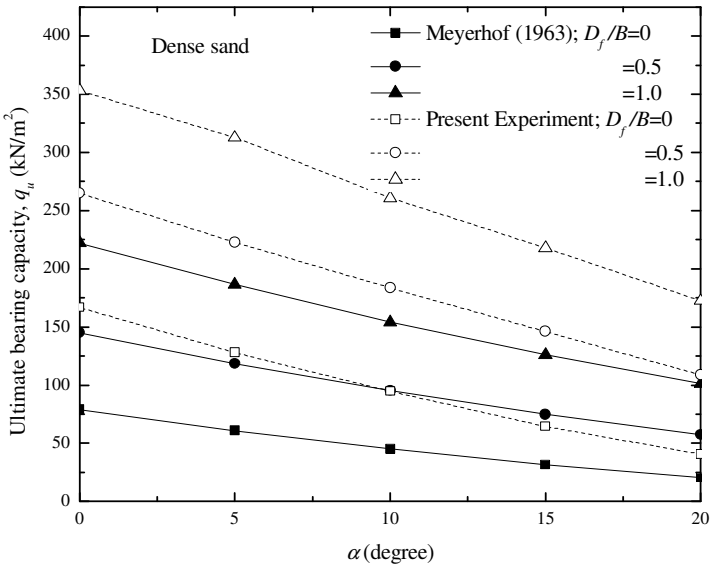

(a)

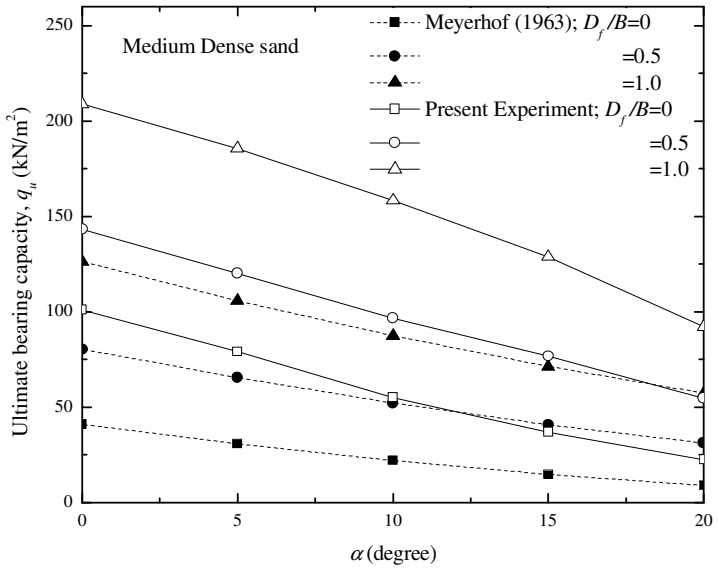

(b)

Figure 4.21: Comparison of ultimate bearing capacities of Present experimental results with Meyerhof (1963) for (a) dense sand and (b) medium dense sand

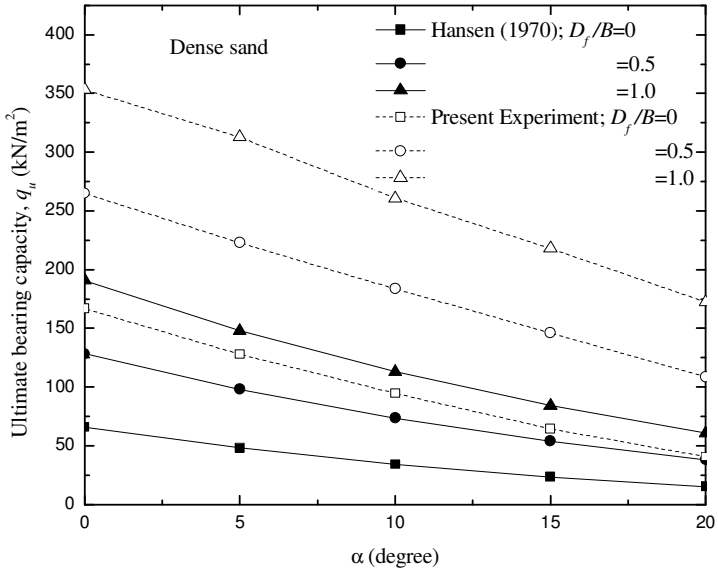

(a)

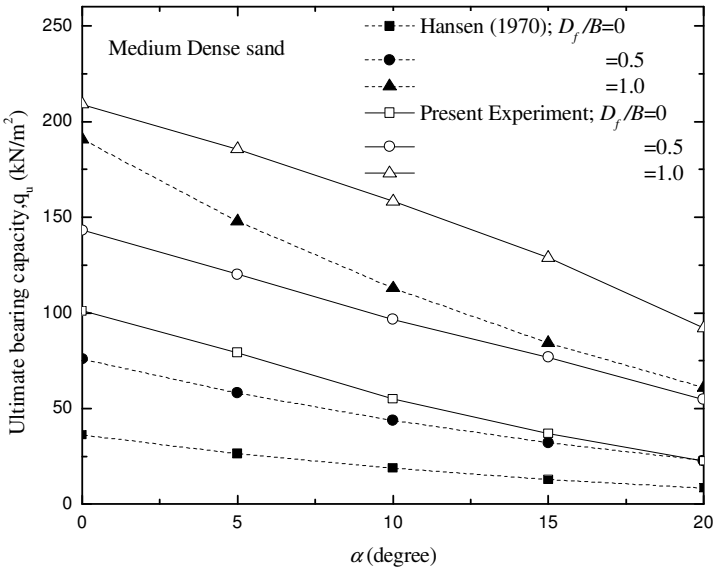

(b)

Figure 4.22: Comparison of ultimate bearing capacities of Present experimental results with Hansen (1970) for (a) dense sand and (b) medium dense sand

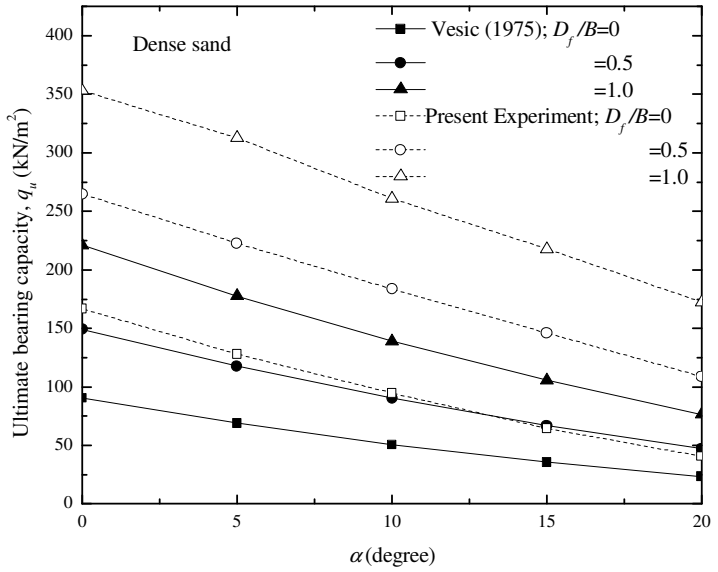

(a)

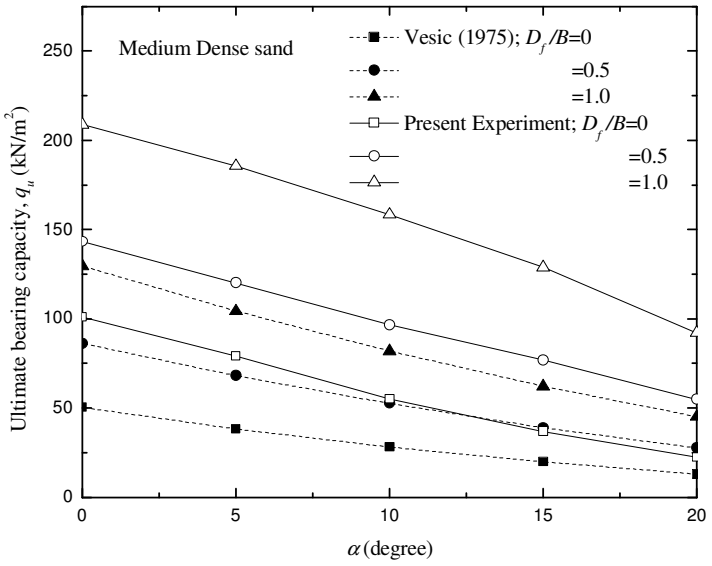

(b)

Figure 4.23: Comparison of ultimate bearing capacities of Present experimental results with Vesic (1975) for (a) dense sand and (b) medium dense sand

Table 4.12. Calculated values of ultimate bearing capacities (q_u) by using formulae of existing theories for centric inclined condition along with Present experimental values

Inclination (α)	e/B	D_f/B	Present Experiment; $q_u \cos\alpha$ (kN/m^2)		Meyerhof (1963); q_u (kN/m^2)		Hansen (1970) ;q_u (kN/m^2)		Vesic (1975); q_u (kN/m^2)	
			$\phi = 37.5^0$	$\phi = 40.8^0$	$\phi = 37.5^0$	$\phi = 40.8^0$	$\phi = 37.5^0$	$\phi = 40.8^0$	$\phi = 37.5^0$	$\phi = 40.8^0$
0	0	0	101.043	166.770	40.98	78.94	36.16	66.03	50.37	90.52
5	0	0	79.159	128.022	30.78	60.78	26.37	48.15	38.28	68.79
10	0	0	55.068	94.679	22.04	44.99	18.72	34.18	28.15	50.60
15	0	0	36.957	64.437	14.75	31.57	12.81	23.38	19.77	35.53
20	0	0	22.586	40.564	8.92	20.52	8.32	15.19	12.97	23.31
0	0	0.5	143.226	264.870	80.45	144.86	75.78	128.43	86.21	149.03
5	0	0.5	120.204	222.818	65.41	118.52	58.05	98.05	68.13	117.51
10	0	0.5	96.611	183.561	52.18	95.17	43.70	73.53	52.48	90.30
15	0	0.5	76.756	145.931	40.78	74.81	32.12	53.79	38.99	66.90
20	0	0.5	54.761	108.784	31.20	57.42	22.84	38.06	27.48	47.00
0	0	1	208.953	353.160	126.42	222.04	115.40	190.82	129.60	221.20
5	0	1	185.681	312.727	105.82	186.32	89.73	147.94	104.26	177.61

Inclination (α)	e/B	D_f/B	Present Experiment; $q_u \cos\alpha$ (kN/m^2)		Meyerhof (1963); q_u (kN/m^2)		Hansen (1970) ;q_u (kN/m^2)		Vesic (1975); q_u (kN/m^2)	
10	0	1	158.442	260.850	87.45	154.26	68.68	112.87	81.92	139.27
15	0	1	128.875	217.950	71.31	125.87	51.42	84.20	62.25	105.59
20	0	1	92.190	172.395	57.40	101.14	37.36	60.93	45.04	76.21

Using Eqs. 2.21 and 2.22 as given by Muhs and Weiss (1973) the ratio ($q_{u(v)}/q_{u(\alpha=0)}$) are evaluated and plotted in Figure 4.24 along with experimental values for different load inclination (α=0-20°). The values are shown in Table 4.13. The computed values as per Muhs and Weiss (1973) is in good agreement with experimental values for both dense sand and medium dense sand.

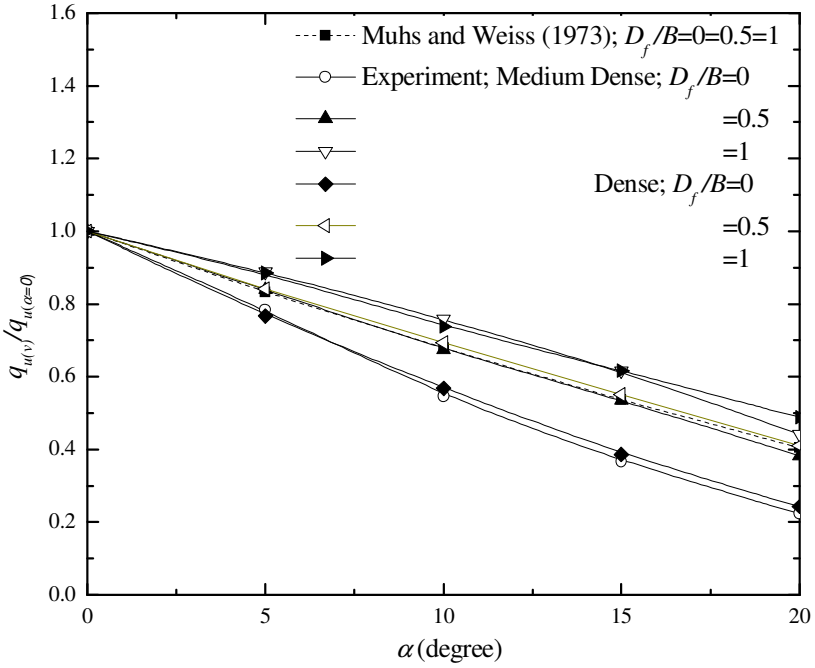

Figure 4.24: Comparison of Present experimental results with Muhs and Weiss (1973)

Table 4.13. Calculated values of Muhs and Weiss (1973) ratio for centric inclined condition along with Present experimental values

Inclination (α)	e/B	D_f/B	Present Experiment		Muhs and Weiss (1973)
			$\phi = 37.5^0$	$\phi = 40.8^0$	$(1-\tan\alpha)^2$
0	0	0	1.00	1.00	1.00
5	0	0	0.78	0.77	0.83
10	0	0	0.54	0.57	0.68
15	0	0	0.37	0.39	0.54
20	0	0	0.22	0.24	0.40
0	0	0.5	1.00	1.00	1.00
5	0	0.5	0.84	0.84	0.83
10	0	0.5	0.67	0.69	0.68
15	0	0.5	0.54	0.55	0.54
20	0	0.5	0.38	0.41	0.40
0	0	1	1.00	1.00	1.00
5	0	1	0.89	0.89	0.83
10	0	1	0.76	0.74	0.68
15	0	1	0.62	0.62	0.54
20	0	1	0.44	0.49	0.40

By using finite element method, Loukidis et al. (2008) proposed an equation for inclination factor as mentioned in Eq. 2.40 for surface footing. The experimental values of ultimate bearing capacity are plotted in Figure 4.25 along with the values obtained by using equations given by Loukidis et al. (2008). The same has been presented in Table 4.14. The nature of variation of bearing capacity with load inclination is in good agreement.

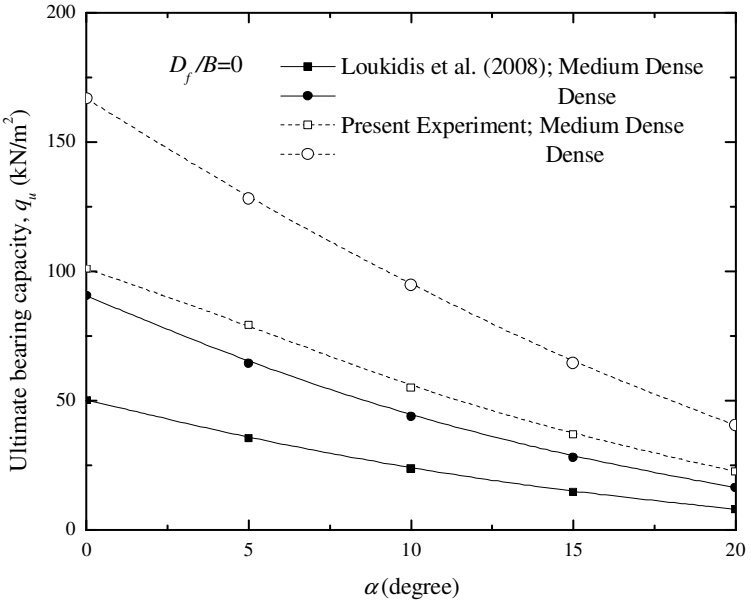

Figure 4.25: Comparison of Present experimental results with Loukidis et al. (2008)

Table 4.14. Calculated values of ultimate bearing capacities by using formula of Loukidis et al. (2008) for centric inclined condition along with Present experimental values

Inclination (α)	e/B	D_f/B	Present Experiment; q_u cosα (kN/m^2)		Loukidis et al. (2008); q_u (kN/m^2)	
			$\phi = 37.5^0$	$\phi = 40.8^0$	$\phi = 37.5^0$	$\phi = 40.8^0$
0	0	0	101.043	166.770	50.37	90.52
5	0	0	79.159	128.022	35.44	64.48
10	0	0	55.068	94.679	23.68	43.95
15	0	0	36.957	64.437	14.67	28.12
20	0	0	22.586	40.564	8.07	16.37

The failure surfaces in all these experiments with centric inclined loading conditions have been observed. Figure 4.26 shows the failure surface as observed for the condition i.e. D_f/B=0, α=20^0, e/B=0. The sliding of the foundation has been observed which is due to horizontal component of the inclined load. It is also seen that the deformation of sand

layer is prominent up to a depth of 0.5B in the vertical direction and laterally up to a distance of near about 2B.

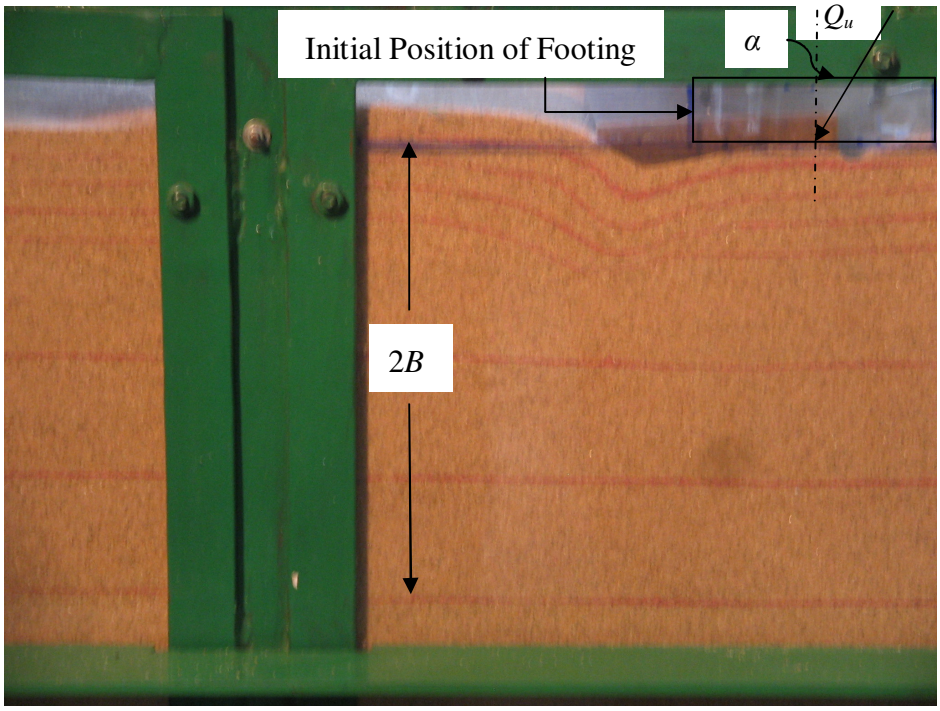

Figure 4.26: Photographic image of failure surface observed in medium dense sand at $D_f/B = 0$, $\alpha = 20°$ and $e/B = 0$

4.3.4 Eccentric Inclined Loading Conditions

Seventy two tests have been conducted with loads applied both eccentric and inclined. The combination of parameters chosen for these experiments is listed in Table 4.13.

Table 4.15. Model test parameters for the case of Eccentric Inclined Loading condition

Sand type	Unit weight of compaction (kN/m³)	Relative density of sand (%)	Friction angle ϕ – direct shear test (degree)	$\frac{D_f}{B}$	$\frac{e}{B}$	Load Inclination, α (degree)
Dense	14.36	69	40.8	0 0.5 1.0	0.05 0.1 0.15	5 10 15 20
Medium dense	13.97	51	37.5	0 0.5	0.05 0.1	5 10

Sand type	Unit weight of compaction (kN/m³)	Relative density of sand (%)	Friction angle ϕ – direct shear test (degree)	$\frac{D_f}{B}$	$\frac{e}{B}$	Load Inclination, α (degree)
				1.0	0.15	15 20

The variation of ubc with load inclination at all embedment ratios and eccentricity ratios for both dense sand and medium dense sand have been observed. Figure 4.27 shows one such plot of the nature of load-settlement curve with load inclination at a particular embedment ratio D_f/B = 0.5 and e/B = 0.05 in medium dense sand. It is seen from the graph that the ultimate bearing capacity decreases with increase in load inclination. This is true for all eccentricities and all depth of embedment. Similarly, the variation of ubc with load eccentricity at all embedment ratios and load inclinations for both dense sand and medium dense sand have been observed. One combination of such plot is shown in Figure 4.28 where the variation of ubc with e/B at a particular embedment ratio D_f/B = 1.0 and $\alpha = 15^0$ in dense sand is presented. It is observed that the ultimate bearing capacity decreases with increase in e/B ratio. The ubc increases with increase in embedment ratio (D_f/B) for all eccentricities and all load inclinations. One such variation of ubc with embedment ratio (D_f/B) at e/B = 0.15 and $\alpha = 20^0$ in medium dense sand is shown in Figure 4.29. It is also observed that the bearing capacity increases with increase in relative density for all combinations of D_f/B, e/B and α. One such plot is shown in Figure 4.30.

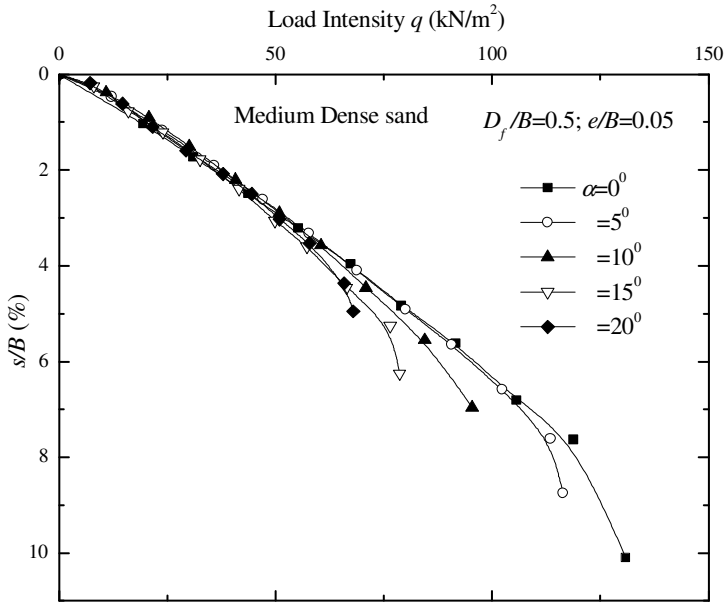

Figure 4.27: Variation of load-settlement curve with load inclination α at D_f/B=0.5 and e/B=0.05 in medium dense sand

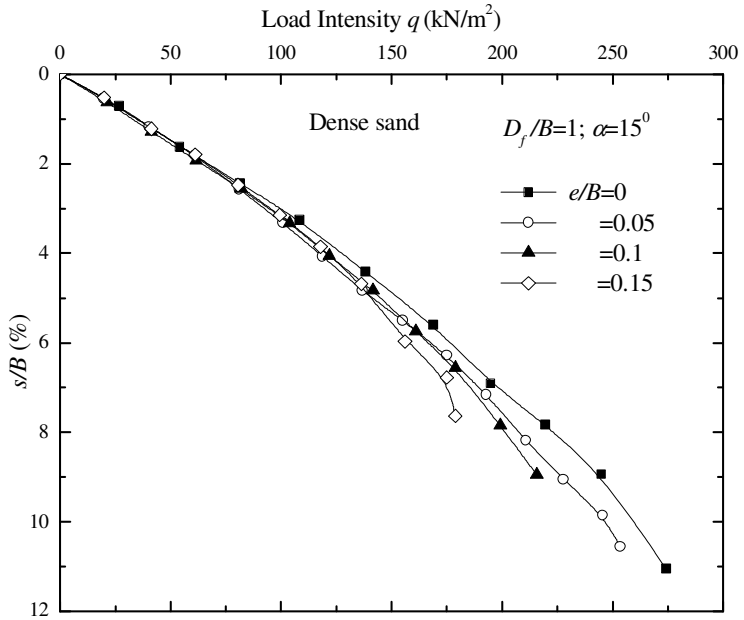

Figure 4.28: Variation of load-settlement curve with e/B at D_f/B=1.0 and α =15^0 in dense sand

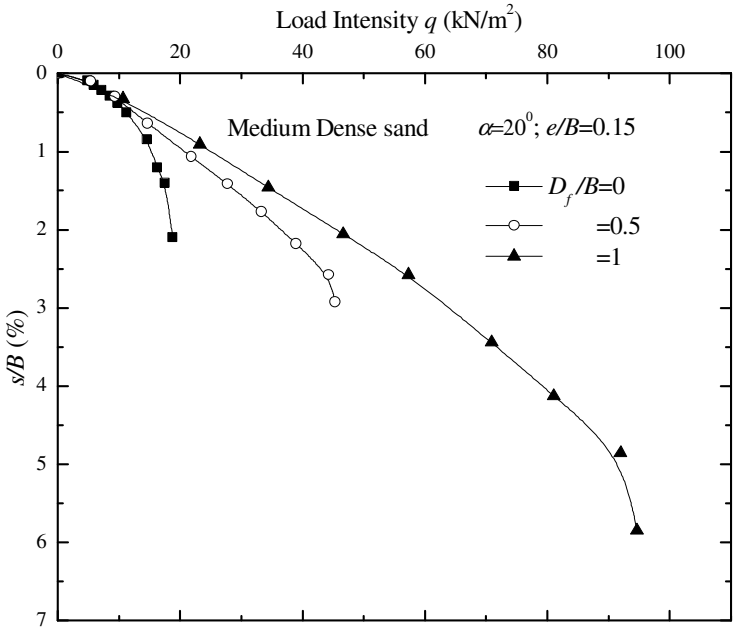

Figure 4.29: Variation of load-settlement curve with embedment ratio (D_f/B) at e/B =0.15 and α =20^0 in medium dense sand

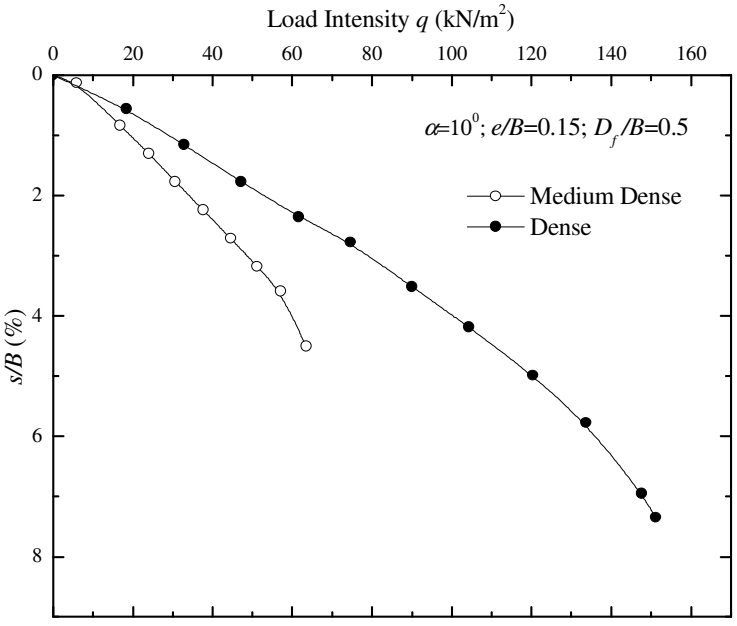

Figure 4.30: Variation of load-settlement curve with Relative Density (D_r) at e/B =0.15, α =10^0 and D_f/B=0.5

Figure 4.31 shows the load arrangement for the test [$D_f/B = 0$, $e/B = 0.15$, and $\alpha = 20^0$]. The photographic images of failure surface developed at ultimate stage for one of the tests is shown in Figure 4.32. From the figure it is observed that the failure surface is significantly developed up to a depth of $0.5B$ below the base of the footing, whereas in case of footing subjected to vertical and centric load the development of the failure surface is seen up to a depth of $1.5B$ (Figure 4.8) from the base of the footing. At the time of failure sliding of the footing occurs along with tilting.

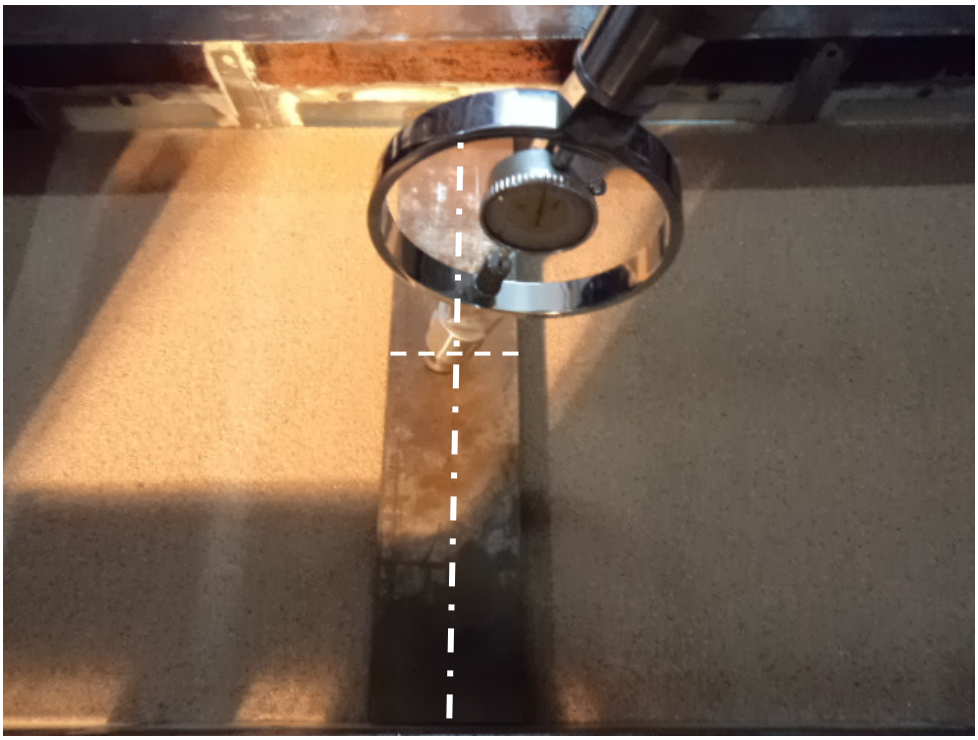

Figure 4.31: Photographic image of load arrangement for the test at $D_f/B = 0$, $\alpha = 20°$ and $e/B = 0.15$

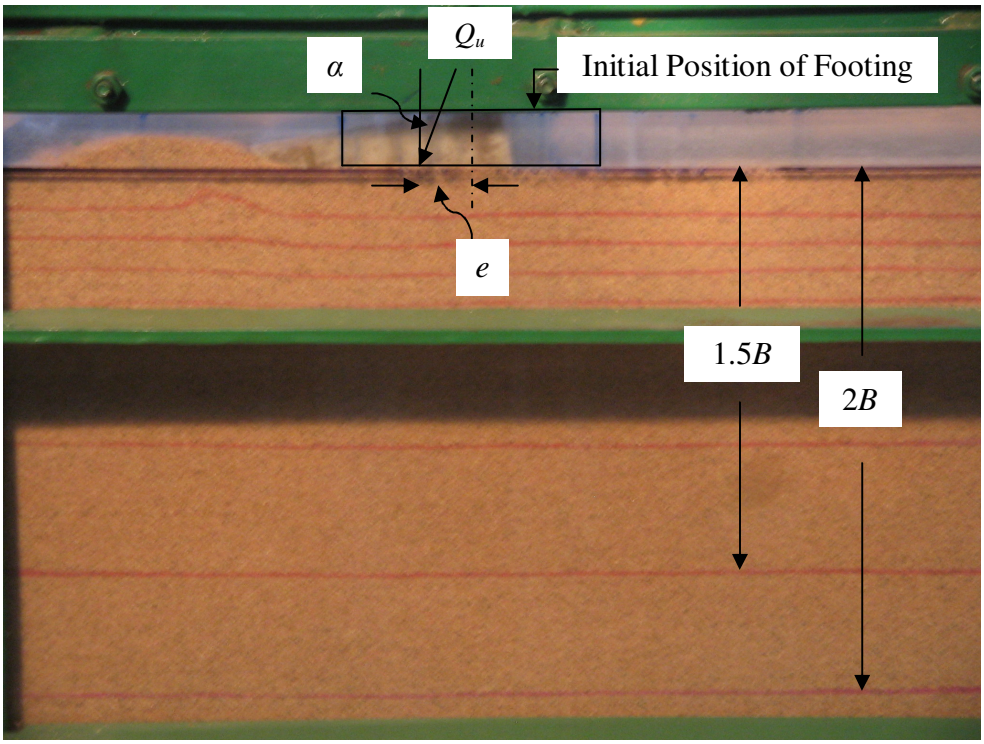

Figure 4.32: Photographic image of the failure surface observed in dense sand at $D_f/B = 0$, $\alpha = 15°$ and $e/B = 0.15$

4.4 Analysis of Test Results

The ultimate bearing capacities of all tests determined from experimental model tests under section 4.3 are given in Table 4.16 (Col. 5) for ready reference. As discussed in section 4.1, in order to quantify certain parameters like $e/B, \alpha, D_f/B$, and D_r all the model test results have been analysed using Nonlinear Regression Analysis Program (NLREG). NLREG performs statistical regression analysis to estimate the values of parameters for linear, multivariate, polynomial, logistic, exponential, and general nonlinear functions. The regression analysis determines the values of the coefficients that cause the function to best fit the observed data that is being provided. The reduction factor concept as discussed in section 4.1 use the proposed Eqs. 4.4 and 4.5 to predict the ultimate bearing

capacity of shallow foundation subjected to eccentric and inclined load. The following procedure is adopted to analyse the test results and develop the reduction factor when the line of load application is towards the center line of the footing.

Step 1: For vertical loading conditions (i.e. α=0), Eq. (4.5) takes the form

$$RF = \left[1 - a\left(\frac{e}{B}\right)^m\right] \tag{4.6}$$

With α = 0 and, for a given D_f /B and given sand type (i.e. dense or medium dense), regression analyses is performed to obtain the magnitudes of a and m.

Step 2: Using the values of a and m obtained in Step 1 and Eq. (4.5), for a given D_f /B and sand type, a regression analysis is performed to obtain the value of n for $\alpha > 0°$.

The values of a, m and n obtained from analyses described above are shown in Table 4.17. It can be seen from Table 4.17 that the variations of a and m with D_f /B are very minimal; however, the value of n decreases with the increase in embedment ratio. The average values of a and m are 2.14 and 0.92 respectively.

Considering the uncertainties involved in any experimental evaluation of ultimate bearing capacity, we can assume without loss of much accuracy

$$a \approx 2 \tag{4.7}$$

$$m \approx 1 \tag{4.8}$$

$$n \approx 2 - \left(\frac{D_f}{B}\right) \tag{4.9}$$

The experimental values of *RF* defined by Eq. (4.4) are shown in Col. 6 of Table 4.16. In computing the experimental *RF* values, the first row of values for both dense and medium dense sands (where $D_f/B = 0$, $\alpha = 0$ and $e/B = 0$) are used as the reference values (i.e. denominator). For comparison purposes, the predicted values of the reduction factor *RF* obtained using Eqs. (4.5), (4.7), (4.8) and (4.9) are shown in Col. 7 of Table 4.16. The deviations of the predicted values of *RF* from those obtained experimentally are shown in Col. 8 of Table 4.16. In most cases the deviations are ±15% or less; however, in some cases, the deviations are 25 to 30%. Thus Eqs. (4.5), (4.7), (4.8) and (4.9) provide a reasonable good and simple approximation to estimate the ultimate bearing capacity of strip foundations ($0 \le D_f/B \le 1$) subjected to eccentric inclined loading. Or

$$q_{u(D_f/B,\, e/B,\, \alpha/\phi)} = q_{u(D_f/B,\, e/B=0,\, \alpha/\phi=0)} \left[1 - 2\left(\frac{e}{B}\right)\right]\left(1 - \frac{\alpha}{\phi}\right)^{2-(D_f/B)} \qquad (4.10)$$

Table 4.16. Model test results

Sand type (1)	$\frac{D_f}{B}$ (2)	α (deg) (3)	$\frac{e}{B}$ (4)	Experimental q_u (kN/m^2) (5)	Experimental *RF* [Eq. (4.4)] (6)	Calculated *RF* [Eqs. 4.5, 4.7, 4.8, and 4.9] (7)	Deviation—$\frac{\text{Col. 7} - \text{Col. 6}}{\text{Col. 7}}$ (%) (8)
Dense	0	0	0	**166.77**	1.0	1	0
	0	0	0.05	133.42	0.8	0.9	11.11
	0	0	0.1	109.87	0.659	0.8	17.65
	0	0	0.15	86.33	0.518	0.7	26.05
	0	5	0	128.51	0.771	0.77	-0.09
	0	5	0.05	103.01	0.618	0.693	10.86
	0	5	0.1	86.33	0.518	0.616	15.96
	0	5	0.15	65.73	0.394	0.539	26.87
	0	10	0	96.14	0.576	0.570	-1.16
	0	10	0.05	76.52	0.459	0.513	10.54
	0	10	0.1	62.78	0.376	0.456	17.42
	0	10	0.15	51.99	0.312	0.399	21.85
	0	15	0	66.71	0.4	0.4	-0.03

Table 4.16 (Continued)

Sand type (1)	$\frac{D_f}{B}$ (2)	α (deg) (3)	$\frac{e}{B}$ (4)	Experimental q_u (kN/m^2) (5)	Experimental RF [Eq. (4.4)] (6)	Calculated RF [Eqs. 4.5, 4.7, 4.8, and 4.9] (7)	Deviation—$\frac{\text{Col. 7} - \text{Col. 6}}{\text{Col. 7}}$ (%) (8)
	0	15	0.05	53.96	0.324	0.36	10.1
	0	15	0.1	44.15	0.265	0.32	17.25
	0	15	0.15	35.12	0.211	0.28	24.77
	0	20	0	43.16	0.259	0.26	0.41
	0	20	0.05	34.83	0.209	0.234	10.72
	0	20	0.1	29.43	0.176	0.208	15.13
	0	20	0.15	23.54	0.141	0.182	22.4
	0.5	0	0	264.87	1.0	1.0	0
	0.5	0	0.05	226.61	0.856	0.9	4.94
	0.5	0	0.1	195.22	0.737	0.8	7.87
	0.5	0	0.15	164.81	0.622	0.7	11.11
	0.5	5	0	223.67	0.844	0.822	-2.74
	0.5	5	0.05	193.26	0.73	0.74	1.37
	0.5	5	0.1	165.79	0.626	0.658	4.81
	0.5	5	0.15	140.28	0.530	0.575	7.95
	0.5	10	0	186.39	0.704	0.656	-7.29
	0.5	10	0.05	160.88	0.607	0.59	-2.9
	0.5	10	0.1	137.34	0.519	0.525	1.18
	0.5	10	0.15	116.74	0.441	0.459	4
	0.5	15	0	151.07	0.57	0.503	-13.43
	0.5	15	0.05	129.49	0.489	0.453	-8.03
	0.5	15	0.1	111.83	0.422	0.402	-4.96
	0.5	15	0.15	94.18	0.356	0.352	-1.01
	0.5	20	0	115.76	0.437	0.364	-20.06
	0.5	20	0.05	98.1	0.37	0.328	-13.05
	0.5	20	0.1	85.35	0.322	0.291	-10.65
	0.5	20	0.5	72.59	0.274	0.255	-7.56
	1.0	0	0	353.16	1.0	1.0	0
	1.0	0	0.05	313.92	0.889	0.9	1.23
	1.0	0	0.1	278.6	0.789	0.8	1.39
	1.0	0	0.15	245.25	0.694	0.7	0.79
	1.0	5	0	313.92	0.889	0.877	-1.3
	1.0	5	0.05	277.62	0.786	0.79	0.46
	1.0	5	0.1	241.33	0.683	0.702	2.65
	1.0	5	0.15	215.82	0.611	0.614	0.51
	1.0	10	0	264.87	0.750	0.755	0.65
	1.0	10	0.05	239.36	0.678	0.679	0.24
	1.0	10	0.1	212.88	0.603	0.604	0.19
	1.0	10	0.15	188.35	0.533	0.528	-0.93

Table 4.16 (Continued)

Sand type (1)	$\frac{D_f}{B}$ (2)	α (deg) (3)	$\frac{e}{B}$ (4)	Experimental q_u (kN/m^2) (5)	Experimental RF [Eq. (4.4)] (6)	Calculated RF [Eqs. 4.5, 4.7, 4.8, and 4.9] (7)	Deviation—$\frac{\text{Col. 7} - \text{Col. 6}}{\text{Col. 7}}$ (%) (8)
	1.0	15	0	225.63	0.639	0.632	-1.03
	1.0	15	0.05	206.01	0.583	0.569	-2.5
	1.0	15	0.1	179.52	0.508	0.506	-0.48
	1.0	15	0.15	155.98	0.442	0.443	0.22
	1.0	20	0	183.45	0.519	0.51	-1.89
	1.0	20	0.05	166.77	0.472	0.459	-2.92
	1.0	20	0.1	143.23	0.406	0.408	0.56
	1.0	20	0.15	126.55	0.358	0.357	-0.41
Medium dense	0	0	0	**101.04**	1.0	1.0	0
	0	0	0.05	84.37	0.835	0.9	7.23
	0	0	0.1	68.67	0.68	0.8	15.05
	0	0	0.15	54.94	0.544	0.7	22.33
	0	5	0	79.46	0.786	0.751	-4.7
	0	5	0.05	63.77	0.631	0.676	6.65
	0	5	0.1	52.97	0.524	0.601	12.75
	0	5	0.15	42.18	0.417	0.526	20.6
	0	10	0	55.92	0.533	0.538	-2.9
	0	10	0.05	47.09	0.466	0.484	3.71
	0	10	0.1	38.46	0.381	0.43	11.54
	0	10	0.15	31.39	0.311	0.376	17.47
	0	15	0	38.26	0.379	0.36	-5.18
	0	15	0.05	32.37	0.32	0.324	1.11
	0	15	0.1	26.98	0.267	0.288	7.3
	0	15	0.15	20.6	0.204	0.252	19.09
	0	20	0	24.03	0.238	0.218	-9.22
	0	20	0.05	19.62	0.294	0.196	0.93
	0	20	0.1	16.68	0.165	0.174	5.27
	0	20	0.15	13.34	0.132	0.152	13.39
	0.5	0	0	143.23	1.0	1.0	0
	0.5	0	0.05	123.61	0.863	0.9	4.11
	0.5	0	0.1	103.99	0.726	0.8	9.25
	0.5	0	0.15	87.31	0.61	0.7	12.92
	0.5	5	0	120.66	0.842	0.807	-4.42
	0.5	5	0.05	103.99	0.726	0.726	0.02
	0.5	5	0.1	90.25	0.63	0.645	2.37
	0.5	5	0.15	72.59	0.507	0.565	10.26
	0.5	10	0	98.1	0.685	0.628	-9.07
	0.5	10	0.05	84.86	0.592	0.565	-4.83
	0.5	10	0.1	72.59	0.507	0.502	-0.89

Table 4.16 (Continued)

Sand type (1)	$\frac{D_f}{B}$ (2)	α (deg) (3)	$\frac{e}{B}$ (4)	Experimental q_u (kN/m^2) (5)	Experimental RF [Eq. (4.4)] (6)	Calculated RF [Eqs. 4.5, 4.7, 4.8, and 4.9] (7)	Deviation—$\frac{\text{Col. 7} - \text{Col. 6}}{\text{Col. 7}}$ (%) (8)
	0.5	10	0.15	60.82	0.425	0.44	3.4
	0.5	15	0	79.46	0.555	0.465	-19.37
	0.5	15	0.05	67.89	0.474	0.418	-13.31
	0.5	15	0.1	56.9	0.397	0.372	-6.85
	0.5	15	0.15	48.07	0.336	0.325	-3.16
	0.5	20	0	58.27	0.407	0.319	-27.62
	0.5	20	0.05	50.03	0.349	0.287	-21.75
	0.5	20	0.1	43.16	0.301	0.255	-18.17
	0.5	20	0.15	36.3	0.253	0.223	-13.56
	1.0	0	0	208.95	1.0	1.0	0
	1.0	0	0.05	193.26	0.925	0.9	-2.76
	1.0	0	0.1	175.6	0.84	0.8	-5.05
	1.0	0	0.15	156.96	0.751	0.7	-7.31
	1.0	5	0	186.39	0.892	0.867	-2.93
	1.0	5	0.05	168.73	0.808	0.78	-3.53
	1.0	5	0.1	153.04	0.732	0.693	-5.63
	1.0	5	0.15	137.34	0.657	0.607	-8.34
	1.0	10	0	160.88	0.77	0.733	-4.99
	1.0	10	0.05	144.21	0.69	0.66	-4.57
	1.0	10	0.1	129.49	0.62	0.587	-5.63
	1.0	10	0.15	112.82	0.54	0.513	-5.18
	1.0	15	0	133.42	0.638	0.6	-6.42
	1.0	15	0.05	118.7	0.568	0.54	-5.2
	1.0	15	0.1	106.93	0.512	0.48	-6.61
	1.0	15	0.15	94.18	0.451	0.42	-7.31
	1.0	20	0	98.1	0.469	0.467	-0.6
	1.0	20	0.05	92.21	0.441	0.42	-5.07
	1.0	20	0.1	84.37	0.404	0.373	-8.15
	1.0	20	0.15	75.54	0.362	0.327	-10.66

Table 4.17. Variation of a, m and n [Eq. (4.5)] along with R^2 values

Sand type	$\frac{D_f}{B}$	a	m	R^2	n	R^2
Dense	0	2.23	0.81	0.99	1.98	0.99
	0.5	2.0	0.88	1.0	1.23	0.99
	1.0	1.76	0.92	1.0	0.97	0.99
Medium dense	0	2.59	0.91	0.99	1.868	0.99
	0.5	2.31	0.93	0.99	1.17	0.99
	1.0	1.97	1.09	0.99	0.95	0.99

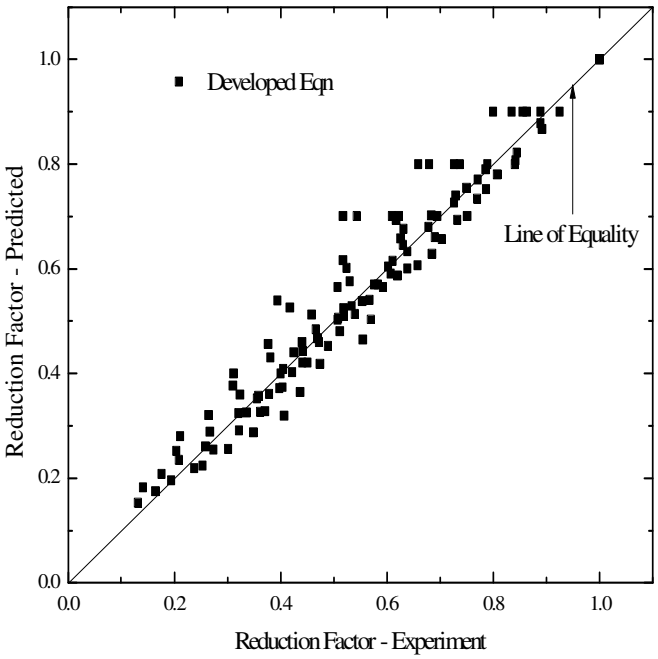

Figure 4.33: Comparison of present experimental results with developed empirical equation

Figure 4.33 shows the comparison of experimental reduction factor with developed empirical reduction factor. The comparison seems to be reasonably good.

4.5 Comparison

4.5.1 Comparison with Meyerhof [1963]

The ultimate bearing capacity of shallow strip foundations subjected to eccentrically inclined load on granular soil proposed by Meyerhof (1963) is

$$q_u = qN_q s_q d_q i_q + \frac{1}{2}\gamma B' N_\gamma s_\gamma d_\gamma i_\gamma \qquad (4.11)$$

All expressions for various factors and notations used in Eq. 4.11 have been described in section 2.2.4.

Meyerhof's equation for inclined and eccentric load considers **(q_u) to be vertical**; whereas in the present analysis q_u is considered **to be inclined** at an angle (α).

The reduction factor *RF* corresponding to Meyerhof (1963) can be written as

$$RF = \frac{\left(\frac{q_u \times B'}{B}\right)\left(\frac{1}{\cos\alpha}\right)}{q_{u\left(e/B=0,\alpha/\phi=0,D_f/B\right)}} = \frac{q_{u\left(e/B,\alpha/\phi,D_f/B\right)}}{q_{u\left(e/B=0,\alpha/\phi=0,D_f/B\right)}} \sec\alpha\left(\frac{B'}{B}\right) \tag{4.12}$$

where q_u = ultimate bearing capacity applied vertically

The comparison of the values of *RF* using Meyorhof's method as discussed above has been made with those using present developed equation and experimental *RF* values. The same has been presented in the Table 4.18.

Table 4.18 Reduction Factor Comparison of Meyerhof (1963) with Present results

Sand type	$\frac{D_f}{B}$	α (deg)	$\frac{e}{B}$	Pred. *RF* [Eq. 4.10]	*RF* corresponding to Meyerhof (1963) Eq. (4.12)	Expt. *RF* [Eq. (4.4)]
Dense	0	0	0	1.000	1.000	1.000
	0	0	0.05	0.900	0.810	0.800
	0	0	0.1	0.800	0.640	0.659
	0	0	0.15	0.700	0.490	0.518
	0	5	0	0.770	0.773	0.771
	0	5	0.05	0.693	0.626	0.618
	0	5	0.1	0.616	0.495	0.518
	0	5	0.15	0.539	0.379	0.394
	0	10	0	0.570	0.579	0.576
	0	10	0.05	0.513	0.469	0.459
	0	10	0.1	0.456	0.370	0.376
	0	10	0.15	0.399	0.284	0.312
	0	15	0	0.400	0.414	0.400
	0	15	0.05	0.360	0.335	0.324
	0	15	0.1	0.320	0.265	0.265
	0	15	0.15	0.280	0.203	0.211

Table 4.18 (Continued)

Sand type	$\frac{D_f}{B}$	α (deg)	$\frac{e}{B}$	Pred. *RF* [Eq. 4.10]	*RF* corresponding to Meyerhof (1963) Eq. (4.12)	Expt. *RF* [Eq. (4.4)]
	0	20	0	0.260	0.277	0.259
	0	20	0.05	0.234	0.224	0.209
	0	20	0.1	0.208	0.177	0.176
	0	20	0.15	0.182	0.136	0.141
	0.5	0	0	1.000	1.000	1.000
	0.5	0	0.05	0.900	0.855	0.856
	0.5	0	0.1	0.800	0.721	0.737
	0.5	0	0.15	0.700	0.597	0.622
	0.5	5	0	0.822	0.821	0.844
	0.5	5	0.05	0.740	0.705	0.730
	0.5	5	0.1	0.658	0.597	0.626
	0.5	5	0.15	0.575	0.497	0.530
	0.5	10	0	0.656	0.667	0.704
	0.5	10	0.05	0.590	0.575	0.607
	0.5	10	0.1	0.525	0.489	0.519
	0.5	10	0.15	0.459	0.410	0.441
	0.5	15	0	0.503	0.535	0.570
	0.5	15	0.05	0.453	0.464	0.489
	0.5	15	0.1	0.402	0.397	0.422
	0.5	15	0.15	0.352	0.335	0.356
	0.5	20	0	0.364	0.422	0.437
	0.5	20	0.05	0.328	0.369	0.370
	0.5	20	0.1	0.291	0.318	0.322
	0.5	20	0.15	0.255	0.271	0.274
	1	0	0	1.000	1.000	1.000
	1	0	0.05	0.900	0.878	0.889
	1	0	0.1	0.800	0.763	0.789
	1	0	0.15	0.700	0.656	0.694
	1	5	0	0.877	0.842	0.889
	1	5	0.05	0.790	0.742	0.786
	1	5	0.1	0.702	0.648	0.683
	1	5	0.15	0.614	0.559	0.611
	1	10	0	0.755	0.705	0.750
	1	10	0.05	0.679	0.625	0.678
	1	10	0.1	0.604	0.548	0.603

Table 4.18 (Continued)

Sand type	$\frac{D_f}{B}$	α (deg)	$\frac{e}{B}$	Pred. *RF* [Eq. 4.10]	*RF* corresponding to Meyerhof (1963) Eq. (4.12)	Expt. *RF* [Eq. (4.4)]
	1	10	0.15	0.528	0.475	0.533
	1	15	0	0.632	0.587	0.639
	1	15	0.05	0.569	0.522	0.583
	1	15	0.1	0.506	0.461	0.508
	1	15	0.15	0.443	0.402	0.442
	1	20	0	0.510	0.485	0.519
	1	20	0.05	0.459	0.434	0.472
	1	20	0.1	0.408	0.385	0.406
	1	20	0.15	0.357	0.338	0.358
Medium dense	0	0	0	1.000	1.000	1.000
	0	0	0.05	0.900	0.810	0.835
	0	0	0.1	0.800	0.640	0.680
	0	0	0.15	0.700	0.490	0.544
	0	5	0	0.751	0.754	0.786
	0	5	0.05	0.676	0.611	0.631
	0	5	0.1	0.601	0.483	0.524
	0	5	0.15	0.526	0.369	0.417
	0	10	0	0.538	0.546	0.553
	0	10	0.05	0.484	0.442	0.466
	0	10	0.1	0.430	0.349	0.381
	0	10	0.15	0.376	0.268	0.311
	0	15	0	0.360	0.373	0.379
	0	15	0.05	0.324	0.302	0.320
	0	15	0.1	0.288	0.239	0.267
	0	15	0.15	0.252	0.183	0.204
	0	20	0	0.218	0.232	0.238
	0	20	0.05	0.196	0.188	0.194
	0	20	0.1	0.174	0.148	0.165
	0	20	0.15	0.152	0.114	0.132
	0.5	0	0	1.000	1.000	1.000
	0.5	0	0.05	0.900	0.858	0.863
	0.5	0	0.1	0.800	0.727	0.726
	0.5	0	0.15	0.700	0.605	0.610
	0.5	5	0	0.807	0.816	0.842
	0.5	5	0.05	0.726	0.704	0.726

Table 4.18 (Continued)

Sand type	$\frac{D_f}{B}$	α (deg)	$\frac{e}{B}$	Pred. *RF* [Eq. 4.10]	*RF* corresponding to Meyerhof (1963) Eq. (4.12)	Expt. *RF* [Eq. (4.4)]
	0.5	5	0.1	0.645	0.599	0.630
	0.5	5	0.15	0.565	0.501	0.507
	0.5	10	0	0.628	0.659	0.685
	0.5	10	0.05	0.565	0.571	0.592
	0.5	10	0.1	0.502	0.489	0.507
	0.5	10	0.15	0.440	0.412	0.425
	0.5	15	0	0.465	0.525	0.555
	0.5	15	0.05	0.418	0.458	0.474
	0.5	15	0.1	0.372	0.395	0.397
	0.5	15	0.15	0.325	0.336	0.336
	0.5	20	0	0.319	0.413	0.407
	0.5	20	0.05	0.287	0.363	0.349
	0.5	20	0.1	0.255	0.316	0.301
	0.5	20	0.15	0.223	0.272	0.253
	1	0	0	1.000	1.000	1.000
	1	0	0.05	0.900	0.881	0.925
	1	0	0.1	0.800	0.769	0.840
	1	0	0.15	0.700	0.663	0.751
	1	5	0	0.867	0.840	0.892
	1	5	0.05	0.780	0.743	0.808
	1	5	0.1	0.693	0.652	0.732
	1	5	0.15	0.607	0.564	0.657
	1	10	0	0.733	0.702	0.770
	1	10	0.05	0.660	0.625	0.690
	1	10	0.1	0.587	0.550	0.620
	1	10	0.15	0.513	0.479	0.540
	1	15	0	0.600	0.584	0.639
	1	15	0.05	0.540	0.522	0.568
	1	15	0.1	0.480	0.463	0.512
	1	15	0.15	0.420	0.406	0.451
	1	20	0	0.467	0.483	0.469
	1	20	0.05	0.420	0.435	0.441
	1	20	0.1	0.373	0.388	0.404
	1	20	0.15	0.327	0.342	0.362

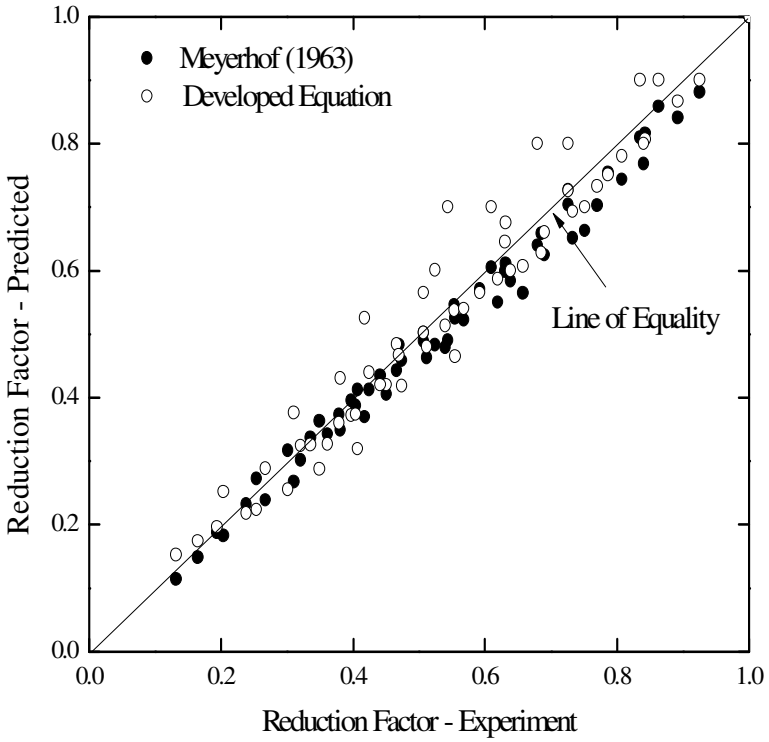

Figure 4.34: Comparison of Present results with Meyerhof (1963)

Table 4.18 and Figure 4.34 show the comparison, and the agreement is reasonably good.

4.5.2 Comparison with Saran and Agarwal [1991]

As discussed in section 2.2.4, Saran and Agarwal (1991) proposed an equation for the determination of ultimate bearing capacity of footing under eccentric and inclined load. They presented the bearing capacity factors N_c, N_q and N_γ in tabular and graphical forms. To compare their results with the present results, N_q and N_γ values (*e/B*=0, 0.1, $\alpha=0^0$, 10^0 and 20^0) are digitized from the graph given by Saran and Agarwal (1991) for medium dense sand ($\phi = 37.5^0$). Using Eqs. (2.36) as proposed by Saran and Agarwal (1991) and (4.4), values of *RF* for bearing capacity corresponding to Saran and Agarwal (1991) is calculated and compared with present Predicted and Experimental *RF* values. This is shown in Table 4.19.

Table 4.19. Comparison of Reduction Factors corresponding to Saran and Agarwal (1991) along with Present results

Experiment No. (1)	$\frac{D_f}{B}$ (2)	α (deg) (3)	$\frac{e}{B}$ (4)	*RF* corresponding to Saran and Agarwal (1991) [Eqs. (2.36) and (4.4)] (5)	Experimental *RF* [Eq. (4.4)] (6)	Predicted *RF* [Eq. 4.10] (7)	Deviation—$\frac{\text{Col.7} - \text{Col.5}}{\text{Col.7}}$ (%) (8)
1	0	0	0	1.0	1.0	1	-0.06
2	0	0	0.1	0.54	0.68	0.8	32.89
3	0	10	0	0.44	0.553	0.538	18.44
4	0	10	0.1	0.33	0.381	0.43	23.17
5	0	20	0	0.36	0.238	0.218	-67.37
6	0	20	0.1	0.18	0.165	0.174	-5.12
7	0.5	0	0	1.0	1.0	1.0	0.02
8	0.5	0	0.1	0.6	0.726	0.8	25.26
9	0.5	10	0	0.52	0.685	0.628	17.85
10	0.5	10	0.1	0.38	0.507	0.502	23.61
11	0.5	20	0	0.38	0.407	0.319	-19.81
12	0.5	20	0.1	0.22	0.301	0.255	13.17
13	1.0	0	0	1.0	1.0	1.0	-0.01
14	1.0	0	0.1	0.63	0.84	0.8	21.31
15	1.0	10	0	0.56	0.77	0.733	24.23
16	1.0	10	0.1	0.41	0.62	0.587	29.92
17	1.0	20	0	0.39	0.469	0.467	16.19
18	1.0	20	0.1	0.24	0.404	0.373	35.41

Most of the values of *RF* computed by Saran and Agarwal (1991) are found to be deviated in the range of 30% from the present results as shown in Table 4.19 and Figure 4.35.

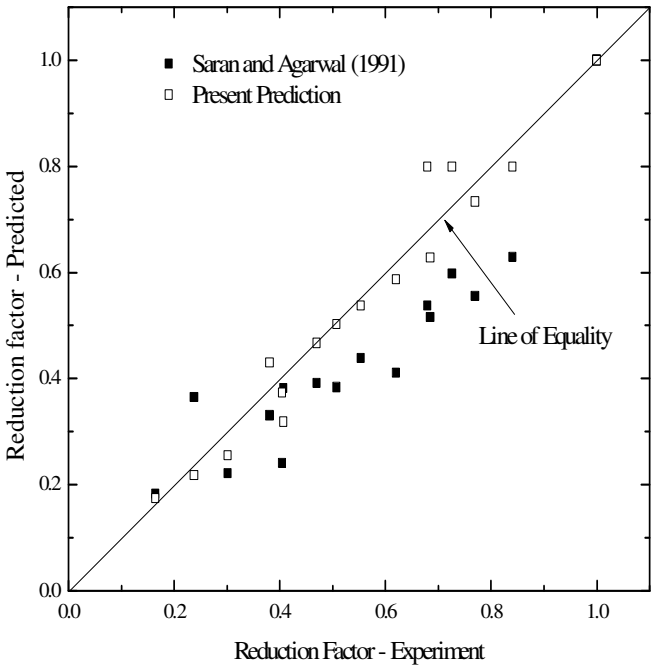

(a)

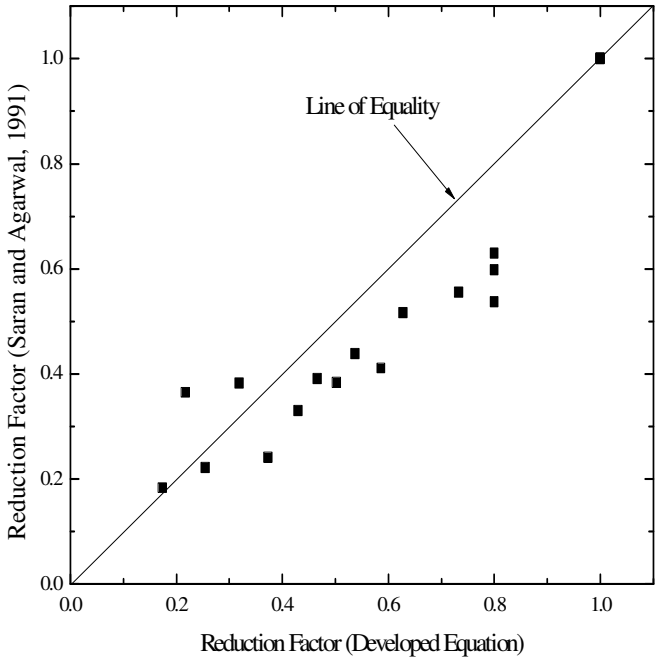

(b)

Figure 4.35: Comparison: (a) Present results with Saran and Agarwal (1991), (b) Present predicted *RF* with *RF* corresponding to Saran and Agarwal (1991)

4.5.3 Comparison with Loukidis et al. [2008]

Recently, Loukidis et al. (2008) developed an equation for combined inclination-eccentricity factor f_{ie} using finite element method for surface foundation (D_f/B = 0) as given by:

$$f_{ie} = \left[1 - \sqrt{3.7\left(\frac{e}{B}\right)^2 + 2.1(\tan\alpha)^2 + 1.5\left(\frac{e}{B}\right)\tan\alpha}\right]^2 \tag{4.13}$$

$$\begin{aligned} q_{u(e/B,\alpha)} &= \left(\frac{V_L}{\cos\alpha}\right)\left(\frac{1}{B}\right) \\ &= \frac{\frac{1}{2}\gamma B^2 N_\gamma f_{ie}}{B\cos\alpha} \\ &= \frac{1}{2}\gamma B N_\gamma \left(\frac{f_{ie}}{\cos\alpha}\right) \end{aligned} \tag{4.14}$$

where $q_{u(e/B,\ \alpha)}$ = Ultimate bearing capacity of strip footing at an eccentricity e and inclination α; V_L = (Vertical) limit load on a strip footing resting over the surface of an uncemented sand deposit subjected to eccentric and inclined load.

The reduction factor *RF* corresponding to Loukidis et al. (2008) can be written as

$$RF = \frac{f_{ie}}{\cos\alpha} \tag{4.15}$$

The reduction factors computed using Eq. (4.15) is compared with those obtained from Eqs. (4.10) and (4.4) in Figures 4.36 and 4.37 and also in Table 4.20. The comparison seems to be good.

Table 4.20. Comparison of Reduction Factors Obtained from Eqs. (4.15) and (4.13) with Eq. (4.10) for $D_f/B = 0$

Experiment No. (1)	α (deg) (2)	$\frac{e}{B}$ (3)	Loukidis et al. (2008) *RF* [Eqs. (4.13) and (4.15)] (4)	Dense sand [Eq. (4.10)] (5)	Medium dense sand [Eq. (4.10)] (6)
1	0	0	1.0	1	1.0
2	0	0.05	0.817	0.9	0.9
3	0	0.1	0.652	0.8	0.8
4	0	0.15	0.506	0.7	0.7
5	5	0	0.766	0.77	0.751
6	5	0.05	0.677	0.693	0.676
7	5	0.1	0.554	0.616	0.601
8	5	0.15	0.431	0.539	0.526
9	10	0	0.563	0.570	0.538
10	10	0.05	0.503	0.513	0.484
11	10	0.1	0.418	0.456	0.43
12	10	0.15	0.326	0.399	0.376
13	15	0	0.388	0.4	0.36
14	15	0.05	0.343	0.36	0.324
15	15	0.1	0.283	0.32	0.288
16	15	0.15	0.217	0.28	0.252
17	20	0	0.238	0.26	0.218
18	20	0.05	0.205	0.234	0.196
19	20	0.1	0.164	0.208	0.174
20	20	0.15	0.119	0.182	0.152

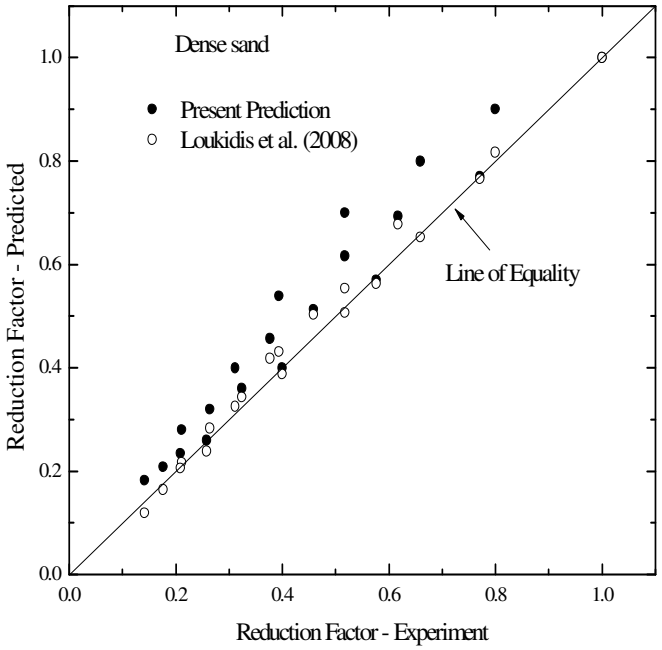

Figure 4.36: Comparison of Present results with Loukidis et al. (2008) for dense sand.

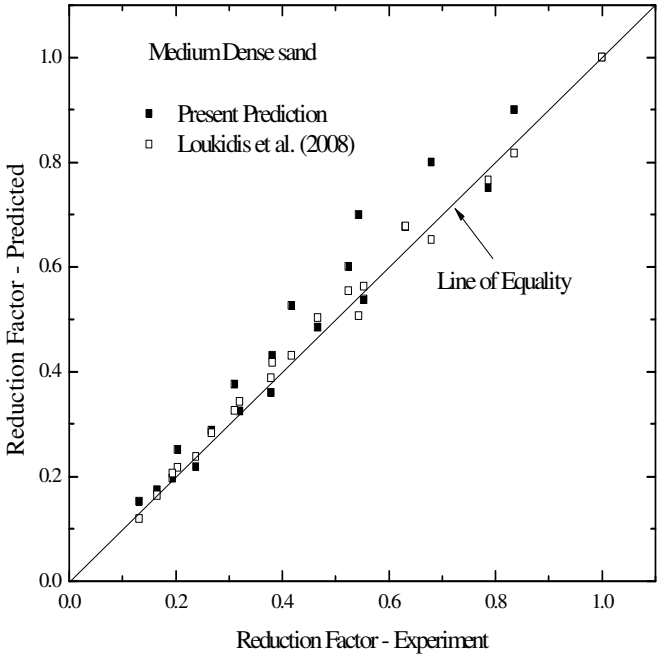

Figure 4.37: Comparison of Present results with Loukidis et al. (2008) for medium dense sand.

4.6 Conclusions

The results of a number of laboratory model tests conducted to determine the ultimate bearing capacity of a strip foundation supported by sand and subjected to an eccentrically inclined load with an embedment ratio (D_f /B) varying from zero to one have been reported. Tests are conducted on dense and medium dense sand. The load eccentricity ratio e/B is varied from 0 to 0.15, and the load inclination α is varied from 0^0 to 20° (i.e. $\alpha/\phi \approx 0$ to 0.5). Based on the test results and within the range of parameters studied, following conclusions are drawn:

- An empirical relationship for reduction factor in predicting ultimate bearing capacity has been proposed.

- A comparison between the reduction factors obtained from the empirical relationships and those obtained from experiments shows, in general, a variation of ±15% or less. In some cases, the deviation is about 25 to 30%.

- The developed reduction factor is also in well agreement with existing theories.

5. ULTIMATE BEARING CAPACITY OF ECCENTRICALLY INCLINED LOADED STRIP FOOTING ON GRANULAR SOIL WHEN THE LINE OF LOAD APPLICATION IS AWAY FROM THE CENTER LINE OF THE FOOTING

5.1 Introduction

Shallow strip foundations are at times subjected to eccentrically inclined loads. Figure 5.1 shows two possible modes of load application. In this figure B is the width of the foundation, e is the load eccentricity, α is the load inclination, and Q_u is the ultimate load per unit length of the foundation. In Figure 5.1(a) the line of load application of the foundation is inclined towards the center line of the foundation and is referred to as *partially compensated* by Perloff and Baron (1976). It is also possible for the line of load application on the foundation to be inclined away from the center line of the foundation as shown in Figure 5.1(b). Perloff and Baron (1976) called this type of loading as *reinforced* case.

The results of practically all studies relating to the bearing capacity of a shallow foundation subjected to eccentrically inclined load presently available in the literature, though fairly limited, consider the so-called *partially compensated* case. This chapter deals with the study for the *reinforced* type of loading [Figure 5.1(b)].

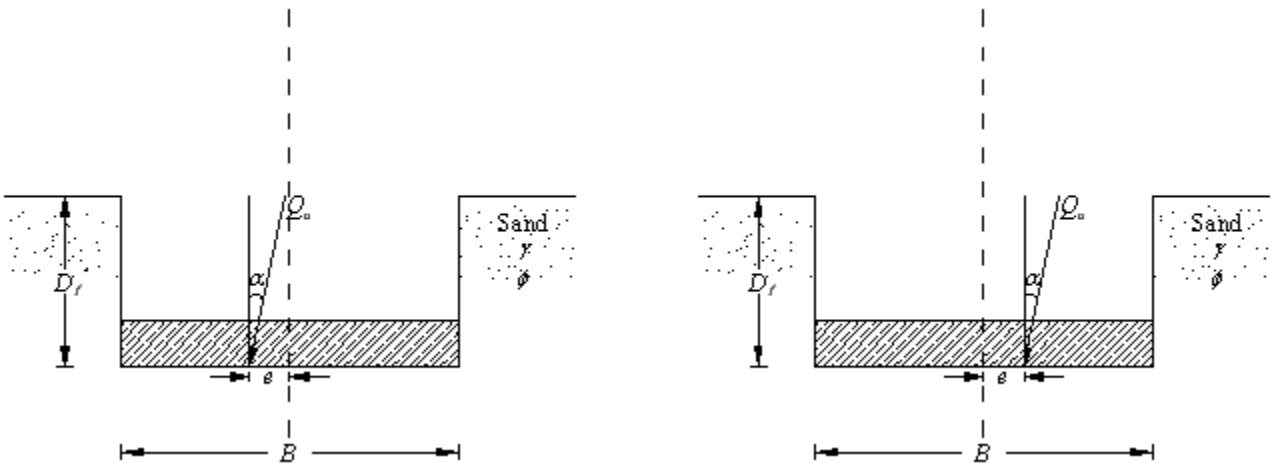

Figure 5.1: Eccentrically inclined load on a strip foundation: (a) *Partially compensated* case, (b) *Reinforced* case

Based on a review of published theoretical and experimental studies related to the estimation of ultimate bearing capacity of shallow strip foundation subjected to eccentrically inclined loading, most of the cases are pertaining to the *partially compensated* condition as mentioned in Chapter 4. In order to quantify certain parameters, for a given value of D_f/B, a reduction factor *RF* as developed in Eq. (4.10) can be developed based on the concept advanced in Eq. (4.5) for load eccentricity and the inclination factors. Or,

$$RF = \frac{q_{u(D_f/B,\, e/B,\, \alpha/\phi)}}{q_{u(D_f/B,\, e/B=0,\, \alpha/\phi=0)}} \tag{5.1}$$

where $q_{u(D_f/B,\, e/B,\, \alpha/\phi)}$ = ultimate bearing capacity with eccentricity ratio e/B and inclination ratio α/ϕ at an embedment ratio D_f/B and $q_{u(D_f/B,\, e/B=0,\, \alpha/\phi=0)}$ = ultimate bearing capacity with centric vertical loading (e/B = 0 and α/ϕ = 0) at the same embedment ratio D_f/B.

Thus it can initially be assumed that

$$RF = \left[1 - a\left(\frac{e}{B}\right)^m\right]\left(1 - \frac{\alpha}{\phi}\right)^n \tag{5.2}$$

where a, m, n = factors which are functions of D_f/B.

The purpose of this chapter is to analyse the results of laboratory model tests conducted on a strip foundation with varying D_f/B, e/B and α to quantify certain coefficients as given in Eq. (5.2).

5.2 Experimental Module

Seventy eight numbers of laboratory model tests were conducted out of which six tests in central vertical condition (i.e. Test No. 1, 14, 27, 40, 53, and 66) are common with test sequence as mentioned in Chapter 4. The details of the tests are mentioned in Table 5.1 and Table 5.2.

Table 5.1. Sequence of Model Tests on Dense sand as per Figure 5.1(b)

Test No.	*e/B*	*α*	D_f/B
1	0	0	0
2-5	0.05	5^0, 10^0, 15^0, 20^0	0
6-9	0.1	5^0, 10^0, 15^0, 20^0	0
10-13	0.15	5^0, 10^0, 15^0, 20^0	0
14	0	0	0.5
15-18	0.05	5^0, 10^0, 15^0, 20^0	0.5
19-22	0.1	5^0, 10^0, 15^0, 20^0	0.5
23-26	0.15	5^0, 10^0, 15^0, 20^0	0.5

27	0	0	1.0
28-31	0.05	5^0, 10^0, 15^0, 20^0	1.0
32-35	0.1	5^0, 10^0, 15^0, 20^0	1.0
36-39	0.15	5^0, 10^0, 15^0, 20^0	1.0

Table 5.2. Sequence of Model Tests on Medium Dense sand as per Figure 5.1(b)

Test No.	*e/B*	α	D_f/B
40	0	0	0
41-44	0.05	5^0, 10^0, 15^0, 20^0	0
45-48	0.1	5^0, 10^0, 15^0, 20^0	0
49-52	0.15	5^0, 10^0, 15^0, 20^0	0
53	0	0	0.5
54-57	0.05	5^0, 10^0, 15^0, 20^0	0.5
58-61	0.1	5^0, 10^0, 15^0, 20^0	0.5
62-65	0.15	5^0, 10^0, 15^0, 20^0	0.5
66	0	0	1.0
67-70	0.05	5^0, 10^0, 15^0, 20^0	1.0
71-74	0.1	5^0, 10^0, 15^0, 20^0	1.0
75-78	0.15	5^0, 10^0, 15^0, 20^0	1.0

5.3 Model Test Results

The ultimate bearing capacities q_u obtained from the present model tests are given in Table 5.3 (Column 5). Other ultimate bearing capacity test results for vertical loading

conditions (α = 0 with *e*/*B* varying from 0.05 to 0.15) relevant to the present study as mentioned in case of *partially compensated* type (Chapter 4) are summarized in Table 5.4. It needs to be mentioned however that, in the majority of eccentrically inclined loading (*reinforced* type) cases, the failure mode is local shear type as defined by Vesic (1973). The application of load considering both eccentricity and inclination for one of the test is shown in Figure 5.2.

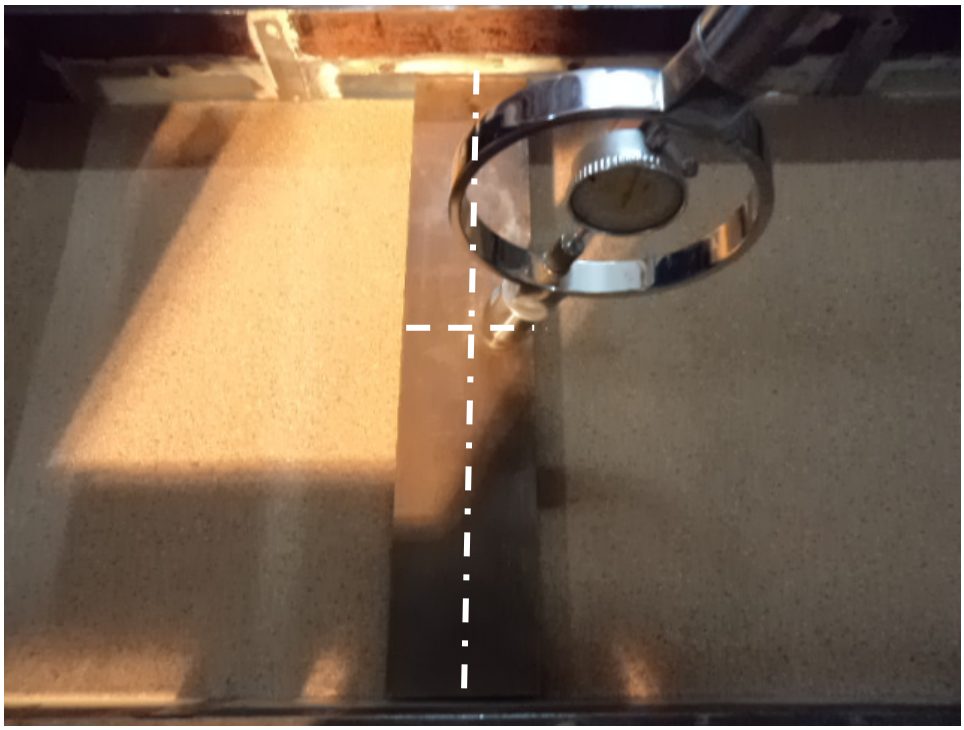

Figure 5.2: Photograph of load application for the test [$e/B = 0.15$, $\alpha = 20^0$ and $D_f/B = 0$] when the line of load application is away from the center line of the footing

As observed in the case of *partially compensated* type of loading, the ultimate bearing capacity (ubc) decreases with increase in the values of *e*/*B* and α for the case of *reinforced* type of loading. Similarly increase in ubc occurs with increase in D_f/B and relative density of sand as seen with partially compensated type of loading. These are shown in Figures 5.3 through 5.6.

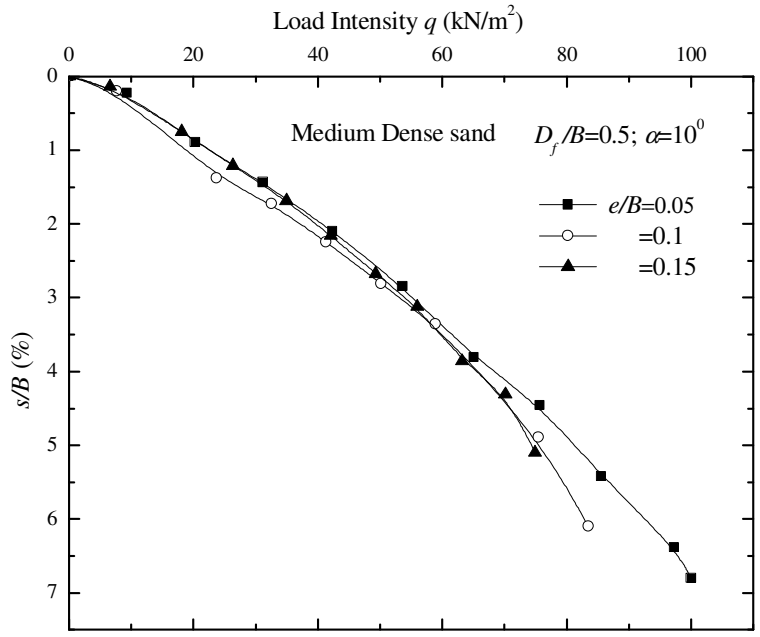

Figure 5.3: Variation of load-settlement curve with e/B at D_f/B=0.5, α=10^0 in medium dense sand

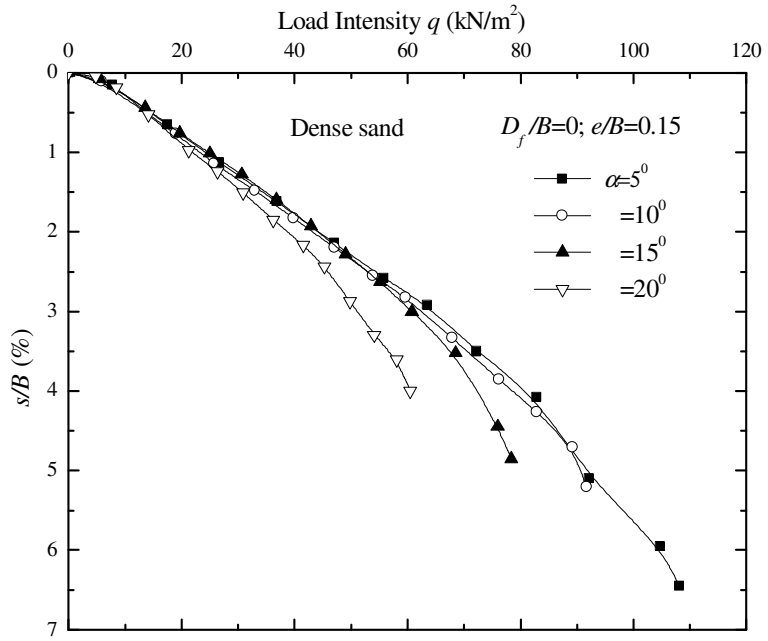

Figure 5.4: Variation of load-settlement curve with load inclination (α) at D_f/B=0, e/B = 0.15 in dense sand

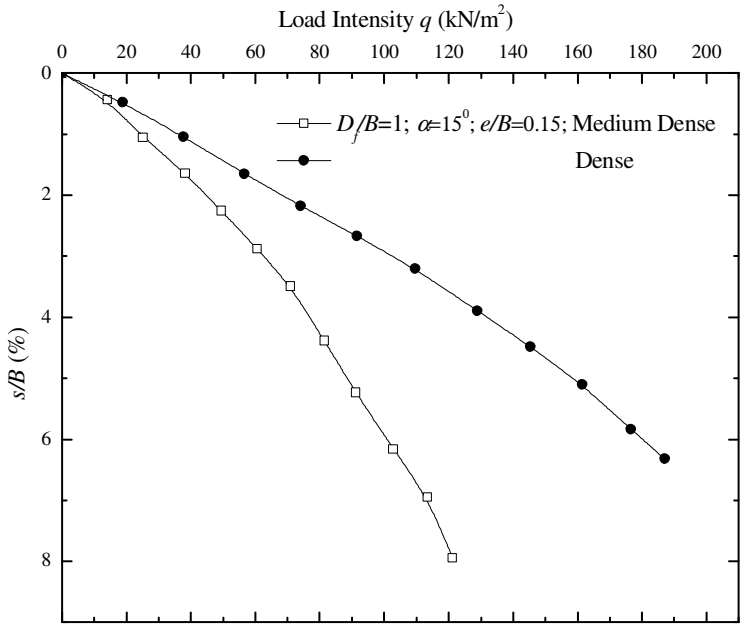

Figure 5.5: Variation of load-settlement curve with relative density (D_r) *at* D_f/B=1, α=15^0, e/B =0.15

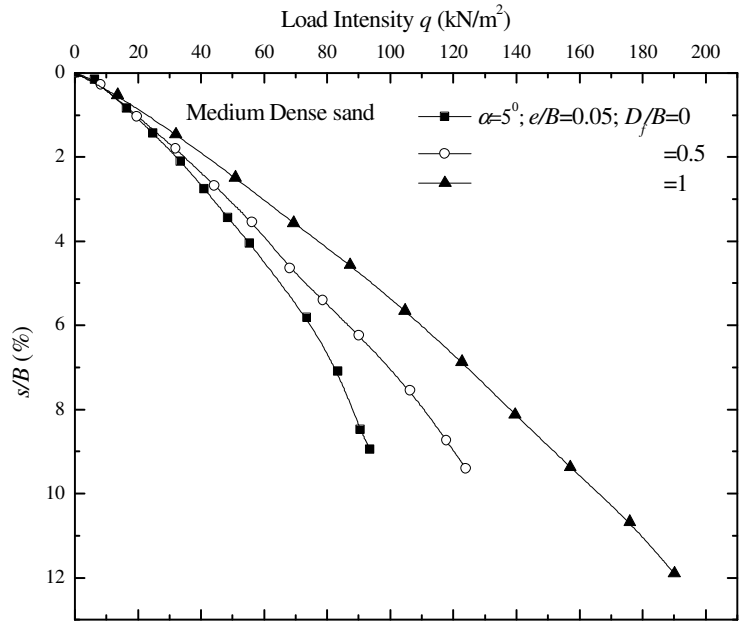

Figure 5.6: Variation of load-settlement curve with D_f/B *at* α=5^0, e/B =0.05 in medium dense sand

A comparison has been made with the ultimate bearing capacities of partially compensated and reinforced type of footings as discussed. Figures 5.7 and 5.8 show plots of the ratio of the ultimate bearing capacities—(q_u–reinforced) determined from the present tests (Table 5.3) to (q_u–partially compensated) provided in Chapter 4 for similar values of D_f/B, e/B (>0) and α (>0). These figures show that:

a. For given values of D_f/B and e/B, the magnitude of (q_u–reinforced)/(q_u–partially compensated) increases with the load inclination α.
b. Generally speaking, for similar values of α and e/B, the ratio shows a tendency to decrease with the increase in embedment ratio.
c. For a given value of D_f/B and α, the ratio increases with the increase in e/B.

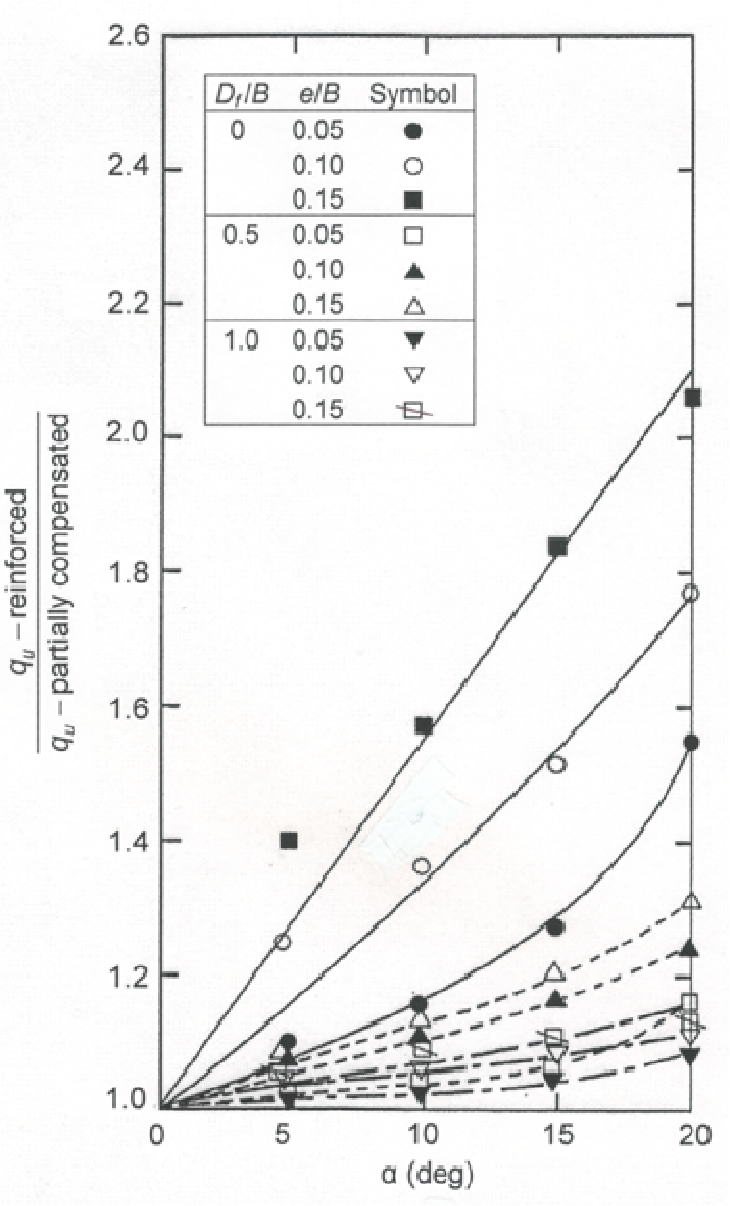

Figure 5.7: Plot of (q_u–reinforced)/(q_u–partially compensated) for cases of eccentrically inclined loading in dense sand

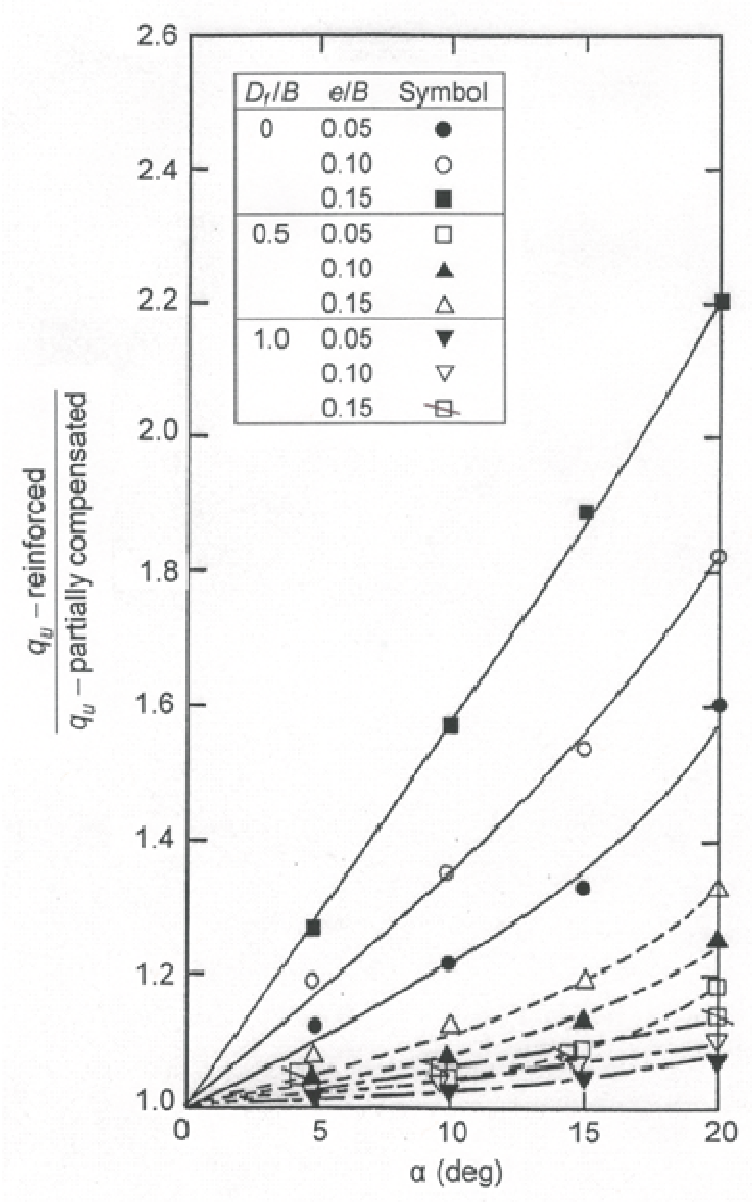

Figure 5.8: Plot of (q_u–reinforced)/(q_u–partially compensated) for cases of eccentrically inclined loading in medium dense sand

Figures 5.9 and 5.10 show the plots of the ratio of (s_u/B-reinforced) obtained from the present tests to (s_u/B-partially compensated) obtained from the tests reported in Chapter 4 (s_u = average settlement along the center line of the foundation at ultimate load) for similar values of D_f/B, e/B (>0) and α (>0). As expected, in any model test program of

this type, the plots are somewhat scattered. However, based on the results shown in these figures, the following general observations can be made:

a. For any given value of D_f/B, the settlement ratio increases with the angle of load inclination α.

b. For similar values of α and e/B, the settlement ratio in general tends to decrease with the increase in D_f/B.

c. For a given D_f/B and α, there is a tendency for the settlement ratio to remain the same irrespective of the value of e/B.

d. For the range of tests conducted, the average value of the settlement ratio is about 1 at $\alpha = 5^\circ$ and increase to about 1.4 at $\alpha = 20^\circ$.

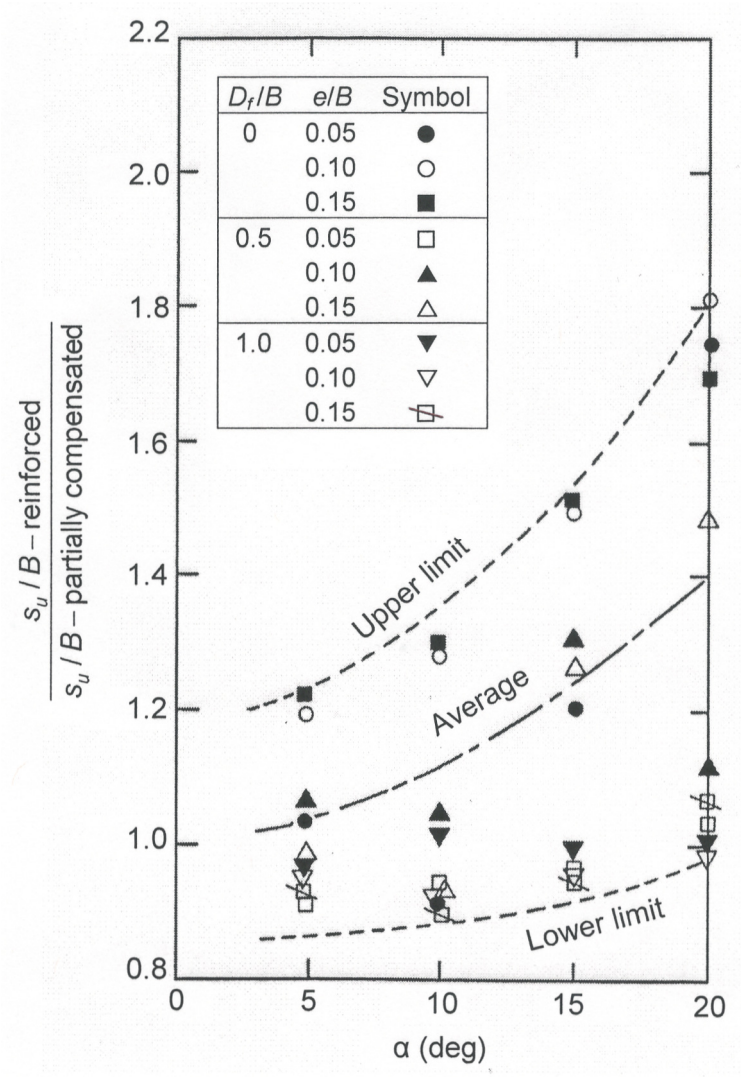

Figure 5.9: Plot of (s_u/B-reinforced)/(s_u/B-partially compensated) for cases of eccentrically inclined loading in dense sand

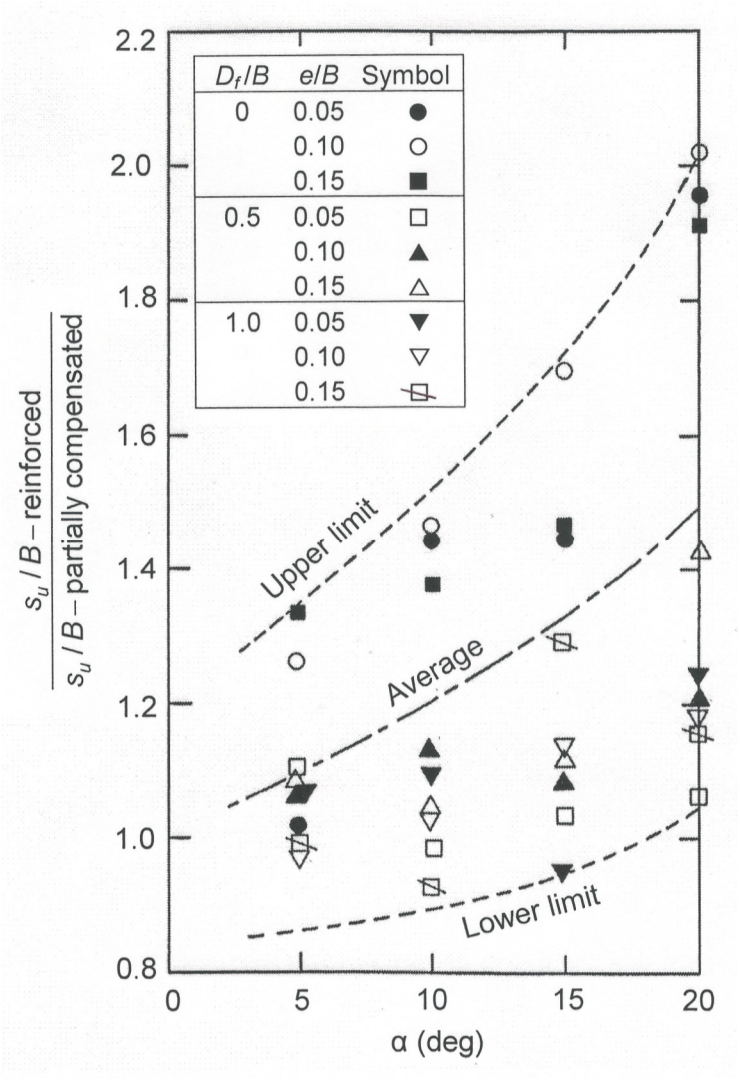

Figure 5.10: Plot of (s_u/B-reinforced)/(s_u/B-partially compensated) for cases of eccentrically inclined loading in medium dense sand

Figures 5.11 and 5.12 show plots of the ratio of the ultimate bearing capacities—(q_u–partially compensated) to (q_u–central vertical) for similar values of D_f /B, e/B (>0) and α (>0). These figures show that:

- For given values of D_f/B and e/B, the magnitude of (q_u–partially compensated)/(q_u–central vertical) decreases with increase in the load inclination α.

- For similar values of α and e/B, the ratio shows a tendency to increase with the increase in embedment ratio (D_f/B).
- For a given value of D_f/B and α, the ratio decreases with the increase in e/B.

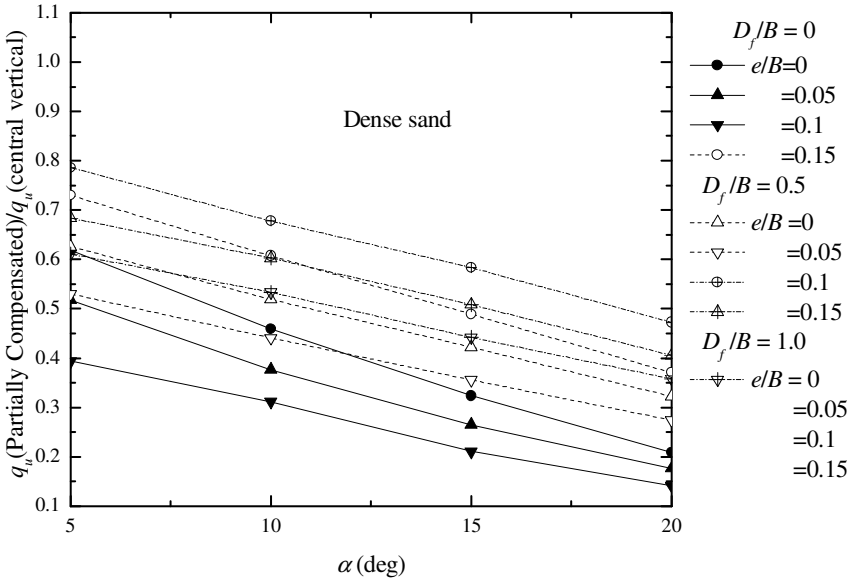

Figure 5.11: Plot of (q_u– partially compensated)/(q_u–central vertical) for cases of eccentrically inclined loading in dense sand

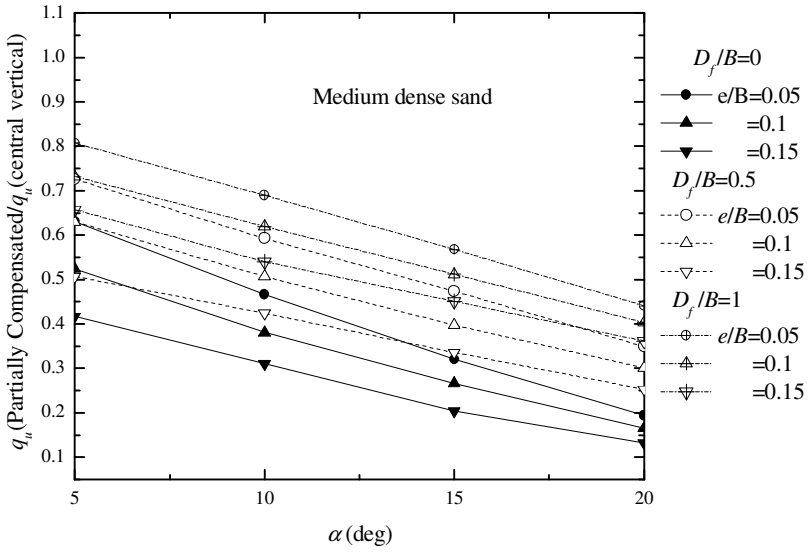

Figure 5.12: Plot of (q_u– partially compensated)/(q_u–central vertical) for cases of eccentrically inclined loading in medium dense sand

Similar types of results were found in Figures 5.13 and 5.14 which show plots of the ratio of the ultimate bearing capacities— (q_u–reinforced)/(q_u–central vertical). The values are also presented in Table 5.3.

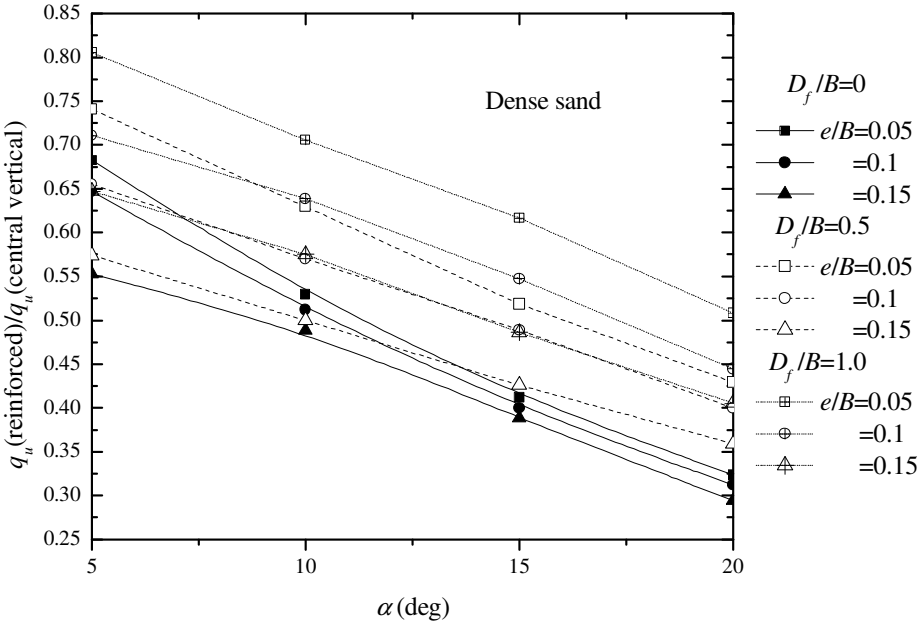

Figure 5.13: Plot of (q_u–reinforced)/(q_u–central vertical) for cases of eccentrically inclined loading in dense sand

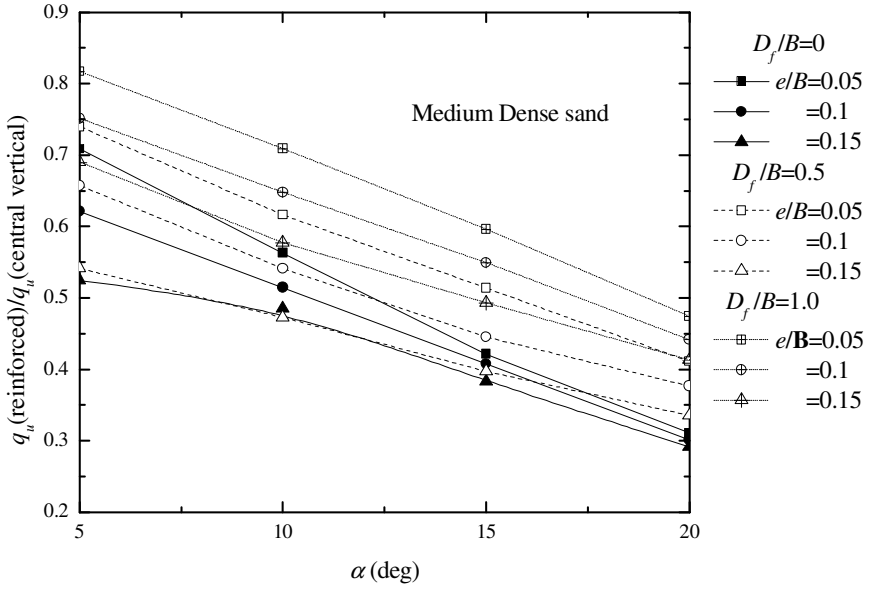

Figure 5.14: Plot of (q_u–reinforced)/(q_u–central vertical) for cases of eccentrically inclined loading in medium dense sand

Table 5.3. Ratio of ultimate bearing capacity q_u in both conditions i.e. partially compensated and reinforced case with ultimate bearing capacity q_u in central vertical condition

Sand Type	*e/B*	α	D_f/B	$q_{u(pc)}$ (kN/m^2)	$q_{u(R)}$ (kN/m^2)	$q_{u(pc)}/q_{u(cv)}$	$q_{u(R)}/q_{u(cv)}$
Dense sand	0.05	5	0	103.005	113.796	0.62	0.68
	0.05	10	0	76.518	88.29	0.46	0.53
	0.05	15	0	53.955	68.67	0.32	0.41
	0.05	20	0	34.826	53.955	0.21	0.32
	0.1	5	0	86.328	107.91	0.52	0.65
	0.1	10	0	62.784	85.347	0.38	0.51
	0.1	15	0	44.145	66.708	0.26	0.40
	0.1	20	0	29.430	51.993	0.18	0.31
	0.15	5	0	65.727	92.214	0.39	0.55
	0.15	10	0	51.993	81.423	0.31	0.49
	0.15	15	0	35.120	64.746	0.21	0.39
	0.15	20	0	23.544	49.05	0.14	0.29
	0.05	5.00	0.50	193.26	196.2	0.73	0.74
	0.05	10.00	0.50	160.88	166.77	0.61	0.63
	0.05	15.00	0.50	129.49	137.34	0.49	0.52
	0.05	20.00	0.50	98.10	113.796	0.37	0.43
	0.10	5.00	0.50	165.79	173.637	0.63	0.66
	0.10	10.00	0.50	137.34	151.074	0.52	0.57
	0.10	15.00	0.50	111.83	129.492	0.42	0.49
	0.10	20.00	0.50	85.35	105.948	0.32	0.40
	0.15	5.00	0.50	140.28	152.055	0.53	0.57
	0.15	10.00	0.50	116.74	132.435	0.44	0.50
	0.15	15.00	0.50	94.18	112.815	0.36	0.43
	0.15	20.00	0.50	72.59	95.157	0.27	0.36
	0.05	5.00	1.00	277.62	284.49	0.79	0.81
	0.05	10.00	1.00	239.36	249.174	0.68	0.71
	0.05	15.00	1.00	206.01	217.782	0.58	0.62

Sand Type	*e/B*	α	D_f/B	$q_{u(pc)}$ (kN/m^2)	$q_{u(R)}$ (kN/m^2)	$q_{u(pc)}/q_{u(cv)}$	$q_{u(R)}/q_{u(cv)}$
	0.05	20.00	1.00	166.77	179.523	0.47	0.51
	0.10	5.00	1.00	241.33	251.136	0.68	0.71
	0.10	10.00	1.00	212.88	225.63	0.60	0.64
	0.10	15.00	1.00	179.52	193.257	0.51	0.55
	0.10	20.00	1.00	143.23	156.96	0.41	0.44
	0.15	5.00	1.00	215.82	228.573	0.61	0.65
	0.15	10.00	1.00	188.35	203.067	0.53	0.58
	0.15	15.00	1.00	155.98	171.675	0.44	0.49
	0.15	20.00	1.00	126.55	143.226	0.36	0.41
Medium dense sand	0.05	5	0	63.765	71.613	0.63	0.71
	0.05	10	0	47.088	56.898	0.47	0.56
	0.05	15	0	32.373	42.5754	0.32	0.42
	0.05	20	0	19.62	31.392	0.19	0.31
	0.1	5	0	52.974	62.784	0.52	0.62
	0.1	10	0	38.4552	51.993	0.38	0.51
	0.1	15	0	26.9775	41.202	0.27	0.41
	0.1	20	0	16.677	30.411	0.17	0.30
	0.15	5	0	42.183	52.974	0.42	0.52
	0.15	10	0	31.392	49.05	0.31	0.49
	0.15	15	0	20.601	38.6514	0.20	0.38
	0.15	20	0	13.3416	29.43	0.13	0.29
	0.05	5	0.5	103.986	105.948	0.73	0.74
	0.05	10	0.5	84.8565	88.29	0.59	0.62
	0.05	15	0.5	67.8852	73.575	0.47	0.51
	0.05	20	0.5	50.031	58.86	0.35	0.41
	0.1	5	0.5	90.252	94.176	0.63	0.66
	0.1	10	0.5	72.594	77.499	0.51	0.54
	0.1	15	0.5	56.898	63.765	0.40	0.45
	0.1	20	0.5	43.164	53.955	0.30	0.38
	0.15	5	0.5	72.594	77.499	0.51	0.54

Sand Type	e/B	α	D_f/B	$q_{u(pc)}$ (kN/m^2)	$q_{u(R)}$ (kN/m^2)	$q_{u(pc)}/q_{u(cv)}$	$q_{u(R)}/q_{u(cv)}$
	0.15	10	0.5	60.822	67.689	0.42	0.47
	0.15	15	0.5	48.069	56.898	0.34	0.40
	0.15	20	0.5	36.297	48.069	0.25	0.34
	0.05	5	1	168.732	170.694	0.81	0.82
	0.05	10	1	144.207	148.131	0.69	0.71
	0.05	15	1	118.701	124.587	0.57	0.60
	0.05	20	1	92.214	99.081	0.44	0.47
	0.1	5	1	153.036	156.96	0.73	0.75
	0.1	10	1	129.492	135.378	0.62	0.65
	0.1	15	1	106.929	114.777	0.51	0.55
	0.1	20	1	84.366	92.214	0.40	0.44
	0.15	5	1	137.34	144.207	0.66	0.69
	0.15	10	1	112.815	120.663	0.54	0.58
	0.15	15	1	94.176	103.005	0.45	0.49
	0.15	20	1	75.537	86.328	0.36	0.41

Note: $q_{u(pc)}$=ultimate bearing capacity in partially compensated condition; $q_{u(R)}$=ultimate bearing capacity in reinforced condition; $q_{u(cv)}$=ultimate bearing capacity in central vertical condition.

Figures 5.15 and 5.16 show the plots of the ratio of (s_u/B- partially compensated) to (s_u/B- central vertical) for similar values of D_f/B, e/B (>0) and α (>0). As expected, in any model test program of this type, the plots are somewhat scattered. However, based on the results shown in these figures, the following general observations can be made:

- For any given value of D_f/B, the settlement ratio decreases with the angle of load inclination α.

- For the range of tests conducted, the average value of the settlement ratio is near about 0.6 at α = 5º and decrease to about 0.3 at α = 20º.

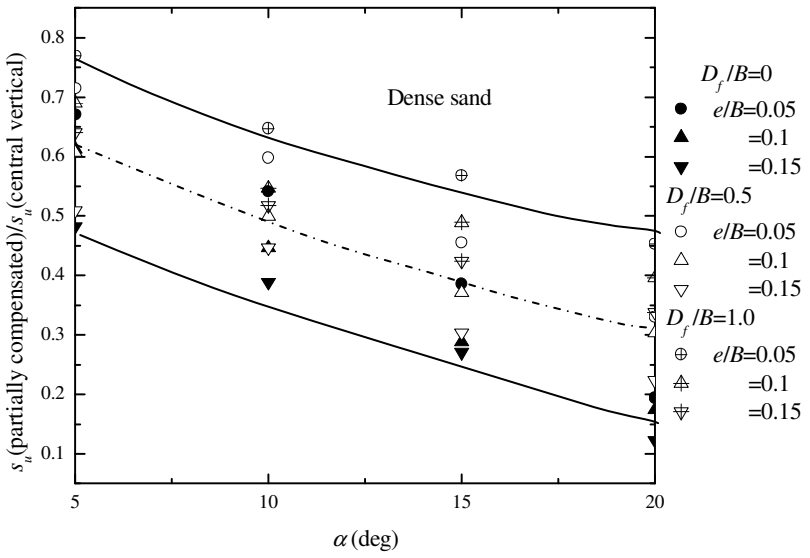

Figure 5.15: Plot of (s_u– partially compensated)/(s_u–central vertical) for cases of eccentrically inclined loading in dense sand

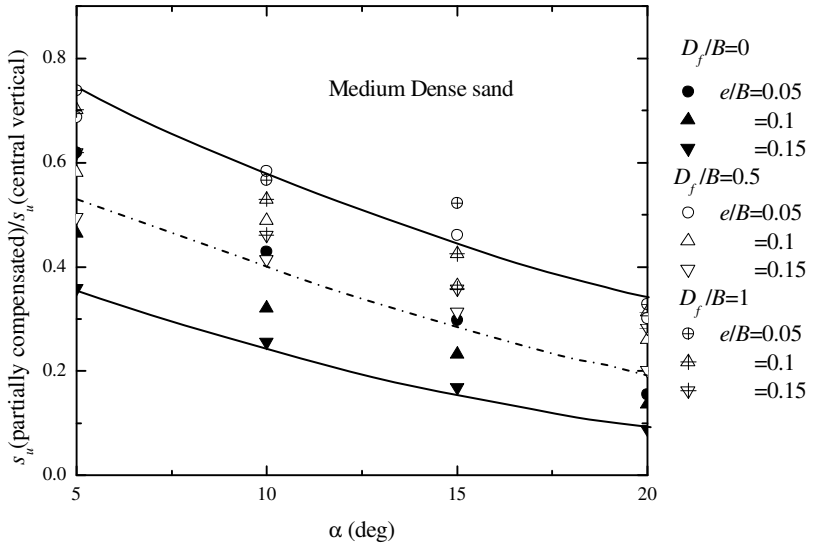

Figure 5.16: Plot of (s_u– partially compensated)/(s_u–central vertical) for cases of eccentrically inclined loading in medium dense sand

Figures 5.17 and 5.18 show the plots of the ratio of (s_u/B- reinforced) to (s_u/B-central vertical) obtained from the tests (s_u = average settlement along the center line of the foundation at ultimate load) for similar values of D_f/B, e/B (>0) and α (>0). However, based on the results shown in these figures, the following general observations can be made:

a. For any given value of D_f /B, the settlement ratio decreases with the angle of load inclination α.

b. For the range of tests conducted, the average value of the settlement ratio is near about 0.62 at α = 0º and decrease to about 0.36 at α = 20º.

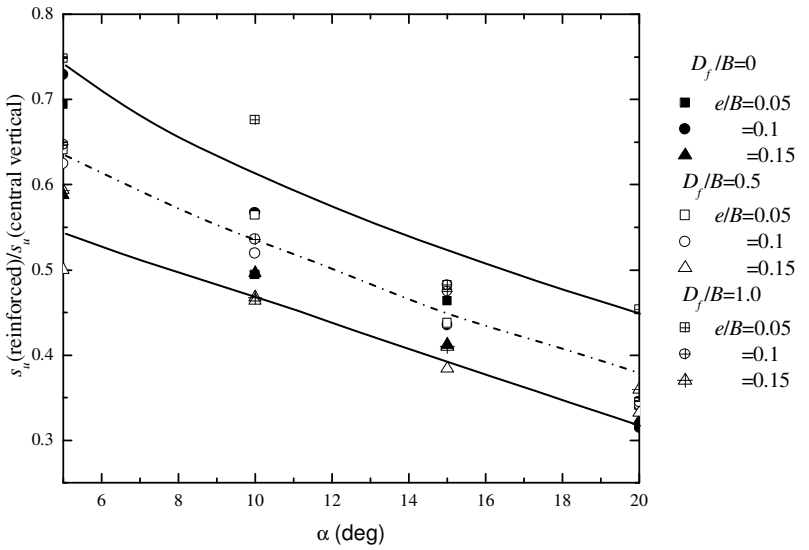

Figure 5.17: Plot of (s_u– reinforced)/(s_u–central vertical) for cases of eccentrically inclined loading in dense sand

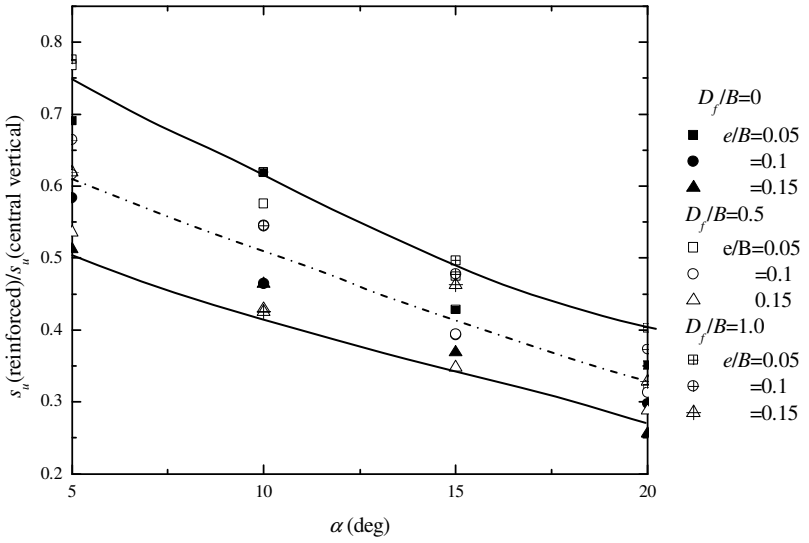

Figure 5.18: Plot of (s_u– reinforced)/(s_u–central vertical) for cases of eccentrically inclined loading in medium dense sand

Figures 5.19 and 5.20 show plots of the ultimate bearing capacities—(q_u–partially compensated) with α. These figures show that:

- For given values of D_f/B and e/B, the magnitude of (q_u– partially compensated) decreases with the load inclination α.
- For similar values of α and e/B, the magnitude of (q_u– partially compensated) shows a tendency to increase with the increase in embedment ratio.
- For a given value of D_f /B and α, the magnitude of (q_u– partially compensated) decreases with the increase in e/B.

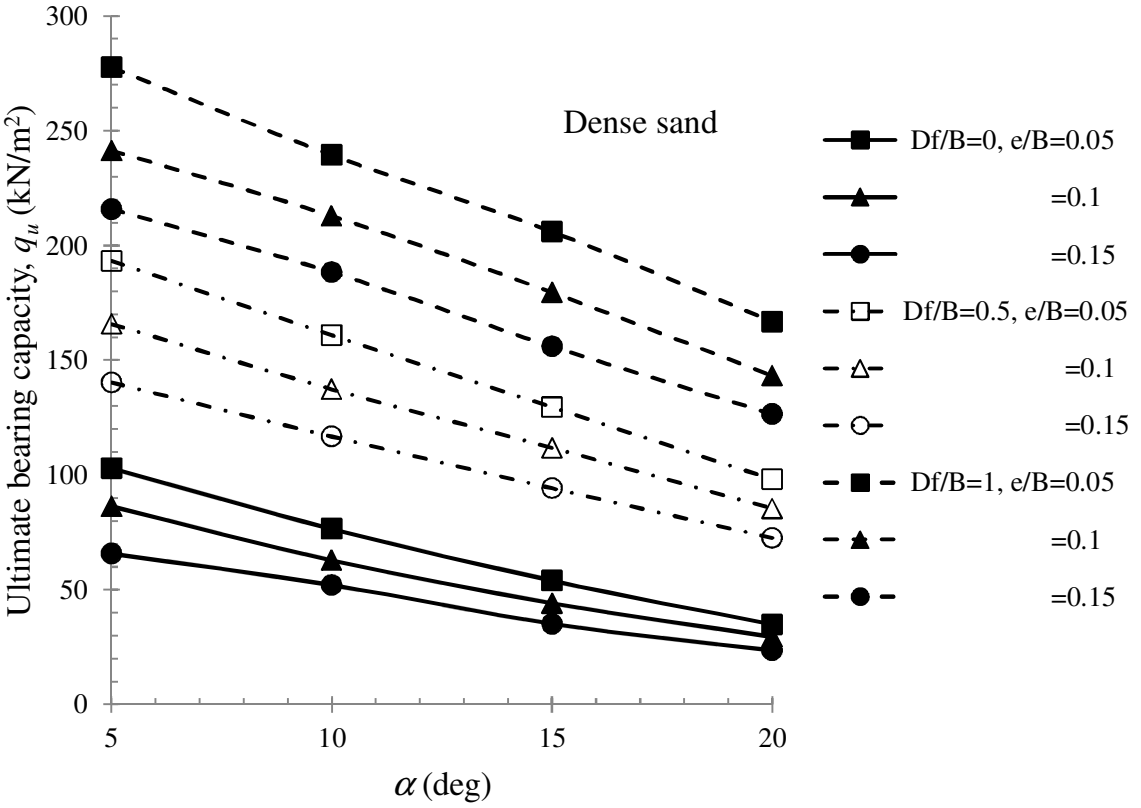

Figure 5.19: Plot of q_u with α for partially compensated case in dense sand

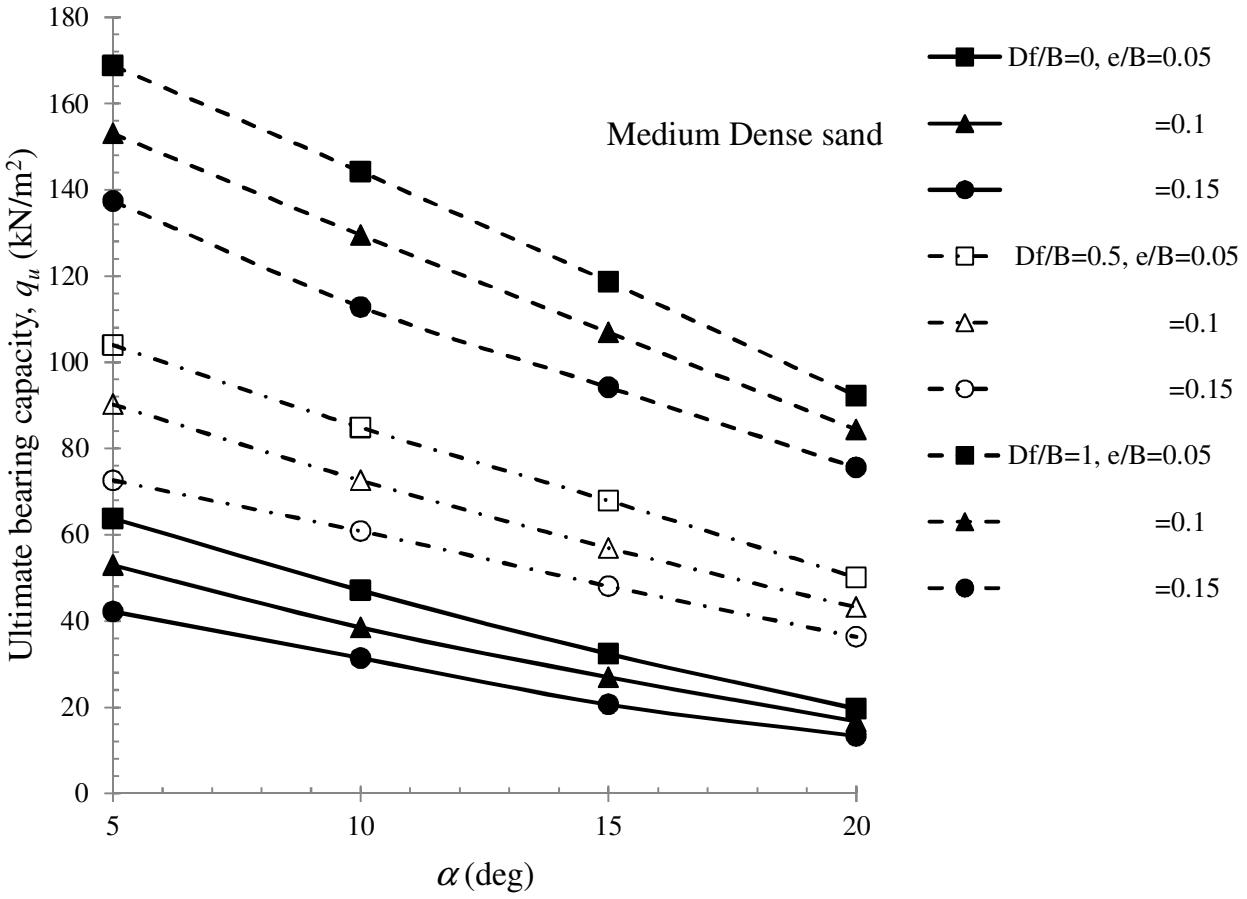

Figure 5.20: Plot of q_u with α for partially compensated case in medium dense sand

Figures 5.21 and 5.22 show plots of the ultimate bearing capacities—(q_u–reinforced) with α, for similar values of D_f/B, e/B (>0) and α (>0). These figures show that:

a. For given values of D_f/B and e/B, the magnitude of (q_u–reinforced) decreases with the load inclination α.

b. For surface condition, the variation of magnitude of (q_u–reinforced) for any value of e/B and α is in a narrow range.

c. For similar values of α and e/B, the magnitude of (q_u–reinforced) shows a tendency to increase with the increase in embedment ratio.

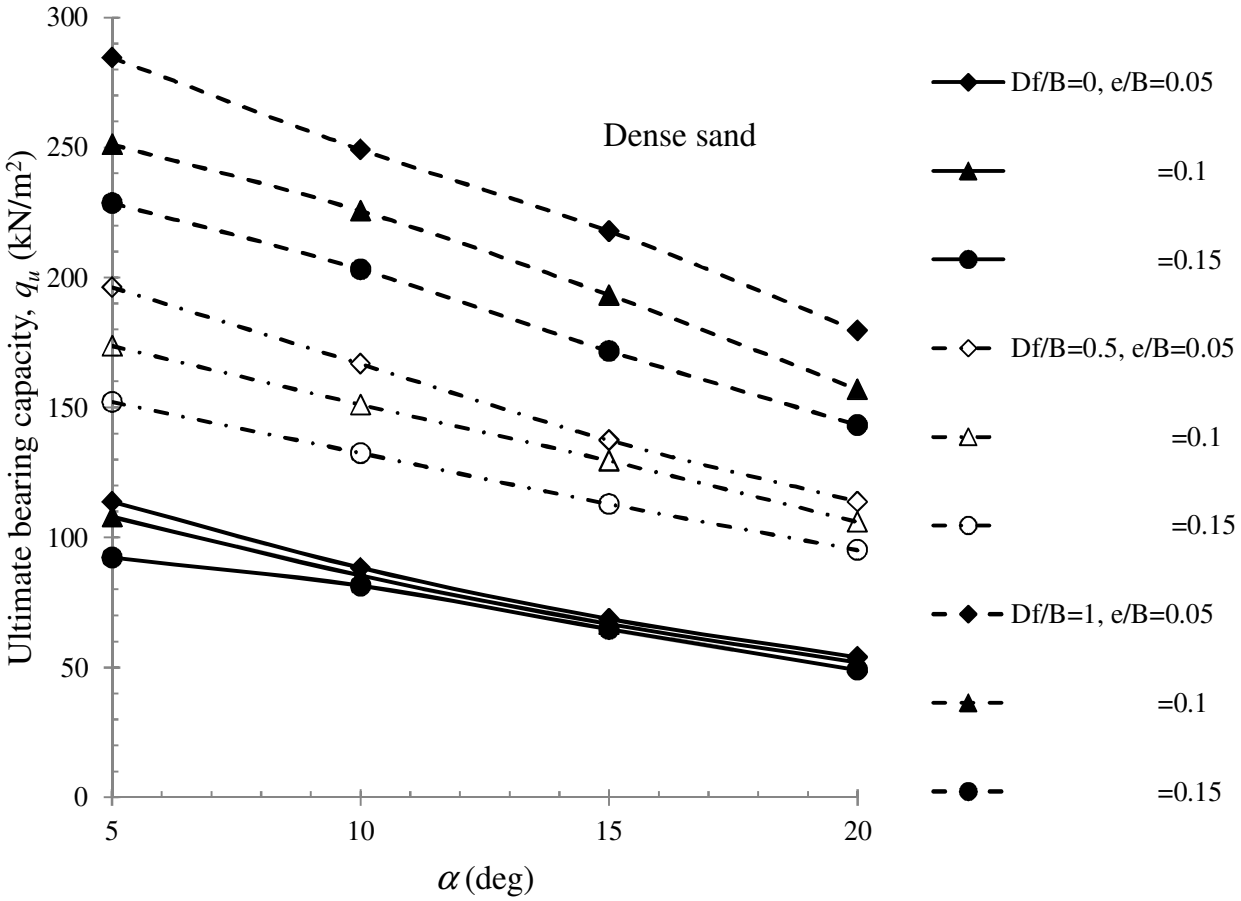

Figure 5.21: Plot of q_u with α for reinforced case in dense sand

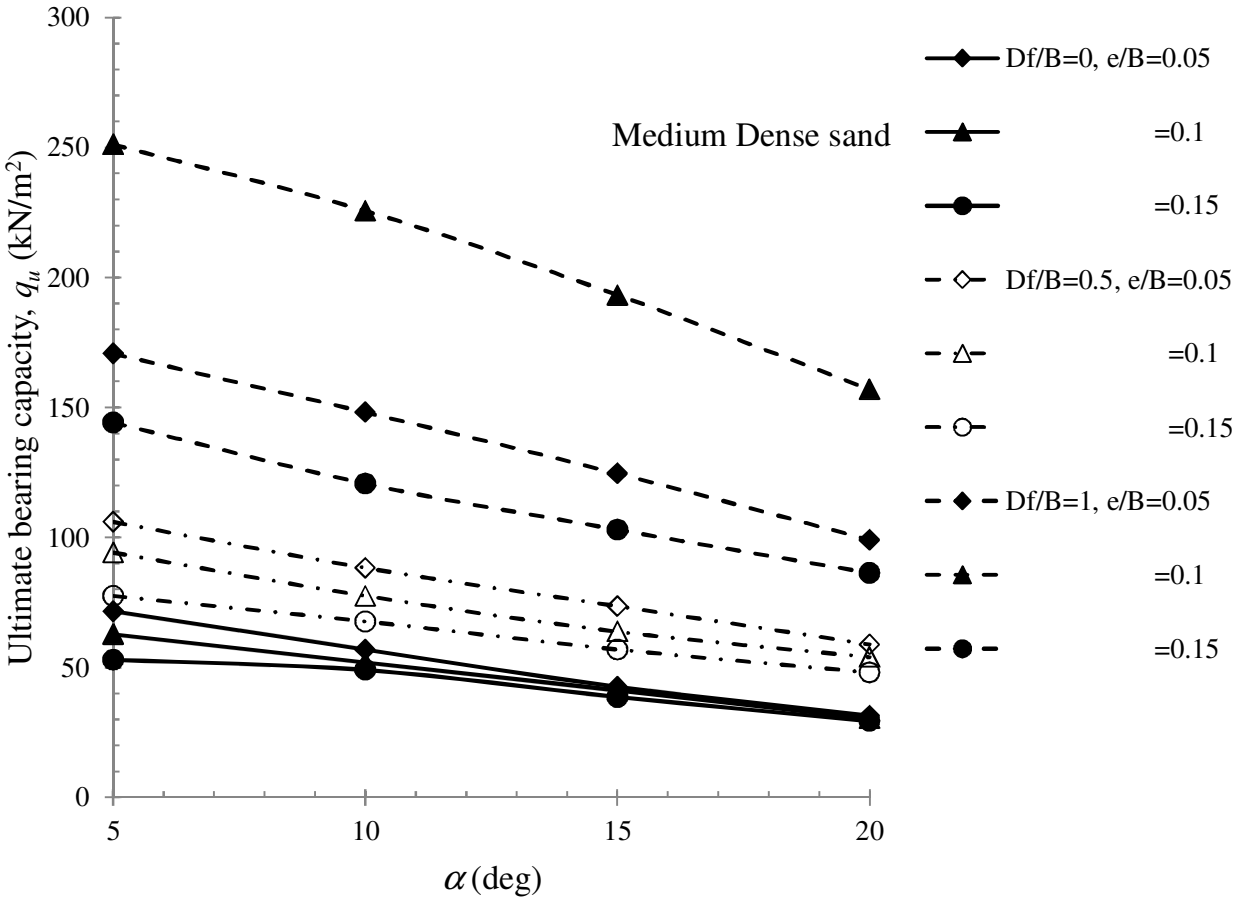

Figure 5.22: Plot of q_u with α for reinforced case in medium dense sand

The photographic images of failure surface developed at ultimate stage for one of the tests for reinforced condition is shown in Figure 5.23 for dense sand at $D_f/B = 1$, $\alpha = 20°$ and $e/B = 0.15$. The failure surface is well developed up to a depth of $2B$ from the bottom of the footing in the vertical direction and near about $2.5B$ in the horizontal direction from the edge of the footing.

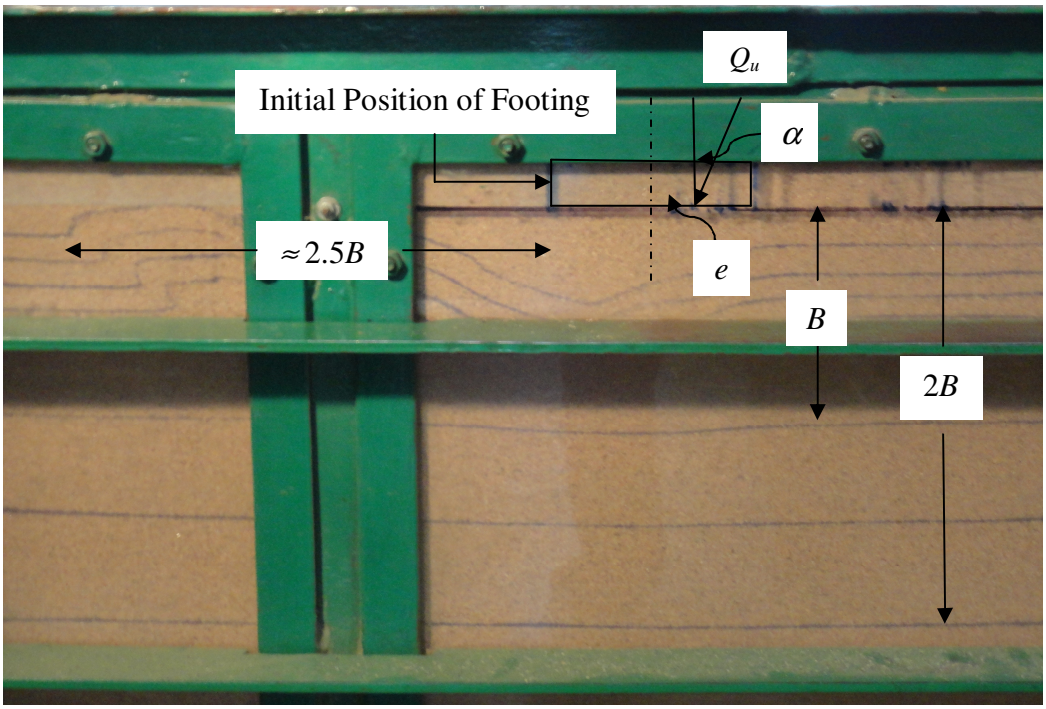

Figure 5.23: Photographic image of the failure surface observed in dense sand at D_f/B = 1, $\alpha = 20°$ and $e/B = 0.15$ in *reinforced* condition

5.4 Analysis of Test Results

In Chapter 4, a two-step procedure is adopted to analyse the experimental ultimate bearing capacities obtained for tests conducted with eccentrically inclined load for the *partially compensated* case. According to that analysis, the reduction factor *RF* may be expressed as

$$RF = \frac{q_{u(D_f/B,\, e/B,\, \alpha/\phi)}}{q_{u(D_f/B,\, e/B=0,\, \alpha/\phi=0)}} = \left[1 - a\left(\frac{e}{B}\right)^m\right]\left(1 - \frac{\alpha}{\phi}\right)^n \qquad (5.3)$$

where $q_{u(D_f/B,\, e/B,\, \alpha/\phi)}$ = ultimate bearing capacity with eccentricity ratio e/B and inclination ratio α/ϕ at an embedment ratio D_f/B and $q_{u(D_f/B,\, e/B=0,\, \alpha/\phi=0)}$ = ultimate bearing capacity with centric vertical loading ($e/B = 0$ and $\alpha/\phi = 0$) at the same embedment ratio D_f/B.

Similar procedure is adopted in this case to analyse the test results given in Tables 5.4 and 5.5. As a first step, considering the tests with vertical load (α = 0, i.e. α/ϕ = 0) regression analyses are performed which give the values of a and m. These values are mentioned along with the R^2 values in Table 5.6. The average values of a and m are 2.14 and 0.92 respectively; however, for simplicity and considering the scattering in an experimental program like this, we can approximate

- $a \approx 2$
- $m \approx 1$

These values are the same as those reported in Chapter 4. Substituting these approximate values of a and m into Eq. (5.3), we obtain

$$RF = \left[1 - 2\left(\frac{e}{B}\right)\right]\left(1 - \frac{\alpha}{\phi}\right)^n \tag{5.4}$$

In the second step, Eq. (5.4) is used to conduct regression analyses for the ultimate bearing capacities obtained with eccentrically inclined loading (Table 5.4) to determine the value of n at varying embedment ratios (for $\alpha > 0$ and $e/B > 0$). These values are given in Table 5.6 along with the R^2 values. It appears that these values of n can be approximated as

$$n \approx 1.5 - 0.7\left(\frac{D_f}{B}\right) \tag{5.5}$$

Table 5.7 also shows the variation of n with embedment ratio calculated from Eq. (5.5). These values are fairly close to the experimental values, thus it can be concluded that Eq. (5.5) is a reasonable approximation. Combining Eqs. (5.4) and (5.5)

$$RF = \left[1 - 2\left(\frac{e}{B}\right)\right]\left(1 - \frac{\alpha}{\phi}\right)^{1.5-0.7(D_f/B)} \tag{5.6}$$

Table 5.4 shows the experimental variation of *RF* in Column 6, and the *RF* calculated based on Eq. (5.6) is shown in Column 7. Column 8 of Table 5.3 shows the deviations of the reduction factor calculated using Eq. (5.6) compared to those obtained experimentally. In most cases the deviation is ±10% or less. There are only a few cases where the deviation is about 15% and about 30% in one case. Hence, Eq. (5.6) can be used to obtain a reasonable prediction of the reduction factor and, thus, the ultimate bearing capacity for shallow strip foundation with eccentrically inclined load via Eq. (5.3).

Table 5.4. Model Test Results

Sand type (1)	$\frac{D_f}{B}$ (2)	α (deg) (3)	$\frac{e}{B}$ (4)	Experimental q_u (kN/m^2) (5)	Experimental *RF* (6)	Calculated *RF* [Eq. (5.6)] (7)	Deviation—$\frac{\text{Col. 7} - \text{Col. 6}}{\text{Col. 7}}$ (%) (8)
Dense	0	0	0	**166.77**	1.0	1.0	0
	0	5	0.05	113.8	0.682	0.74	7.76
	0	5	0.1	107.91	0.647	0.66	1.59
	0	5	0.15	92.21	0.553	0.58	3.89
	0	10	0.05	88.29	0.529	0.59	10.32
	0	10	0.1	85.35	0.512	0.52	2.47
	0	10	0.15	81.42	0.488	0.46	-6.34
	0	15	0.05	68.67	0.412	0.45	9.02
	0	15	0.1	66.71	0.4	0.4	0.57
	0	15	0.15	64.75	0.388	0.35	-10.3
	0	20	0.05	53.96	0.324	0.33	1.24
	0	20	0.1	51.99	0.312	0.29	-7.06
	0	20	0.15	49.05	0.294	0.25	-15.43
	0.5	0	0	264.87	1.0	1.0	0
	0.5	5	0.05	196.2	0.741	0.77	4.34
	0.5	5	0.1	173.64	0.656	0.69	4.76
	0.5	5	0.15	152.06	0.574	0.60	4.68

Table 5.3 (Continued)

Sand type (1)	$\frac{D_f}{B}$ (2)	α (deg) (3)	$\frac{e}{B}$ (4)	Experimental q_u (kN/m^2) (5)	Experimental RF (6)	Calculated RF [Eq. (5.6)] (7)	Deviation—$\frac{\text{Col. 7} - \text{Col. 6}}{\text{Col. 7}}$ (%) (8)
	0.5	10	0.05	166.77	0.630	0.65	3.34
	0.5	10	0.1	151.07	0.570	0.58	1.49
	0.5	10	0.15	132.44	0.5	0.51	1.3
	0.5	15	0.05	137.34	0.519	0.53	2.41
	0.5	15	0.1	129.49	0.489	0.47	-3.52
	0.5	15	0.15	112.82	0.426	0.41	-3.07
	0.5	20	0.05	113.8	0.43	0.41	-3.59
	0.5	20	0.1	105.95	0. 4	0.37	-8.51
	0.5	20	0.15	95.16	0.359	0.32	-11.38
	1.0	0	0	353.16	1.0	1.0	0
	1.0	5	0.05	284.49	0.806	0.81	0.63
	1.0	5	0.1	251.14	0.711	0.72	1.31
	1.0	5	0.15	228.57	0.647	0.63	-2.65
	1.0	10	0.05	249.17	0.706	0.72	1.83
	1.0	10	0.1	225.63	0.639	0.64	-0.01
	1.0	10	0.15	203.07	0.575	0.56	-2.86
	1.0	15	0.05	217.78	0.617	0.62	1.14
	1.0	15	0.1	193.26	0.547	0.55	1.3
	1.0	15	0.15	171.68	0.486	0.49	-0.2
	1.0	20	0.05	179.52	0.508	0.53	3.18
	1.0	20	0.1	156.96	0.444	0.47	4.76
	1.0	20	0.15	143.23	0.406	0.41	0.68
Medium dense	0	0	0	**101.04**	1.0	1.0	0
	0	5	0.05	71.61	0.709	0.73	2.4
	0	5	0.1	62.78	0.621	0.65	3.73
	0	5	0.15	52.97	0.524	0.56	7.17
	0	10	0.05	56.9	0.563	0.57	0.37
	0	10	0.1	51.99	0.515	0.5	-2.42
	0	10	0.15	49.05	0.485	0.44	-10.43
	0	15	0.05	42.58	0.421	0.42	-0.74
	0	15	0.1	41.2	0.408	0.37	-9.67
	0	15	0.15	38.65	0.383	0.33	-17.58
	0	20	0.05	31.39	0.311	0.29	-8.28
	0	20	0.1	30.41	0.301	0.26	-18.01
	0	20	0.15	29.43	0.291	0.22	-30.52
	0.5	0	0	143.23	1.0	1.0	0
	0.5	5	0.05	105.95	0.74	0.76	3.11
	0.5	5	0.1	94.18	0.658	0.68	3.11
	0.5	5	0.15	77.5	0.541	0.59	8.87

Table 5.3 (Continued)

Sand type (1)	$\frac{D_f}{B}$ (2)	α (deg) (3)	$\frac{e}{B}$ (4)	Experimental q_u (kN/m^2) (5)	Experimental RF (6)	Calculated RF [Eq. (5.6)] (7)	Deviation—$\frac{\text{Col. 7} - \text{Col. 6}}{\text{Col. 7}}$ (%) (8)
	0.5	10	0.05	88.29	0.616	0.63	2.15
	0.5	10	0.1	77.5	0.541	0.56	3.38
	0.5	10	0.15	67.69	0.473	0.49	3.55
	0.5	15	0.05	73.58	0.514	0.5	-2.71
	0.5	15	0.1	63.77	0.445	0.44	-0.14
	0.5	15	0.15	56.9	0.397	0.39	-2.12
	0.5	20	0.05	58.86	0.411	0.37	-9.7
	0.5	20	0.1	53.96	0.377	0.33	-13.13
	0.5	20	0.15	48.07	0.336	0.29	-15.18
	1.0	0	0	208.95	1.0	1.0	0
	1.0	5	0.05	170.69	0.817	0.8	-1.78
	1.0	5	0.1	156.96	0.751	0.71	-5.29
	1.0	5	0.15	144.21	0.69	0.62	-10.55
	1.0	10	0.05	148.13	0.709	0.7	-0.95
	1.0	10	0.1	135.38	0.648	0.62	-3.79
	1.0	10	0.15	120.66	0.577	0.55	-5.73
	1.0	15	0.05	124.59	0.596	0.6	0.31
	1.0	15	0.1	114.78	0.549	0.53	-3.32
	1.0	15	0.15	103.01	0.493	0.47	-5.97
	1.0	20	0.05	99.08	0.474	0.49	3.06
	1.0	20	0.1	92.21	0.441	0.43	-1.5
	1.0	20	0.15	86.33	0.413	0.38	-8.59

Table 5.5. Experimental Ultimate Bearing Capacity for Vertical Loading ($\alpha = 0$)

Sand type	$\frac{D_f}{B}$	$\frac{e}{B}$	q_u (kN/m^2)
Dense	0	0.05	133.42
	0	0.10	109.87
	0	0.15	86.33
	0.5	0.05	226.61
	0.5	0.10	195.22
	0.5	0.15	164.81
	1.0	0.05	313.92
	1.0	0.10	278.60
	1.0	0.15	245.26
Medium Dense	0	0.05	84.37

Sand type	$\frac{D_f}{B}$	$\frac{e}{B}$	q_u (kN/m^2)
	0	0.10	68.67
	0	0.15	54.94
	0.5	0.05	123.61
	0.5	0.10	103.99
	0.5	0.15	87.31
	1.0	0.05	193.26
	1.0	0.10	175.60
	1.0	0.15	156.96

Table 5.6. Values of a and m based on Regression Analyses (for $\alpha = 0$ —Tables 5.1 and 5.2) along with R^2 value

Sand type	$\frac{D_f}{B}$	a	m	R^2
Dense	0	2.23	0.81	0.99
	0.5	2.0	0.88	1.0
	1.0	1.76	0.92	1.0
Medium Dense	0	2.59	0.91	0.99
	0.5	2.31	0.93	0.99
	1.0	1.97	1.09	0.99
Average		2.14 ≈ 2.0	0.92 ≈ 1	

Table 5.7. Values of n Based on Regression Analyses (for $\alpha > 0$ and $e/B \geq 0$) along with R^2 value

Sand type	$\frac{D_f}{B}$	n	R^2	n [from Eq. (5.5)]
Dense	0	1.53	0.93	1.5
	0.5	1.13	0.96	1.15
	1.0	0.83	0.99	0.8
Medium Dense	0	1.37	0.98	1.5
	0.5	1.11	0.94	1.15
	1.0	0.75	0.96	0.8

5.5 Comparison

5.5.1 Comparison with Loukidis et al. [2008]

Loukidis et al. (2008) developed an equation for combined inclination-eccentricity factor f_{ie} using finite element method for surface foundation ($D_f/B = 0$) as given by Eq. 4.13 and 4.14 as discussed in Chapter 4. This equation can take the load inclination clockwise as well as anti-clockwise. A comparison has been made in Chapter 4 for the partially compensated condition by using angles in anti-clockwise direction. In this chapter the comparison has been made with results from present analysis with results by using Eqs. proposed by Loukidis et al. (2008) in clockwise direction which simulates to the condition of reinforced footing. It is to be noted that the equations given by Loukidis et al. (2008) are for surface footings (D_f/B=0) whereas the present prediction is for all depth of footing ($0 \leq D_f/B \leq 1$).

The reduction factor *RF* corresponding to Loukidis et al. (2008) can be written as

$$RF = \frac{f_{ie}}{\cos\alpha} \tag{5.7}$$

The comparisons have been shown in Figures 5.24 and 5.25. Also the comparisons are presented in Table 5.8. It appears that the results from both analyses are in good agreement.

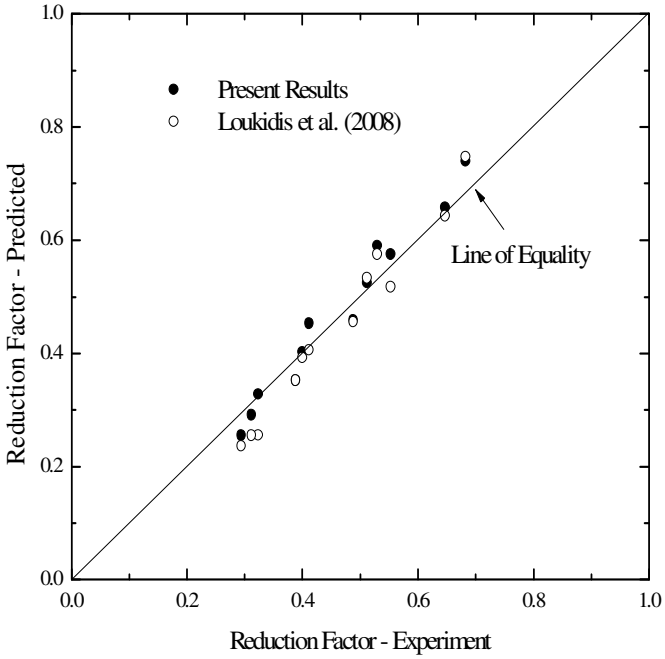

Figure 5.24: Comparison of Present results with Loukidis et al. (2008) for dense sand.

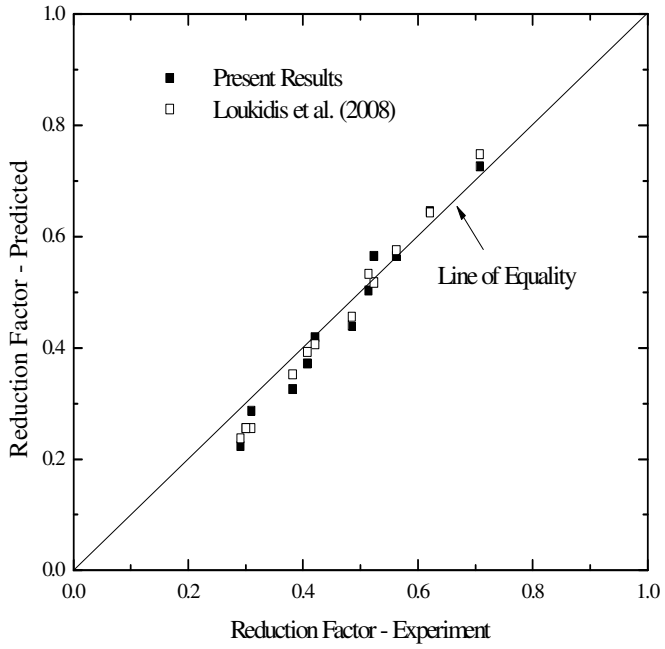

Figure 5.25: Comparison of Present results with Loukidis et al. (2008) for medium dense sand.

Table 5.8. Comparison of Reduction Factors Obtained from Eq. (5.7) with Eq. (5.6) for $D_f/B = 0$

Experiment No. (1)	α (deg) (2)	$\frac{e}{B}$ (3)	Loukidis et al. (2008) *RF* [Eq. (5.7)] (4)	Dense sand [Eq. (5.6)] (5)	Medium dense sand [Eq. (5.6)] (6)
1	5	0.05	0.748	0.74	0.726
2	5	0.1	0.643	0.658	0.645
3	5	0.15	0.517	0.575	0.565
4	10	0.05	0.575	0.590	0.565
5	10	0.1	0.533	0.525	0.502
6	10	0.15	0.456	0.459	0.44
7	15	0.05	0.406	0.453	0.418
8	15	0.1	0.393	0.402	0.372
9	15	0.15	0.352	0.352	0.325
10	20	0.05	0.256	0.328	0.287
11	20	0.1	0.255	0.291	0.255
12	20	0.15	0.237	0.255	0.223

5.6 Conclusions

Analysis of a number of laboratory model test results for the ultimate bearing capacity of shallow strip foundation under eccentrically inclined load is presented. This study relates to the case of *reinforced* type of loading [Figure 5.1(b)]. It complements the previous study as mentioned in Chapter 4 which is for *partially compensated* type of loading. Based on this study and the results of the Chapter 4, the following general conclusions can be drawn.

- For $\alpha = 0$ and $0 \le D_f/B \le 1$,

$$RF = 1 - 2\left(\frac{e}{B}\right)$$

This is common to *reinforced* and *partially compensated* cases.

- For $e/B = 0$, $0 \le D_f/B \le 1$ and $\alpha > 0$, the reduction factor

$$RF = \left(1 - \frac{\alpha}{\phi}\right)^{2-(D_f/B)}$$

This is common to *reinforced* and *partially compensated* cases.

- For *partially compensated* case with $e/B > 0$

$$RF = \left[1 - 2\left(\frac{e}{B}\right)\right]\left(1 - \frac{\alpha}{\phi}\right)^{2-(D_f/B)} \quad \text{[Eqn. 4.7]}$$

- For *reinforced* case with $e/B > 0$

$$RF = \left[1 - 2\left(\frac{e}{B}\right)\right]\left(1 - \frac{\alpha}{\phi}\right)^{1.5-0.7(D_f/B)}$$

- For given values of D_f/B and e/B, the magnitude of (q_u–reinforced)/(q_u–partially compensated) increases with the load inclination α.
- For similar values of α and e/B, the above ratio shows a tendency to decrease with the increase in embedment ratio (D_f/B).
- For a given value of D_f/B and α, the ratio (q_u–reinforced)/(q_u–partially compensated) increases with the increase in e/B.
- At ultimate load, the settlement ratio of s_u in the *reinforced* case to s_u in the *partially compensated* case can be approximated as follows

$$\frac{s_u - \text{reinforced}}{s_u - \text{partially compensated}} \approx \begin{cases} 1 \text{ at } \alpha = 5^\circ \\ \text{to} \\ 1.4 \text{ at } \alpha = 20^\circ \end{cases}$$

- For *reinforced* case, the comparison of results from present prediction with Loukidis et al. (2008) is in good agreement for surface condition ($D_f/B = 0$).

6. PREDICTION OF ULTIMATE BEARING CAPACITY OF ECCENTRICALLY INCLINED LOADED STRIP FOOTING BY ANN: PART I

6.1 Introduction

The computation of ultimate bearing capacity of shallow foundations on granular soil when subjected to eccentric and inclined load has been explained in Chapter 4 by using reduction factor method. The analysis gives fairly good prediction as compared to other existing theories. In this chapter, it is desired to predict the ultimate bearing capacity under above conditions using neural network model. This model uses a database of large number of model tests carried out in a calibration tank as discussed in Chapter 4 to estimate the reduction factor in case when the resultant load (eccentric and inclined) acts towards the center line of the footing [Figure 6.1]. The concept of Reduction Factor (*RF*) i.e. the ratio of the ultimate bearing capacity of the foundation subjected to an eccentrically inclined load to the ultimate bearing capacity of the foundation subjected to a centric vertical load has been adopted.

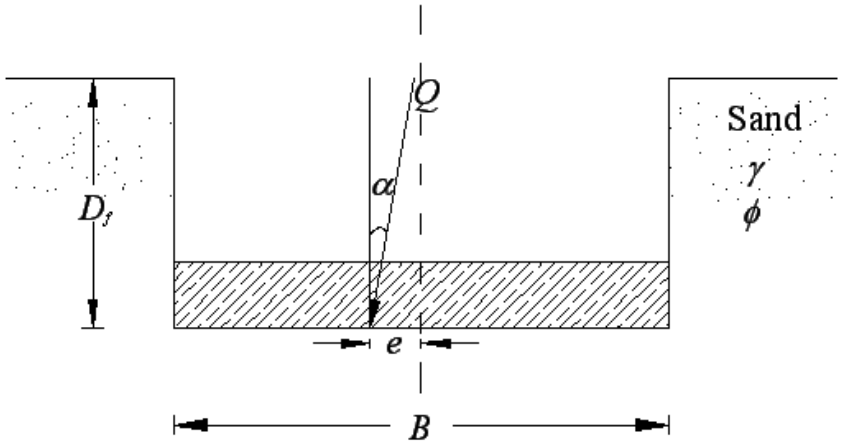

Figure 6.1: Partially Compensated Footing (Perloff and Baron 1976)

6.2 Overview of Artificial Neural Network

6.2.1 Biological model of a neuron

The neuron is the basic unit for processing the signals in the biological nervous system. Each neuron receives and processes the signals from other neurons through the input paths called dendrites (Figure 6.2). The dendrites collect the signals and send them to the cell body, or the soma of the neuron, which sums the incoming signals. If the charge of the collected signals is strong enough, the neuron is activated and produces an output signal; otherwise the neuron remains inactive. The output signal is then transmitted to the neighboring neurons through an output structure called the axon. The axon of a neuron divides and connects to dendrites of the neighboring neurons through junctions called synapses.

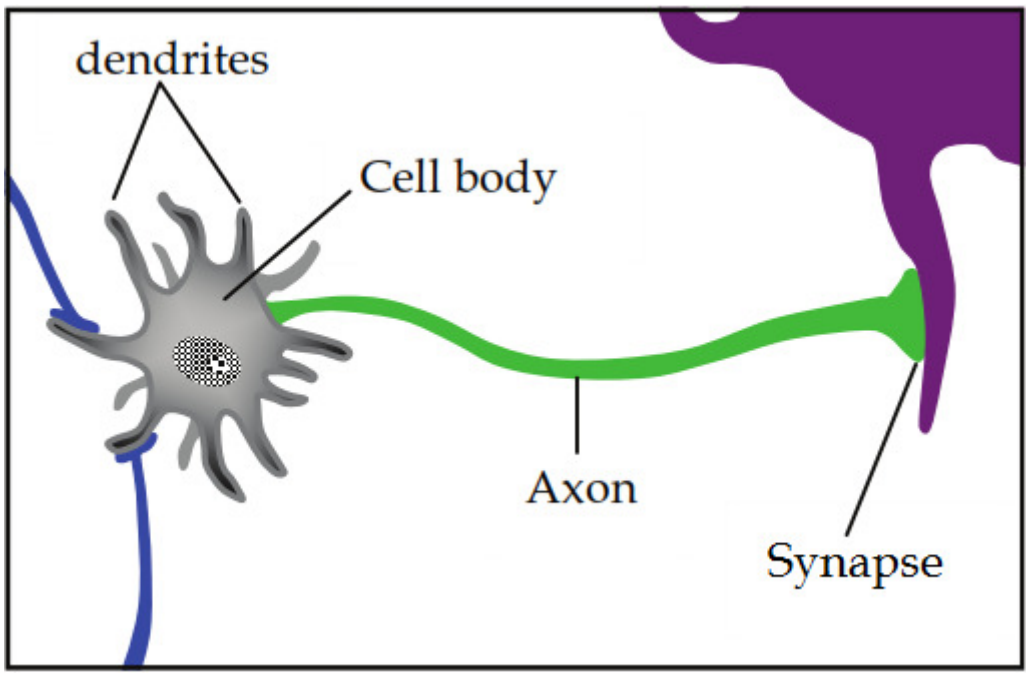

Figure 6.2: Biological neuron (after Park, 2011)

6.2.2 The concept of Artificial Neural Network

Artificial neural networks (ANNs) are a form of artificial intelligence, which, in their architecture, attempt to simulate the biological structure of the human brain and nervous system (Shahin et al. 2002). Typically, the architecture of ANNs consists of a series of processing elements (PEs), or nodes, that are usually arranged in layers: an input layer, an output layer and one or more hidden layers, as shown in Figure 6.3. The determination of number of hidden layers and the number of neurons in each hidden layer is a significant task. The number of hidden layers is usually determined first and is a critical step. The number of hidden layers required generally depends on the complexity of the relationship between the input parameters and the output value (Park, 2011).

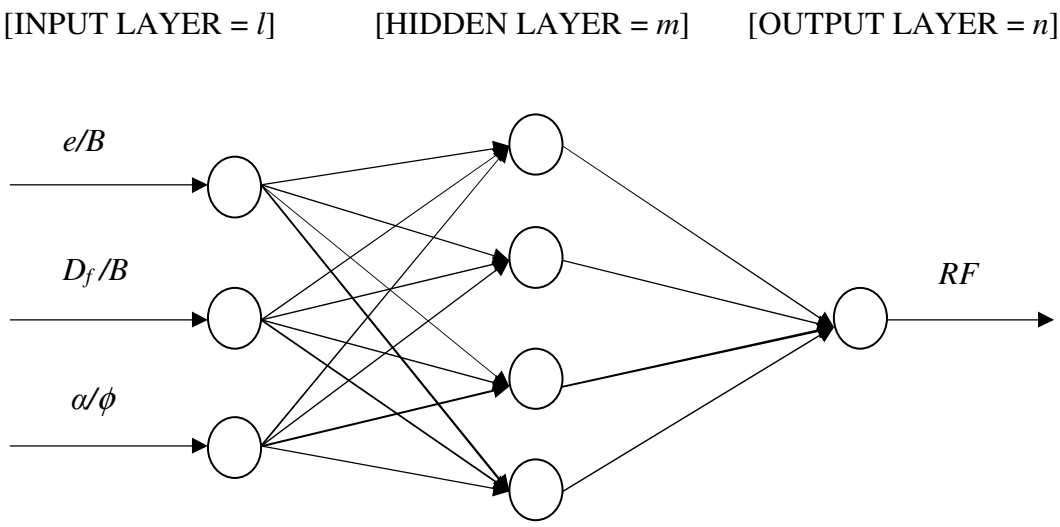

Figure 6.3: The ANN Architecture.

ANNs learn from data set presented to them and use these data to adjust their weights in an attempt to capture the relationship between the model input variables and the corresponding outputs. Consequently, Artificial Neural Networks do not need prior knowledge regarding the nature of the mathematical relationship between the input and

output variables. This is one of the main benefits of ANNs over most empirical and statistical methods (Jaksa et al. 2008).

6.2.3 Application of ANN in Geotechnical Engineering

Based on the literature review it has been reported that ANNs have been applied successfully to many geotechnical engineering problems such as predicting pile capacity, shallow foundations, modelling soil behaviour, site characterisation, earth retaining structures, settlement of structures, slope stability, design of tunnels and underground openings, liquefaction, soil permeability and hydraulic conductivity, soil compaction, soil swelling and classification of soils. A comprehensive review report on the applications of ANNs in geotechnical engineering is presented by Shahin et al. (2008) and Park (2011).

6.3 Problem Definition

Extensive laboratory model tests have been conducted on a strip footing lying over sand bed subjected to an eccentrically inclined load (the line of load application is towards the center line of the footing as shown in Figure 6.1) to determine the ultimate bearing capacity. Based on the laboratory test results, a neural network model is developed to predict the ultimate bearing capacity of the footing. The ultimate bearing capacity of footing at any depth of embedment subjected to eccentric and inclined load can be determined by knowing the ultimate bearing capacity of footing subjected to centric and vertical load at that depth of embedment and the corresponding reduction factor. This reduction factor (*RF*) is the ratio of the ultimate bearing capacity of the foundation subjected to an eccentrically inclined load to the ultimate bearing capacity of the foundation subjected to a centric vertical load at the same depth of embedment. Different

sensitivity analysis is carried out to evaluate the parameters affecting the reduction factor. Emphasis is placed on the construction of neural interpretation diagram, based on the weights of the developed neural network model, to find out direct or inverse effect of input parameters on the output. A prediction model equation is established with the weights of the neural network as the model parameters. Finally, the predictions from ANN, and those from developed empirical equation in Chapter 4, are compared with the existing theories.

6.4 Database and Preprocessing

The extensive database of laboratory experimental data as presented in Chapter 4 has been considered for the analysis in this chapter. The laboratory test data consist of parameters like load eccentricity (e), load inclination (α), embedment ratio (D_f /B), friction angle (ϕ) and ultimate bearing capacity (q_u). One hundred and twenty numbers of laboratory model tests results as conducted in this series have been considered for analysis. In this ANN model, the three dimensionless input parameters are e/B, α/ϕ and D_f /B, and the output is the reduction factor (RF). The reduction factor (RF) is given by

$$RF = \frac{q_{u(D_f/B,\, e/B,\, \alpha/\phi)}}{q_{u(D_f/B,\, e/B=0,\, \alpha/\phi=0)}} \tag{6.1}$$

where $q_{u(D_f/B,\, e/B,\, \alpha/\phi)}$ = ultimate bearing capacity with eccentricity ratio e/B and inclination ratio α/ϕ at an embedment ratio D_f /B and $q_{u(D_f/B,\, e/B=0,\, \alpha/\phi=0)}$ = ultimate bearing capacity with centric vertical loading (i.e., e/B = 0 and α/ϕ = 0) at the same embedment ratio D_f/B.

Out of 120 test records shown in Table 6.1, 90 tests are considered for training and the remaining 30 are reserved for testing. Each record represents a complete model test where an eccentrically inclined loaded strip footing is subjected to failure. All the variables (i.e. inputs and output) are normalized in the range [-1, 1] before training. A feedforward backpropagation neural network is used with hyperbolic tangent sigmoid function and linear function as the transfer function. The backpropagation algorithm trains the network by iteratively adjusting all the connection weights among neurons, with the goal of finding a set of connection weights that minimizes the error of the network, i.e. sum-of-the-squares between the actual and predicted output (least squares error function, Olden 2000). A feedforward neural network has one-way connections to other units so that each unit can only be connected to units in later layers. Inputs are passed from layer to layer in a feed-forward manner. In the model, each input unit is connected to each hidden unit and then each hidden unit is connected to each output unit (Ozesmi and Ozesmi 1999). The network is trained (learning) with Levenberg–Marquardt (LM) algorithm as it is efficient in comparison to gradient descent backpropagation algorithm (Goh et al. 2005; Das and Basudhar 2006). The ANN has been implemented using MATLAB V 7.11.0 (R2010b).

Table 6.1. Dataset used for training and testing of ANN model [Chapter 4]

Data Type (1)	Expt. No. (2)	$\frac{e}{B}$ (3)	$\frac{D_f}{B}$ (4)	$\frac{\alpha}{\phi}$ (5)	Experimental q_u (kN/m^2) (6)	Experimental RF [Eq. (6.1)] (7)	Calculated RF [Eq. (6.17)] (8)
Training	1	0.05	0	0	133.42	0.800	0.900
	2	0.1	0	0	109.87	0.659	0.800
	3	0.15	0	0	86.33	0.518	0.700
	4	0	0	0.123	128.51	0.771	0.770
	5	0.05	0	0.123	103.01	0.618	0.693
	6	0.1	0	0.123	86.33	0.518	0.616
	7	0	0	0.245	96.14	0.576	0.570
	8	0.05	0	0.245	76.52	0.459	0.513
	9	0.15	0	0.245	51.99	0.312	0.399
	10	0	0	0.368	66.71	0.400	0.400
	11	0.1	0	0.368	44.15	0.265	0.320
	12	0.15	0	0.368	35.12	0.211	0.280
	13	0.05	0	0.49	34.83	0.209	0.234
	14	0.1	0	0.49	29.43	0.176	0.208
	15	0.15	0	0.49	23.54	0.141	0.182
	16	0	0.5	0	264.87	1.000	1.000
	17	0.05	0.5	0	226.61	0.856	0.900
	18	0.1	0.5	0	195.22	0.737	0.800
	19	0	0.5	0.123	223.67	0.844	0.822
	20	0.05	0.5	0.123	193.26	0.730	0.740
	21	0.15	0.5	0.123	140.28	0.530	0.575
	22	0	0.5	0.245	186.39	0.704	0.656
	23	0.1	0.5	0.245	137.34	0.519	0.525
	24	0.15	0.5	0.245	116.74	0.441	0.459
	25	0.05	0.5	0.368	129.49	0.489	0.453
	26	0.1	0.5	0.368	111.83	0.422	0.402
	27	0.15	0.5	0.368	94.18	0.356	0.352
	28	0	0.5	0.49	115.76	0.437	0.364
	29	0.05	0.5	0.49	98.10	0.370	0.328
	30	0.15	0.5	0.49	72.59	0.274	0.255
	31	0	1	0	353.16	1.000	1.000
	32	0.1	1	0	278.60	0.789	0.800
	33	0.15	1	0	245.25	0.694	0.700
	34	0.05	1	0.123	277.62	0.786	0.790
	35	0.1	1	0.123	241.33	0.683	0.702
	36	0.15	1	0.123	215.82	0.611	0.614

Table 6.1 (continued)

Data Type (1)	Expt. No. (2)	$\frac{e}{B}$ (3)	$\frac{D_f}{B}$ (4)	$\frac{\alpha}{\phi}$ (5)	Experimental q_u (kN/m^2) (6)	Experimental RF [Eq. (6.1)] (7)	Calculated RF [Eq. (6.17)] (8)
	37	0	1	0.245	264.87	0.750	0.755
	38	0.05	1	0.245	239.36	0.678	0.679
	39	0.1	1	0.245	212.88	0.603	0.604
	40	0	1	0.368	225.63	0.639	0.632
	41	0.1	1	0.368	179.52	0.508	0.506
	42	0.15	1	0.368	155.98	0.442	0.443
	43	0.05	1	0.49	166.77	0.472	0.459
	44	0.1	1	0.49	143.23	0.406	0.408
	45	0.15	1	0.49	126.55	0.358	0.357
	46	0	0	0	101.04	1.000	1.000
	47	0.05	0	0	84.37	0.835	0.900
	48	0.15	0	0	54.94	0.544	0.700
	49	0	0	0.133	79.46	0.786	0.751
	50	0.1	0	0.133	52.97	0.524	0.601
	51	0.15	0	0.133	42.18	0.417	0.526
	52	0.05	0	0.267	47.09	0.466	0.484
	53	0.1	0	0.267	38.46	0.381	0.430
	54	0.15	0	0.267	31.39	0.311	0.376
	55	0	0	0.4	38.26	0.379	0.360
	56	0.05	0	0.4	32.37	0.320	0.324
	57	0.1	0	0.4	26.98	0.267	0.288
	58	0	0	0.533	24.03	0.238	0.218
	59	0.05	0	0.533	19.62	0.194	0.196
	60	0.15	0	0.533	13.34	0.132	0.152
	61	0	0.5	0	143.23	1.000	1.000
	62	0.1	0.5	0	103.99	0.726	0.800
	63	0.15	0.5	0	87.31	0.610	0.700
	64	0.05	0.5	0.133	103.99	0.726	0.726
	65	0.1	0.5	0.133	90.25	0.630	0.645
	66	0.15	0.5	0.133	72.59	0.507	0.565
	67	0	0.5	0.267	98.10	0.685	0.628
	68	0.05	0.5	0.267	84.86	0.592	0.565
	69	0.1	0.5	0.267	72.59	0.507	0.502
	70	0	0.5	0.4	79.46	0.555	0.465
	71	0.05	0.5	0.4	67.89	0.474	0.418
	72	0.15	0.5	0.4	48.07	0.336	0.325
	73	0	0.5	0.533	58.27	0.407	0.319
	74	0.1	0.5	0.533	43.16	0.301	0.255

Table 6.1 (continued)

Data Type (1)	Expt. No. (2)	$\frac{e}{B}$ (3)	$\frac{D_f}{B}$ (4)	$\frac{\alpha}{\phi}$ (5)	Experimental q_u (kN/m^2) (6)	Experimental RF [Eq. (6.1)] (7)	Calculated RF [Eq. (6.17)] (8)
	75	0.15	0.5	0.533	36.30	0.253	0.223
	76	0.05	1	0	193.26	0.925	0.900
	77	0.1	1	0	175.60	0.840	0.800
	78	0.15	1	0	156.96	0.751	0.700
	79	0	1	0.133	186.39	0.892	0.867
	80	0.05	1	0.133	168.73	0.808	0.780
	81	0.1	1	0.133	153.04	0.732	0.693
	82	0	1	0.267	160.88	0.770	0.733
	83	0.05	1	0.267	144.21	0.690	0.660
	84	0.15	1	0.267	112.82	0.540	0.513
	85	0	1	0.4	133.42	0.638	0.600
	86	0.1	1	0.4	106.93	0.512	0.480
	87	0.15	1	0.4	94.18	0.451	0.420
	88	0.05	1	0.533	92.21	0.441	0.420
	89	0.1	1	0.533	84.37	0.404	0.373
	90	0.15	1	0.533	75.54	0.362	0.327
Testing	1	0	0	0	166.77	1.0	1.000
	2	0.15	0	0.123	65.73	0.394	0.539
	3	0.1	0	0.245	62.78	0.376	0.456
	4	0.05	0	0.368	53.96	0.324	0.360
	5	0	0	0.490	43.16	0.259	0.260
	6	0.15	0.5	0	164.81	0.622	0.700
	7	0.1	0.5	0.123	165.79	0.626	0.658
	8	0.05	0.5	0.245	160.88	0.607	0.590
	9	0	0.5	0.368	151.07	0.570	0.503
	10	0.1	0.5	0.490	85.35	0.322	0.291
	11	0.05	1	0	313.92	0.889	0.900
	12	0	1	0.123	313.92	0.889	0.877
	13	0.15	1	0.245	188.35	0.533	0.528
	14	0.05	1	0.368	206.01	0.583	0.569
	15	0	1	0.49	183.45	0.519	0.510
	16	0.1	0	0	68.67	0.680	0.800
	17	0.05	0	0.133	63.77	0.631	0.676
	18	0	0	0.267	55.92	0.553	0.538
	19	0.15	0	0.4	20.60	0.204	0.252
	20	0.1	0	0.533	16.68	0.165	0.174
	21	0.05	0.5	0	123.61	0.863	0.900
	22	0	0.5	0.133	120.66	0.842	0.807

Table 6.1 (continued)

Data Type (1)	Expt. No. (2)	$\frac{e}{B}$ (3)	$\frac{D_f}{B}$ (4)	$\frac{\alpha}{\phi}$ (5)	Experimental q_u (kN/m^2) (6)	Experimental RF [Eq. (6.1)] (7)	Calculated RF [Eq. (6.17)] (8)
	23	0.15	0.5	0.267	60.82	0.425	0.440
	24	0.1	0.5	0.4	56.90	0.397	0.372
	25	0.05	0.5	0.533	50.03	0.349	0.287
	26	0	1	0	208.95	1.000	1.000
	27	0.15	1	0.133	137.34	0.657	0.607
	28	0.1	1	0.267	129.49	0.620	0.587
	29	0.05	1	0.4	118.70	0.568	0.540
	30	0	1	0.533	98.10	0.469	0.467

6.5 Results and Discussion

The maximum, minimum, average and standard deviation values of the three input and one output parameters used in the ANN model are presented in Table 6.2. The schematic diagram of ANN architecture is shown in Figure 6.3. The number of hidden layer neurons is varied and the mean square error (mse) is noted. The minimum mse is found to be 0.001 when there are three neurons in the hidden layer [Figure 6.4]. Therefore, the final ANN architecture is retained as 3-3-1 [i.e. 3 (input) – 3 (hidden layer neuron) – 1 (Output)]. Mean Square Error (MSE) is defined as

$$MSE = \frac{\sum_{i=1}^{n} \left(RF_i - RF_p\right)^2}{n} \tag{6.2}$$

Coefficient of Efficiency, R^2 is expressed as

$$R^2 = \frac{E_1 - E_2}{E_1} \tag{6.3}$$

where

$$E_1 = \sum_{i=1}^{n} \left(RF_i - \overline{RF}\right)^2 \tag{6.3a}$$

and

$$E_2 = \sum_{i=1}^{n} \left(RF_P - RF_i \right)^2 \tag{6.3b}$$

where $RF_i, \overline{RF}, and\ RF_p$ are the experimental, average experimental and predicted RF value respectively and n = number of training data.

Table 6.2. Statistical values of the parameters

Parameter	Maximum value	Minimum value	Average value	Standard Deviation
e/B	0.15	0	0.075	0.056
D_f/B	1	0	0.5	0.408
α/ϕ	0.533	0	0.256	0.181
RF	1.0	0.132	0.555	0.217

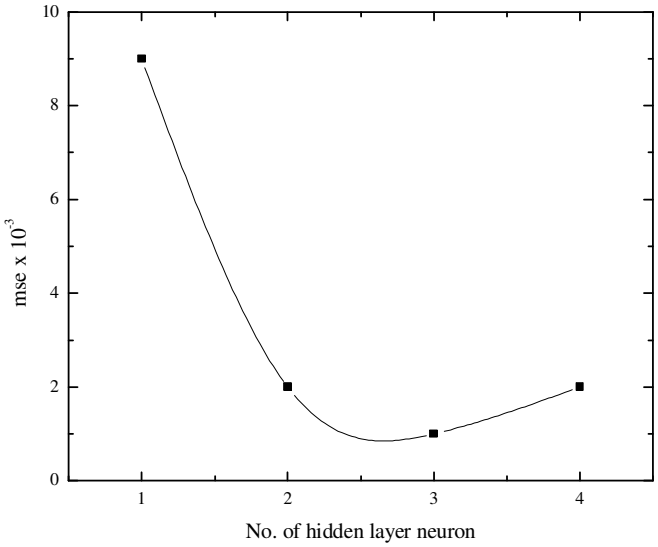

Figure 6.4: Variation of hidden layer neurons with mean square error (mse)

The coefficient of efficiency (R^2) for training and testing data are found to be 0.995 and 0.993, respectively, as shown in Figures 6.5 and 6.6. Data used in this analysis have been obtained from laboratory model tests carried out in duplicate, in a calibration chamber,

the details of which are given in Chapter 3 and 4. All the data used in the training and the testing are from the same source and are of same nature. Probably, this may be one of the causes for better fitting in both testing and training phase as well. The weights and biases of the network are presented in Table 6.3. These weights and biases can be utilized for interpretation of relationship between the inputs and output, sensitivity analysis and framing an ANN model in the form of an equation. The residual analysis is carried out by calculating the residuals from the experimental reduction factor and predicted reduction factor for training data set. Residual (e_r) can be defined as the difference between the experimental and predicted *RF* value and is given by

$$e_r = RF_i - RF_p \tag{6.4}$$

The residuals are plotted with the experiment number as shown in Figure 6.7. It is observed that the residuals are distributed evenly along the center line of the plot. Therefore, it can be said that the network is well trained and can be used for prediction with reasonable accuracy.

Table 6.3. Values of connection weights and biases

Neuron	Weight				Bias	
	w_{ik}			w_k		
	e/B	D_f/B	α/ϕ	*RF*	b_{hk}	b_0
Hidden Neuron 1 (k=1)	-0.0523	0.6833	-0.5784	9.3907	-0.0116	1.0177
Hidden Neuron 2 (k=2)	0.0401	-0.7286	0.6003	8.5052	0.0298	
Hidden Neuron 3 (k=3)	0.3693	0.0724	0.4722	-1.4541	1.2362	

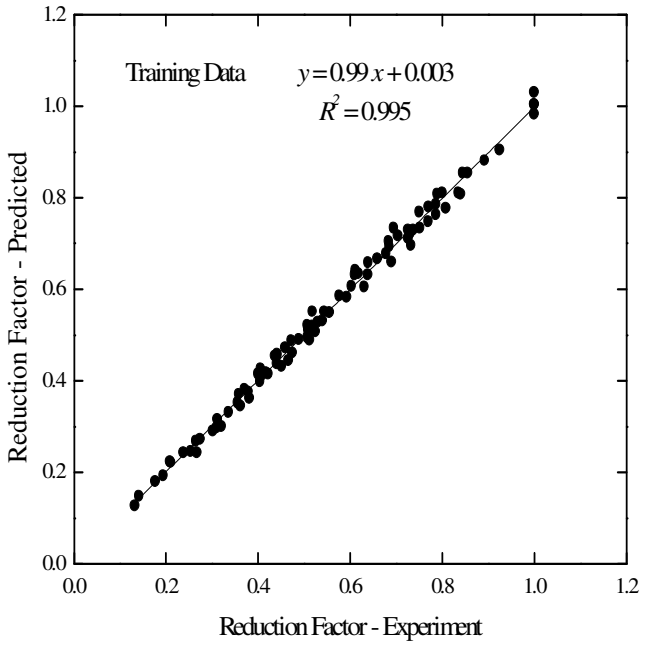

Figure 6.5: Correlation between Predicted Reduction Factor with Experimental Reduction Factor for training data.

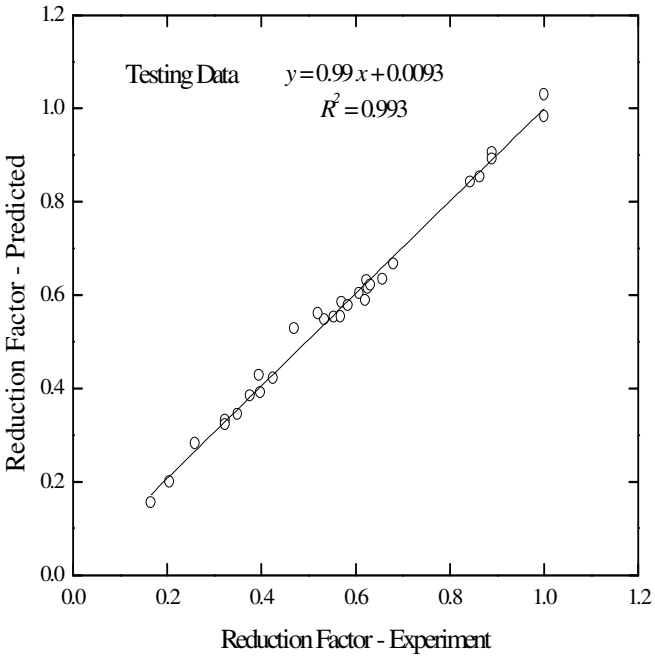

Figure 6.6: Correlation between Predicted Reduction Factor with Experimental Reduction Factor for testing data.

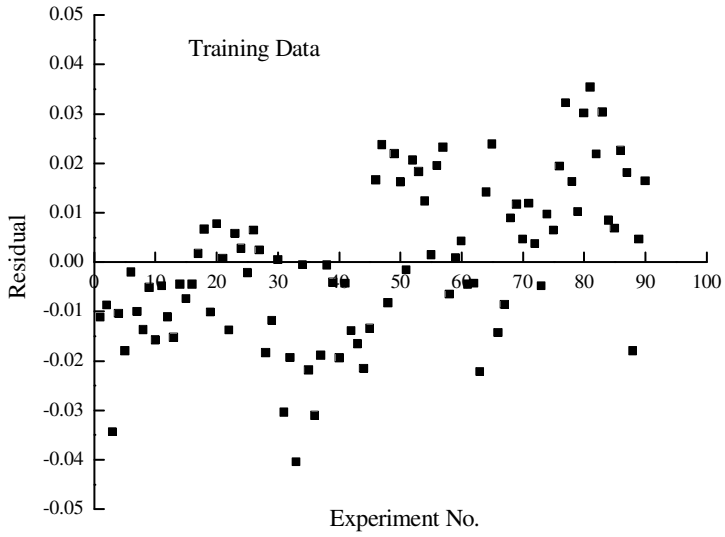

Figure 6.7: Residual distribution of training data

6.5.1 Sensitivity Analysis

Sensitivity analysis is carried out for selection of important input variables. Different approaches have been suggested to select the important input variables. The Pearson correlation coefficient is defined as one of the variable ranking criteria in selecting proper inputs for the ANN (Guyon and Elisseeff 2003; Wilby et al. 2003). Goh (1994) and Shahin et al. (2002) have used Garson's algorithm (Garson 1991) in which the input-hidden and hidden-output weights of trained ANN model are partitioned and the absolute values of the weights are taken to select the important input variables. It does not provide information on the effect of input variables in terms of direct or inverse relation to the output. Olden et al. (2004) proposed a connection weight approach based on the NID, in which the actual values of input-hidden and hidden-output weights are taken. It sums the products across all the hidden neurons, which is defined as S_i. The relative inputs are corresponding to absolute S_i values, where the most important input corresponds to

highest S_i value. The details of connection weight approach are presented in Olden et al. (2004).

Table 6.4 shows the cross correlation of inputs with the reduction factor. From the table it is observed that *RF* is highly correlated to α/ϕ with a cross correlation values of 0.79, followed by *e/B* and D_f/B. The relative importance of the three input parameters as per Garson's algorithm is presented in Table 6.5. The α/ϕ is found to be the most important input parameter with the relative importance value being 46.5% followed by 37.7% for D_f/B and 15.8% for *e/B*. The relative importance of the present input variables, as calculated following the connection weight approach (Olden et al. 2004) is also presented in Table 6.5. α/ϕ is found to be the most important input parameter (S_i value = -1.012) followed by *e/B* (S_i value = -0.687) and D_f/B (S_i value = 0.115). The S_i values being negative imply that both α/ϕ and *e/B* are indirectly related and D_f/B is directly related to *RF* values. In other words, increasing α/ϕ or *e/B* will lead to a reduction in the *RF* and hence leads to lower ultimate bearing capacity. Increasing D_f/B increases the *RF*, and hence increases the bearing capacity.

Table 6.4. Cross-correlation of the input and output for the reduction factor

Parameters	*e/B*	D_f/B	α/ϕ	*RF*
e/B	1	0	0	-0.44
D_f/B		1	0	0.37
α/ϕ			1	-0.79
RF				1

Table 6.5. Relative Importance of different inputs as per Garson's algorithm and connection weight approach

Parameters	Garson's algorithm		Connection weight approach	
(1)	Relative Importance (%) (2)	Ranking of inputs as per relative importance (3)	S_i values as per Connection weight approach (4)	Ranking of inputs as per relative importance (5)
e/B	15.8	3	-0.687	2
D_f/B	37.7	2	0.115	3
α/ϕ	46.5	1	-1.012	1

6.5.2 Neural Interpretation Diagram (NID)

Ozesmi and Ozesmi (1999) proposed neural interpretation diagram (NID) for visual interpretation of the connection weight among the neurons. For the present study with the weights as obtained and shown in Table 6.3, a Neural Interpretation Diagram is presented in Figure 6.8. The lines joining the input-hidden and hidden-output neurons represent the weights. The positive weights are represented by solid lines and negative weights by dashed lines and the thickness of the line is proportional to its magnitude. The relationship between the input and output is determined in two steps. Direct proportionality of the input variables is depicted by positive input-hidden and positive hidden-output weights, or negative input-hidden and negative hidden-output weights. The positive input-hidden and negative hidden-output; negative input-hidden and positive hidden-output weight indicates the inverse proportionality of the input variables. Therefore, the multiplication of actual weights of input-hidden and hidden-output rather than multiplication of absolute weights indicate the effect of that input variable on the

output. The input directly related to the output is represented with a grey circle and that having inverse effect with blank circle.

It is seen from Table 6.5 (4th Column) that S_i values for parameters (e/B) and (α/ϕ) are negative indicating that both the parameters (e/B) and (α/ϕ) are inversely related to whereas S_i value for parameter (D_f/B) being positive is directly related to RF values. This is shown in Figure 6.8. Therefore, the developed ANN model is not a "black box" and could explain the physical effect of the input parameters on the output.

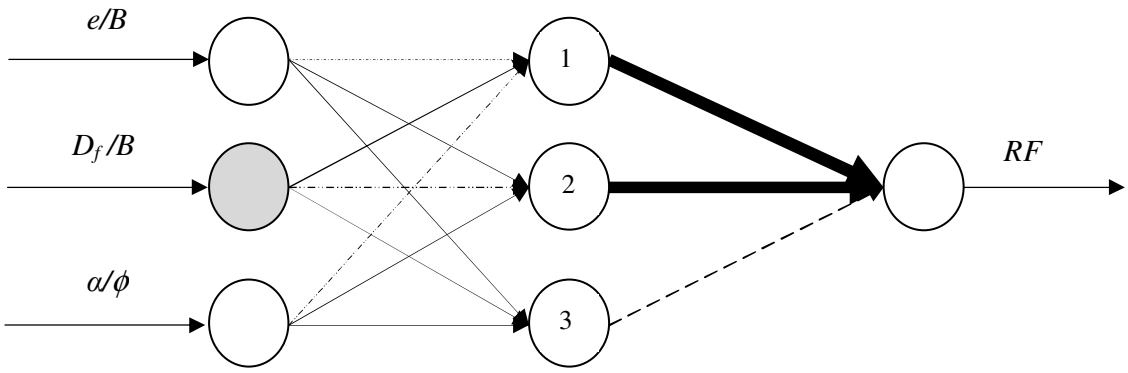

Figure 6.8: Neural Interpretation Diagram (NID) showing lines representing connection weights and effects of inputs on Reduction Factor (RF)

6.5.3 ANN model equation for the Reduction Factor based on trained neural network

A model equation is developed with the weights obtained from trained neural network as the model parameters (Goh et al. 2005). The mathematical equation relating input parameters (e/B, D_f/B, and α/ϕ) to output (Reduction Factor) can be given by

$$RF_n = f_n\left\{b_0 + \sum_{k=1}^{h}\left[w_k f_n\left(b_{hk} + \sum_{i=1}^{m} w_{ik} X_i\right)\right]\right\} \qquad (6.5)$$

where RF_n = normalized value of RF in the range [-1, 1], f_n = transfer function, h = no. of neurons in the hidden layer, X_i = normalized value of inputs in the range [-1, 1], m = no. of input variables, w_{ik} = connection weight between i^{th} layer of input and k^{th} neuron of hidden layer, w_k = connection weight between k^{th} neuron of hidden layer and single output neuron, b_{hk} = bias at the k^{th} neuron of hidden layer, and b_o = bias at the output layer.

The model equation for Reduction Factor of shallow strip foundations subjected to eccentrically inclined load is formulated using the values of the weights and biases shown in Table 6.3 as per the following steps.

Step – 1

The input parameters are normalized in the range [-1, 1] by the following expressions

$$X_n = 2\left(\frac{X_1 - X_{\min}}{X_{\max} - X_{\min}}\right) - 1 \tag{6.6}$$

where, X_n = Normalized value of input parameter X_1, and X_{max} and X_{min} are maximum and minimum values of the input parameter X_1 in the data set.

Step – 2

Calculate the normalized value of reduction factor (RF_n) using the following expressions

$$A_1 = -0.0523\left(\frac{e}{B}\right)_n + 0.6833\left(\frac{D_f}{B}\right)_n - 0.5784\left(\frac{\alpha}{\phi}\right)_n - 0.0116 \tag{6.7}$$

$$A_2 = 0.0401\left(\frac{e}{B}\right)_n - 0.7286\left(\frac{D_f}{B}\right)_n + 0.6003\left(\frac{\alpha}{\phi}\right)_n + 0.0298 \tag{6.8}$$

$$A_3 = 0.3693\left(\frac{e}{B}\right)_n + 0.0724\left(\frac{D_f}{B}\right)_n + 0.4722\left(\frac{\alpha}{\phi}\right)_n + 1.2362 \tag{6.9}$$

$$B_1 = 9.3907\left(\frac{e^{A_1} - e^{-A_1}}{e^{A_1} + e^{-A_1}}\right) \tag{6.10}$$

$$B_2 = 8.5052\left(\frac{e^{A_2} - e^{-A_2}}{e^{A_2} + e^{-A_2}}\right) \tag{6.11}$$

$$B_3 = -1.4541\left(\frac{e^{A_3} - e^{-A_3}}{e^{A_3} + e^{-A_3}}\right) \tag{6.12}$$

$$C_1 = 1.0177 + B_1 + B_2 + B_3 \tag{6.13}$$

$$RF_n = C_1 \tag{6.14}$$

Step – 3

Denormalize the RF_n value obtained from Eq. (6.14) to actual RF as

$$RF = 0.5(RF_n + 1)(RF_{\max} - RF_{\min}) + RF_{\min} \tag{6.15}$$

$$RF = 0.5(RF_n + 1)(1 - 0.132) + 0.132 \tag{6.16}$$

6.6 Comparison

6.6.1 Comparison with Developed Empirical Equation

An empirical equation for ultimate bearing capacity is developed based on laboratory model tests data for prediction of reduction factor (RF) as discussed in Chapter 4, which can be expressed as

$$RF = \frac{q_{u(D_f/B, e/B, \alpha/\phi)}}{q_{u(D_f/B, e/B=0, \alpha/\phi=0)}} = \left[1 - 2\left(\frac{e}{B}\right)\right]\left[1 - \left(\frac{\alpha}{\phi}\right)\right]^{\left(2 - \frac{D_f}{B}\right)} \tag{6.17}$$

The results for reduction factor (*RF*) obtained from developed ANN equation (Eq. 6.15) are compared with those obtained by use of empirical equation (Eq. 6.17). The comparison is shown in Figures 6.9 and 6.10. It is seen that ANN results are closer to experimental values than those from developed empirical equation [Eq. (6.17)].

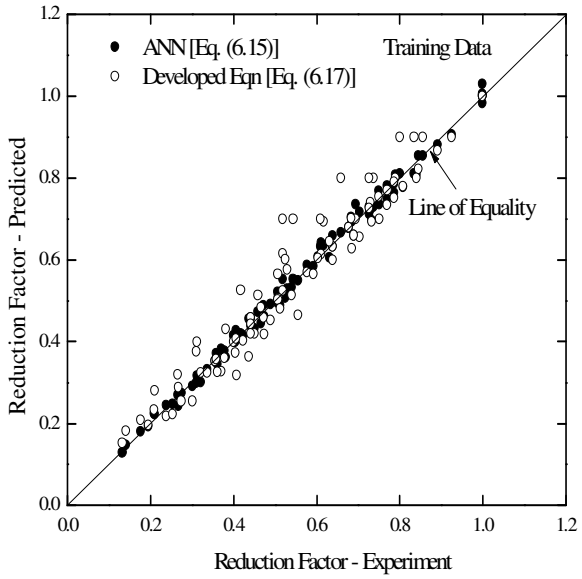

Figure 6.9: Comparison of ANN results with Experimental *RF* and Eq. 6.17 for training data

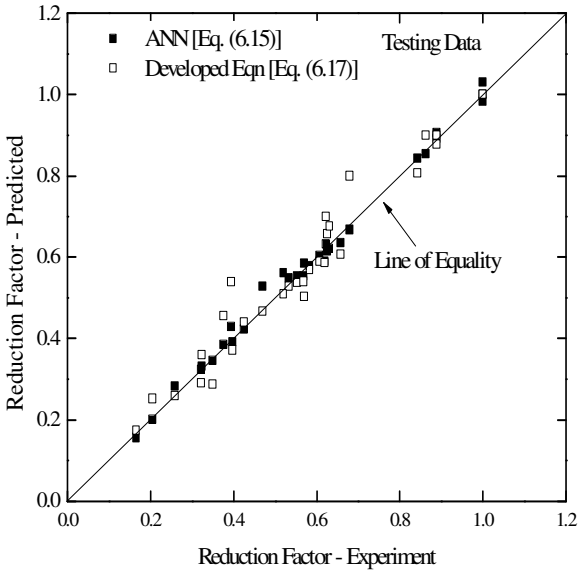

Figure 6.10: Comparison of ANN results with Experimental *RF* and Eq. 6.17 for testing data

6.6.2 Comparison with Meyerhof [1963]

As discussed in section 4.5.1 of Chapter 4, the reduction factor (*RF*) corresponding to Meyerhof (1963) can be written as

$$RF = \frac{\left(\frac{q_u \times B^{'}}{B}\right)\left(\frac{1}{\cos\alpha}\right)}{q_{u\left(e/B=0,\alpha/\phi=0,D_f/B\right)}} = \frac{q_{u\left(e/B,\alpha/\phi,D_f/B\right)}}{q_{u\left(e/B=0,\alpha/\phi=0,D_f/B\right)}} \sec\alpha \left(\frac{B^{'}}{B}\right) \tag{6.18}$$

The values so found by using Eq. (6.18) are compared with the reduction factor as given by Eqs. 6.1 and 6.15. This is presented in Figure 6.11. Reasonably good agreements are found.

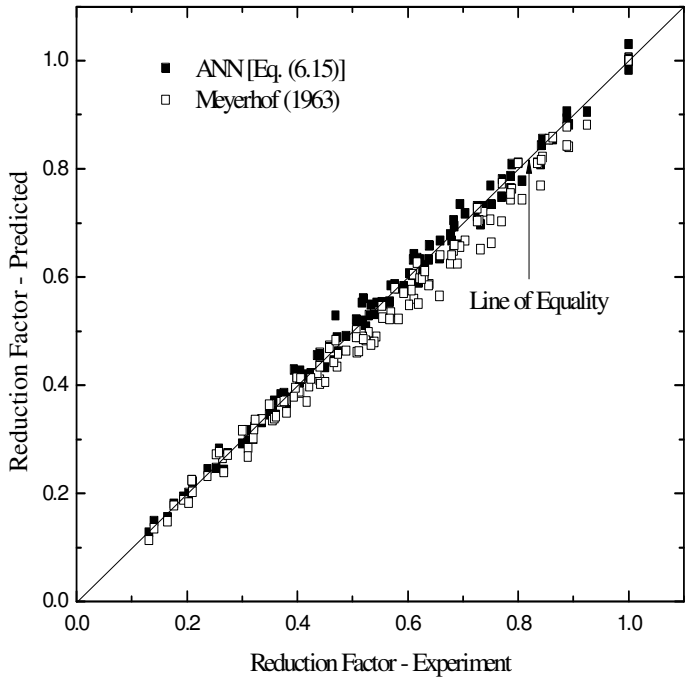

Figure 6.11: Comparison of Present results with Meyerhof (1963)

6.6.3 Comparison with Saran and Agarwal [1991]

The digitized values of N_q and N_γ (e/B=0, 0.1, α=0^0, 10^0 and 20^0) for medium dense sand ($\phi = 37.5^0$) are calculated from the graph originally given by Saran and Agarwal (1991) as discussed in section 2.2.4 and 4.5.2. Using Eqs. (2.36) and (6.1) the reduction factor (*RF*) corresponding to Saran and Agarwal (1991) is calculated and compared with Predicted and Experimental *RF* and shown in Figure 6.12. The *RF* values obtained from Saran and Agarwal (1991) are away from the line of equality as compared to present experimental and predicted results.

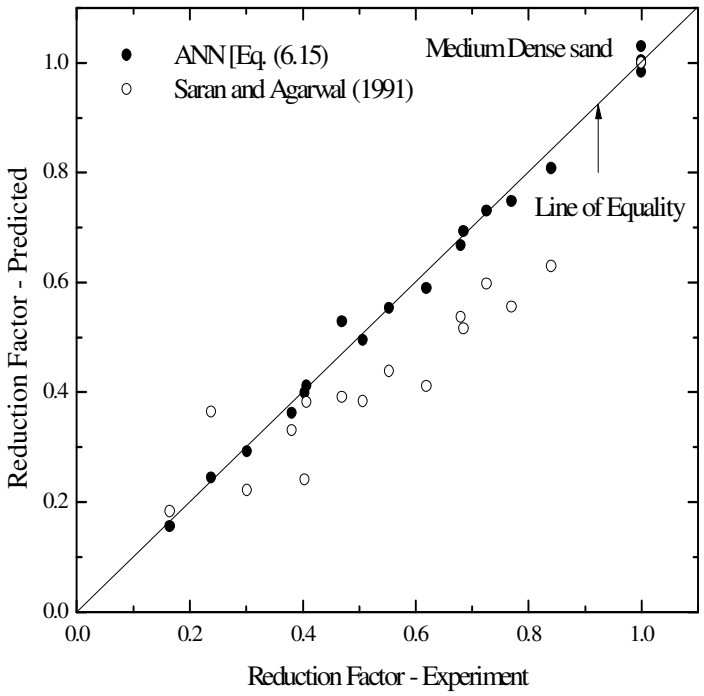

Figure 6.12: Comparison of Present results with Saran and Agarwal (1991) for medium dense sand

6.6.4 Comparison with Loukidis et al. [2008]

As mentioned in section 4.5.3, the reduction factor *RF* corresponding to Loukidis et al. (2008) can be written as

$$RF = \frac{f_{ie}}{\cos\alpha} \tag{6.19}$$

The reduction factors computed using Eq. (6.19) are compared with those obtained from Eqs. (6.15) and (6.1) which are shown in Figures 6.13 and 6.14. It is seen that the values (*RF*) predicted by ANN, developed empirical equation and Loukidis et al. (2008) are in good agreement with experimental values. The values obtained by ANN and Loukidis et al. (2008) are very close to experimental values. However, this is to be mentioned that Loukidis et al. (2008) give the values for surface footing only.

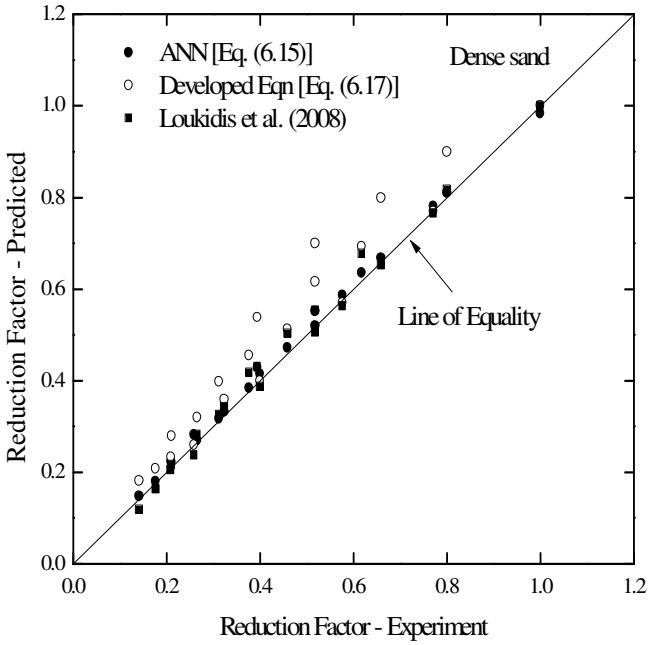

Figure 6.13: Comparison of ANN results with Loukidis et al. (2008) and developed equation [Eq. (6.17)] for dense sand.

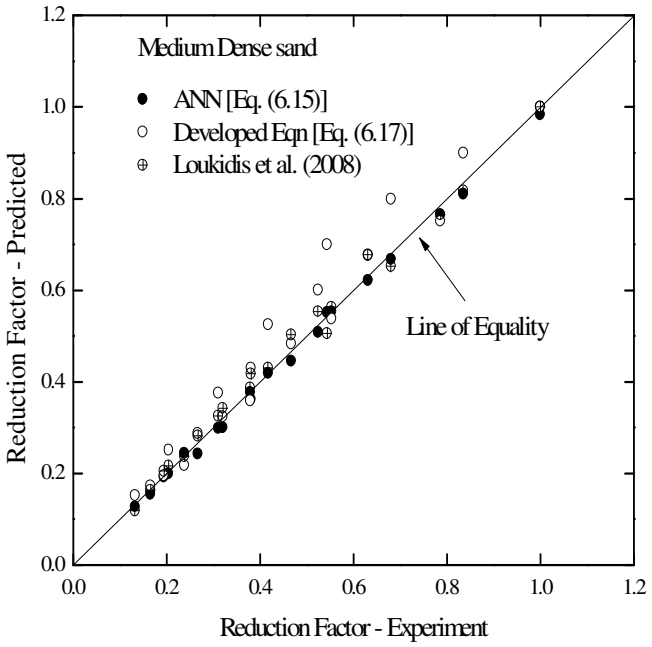

Figure 6.14: Comparison of ANN results with Loukidis et al. (2008) and developed equation [Eq. (6.17)] for medium dense sand.

6.7 Conclusions

Based on developed neural network model, the following conclusions are drawn:

- As per residual analysis, the errors are distributed evenly along the center line. It can be concluded that the network is well trained and can predict the result with reasonable accuracy.
- Based on Pearson correlation coefficient, it is observed that α/ϕ is the most important input parameter followed by e/B and D_f/B.
- As per Garson's algorithm, α/ϕ is found to be the most important input parameter followed by D_f/B and e/B.
- Connection weight approach gives similar results as found in Pearson correlation coefficient

- Sensitivity analysis using Connection weight approach is able to explore the inputs-output relationship as it considers the actual value of trained weights.
- The developed ANN model has explained the physical effect of inputs on the output, as depicted in NID. It is observed that e/B and α/ϕ are inversely related to RF values whereas D_f/B is directly related to RF.
- A model equation is developed based on the trained weights of the ANN.
- The predictability of ANN model is found to be slightly better than the developed empirical equation, Meyerhof (1963) and Loukidis et al. (2008).

7. PREDICTION OF ULTIMATE BEARING CAPACITY OF ECCENTRICALLY INCLINED LOADED STRIP FOOTING BY ANN: PART II

7.1 Introduction

When a shallow strip footing is subjected to eccentric and inclined load, there may be two possible modes of load applications as shown in Figure 7.1. In this figure, B is the width of the footing, e is the load eccentricity, α is the load inclination, and Q_u is the ultimate load per unit length of the footing. As discussed in Chapter 5, when the line of load application of the footing is inclined towards the center line of the footing (Figure 7.1 a) is referred as *partially compensated* (Perloff and Baron 1976). However, there may be another mode of application where the line of load application on the footing is inclined away from the center line as shown in Figure 7.1(b). Perloff and Baron (1976) called this type of loading as *reinforced* case.

In this chapter a neural network model has been developed to predict the ultimate bearing capacity when the line of load application is away from the center line of the footing.

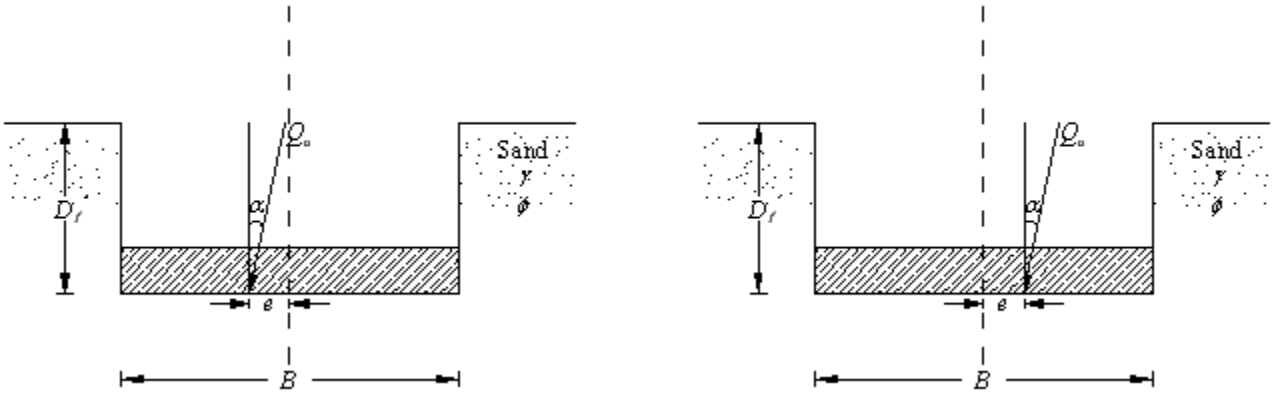

Figure 7.1: Eccentrically inclined load on a strip foundation: (a) *Partially compensated* case, (b) *Reinforced* case

7.2 Problem Definition

The results of laboratory model tests conducted on a strip footing resting over dry sand bed subjected to load arrangement as per Figure 7.1 (b) has been used for determining the ultimate bearing capacity. The details of load tests have been described in Chapter 5. The ultimate bearing capacity of the eccentrically inclined loaded strip foundation at any depth of embedment will be equal to the reduction factor multiplied by the ultimate bearing capacity of strip footing under centric and vertical load at the same depth of embedment. From the laboratory test results, a neural network model is developed to predict the reduction factor to compute the ultimate bearing capacity of an eccentrically inclined loaded strip footing as shown in Figure 7.1 (b). This reduction factor (*RF*) is the ratio of the ultimate bearing capacity of the footing subjected to an eccentrically inclined load to the ultimate bearing capacity of the footing subjected to a centric vertical load. A thorough sensitivity analysis is carried out to evaluate the parameters affecting the reduction factor. Based on the weights of the developed neural network model, a neural interpretation diagram is developed to find out whether the input parameters have direct or inverse effect on the output. A prediction model equation is established with the weights of the neural network as the model parameters. The results are compared with the values based on developed empirical equation as in Chapter 5. Also the results have been compared with those obtained by Loukidis et al. (2008) by using finite element methods for the case of surface footings.

7.3 Database and Preprocessing

The database available in Chapter 5 has been used in the present study. The data consists of parameters like load eccentricity (e), load inclination (α), embedment ratio (D_f /B), friction angle (ϕ) and ultimate bearing capacity (q_u). Seventy eight number of laboratory model tests are carried out. The input parameters for the ANN model are e/B, α/ϕ and D_f /B and the output is the reduction factor (RF). The reduction factor (RF) is given by

$$RF = \frac{q_{u(D_f/B, e/B, \alpha/\phi)}}{q_{u(D_f/B, e/B=0, \alpha/\phi=0)}} \tag{7.1}$$

where, $q_{u(D_f/B, e/B, \alpha/\phi)}$ = ultimate bearing capacity with eccentricity ratio e/B and inclination ratio α/ϕ at an embedment ratio D_f /B and $q_{u(D_f/B, e/B=0, \alpha/\phi=0)}$ = ultimate bearing capacity with centric vertical loading (e/B = 0 and α/ϕ = 0) at the same embedment ratio D_f/B.

Out of 78 test records shown in Table 7.1, 59 tests are considered for training and the remaining 19 are reserved for testing. Each record represents a complete model test where an eccentrically inclined loaded strip footing is subjected to failure. Similar type of preprocessing is adopted here as mentioned in section 6.4.

7.4 Results and Discussion

The maximum, minimum, average and standard deviation values of the three input and one output parameters are presented in Table 7.2. They are computed from the database. The schematic diagram of ANN architecture is shown [Figure 7.2]. The number of hidden layer neurons is varied with mean square error (mse). The minimum mse is found

to be 0.001 for four neurons in the hidden layer [Figure 7.3]. Therefore, the final ANN architecture used in this study will be 3-4-1 [i.e. 3 (input) – 4 (hidden layer neuron) – 1 (Output)] as shown in Figure 7.4.

[INPUT LAYER = *l*] [HIDDEN LAYER = *m*] [OUTPUT LAYER = *n*]

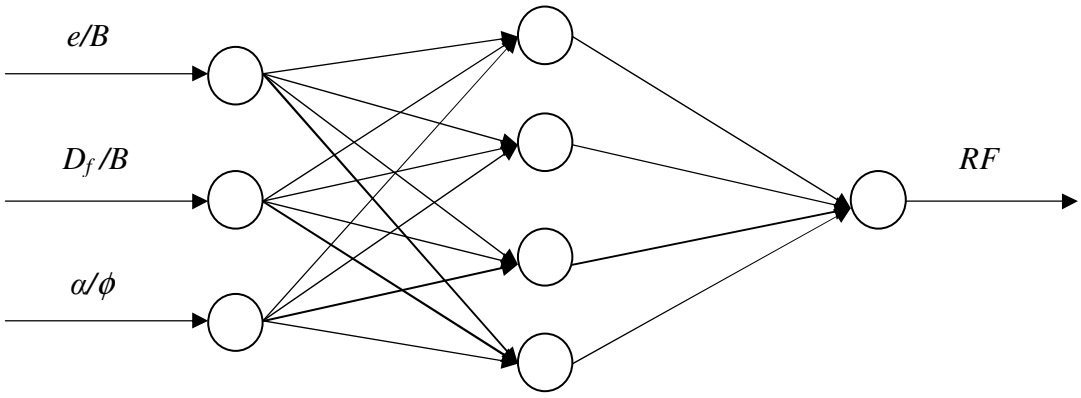

Figure 7.2: The ANN Architecture

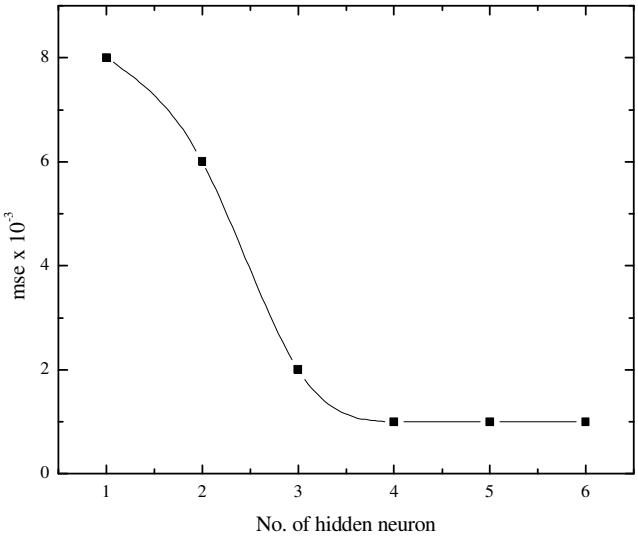

Figure 7.3: Variation of hidden layer neuron with mean square error (mse).

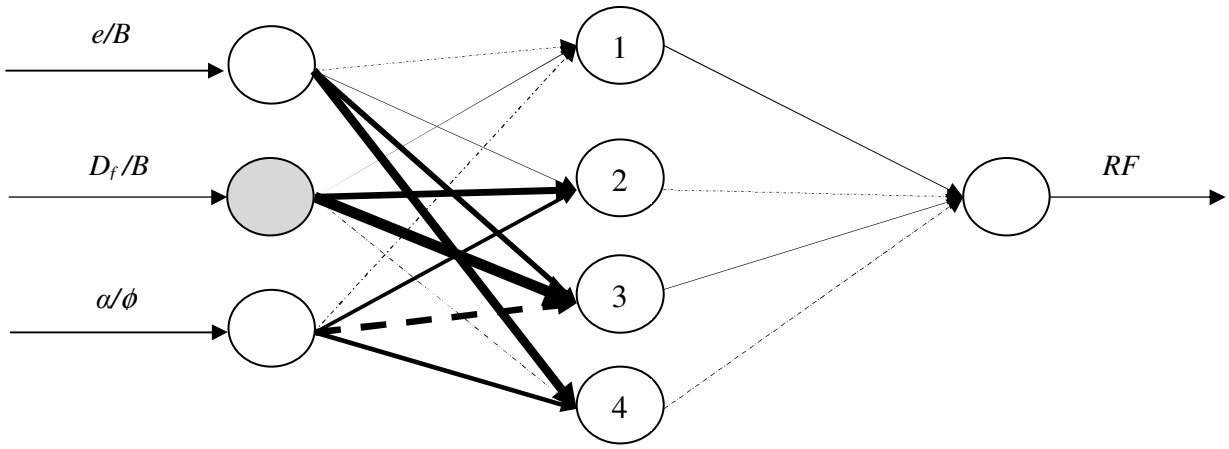

Figure 7.4 NID showing lines of connection weights and effects of inputs on *RF*

Table 7.1. Dataset used for training and testing of ANN model [Chapter 6]

Data Type (1)	Expt No. (2)	$\frac{e}{B}$ (3)	$\frac{D_f}{B}$ (4)	$\frac{\alpha}{\phi}$ (5)	Experimental q_u (kN/m^2) (6)	Experimental *RF* [Eq. (7.1)] (7)	Calculated *RF* [Eq. (7.17)] (8)
Training	1	0.05	0	0.123	113.80	0.682	0.740
	2	0.1	0	0.123	107.91	0.647	0.658
	3	0.05	0	0.245	88.29	0.529	0.590
	4	0.1	0	0.245	85.35	0.512	0.525
	5	0.15	0	0.245	81.42	0.488	0.459
	6	0.05	0	0.368	68.67	0.412	0.453
	7	0.15	0	0.368	64.75	0.388	0.352
	8	0.1	0	0.490	51.99	0.312	0.291
	9	0.15	0	0.490	49.05	0.294	0.255
	10	0	0.5	0.000	264.87	1.000	1.000
	11	0.05	0.5	0.123	196.20	0.741	0.774
	12	0.1	0.5	0.123	173.64	0.656	0.688
	13	0.15	0.5	0.123	152.06	0.574	0.602
	14	0.05	0.5	0.245	166.77	0.630	0.651
	15	0.1	0.5	0.245	151.07	0.570	0.579
	16	0.05	0.5	0.368	137.34	0.519	0.531
	17	0.15	0.5	0.368	112.82	0.426	0.413
	18	0.1	0.5	0.490	105.95	0.400	0.369
	19	0.15	0.5	0.490	95.16	0.359	0.323
	20	0	1	0.000	353.16	1.000	1.000
	21	0.05	1	0.123	284.49	0.806	0.811
	22	0.1	1	0.123	251.14	0.711	0.721
	23	0.05	1	0.245	249.17	0.706	0.719

Table 7.1 (continued)

Data Type (1)	Expt No. (2)	$\frac{e}{B}$ (3)	$\frac{D_f}{B}$ (4)	$\frac{\alpha}{\phi}$ (5)	Experimental q_u (kN/m^2) (6)	Experimental RF [Eq. (7.1)] (7)	Calculated RF [Eq. (7.17)] (8)
	24	0.15	1	0.245	203.07	0.575	0.559
	25	0.05	1	0.368	217.78	0.617	0.624
	26	0.1	1	0.368	193.26	0.547	0.554
	27	0.15	1	0.368	171.68	0.486	0.485
	28	0.1	1	0.490	156.96	0.444	0.467
	29	0.15	1	0.490	143.23	0.406	0.408
	30	0	0	0.000	101.04	1.000	1.000
	31	0.1	0	0.133	62.78	0.621	0.645
	32	0.15	0	0.133	52.97	0.524	0.565
	33	0.05	0	0.267	56.90	0.563	0.565
	34	0.1	0	0.267	51.99	0.515	0.502
	35	0.05	0	0.400	42.58	0.421	0.418
	36	0.15	0	0.400	38.65	0.383	0.325
	37	0.05	0	0.533	31.39	0.311	0.287
	38	0.1	0	0.533	30.41	0.301	0.255
	39	0.15	0	0.533	29.43	0.291	0.223
	40	0	0.5	0.000	143.23	1.000	1.000
	41	0.05	0.5	0.133	105.95	0.740	0.763
	42	0.1	0.5	0.133	94.18	0.658	0.679
	43	0.15	0.5	0.133	77.50	0.541	0.594
	44	0.1	0.5	0.267	77.50	0.541	0.560
	45	0.15	0.5	0.267	67.69	0.473	0.490
	46	0.05	0.5	0.400	73.58	0.514	0.500
	47	0.1	0.5	0.400	63.77	0.445	0.445
	48	0.05	0.5	0.533	58.86	0.411	0.375
	49	0.15	0.5	0.533	48.07	0.336	0.291
	50	0	1	0.000	208.95	1.000	1.000
	51	0.1	1	0.133	156.96	0.751	0.713
	52	0.15	1	0.133	144.21	0.690	0.624
	53	0.05	1	0.267	148.13	0.709	0.702
	54	0.1	1	0.267	135.38	0.648	0.624
	55	0.05	1	0.400	124.59	0.596	0.598
	56	0.1	1	0.400	114.78	0.549	0.532
	57	0.15	1	0.400	103.01	0.493	0.465
	58	0.05	1	0.533	99.08	0.474	0.489
	59	0.15	1	0.533	86.33	0.413	0.380

Table 7.1 (continued)

Data Type (1)	Expt No. (2)	$\frac{e}{B}$ (3)	$\frac{D_f}{B}$ (4)	$\frac{\alpha}{\phi}$ (5)	Experimental q_u (kN/m^2) (6)	Experimental RF [Eq. (7.1)] (7)	Calculated RF [Eq. (7.17)] (8)
Testing	1	0	0	0.000	166.77	1.000	1.000
	2	0.15	0	0.123	92.21	0.553	0.575
	3	0.1	0	0.368	66.71	0.400	0.402
	4	0.05	0	0.490	53.96	0.324	0.328
	5	0.15	0.5	0.245	132.44	0.500	0.507
	6	0.1	0.5	0.368	129.49	0.489	0.472
	7	0.05	0.5	0.490	113.80	0.430	0.415
	8	0.15	1	0.123	228.57	0.647	0.630
	9	0.1	1	0.245	225.63	0.639	0.639
	10	0.05	1	0.490	179.52	0.508	0.525
	11	0.05	0	0.133	71.61	0.709	0.726
	12	0.15	0	0.267	49.05	0.485	0.440
	13	0.1	0	0.400	41.20	0.408	0.372
	14	0.05	0.5	0.267	88.29	0.616	0.630
	15	0.15	0.5	0.400	56.90	0.397	0.389
	16	0.1	0.5	0.533	53.96	0.377	0.333
	17	0.05	1	0.133	170.69	0.817	0.803
	18	0.15	1	0.267	120.66	0.577	0.546
	19	0.1	1	0.533	92.21	0.441	0.435

Table 7.2. Statistical values of the parameters

Parameter	Maximum value	Minimum value	Average value	Standard Deviation
e/B	0.15	0	0.092	0.047
D_f/B	1	0	0. 5	0.408
α/ϕ	0.533	0	0.295	0.162
RF	1	0.291	0.56	0.179

The coefficient of efficiency (R^2) for the training and testing data are found to be 0.994 and 0.988, respectively [Figures 7.5 & 7.6]. Data used in this analysis have been obtained from laboratory model tests carried out in duplicate, in a calibration chamber, the details of which are given in Chapter 3 and 5. All the data used in the training and the testing are

from the same source and are of same nature. Probably, this may be one of the causes for better fitting in both testing and training phase as well. The weights and biases of the network are presented in Table 7.3. The weights and biases can be utilized for interpretation of the relationships between the inputs and output, to carry out a sensitivity analysis, and for framing an ANN model in the form of an equation that can be used for predicting *RF*. The residual analysis is carried out by calculating the residuals from the experimental reduction factor and predicted reduction factor for training data set. Residual (e_r) can be defined as the difference between the experimental and predicted *RF* value and is given by

$$e_r = RF_i - RF_p \tag{7.2}$$

where RF_i and RF_p are the experimental and predicted *RF* value respectively.

The residuals are plotted with the experiment number as shown in Figure 7.7. It is observed that the residuals are distributed evenly along the horizontal axis of the plot. Therefore, it can be said that the network is well trained and can be used for prediction with reasonable accuracy.

Table 7.3. Values of connection weights and biases

Neuron	Weight				Bias	
	w_{ik}			w_k		
	e/B	D_f/B	α/ϕ	*RF*	b_{hk}	b_0
Hidden Neuron 1 (k=1)	-0.4188	0.3928	-0.8511	0.7337	-0.005	0.0972
Hidden Neuron 2 (k=2)	0.17	5.2462	3.1071	-0.1013	3.874	
Hidden Neuron 3 (k=3)	4.0168	8.1273	-4.8781	0.0693	7.3396	
Hidden Neuron 4 (k=4)	6.2788	-0.3513	3.247	-0.2621	4.8671	

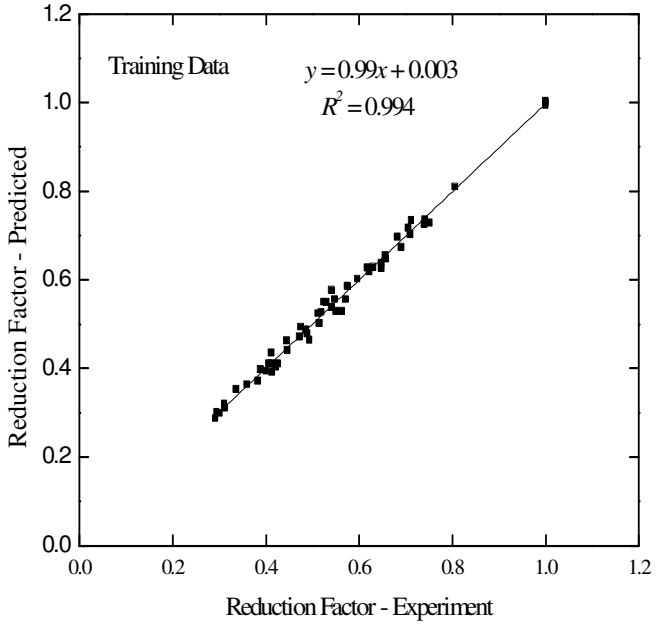

Figure 7.5 Correlation between Predicted Reduction Factor with Experimental Reduction Factor for training data

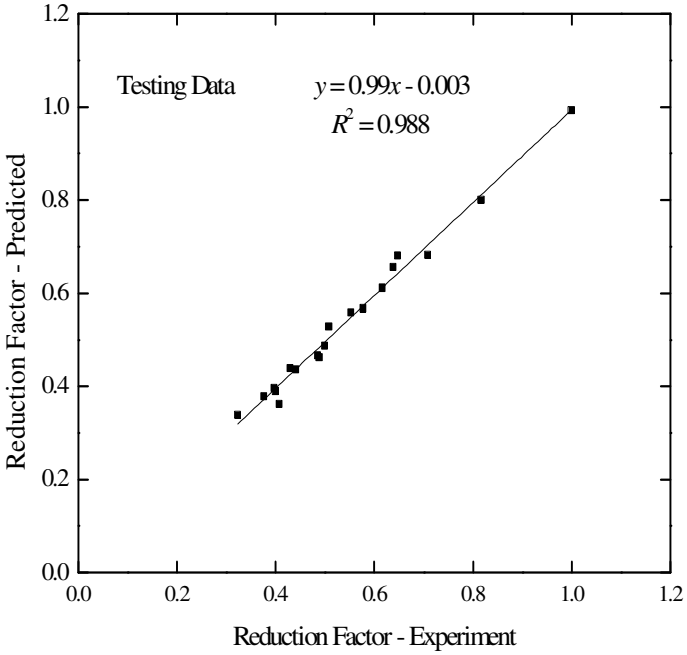

Figure 7.6 Correlation between Predicted Reduction Factor with Experimental Reduction Factor for testing data

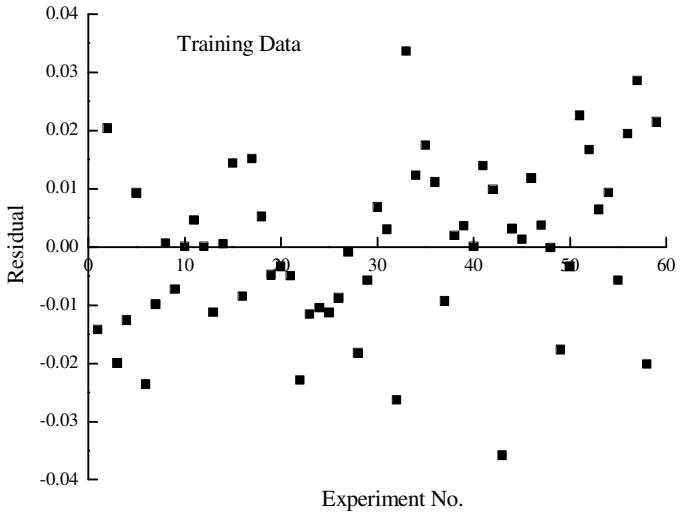

Figure 7.7: Residual distribution of training data

7.4.1 Sensitivity Analysis

Sensitivity analysis is conducted for selection of important input variables. Different approaches like Pearson correlation coefficient (Guyon and Elisseeff 2003; Wilby et al. 2003), Garson's algorithm (Garson 1991; Goh 1995) and connection weight approach method (Olden et al. 2004) are used to identify important input parameters based on the trained weights and biases of neural network model as discussed in Chapter 6.

The sensitivity analysis based on Pearson correlation coefficient is presented in Table 7.4 which shows the cross correlation of inputs with the reduction factor. It is seen that the parameters (e/B) and (α/ϕ) are inter-related with a cross-correlation value of 0.3. This is possibly due to the reinforcing effect. From the table it is observed that RF is highly correlated to α/ϕ with a cross correlation values of 0.87, followed by e/B (=0.59) and D_f/B (=0.28). The sensitivity analysis for the model as per Garson's algorithm is presented in Table 7.5. The α/ϕ is found to be the most important input parameter with the relative importance value being 37.3% followed by 34.1% for D_f/B and 28.6% for

e/B. The relative importance of the input variables as calculated following connection weight approach (Olden et al. 2004) is also presented in Table 7.5. As per connection weight approach method α/ϕ is found to be the most important input parameter (S_i value -2.13) followed by *e/B* (S_i value -1.69) and D_f/B (S_i value 0.41). The S_i values being negative imply that both α/ϕ and *e/B* are indirectly and D_f/B is directly related to *RF* values.

Table 7.4. Cross-correlation of the input and output for the reduction factor

Parameters	*e/B*	D_f/B	α/ϕ	*RF*
e/B	1	0	0.3	-0.59
D_f/B		1	0	0.28
α/ϕ			1	-0.87
RF				1

Table 7.5. Relative Importance of different inputs as per Garson's algorithm and connection weight approach

Parameters	Garson's algorithm		Connection weight approach	
(1)	Relative Importance (%) (2)	Ranking of inputs as per relative importance (3)	S_i values as per Connection weight approach (4)	Ranking of inputs as per relative importance (5)
e/B	28.6	3	-1.6918	2
D_f/B	34.1	2	0.412	3
α/ϕ	37.3	1	-2.128	1

7.4.2 Neural Interpretation Diagram (NID)

Ozesmi and Ozesmi (1999) proposed neural interpretation diagram (NID) for visual interpretation of the connection weight among the neurons. For the present study with the

weights obtained as shown in Table 7.3, a Neural Interpretation Diagram is presented in Figure 7.4. The detail of neural interpretation diagram is enumerated in Chapter 6.

It can be seen from Figure 7.4 and 4th column of Table 7.5 that *e/B* and α/ϕ are inversely related to *RF* values whereas D_f/B is directly related to *RF*. It can be concluded that *RF* value decreases with increase in *e/B* and α/ϕ , but increases with increase in D_f/B. In other words, the developed ANN model is not a "black box" and could explain the physical effect of inputs on the output.

7.4.3 ANN model equation for the Reduction Factor based on trained neural network

A model equation is developed with the weights obtained from trained neural network as the model parameters (Goh et al. 2005). The mathematical equation relating input parameters (*e/B*, D_f/B, α/ϕ) to output (Reduction Factor i.e. *RF*) can be given by

$$RF_n = f_n\left\{b_0 + \sum_{k=1}^{h}\left[w_k f_n\left(b_{hk} + \sum_{i=1}^{m} w_{ik} X_i\right)\right]\right\} \qquad (7.3)$$

where RF_n = normalized value of *RF* in the range [-1, 1], f_n = transfer function, h = no. of neurons in the hidden layer, X_i = normalized value of inputs in the range [-1, 1], m = no. of input variables, w_{ik} = connection weight between i^{th} layer of input and k^{th} neuron of hidden layer, w_k = connection weight between k^{th} neuron of hidden layer and single output neuron, b_{hk} = bias at the k^{th} neuron of hidden layer, and b_o = bias at the output layer.

The model equation for the reduction factor of a shallow strip footing subjected to eccentrically inclined load as shown in Figure 7.1(b) is formulated using the values of the weights and biases shown in Table 7.3 as per the following steps.

Step – 1

The input parameters are normalized in the range [-1, 1] by the following expressions

$$X_n = 2\left(\frac{X_1 - X_{\min}}{X_{\max} - X_{\min}}\right) - 1 \tag{7.4}$$

Where, X_n = Normalized value of input parameter X_1 and X_{max} and X_{min} are maximum and minimum values of input parameter X_1 in the data set.

Step – 2

Calculate the normalized value of reduction factor (RF_n) using the following expressions

$$A_1 = -0.4188\left(\frac{e}{B}\right)_n + 0.3928\left(\frac{D_f}{B}\right)_n - 0.8511\left(\frac{\alpha}{\phi}\right)_n - 0.005 \tag{7.5}$$

$$A_2 = 0.17\left(\frac{e}{B}\right)_n + 5.2462\left(\frac{D_f}{B}\right)_n + 3.1071\left(\frac{\alpha}{\phi}\right)_n + 3.874 \tag{7.6}$$

$$A_3 = 4.0168\left(\frac{e}{B}\right)_n + 8.1273\left(\frac{D_f}{B}\right)_n - 4.8781\left(\frac{\alpha}{\phi}\right)_n + 7.3396 \tag{7.7}$$

$$A_4 = 6.2788\left(\frac{e}{B}\right)_n - 0.3513\left(\frac{D_f}{B}\right)_n + 3.247\left(\frac{\alpha}{\phi}\right)_n + 4.8671 \tag{7.8}$$

$$B_1 = 0.7337\left(\frac{e^{A_1} - e^{-A_1}}{e^{A_1} + e^{-A_1}}\right) \tag{7.9}$$

$$B_2 = -0.1013\left(\frac{e^{A_2} - e^{-A_2}}{e^{A_2} + e^{-A_2}}\right) \tag{7.10}$$

$$B_3 = 0.0693\left(\frac{e^{A_3} - e^{-A_3}}{e^{A_3} + e^{-A_3}}\right) \tag{7.11}$$

$$B_4 = -0.2621\left(\frac{e^{A_4} - e^{-A_4}}{e^{A_4} + e^{-A_4}}\right) \tag{7.12}$$

$$C_1 = 0.0972 + B_1 + B_2 + B_3 + B_4 \tag{7.13}$$

$$RF_n = C_1 \tag{7.14}$$

Step – 3

Denormalize the RF_n value obtained from Eq. (7.14) to actual RF as

$$RF = 0.5(RF_n + 1)(RF_{\max} - RF_{\min}) + RF_{\min} \tag{7.15}$$

$$RF = 0.5(RF_n + 1)(1 - 0.291) + 0.291 \tag{7.16}$$

7.5 Comparison

7.5.1 Comparison with Developed Empirical Equation

In Chapter 5, an empirical equation is developed for reduction factor (RF) in reinforced case and expressed as

$$RF = \frac{q_{u(D_f/B, e/B, \alpha/\phi)}}{q_{u(D_f/B, e/B=0, \alpha/\phi=0)}} = \left[1 - \left(\frac{e}{B}\right)^2\right]\left[1 - \left(\frac{\alpha}{\phi}\right)\right]^{\left(1.5 - 0.7\frac{D_f}{B}\right)} \tag{7.17}$$

Figures 7.8 and 7.9 show the comparison of RF values obtained from Eq. 7.15 (obtained from ANN) with Eqs. (7.17) (obtained by Empirical equation) and (7.1) (obtained from

experiments). It is seen that ANN results are closer to line of equality than the empirical ones from Eq. (7.17).

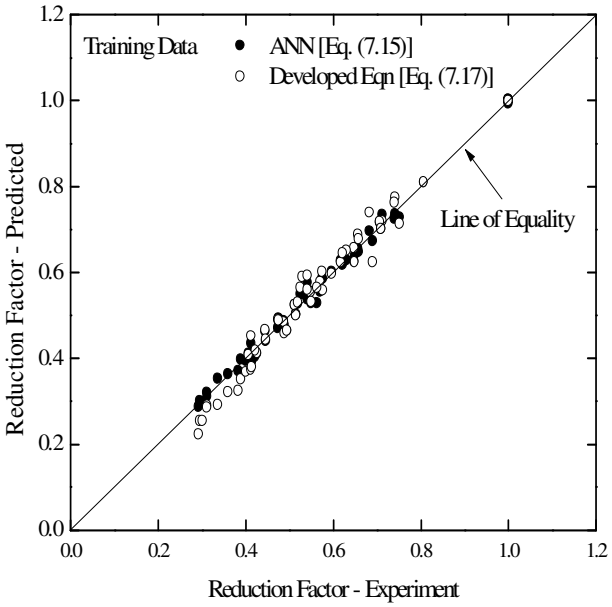

Figure 7.8: Comparison of ANN results with Experimental *RF* and Developed equation for training data

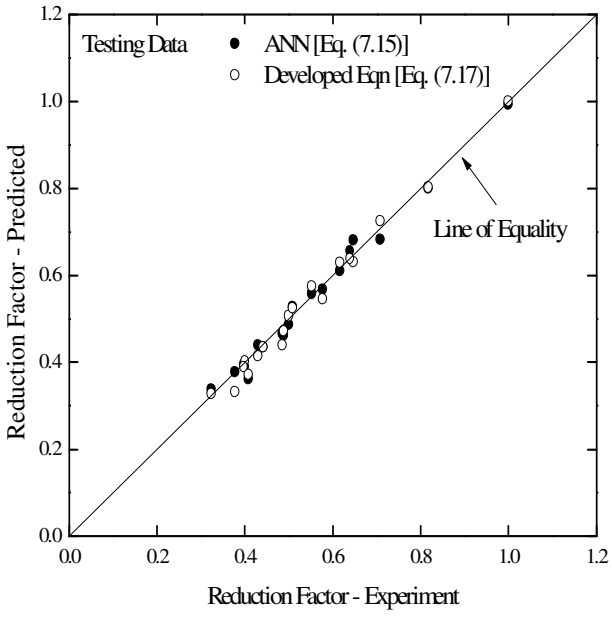

Figure 7.9: Comparison of ANN results with Experimental *RF* and Developed equation for testing data

7.5.2 Comparison with Loukidis et al. [2008]

As discussed in section 5.5.1, using Eqs. for combined eccentricity-inclination factor proposed by Loukidis et al. (2008) and considering load inclination in clockwise direction simulating to the condition of reinforced footing, the reduction factor *RF* corresponding to Loukidis et al. (2008) can be written as

$$RF = \frac{f_{ie}}{\cos\alpha} \tag{7.18}$$

The reduction factors corresponding to Loukidis et al. (2008) obtained by using Eq. (7.18) are shown in Figures 7.10 and 7.11 for dense and medium dense sand along with those values obtained from Eqs. (7.15) (obtained from ANN) and (7.1) (obtained from experiments). The comparison appears to be good.

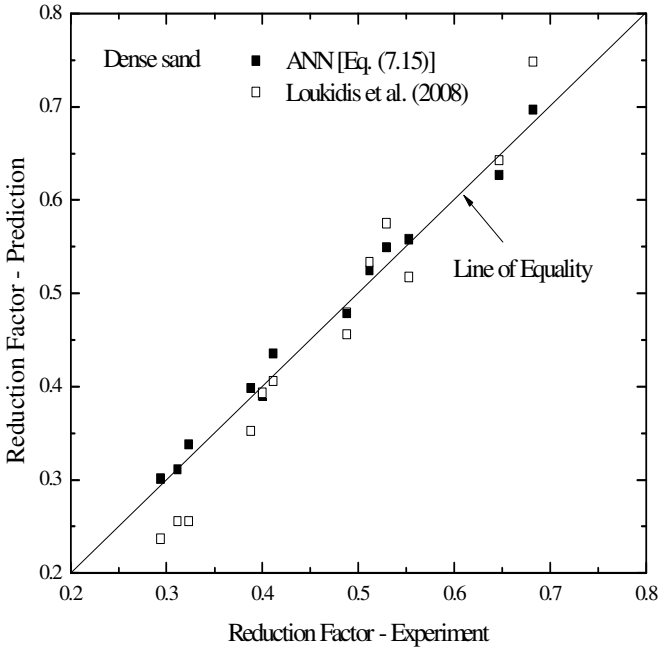

Figure 7.10: Comparison of ANN results with Loukidis et al. (2008) for dense sand

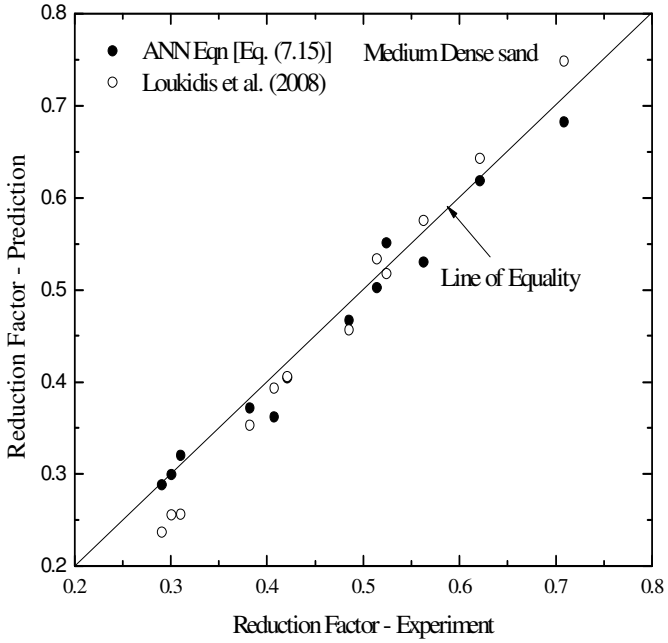

Figure 7.11: Comparison of ANN results with Loukidis et al. (2008) for medium dense sand

7.6 Conclusions

Based on the neural network model developed herein, the following conclusions are drawn.

- Since the errors are distributed evenly along the horizontal axis, the network is well trained and can predict the result with reasonable accuracy.
- α/ϕ is the most important input parameter followed by e/B and D_f/B as observed in Pearson correlation coefficient.
- Similarly, using Garson's algorithm, α/ϕ is found to be the most important input parameter followed by D_f/B and e/B.
- The results obtained by using Connection weight approach are same as Pearson correlation coefficient.

- The developed ANN model has explained the physical effect of inputs on the output, as depicted in NID. It is observed that e/B and α/ϕ are inversely related to RF values whereas D_f/B is directly related to RF.
- A model equation is developed based on the trained weights of the ANN.
- The predictability of ANN model is better than the developed empirical equation.

8. PREDICTION OF ULTIMATE BEARING CAPACITY OF ECCENTRICALLY INCLINED LOADED STRIP FOOTING BY ANN: PART III

8.1 Introduction

There may be two possible modes of load application when a shallow strip footing is subjected to eccentrically inclined loads. Figure 8.1 shows such cases of load applications.

As mentioned in the Chapter 4 and 5, laboratory model tests have been conducted with shallow strip footings subjected to loads which are both eccentric and inclined. The prediction of ultimate bearing capacity in such loading conditions have been mentioned independently in Chapter 6 and 7 when the line of load application is towards the center-line and away from the center line of the footing respectively. In this chapter, the objective is to predict the ultimate bearing capacity in a single formulation when the load is applied either away from the center line or towards the center line of the footing.

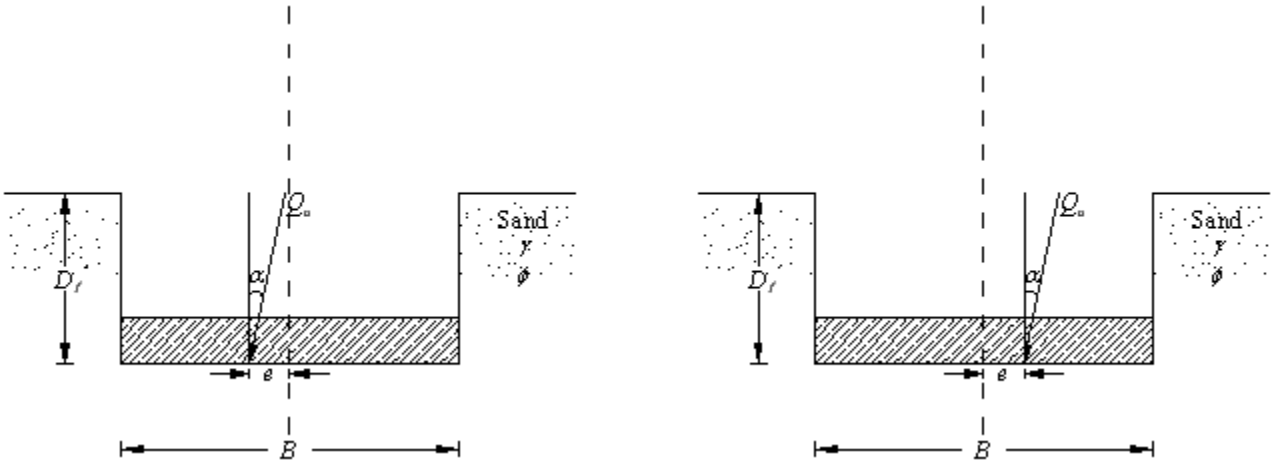

Figure 8.1 Eccentrically inclined load on a strip foundation: (a) *Partially compensated* case, (b) *Reinforced* case

8.2 Database and Preprocessing

The extensive results of laboratory experimental data presented in Chapter 4 and 5 have been considered for study in this chapter. Load tests are carried out on model strip footings subjected to eccentrically inclined loads in the manner as shown in both Figures 8.1(a) and 8.1(b) that are increased to failure. The data consist of parameters like load eccentricity (e), load inclination (α), embedment ratio (D_f /B), friction angle (ϕ) and ultimate bearing capacity (q_u). Results from one hundred and ninety two number of laboratory model tests have been considered in the analysis. The input parameters are e/B, α/ϕ, D_f /B and LA and the output is reduction factor (RF). LA is known as Load Arrangement. It can be defined as

LA = -1 [Line of load application is towards the center line of the footing as shown in Figure 8.1(a)]

= 0 [Centric Vertical and Eccentric Vertical loading condition]

= 1 [Line of load application is away from the center line of the footing as shown in Figure 8.1(b)]

The reduction factor (RF) is given by

$$RF = \frac{q_{u(D_f/B,\, e/B,\, \alpha/\phi,\, LA)}}{q_{u(D_f/B,\, e/B=0,\, \alpha/\phi=0,\, LA=0)}} \tag{8.1}$$

where $q_{u(D_f B,\, e/B,\, \alpha/\varphi,\, LA)}$ = ultimate bearing capacity with eccentricity ratio e/B and inclination ratio α/ϕ and load arrangement LA at an embedment ratio D_f /B and $q_{u(D_f B,\, e/B=0,\, \alpha/\varphi=0,\, LA=0)}$= ultimate settlement corresponding to ultimate bearing capacity

with centric vertical loading ($e/B = 0$, $\alpha/\phi = 0$ and $LA = 0$) at the same embedment ratio D_f/B.

Out of 192 test records shown in Table 8.1, 144 tests are considered for training and the remaining 48 are reserved for testing. Each record represents a complete model test where an eccentrically inclined loaded strip footing is subjected to failure. Similar type of preprocessing is adopted here as discussed in section 6.4.

Table 8.1. Dataset used for training and testing of ANN model

Data Type (1)	Expt. No. (2)	$\frac{e}{B}$ (3)	$\frac{D_f}{B}$ (4)	$\frac{\alpha}{\phi}$ (5)	LA (6)	Experimental q_u (kN/m^2) (7)	Experimental RF [Eq. (8.1)] (8)
Training	1	0.05	0	0	0	133.42	0.800
	2	0.1	0	0	0	109.87	0.659
	3	0.15	0	0	0	86.33	0.518
	4	0	0	0.123	0	128.51	0.771
	5	0.05	0	0.123	-1	103.01	0.618
	6	0.1	0	0.123	-1	86.33	0.518
	7	0	0	0.245	0	96.14	0.576
	8	0.05	0	0.245	-1	76.52	0.459
	9	0.15	0	0.245	-1	51.99	0.312
	10	0	0	0.368	0	66.71	0.400
	11	0.1	0	0.368	-1	44.15	0.265
	12	0.15	0	0.368	-1	35.12	0.211
	13	0.05	0	0.49	-1	34.83	0.209
	14	0.1	0	0.49	-1	29.43	0.176
	15	0.15	0	0.49	-1	23.54	0.141
	16	0	0.5	0	0	264.87	1.000
	17	0.05	0.5	0	0	226.61	0.856
	18	0.1	0.5	0	0	195.22	0.737
	19	0	0.5	0.123	0	223.67	0.844
	20	0.05	0.5	0.123	-1	193.26	0.730
	21	0.15	0.5	0.123	-1	140.28	0.530
	22	0	0.5	0.245	0	186.39	0.704
	23	0.1	0.5	0.245	-1	137.34	0.519
	24	0.15	0.5	0.245	-1	116.74	0.441
	25	0.05	0.5	0.368	-1	129.49	0.489

Table 8.1 (Continued)

Data Type (1)	Expt. No. (2)	$\frac{e}{B}$ (3)	$\frac{D_f}{B}$ (4)	$\frac{\alpha}{\phi}$ (5)	LA (6)	Experimental q_u (kN/m^2) (7)	Experimental RF [Eq. (8.1)] (8)
	26	0.1	0.5	0.368	-1	111.83	0.422
	27	0.15	0.5	0.368	-1	94.18	0.356
	28	0	0.5	0.49	0	115.76	0.437
	29	0.05	0.5	0.49	-1	98.10	0.370
	30	0.1	0.5	0.49	-1	85.35	0.322
	31	0	1	0	0	353.16	1.000
	32	0.05	1	0	0	313.92	0.889
	33	0.15	1	0	0	245.25	0.694
	34	0	1	0.123	0	313.92	0.889
	35	0.1	1	0.123	-1	241.33	0.683
	36	0.15	1	0.123	-1	215.82	0.611
	37	0.05	1	0.245	-1	239.36	0.678
	38	0.1	1	0.245	-1	212.88	0.603
	39	0.15	1	0.245	-1	188.35	0.533
	40	0	1	0.368	0	225.63	0.639
	41	0.05	1	0.368	-1	206.01	0.583
	42	0.1	1	0.368	-1	179.52	0.508
	43	0	1	0.49	0	183.45	0.519
	44	0.05	1	0.49	-1	166.77	0.472
	45	0.15	1	0.49	-1	126.55	0.358
	46	0	0	0	0	101.04	1.000
	47	0.1	0	0	0	68.67	0.680
	48	0.15	0	0	0	54.94	0.544
	49	0.05	0	0.133	-1	63.77	0.631
	50	0.1	0	0.133	-1	52.97	0.524
	51	0.15	0	0.133	-1	42.18	0.417
	52	0	0	0.267	0	55.92	0.553
	53	0.05	0	0.267	-1	47.09	0.466
	54	0.1	0	0.267	-1	38.46	0.381
	55	0	0	0.4	0	38.26	0.379
	56	0.05	0	0.4	-1	32.37	0.320
	57	0.15	0	0.4	-1	20.60	0.204
	58	0	0	0.533	0	24.03	0.238
	59	0.1	0	0.533	-1	16.68	0.165
	60	0.15	0	0.533	-1	13.34	0.132
	61	0.05	0.5	0	0	123.61	0.863
	62	0.1	0.5	0	0	103.99	0.726
	63	0.15	0.5	0	0	87.31	0.610

Table 8.1 (Continued)

Data Type (1)	Expt. No. (2)	$\frac{e}{B}$ (3)	$\frac{D_f}{B}$ (4)	$\frac{\alpha}{\phi}$ (5)	LA (6)	Experimental q_u (kN/m^2) (7)	Experimental RF [Eq. (8.1)] (8)
	64	0	0.5	0.133	0	120.66	0.842
	65	0.05	0.5	0.133	-1	103.99	0.726
	66	0.1	0.5	0.133	-1	90.25	0.630
	67	0	0.5	0.267	0	98.10	0.685
	68	0.05	0.5	0.267	-1	84.86	0.592
	69	0.15	0.5	0.267	-1	60.82	0.425
	70	0	0.5	0.4	0	79.46	0.555
	71	0.1	0.5	0.4	-1	56.90	0.397
	72	0.15	0.5	0.4	-1	48.07	0.336
	73	0.05	0.5	0.533	-1	50.03	0.349
	74	0.1	0.5	0.533	-1	43.16	0.301
	75	0.15	0.5	0.533	-1	36.30	0.253
	76	0	1	0	0	208.95	1.000
	77	0.05	1	0	0	193.26	0.925
	78	0.1	1	0	0	175.60	0.840
	79	0	1	0.133	0	186.39	0.892
	80	0.05	1	0.133	-1	168.73	0.808
	81	0.15	1	0.133	-1	137.34	0.657
	82	0	1	0.267	0	160.88	0.770
	83	0.1	1	0.267	-1	129.49	0.620
	84	0.15	1	0.267	-1	112.82	0.540
	85	0.05	1	0.4	-1	118.70	0.568
	86	0.1	1	0.4	-1	106.93	0.512
	87	0.15	1	0.4	-1	94.18	0.451
	88	0	1	0.533	0	98.10	0.469
	89	0.05	1	0.533	-1	92.21	0.441
	90	0.1	1	0.533	-1	84.37	0.404
	91	0.1	0	0.123	1	107.91	0.647
	92	0.15	0	0.123	1	92.214	0.553
	93	0.05	0	0.245	1	88.29	0.529
	94	0.1	0	0.245	1	85.347	0.512
	95	0.05	0	0.368	1	68.67	0.412
	96	0.15	0	0.368	1	64.746	0.388
	97	0.05	0	0.49	1	53.955	0.324
	98	0.1	0	0.49	1	51.993	0.312
	99	0.15	0	0.49	1	49.05	0.294
	100	0.1	0.5	0.123	1	173.637	0.656
	101	0.15	0.5	0.123	1	152.055	0.574

Table 8.1 (Continued)

Data Type (1)	Expt. No. (2)	$\frac{e}{B}$ (3)	$\frac{D_f}{B}$ (4)	$\frac{\alpha}{\phi}$ (5)	LA (6)	Experimental q_u (kN/m^2) (7)	Experimental RF [Eq. (8.1)] (8)
	102	0.05	0.5	0.245	1	166.77	0.630
	103	0.1	0.5	0.245	1	151.074	0.570
	104	0.15	0.5	0.245	1	132.435	0.500
	105	0.05	0.5	0.368	1	137.34	0.519
	106	0.1	0.5	0.368	1	129.492	0.489
	107	0.05	0.5	0.49	1	113.796	0.430
	108	0.15	0.5	0.49	1	95.157	0.359
	109	0.05	1	0.123	1	284.49	0.806
	110	0.1	1	0.123	1	251.136	0.711
	111	0.15	1	0.123	1	228.573	0.647
	112	0.1	1	0.245	1	225.63	0.639
	113	0.15	1	0.245	1	203.067	0.575
	114	0.05	1	0.368	1	217.782	0.617
	115	0.1	1	0.368	1	193.257	0.547
	116	0.05	1	0.49	1	179.523	0.508
	117	0.15	1	0.49	1	143.226	0.406
	118	0.1	0	0.133	1	62.78	0.621
	119	0.15	0	0.133	1	52.97	0.524
	120	0.05	0	0.267	1	56.90	0.563
	121	0.1	0	0.267	1	51.99	0.515
	122	0.15	0	0.267	1	49.05	0.485
	123	0.05	0	0.4	1	42.58	0.421
	124	0.1	0	0.4	1	41.20	0.408
	125	0.05	0	0.533	1	31.39	0.311
	126	0.15	0	0.533	1	29.43	0.291
	127	0.1	0.5	0.133	1	94.18	0.658
	128	0.15	0.5	0.133	1	77.50	0.541
	129	0.05	0.5	0.267	1	88.29	0.616
	130	0.1	0.5	0.267	1	77.50	0.541
	131	0.05	0.5	0.4	1	73.58	0.514
	132	0.15	0.5	0.4	1	56.90	0.397
	133	0.05	0.5	0.533	1	58.86	0.411
	134	0.1	0.5	0.533	1	53.96	0.377
	135	0.15	0.5	0.533	1	48.07	0.336
	136	0.1	1	0.133	1	156.96	0.751
	137	0.15	1	0.133	1	144.21	0.690
	138	0.05	1	0.267	1	148.13	0.709
	139	0.1	1	0.267	1	135.38	0.648

Table 8.1 (Continued)

Data Type (1)	Expt. No. (2)	$\frac{e}{B}$ (3)	$\frac{D_f}{B}$ (4)	$\frac{\alpha}{\phi}$ (5)	LA (6)	Experimental q_u (kN/m^2) (7)	Experimental RF [Eq. (8.1)] (8)
	140	0.05	1	0.4	1	124.59	0.596
	141	0.1	1	0.4	1	114.78	0.549
	142	0.15	1	0.4	1	103.01	0.493
	143	0.05	1	0.533	1	99.08	0.474
	144	0.15	1	0.533	1	86.33	0.413
Testing	1	0	0	0	0	166.77	1.000
	2	0.15	0	0.123	-1	65.73	0.394
	3	0.1	0	0.245	-1	62.78	0.376
	4	0.05	0	0.368	-1	53.96	0.324
	5	0	0	0.49	0	43.16	0.259
	6	0.15	0.5	0	0	164.81	0.622
	7	0.1	0.5	0.123	-1	165.79	0.626
	8	0.05	0.5	0.245	-1	160.88	0.607
	9	0	0.5	0.368	0	151.07	0.570
	10	0.15	0.5	0.49	-1	72.59	0.274
	11	0.1	1	0	0	278.60	0.789
	12	0.05	1	0.123	-1	277.62	0.786
	13	0	1	0.245	0	264.87	0.750
	14	0.15	1	0.368	-1	155.98	0.442
	15	0.1	1	0.49	-1	143.23	0.406
	16	0.05	0	0	0	84.37	0.835
	17	0	0	0.133	0	79.46	0.786
	18	0.15	0	0.267	-1	31.39	0.311
	19	0.1	0	0.4	-1	26.98	0.267
	20	0.05	0	0.533	-1	19.62	0.194
	21	0	0.5	0	0	143.23	1.000
	22	0.15	0.5	0.133	-1	72.59	0.507
	23	0.1	0.5	0.267	-1	72.59	0.507
	24	0.05	0.5	0.4	-1	67.89	0.474
	25	0	0.5	0.533	0	58.27	0.407
	26	0.15	1	0	0	156.96	0.751
	27	0.1	1	0.133	-1	153.04	0.732
	28	0.05	1	0.267	-1	144.21	0.690
	29	0	1	0.4	0	133.42	0.638
	30	0.15	1	0.533	-1	75.54	0.362
	31	0.05	0	0.123	1	113.796	0.682
	32	0.15	0	0.245	1	81.423	0.488

Table 8.1 (Continued)

Data Type (1)	Expt. No. (2)	$\frac{e}{B}$ (3)	$\frac{D_f}{B}$ (4)	$\frac{\alpha}{\phi}$ (5)	LA (6)	Experimental q_u (kN/m^2) (7)	Experimental RF [Eq. (8.1)] (8)
	33	0.1	0	0.368	1	66.708	0.400
	34	0.05	0.5	0.123	1	196.2	0.741
	35	0.15	0.5	0.368	1	112.815	0.426
	36	0.1	0.5	0.49	1	105.948	0.400
	37	0.05	1	0.245	1	249.174	0.706
	38	0.15	1	0.368	1	171.675	0.486
	39	0.1	1	0.49	1	156.96	0.444
	40	0.05	0	0.133	1	71.61	0.709
	41	0.15	0	0.4	1	38.65	0.383
	42	0.1	0	0.533	1	30.41	0.301
	43	0.05	0.5	0.133	1	105.95	0.740
	44	0.15	0.5	0.267	1	67.69	0.473
	45	0.1	0.5	0.4	1	63.77	0.445
	46	0.05	1	0.133	1	170.69	0.817
	47	0.15	1	0.267	1	120.66	0.577
	48	0.1	1	0.533	1	92.21	0.441

8.3 Results and Discussion

The maximum, minimum, average and standard deviation values of the four inputs and one output parameters used in the ANN model are presented in Table 8.2. They are calculated from the database. The schematic diagram of ANN architecture is shown in Figure 8.2. The number of hidden layer neurons is varied and the mean square error (mse) is noted. The minimum mse is found to be 1.0×10^{-3} when there are five neurons in the hidden layer [Figure 8.3]. Therefore, the final ANN architecture is retained as 4-5-1 [i.e. 4 (input) – 5 (hidden layer neuron) – 1 (Output)].

Table 8.2. Statistical values of the parameters

Parameter	Maximum value	Minimum value	Average value	Standard Deviation
e/B	0.15	0	0.084	0.052
D_f/B	1	0	0.5	0.408

Parameter	Maximum value	Minimum value	Average value	Standard Deviation
α/ϕ	0.533	0	0.28	0.171
LA	1.0	-1.0	0	0.866
RF	1.0	0.132	0.543	0.19

[INPUT LAYER = *l*] [HIDDEN LAYER = *m*] [OUTPUT LAYER = *n*]

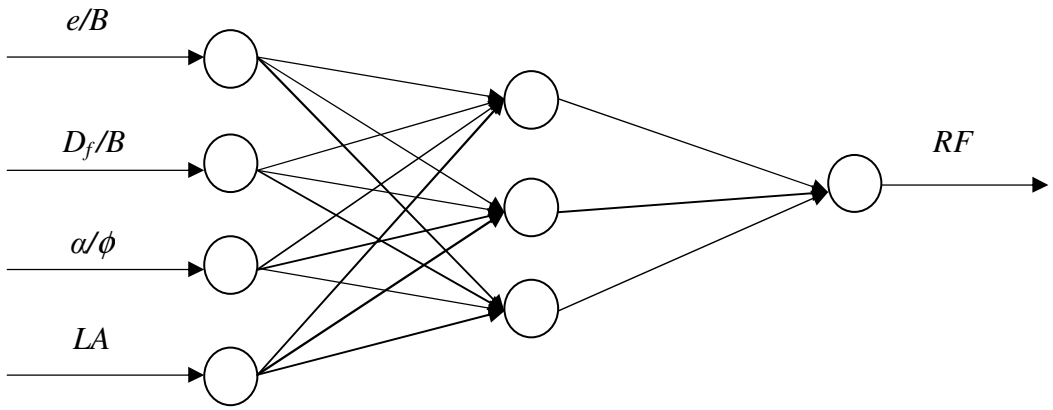

Figure 8.2 The ANN Architecture

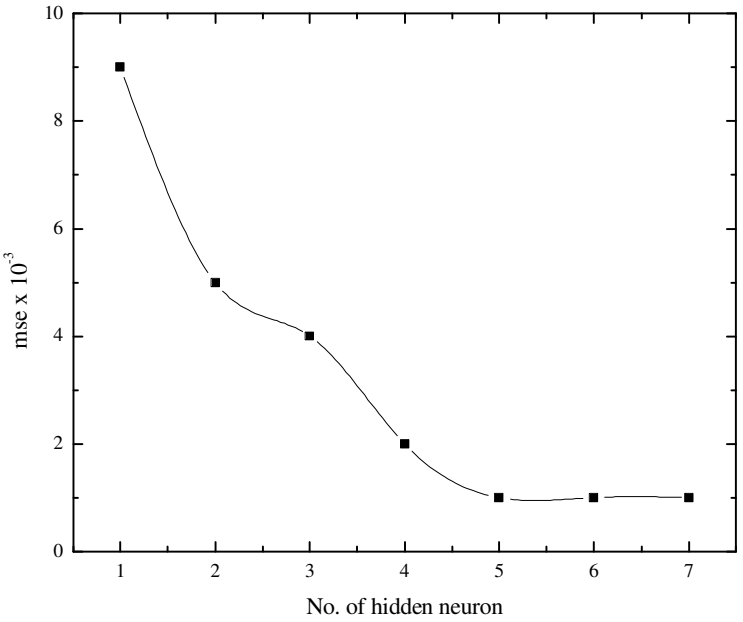

Figure 8.3 Variation of hidden layer neuron with mean square error (mse)

The coefficient of efficiency (R^2) for training and testing data are found to be 0.99 and 0.98 respectively, as shown in Figures 8.4 and 8.5. Data used in this analysis have been obtained from laboratory model tests carried out in duplicate, in a calibration chamber, the details of which are given in Chapter 3, 4 and 6. The weights and biases of the network are presented in Table 8.3. These weights and biases can be utilized for interpretation of relationship between the inputs and output, sensitivity analysis and framing an ANN model in the form of an equation.

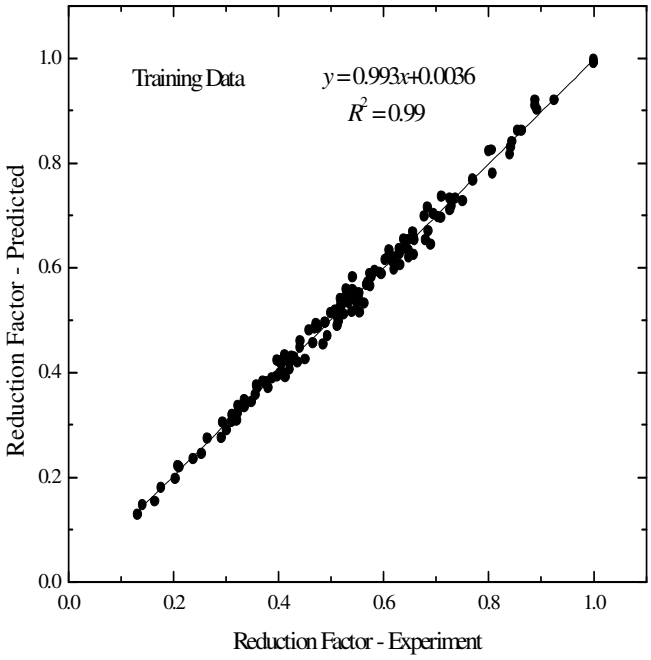

Figure 8.4 Correlation between Predicted Reduction Factor with Experimental Reduction Factor for training data

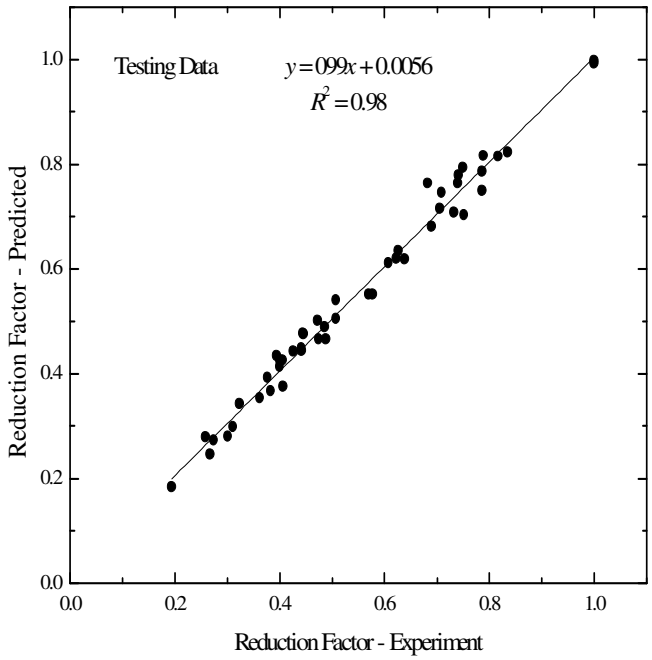

Figure 8.5 Correlation between Predicted Reduction Factor with Experimental Reduction Factor for testing data

Table 8.3. Values of connection weights and biases

Neuron	Weight					Bias	
	w_{ik}				w_k		
	e/B	D_f/B	α/ϕ	*LA*	*RF*	b_{hk}	b_0
Hidden Neuron 1 (k=1)	-1.35	-0.9514	-3.1318	2.0935	0.1861	-4.7877	-0.0064
Hidden Neuron 2 (k=2)	1.1469	-0.3053	1.4808	-3.5185	-0.1399	1.4851	
Hidden Neuron 3 (k=3)	0.8794	0.7097	-1.2318	-0.8993	0.1846	2.3233	
Hidden Neuron 4 (k=4)	-0.231	0.9149	-0.9087	1.0174	0.2944	2.265	
Hidden Neuron 5 (k=5)	0.4031	-0.2417	0.7069	0.1688	-0.7199	0.3686	

The residual analysis is carried out by calculating the residuals from the experimental reduction factor and predicted reduction factor for training data set. Residual (e_r) can be defined as the difference between the experimental and predicted *RF* value and is given by

$$e_r = RF_i - RF_p \tag{8.2}$$

where RF_i and RF_p are experimental and predicted *RF* value respectively.

The residuals are plotted with the experiment number as shown in Figure 8.6. It is observed that the residuals are distributed evenly along the centerline of the plot. Therefore, it can be said that the network is well trained and can be used for prediction with reasonable accuracy.

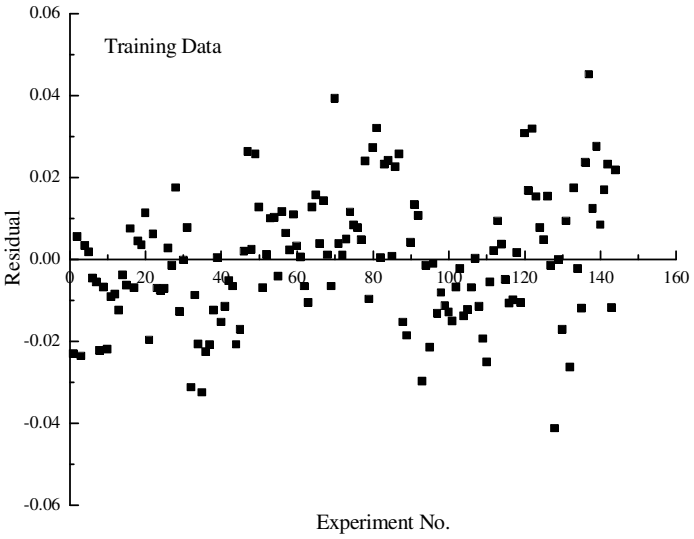

Figure 8.6. Residual distribution of training data

8.3.1 Sensitivity Analysis

Artificial neural networks are data driven approach and the important inputs are selected by conducting sensitivity analysis. Different approaches like Pearson correlation coefficient (Guyon and Elisseeff 2003; Wilby et al. 2003), Garson's algorithm (Garson

1991; Goh 1995) and connection weight approach method (Olden et al. 2004) are used to identify important input parameters based on the trained weights and biases of neural network model (briefly described in Chapter 6).

Table 8.4. Cross-correlation of the input and output for the reduction factor

Parameters	*e/B*	D_f/B	α/ϕ	*LA*	*RF*
e/B	1	0	0.04	0	-0.42
D_f/B		1	0	0	0.37
α/ϕ			1	0	-0.79
LA				1	0.16
RF					1

Table 8.4 shows the cross correlation of inputs with the reduction factor. From the table it is observed that *RF* is highly correlated to α/ϕ with a cross correlation values of 0.79, followed by *e/B*, D_f/B and *LA*. The ranking of the four input parameters as per Garson's algorithm is presented in Table 8.5. The α/ϕ is found to be the most important input parameter with the relative importance value being 34.75% followed by 30.15% for *LA*, 18.68% for *e/B* and 16.42% for D_f/B. The relative importance of the input variables using connection weight approach (Olden et al. 2004) is also presented in Table 8.5. The α/ϕ is found to be the most important input parameter (S_i value = -1.794) followed by *LA* (S_i value = 0.894), *e/B* (S_i value = -0.608) and D_f/B (S_i value = 0.44). The summation of products of input-hidden and hidden-output weights across all the hidden neurons is called as S_i (Olden et al. 2004). The S_i values being negative imply that both α/ϕ and *e/B* are indirectly related whereas *LA* and D_f/B are directly related to *RF* values.

Table 8.5. Relative Importance of different inputs as per Garson's algorithm and connection weight approach

Parameters	Garson's algorithm		Connection weight approach	
(1)	Relative Importance (%) (2)	Ranking of inputs as per relative importance (3)	S_i values as per Connection weight approach (4)	Ranking of inputs as per relative importance (5)
e/B	18.68	3	-0.608	3
D_f/B	16.42	4	0.44	4
α/ϕ	34.75	1	-1.794	1
LA	30.15	2	0.894	2

8.3.2 Neural Interpretation Diagram (NID)

Ozesmi and Ozesmi (1999) proposed a novel approach called as Neural Interpretation Diagram (NID) for visual interpretation of the connection weight among the neurons and to find interrelationship between the inputs and output. Neural interpretation diagram is discussed in detail in Chapter 6.

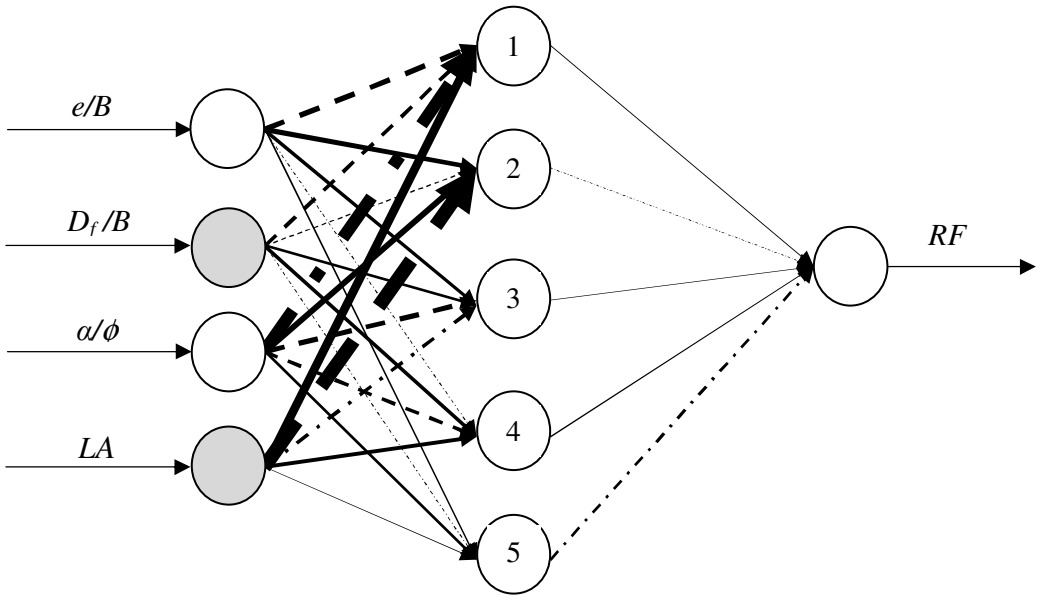

Figure 8.7. Neural Interpretation Diagram (NID) showing lines representing connection weights and effects of inputs on Reduction Factor (*RF*)

It can be seen from Table 8.5 (4th Column) that S_i values for parameters *e/B* and α/ϕ are negative indicating that both the parameters *e/B* and α/ϕ are inversely related to whereas S_i value for parameter *LA* and D_f/B being positive is directly related to *RF* values. This is shown in Figure 8.7. Thus it is inferred that *RF* value increases with increase in *LA* and D_f/B values and decreases with increase in *e/B* and α/ϕ values. Therefore, the developed ANN model is not a "black box" and could explain the physical effect of the input parameters on the output.

8.3.3 ANN model equation for the Reduction Factor based on trained neural network

A model equation is developed with the weights obtained from trained neural network as the model parameters (Goh et al. 2005). The mathematical equation relating input parameters (*e/B,* D_f/B, α/ϕ, *LA*) to output (Reduction Factor) can be given by

$$RF_n = f_n\left\{b_0 + \sum_{k=1}^{h}\left[w_k f_n\left(b_{hk} + \sum_{i=1}^{m} w_{ik} X_i\right)\right]\right\} \tag{8.3}$$

where RF_n = normalized value of RF in the range [-1, 1], f_n = transfer function, h = no. of neurons in the hidden layer, X_i = normalized value of inputs in the range [-1, 1], m = no. of input variables, w_{ik} = connection weight between i^{th} layer of input and k^{th} neuron of hidden layer, w_k = connection weight between k^{th} neuron of hidden layer and single output neuron, b_{hk} = bias at the k^{th} neuron of hidden layer, and b_o = bias at the output layer.

The model equation for Reduction Factor of shallow strip foundations subjected to eccentrically inclined load (both mode of load application) is formulated using the values of the weights and biases shown in Table 8.3 as per the following steps.

Step – 1

The input parameters are normalized in the range [-1 1] by the following expressions

$$X_n = 2\left(\frac{X_1 - X_{\min}}{X_{\max} - X_{\min}}\right) - 1 \tag{8.4}$$

where, X_n = Normalized value of input parameter X_1, and X_{max} and X_{min} are maximum and minimum values of the input parameter X_1 in the data set.

Step – 2

Calculate the normalized value of reduction factor (RF_n) using the following expressions

$$A_1 = -1.35\left(\frac{e}{B}\right)_n - 0.9514\left(\frac{D_f}{B}\right)_n - 3.1318\left(\frac{\alpha}{\phi}\right)_n + 2.0935(LA)_n - 4.7877 \tag{8.5}$$

$$A_2 = 1.1469\left(\frac{e}{B}\right)_n - 0.3053\left(\frac{D_f}{B}\right)_n + 1.4808\left(\frac{\alpha}{\phi}\right)_n - 3.5185(LA)_n + 1.4851 \tag{8.6}$$

$$A_3 = 0.8794\left(\frac{e}{B}\right)_n + 0.7097\left(\frac{D_f}{B}\right)_n - 1.2318\left(\frac{\alpha}{\phi}\right)_n - 0.8993(LA)_n + 2.3233 \tag{8.7}$$

$$A_4 = -0.231\left(\frac{e}{B}\right)_n + 0.9149\left(\frac{D_f}{B}\right)_n - 0.9087\left(\frac{\alpha}{\phi}\right)_n + 1.0174(LA)_n + 2.265 \tag{8.8}$$

$$A_5 = 0.4031\left(\frac{e}{B}\right)_n - 0.2417\left(\frac{D_f}{B}\right)_n + 0.7069\left(\frac{\alpha}{\phi}\right)_n + 0.1688(LA)_n + 0.3686 \tag{8.9}$$

$$B_1 = 0.1861\left(\frac{e^{A_1} - e^{-A_1}}{e^{A_1} + e^{-A_1}}\right) \tag{8.10}$$

$$B_2 = -0.1399\left(\frac{e^{A_2} - e^{-A_2}}{e^{A_2} + e^{-A_2}}\right) \tag{8.11}$$

$$B_3 = 0.1846\left(\frac{e^{A_3} - e^{-A_3}}{e^{A_3} + e^{-A_3}}\right) \tag{8.12}$$

$$B_4 = 0.2944\left(\frac{e^{A_4} - e^{-A_4}}{e^{A_4} + e^{-A_4}}\right) \tag{8.13}$$

$$B_5 = -0.7199\left(\frac{e^{A_5} - e^{-A_5}}{e^{A_5} + e^{-A_5}}\right) \tag{8.14}$$

$$C_1 = -0.0064 + B_1 + B_2 + B_3 + B_4 + B_5 \tag{8.15}$$

$$C_1 = RF_n \tag{8.16}$$

Step – 3

Denormalize the RF_n value obtained from Eq. (8.18) to actual RF as

$$RF = 0.5(RF_n + 1)(RF_{\max} - RF_{\min}) + RF_{\min} \tag{8.17}$$

$$RF = 0.5(RF_n + 1)(1 - 0.132) + 0.132 \tag{8.18}$$

8.4 Comparison

Earlier, in Chapter 6 an ANN model equation is proposed for eccentrically inclined loaded strip foundation considering that the line of load application is towards the center line of the footing which can be expressed as

$$RF_1 = 0.5(RF_n + 1)(1 - 0.132) + 0.132 \tag{8.19}$$

where RF_1 = Reduction Factor for the above loading condition

Similarly, in Chapter 7 an ANN model equation is developed for eccentrically inclined loaded strip foundation when the load is applied away from the center line of the footing that can be expressed as

$$RF_2 = 0.5(RF_n + 1)(1 - 0..291) + 0.291 \tag{8.20}$$

where, RF_2 = Reduction Factor for above case

The plot of reduction factor obtained from Eqs. (8.19) and (8.20) with Eq. (8.17) and Eq. (8.1) is shown in Figure 8.8. Excellent results are found.

The present developed model ANN equation is in well agreement with the empirical equations mentioned in Chapter 4 and 5 along with results from other approaches. The

comparison is shown in Figure 8.9 and also in Table A.1 [Appendix A]. This single equation can predict with reasonable accuracy in both type of loading.

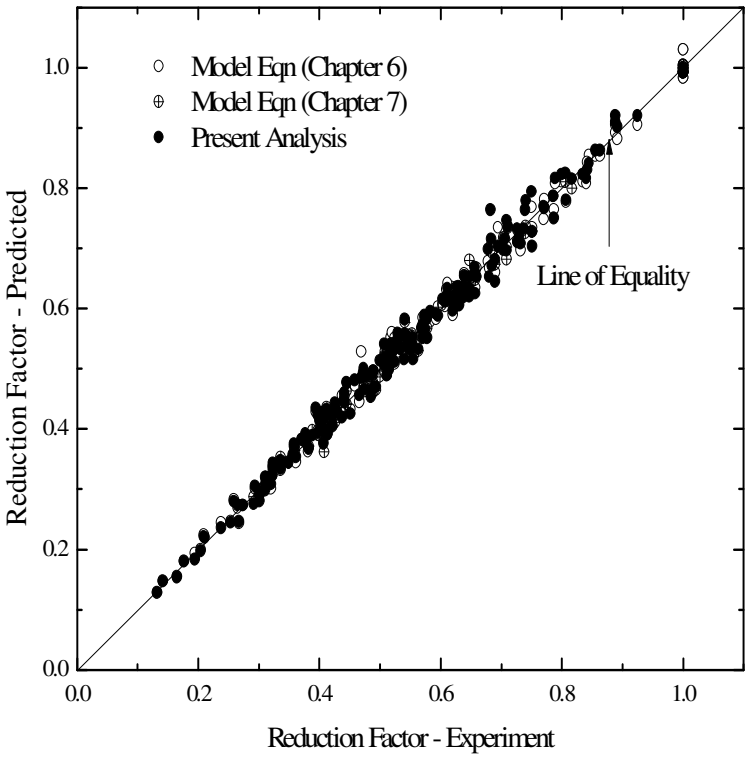

Figure 8.8. Comparison of Reduction Factor of Present analysis with ANN model equation developed in Chapter 6 and 7 for both type of load arrangement

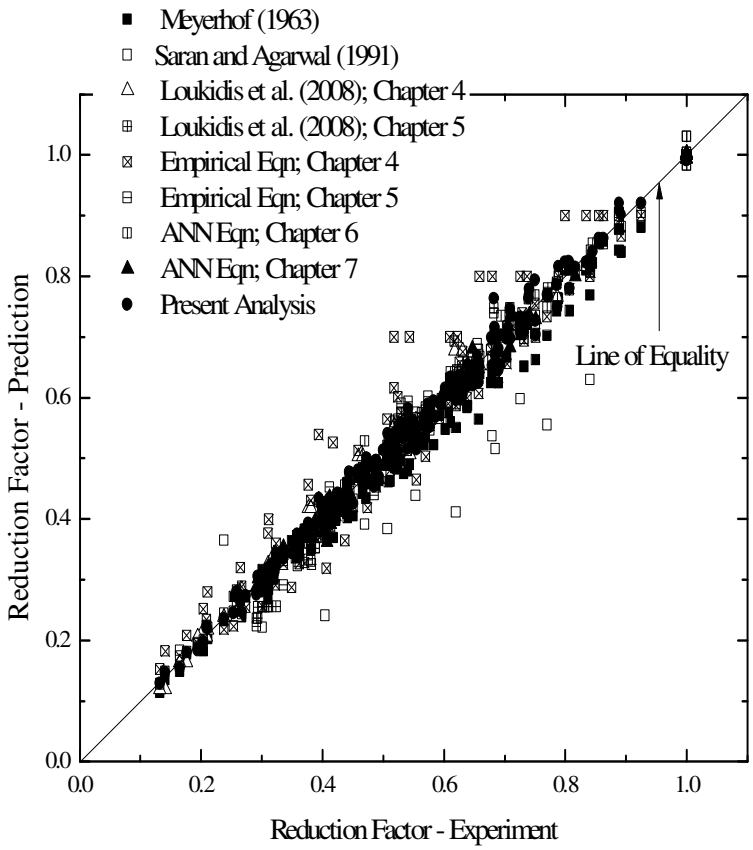

Figure 8.9. Comparison of Reduction Factor of Present analysis with other approaches

8.5 Conclusions

Based on the developed neural network model, following conclusions are drawn:

- As the errors are distributed evenly along the center line, the network is well trained and can predict the result with reasonable accuracy.
- Based on Pearson correlation coefficient, α/ϕ is the most important input parameter followed by e/B, D_f/B and LA.
- Using connection weight approach and Garson's algorithm, α/ϕ is found to be the most important input parameter followed by LA, e/B, and D_f/B.

- The developed ANN model has explained the physical effect of inputs on the output, as depicted in NID. It is observed that e/B and α/ϕ are inversely related to RF values whereas D_f/B and LA are directly related to RF.
- This developed combined ANN model equation can be applicable for either mode of load application to predict ultimate bearing capacity which is in good agreement with other methods.

9. ESTIMATION OF AVERAGE SETTLEMENT OF SHALLOW STRIP FOUNDATION ON GRANULAR SOIL UNDER ECCENTRIC LOADING

9.1 Introduction

For a foundation supported by granular soil within the zone of influence of stress distribution, the elastic settlement is the only component that needs consideration. During the last sixty years or so, a number of procedures have been developed to predict elastic settlement; however, there is a lack of a reliable standardized procedure. This is due to difficulty in getting the undisturbed samples for cohesionless soil and the lack of determination of accurate effective depth of influence zone for loads applied to the foundation.

Despite above problems, several methodologies are available in the literature for settlement analysis such as Terzaghi and Peck (1948), DeBeer and Martens (1957), Alpan (1964), Meyerhof (1965), D'Appolonia et al. (1968), Schmertmann (1970), Schultze and Sherif (1973), Schmertmann et al. (1978), Wahls (1981), Burland and Burbidge (1985), Jeyapalan and Boehm (1986), Leonards and Frost (1988), Berardi and Lancellotta (1991), Nova and Montrasio (1991), Tan and Duncan (1991), Papadopoulos (1992), and Berardi (1992). However, most of them are showing inconsistent performance in settlement predictions for shallow foundation on cohesionless soil. However, the above methods consider the case of vertically centric loaded footing. The settlement analysis for the eccentrically loaded footing is limited in the literature. Therefore, in this chapter, estimation of average settlement of eccentrically loaded embedded footings has been discussed. From the model test results an empirical equation is developed to predict the

ultimate settlement of eccentrically loaded embedded footings by knowing the ultimate settlement of surface footing subjected to centric load. A relation has been established between the ultimate bearing capacity, ultimate settlement, average load per unit area and the corresponding average settlement. Based on the laboratory test results, an empirical procedure has been developed to estimate the average settlement of the foundation while being subjected to an average allowable eccentric load per unit area, where the applied load is vertical.

9.2 Development of an empirical equation from DeBeer's chart (1967)

It is important to keep in mind that the average settlement at ultimate load depends on several factors. It appears that, for preliminary estimation purposes, the variations of $\left[\left(\frac{s_u}{B}\right)_{(D_f/B=0, e/B=0)}\right]$ with γB (γ = unit weight of sand), and D_r (relative density of sand) for circular foundation as provided by DeBeer (1967) are reasonable. Figure 9.1 shows the experimental results of DeBeer (1967) in a nondimensional form (Note: p_a = atmospheric pressure ≈ 100 kN/m^2). The average plots can be approximated as

$$\left(\frac{s_u}{B}\right)_{(D_f\, B=0, e/B=0)}(\%) = 30\, e^{(-0.9 D_r)} + 1.67 \ln\left(\frac{\gamma B}{P_a}\right) - 1 \qquad (9.1)$$

where D_r is expressed as a fraction. For comparison purposes Eq. (9.1) is also plotted in Figure 9.1. The comparison seems to be reasonably good for all relative densities.

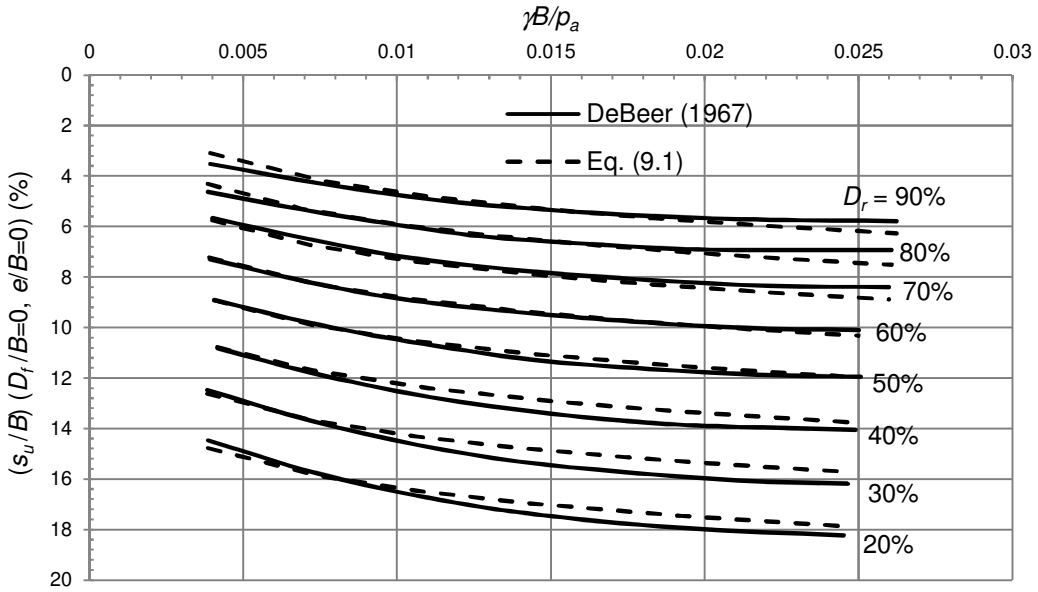

Figure 9.1: Comparison of curve by developed equation with DeBeer's curve

9.3 Average settlement at ultimate load $\left[\left(\frac{s_u}{B}\right)_{(D_f/B,e/B)}\right]$

Figures 9.2 (a) and (b) show the plots of $\left[\left(\frac{s_u}{B}\right)_{(D_f/B,e/B)}\right]$ vs. D_f/B in dense and medium dense sand. As might be expected for any experimental work of this type, there is some scatter.

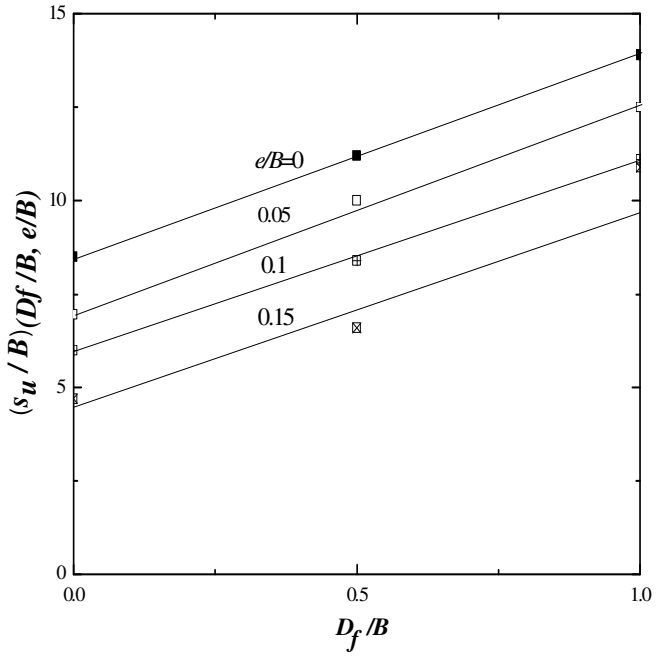

(a)

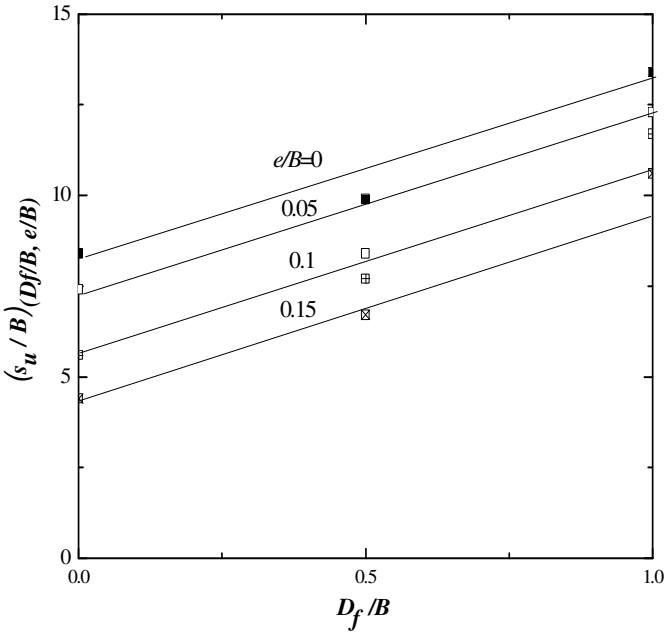

(b)

Figure 9.2: Variation of $(s_u/B)_{(Df/B,\ e/B)}$ with D_f /B and e/B: (a) dense sand, (b) medium dense sand

Thus it can initially be assumed that

$$\left(\frac{s_u}{B}\right)_{(D_f/B,\,e/B=0)} = \left(\frac{s_u}{B}\right)_{(D_f/B=0,\,e/B=0)}\left[1+a\left(\frac{D_f}{B}\right)\right] \tag{9.2}$$

where a = constant to be evaluated based on regression analysis of test results on centric vertical load under different relative densities.

The regression analysis is shown in Table 9.1.

Table 9.1. Values of a based on regression analysis along with R^2

Type of sand	a	R^2
Dense	0.635	1.0
Medium Dense	0.55	0.94
Average	0.593	

However, from Table 9.1 based on the values of a, it appears that for any given e/B,

$$\left(\frac{s_u}{B}\right)_{(D_f/B,\,e/B=0)} \approx \left(\frac{s_u}{B}\right)_{(D_f/B=0,\,e/B=0)}\left[1+0.6\left(\frac{D_f}{B}\right)\right] \tag{9.3}$$

It may thus be reasonable to express the average settlement at ultimate load in the form of a reduction factor. Or

$$RF = \frac{\left(\frac{s_u}{B}\right)_{(D_f/B,\,e/B)}}{\left(\frac{s_u}{B}\right)_{(D_f/B=0,\,e/B=0)}} \tag{9.4}$$

Note that $\left[\left(\frac{s_u}{B}\right)_{(D_f/B=0, e/B=0)}\right]$ is the settlement at ultimate load for a surface foundation with vertical centric load and $\left[\left(\frac{s_u}{B}\right)_{(D_f/B,\, e/B)}\right]$ is the settlement at ultimate load for an embedded foundation with vertical eccentric load.

The reduction factor can be initially taken as

$$RF = \left[1 + 0.6\left(\frac{D_f}{B}\right)\right]\left[1 - b\left(\frac{e}{B}\right)\right] \tag{9.5}$$

where b = constant to be evaluated based on regression analysis of eccentrically loaded test results

The values of b along with R^2 value are shown in Table 9.2.

Table 9.2. Value of b based on regression analysis along with R^2

Type of sand	b	R^2
Dense	2.18	0.94
Medium Dense	2.06	0.87
Average	2.17	

So, the reduction factor can be approximated as

$$RF \approx \left[1 + 0.6\left(\frac{D_f}{B}\right)\right]\left[1 - 2.15\left(\frac{e}{B}\right)\right] \tag{9.6}$$

Table 9.3 columns 6 – 8 show the experimental values of *RF*, *RF* calculated from Eq. (9.6), and the deviations of the experimental values from those calculated using Eq. (9.6).

The experimental values compare reasonably well with those estimated by using the empirical relationship.

Hence using Eqs. (9.1), (9.4) and (9.6), one can estimate the general magnitude of $\left[\left(\frac{s_u}{B}\right)_{(D_f/B,e/B)}\right]$.

9.4 Average load per unit area and Average settlement relationship

In order to develop a load-settlement relationship for shallow strip foundation subjected to eccentric loading, the following parameters can be defined:

$$\alpha = \frac{q_{(D_f/B,e/B)}}{q_{u(D_f/B,e/B)}} \tag{9.7}$$

and

$$\beta = \frac{\left(\frac{s}{B}\right)_{(D_f/B,e/B)}}{\left(\frac{s_u}{B}\right)_{(D_f/B,e/B)}} \tag{9.8}$$

where $q_{(D_f/B,e/B)}$ and $\left(\frac{s}{B}\right)_{(D_f/B,e/B)}$ are respectively the average load per unit area, and the corresponding settlement ratio at a given D_f/B and e/B.

The load-settlement curves of twenty four numbers of tests in the database are estimated by using the hyperbolic fitting method as mentioned in Eq. 9.9.

$$\beta = \frac{\alpha}{a(\alpha)+b} \tag{9.9}$$

The value of *a* and *b* are found to be -0.427 and 1.436 respectively. Figure 9.3 shows the experimental variation of β vs. α for dense and medium dense sands. The average variation obtained by hyperbolic fitting gives a relationship which can be approximated as,

$$\beta = \frac{\alpha}{1.43 - 0.43\alpha} \tag{9.10}$$

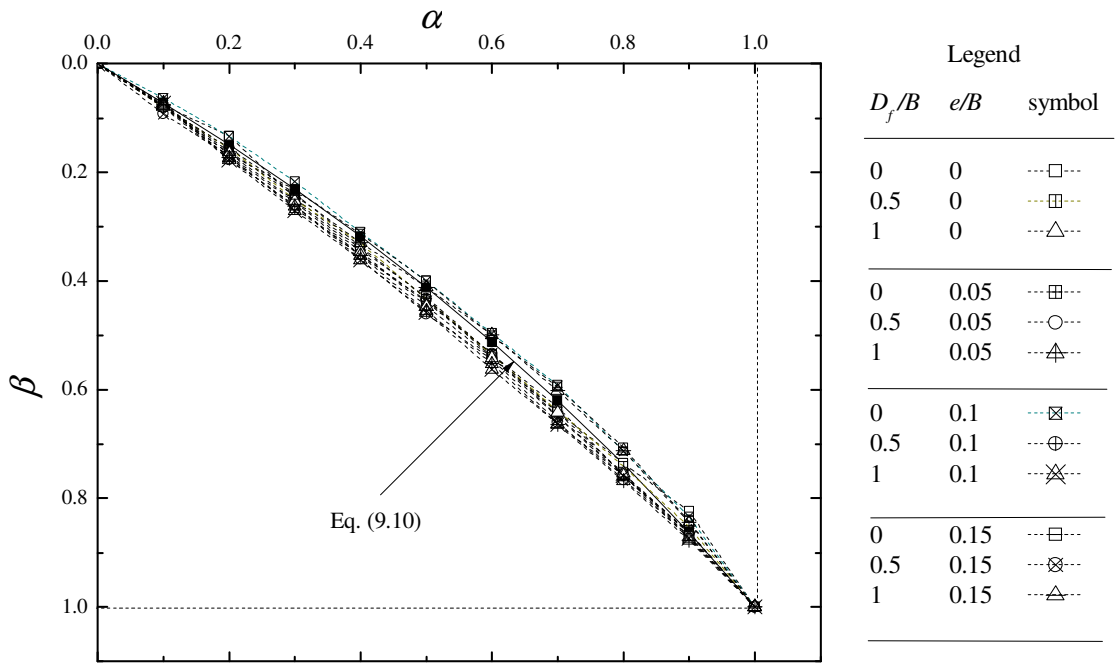

(a)

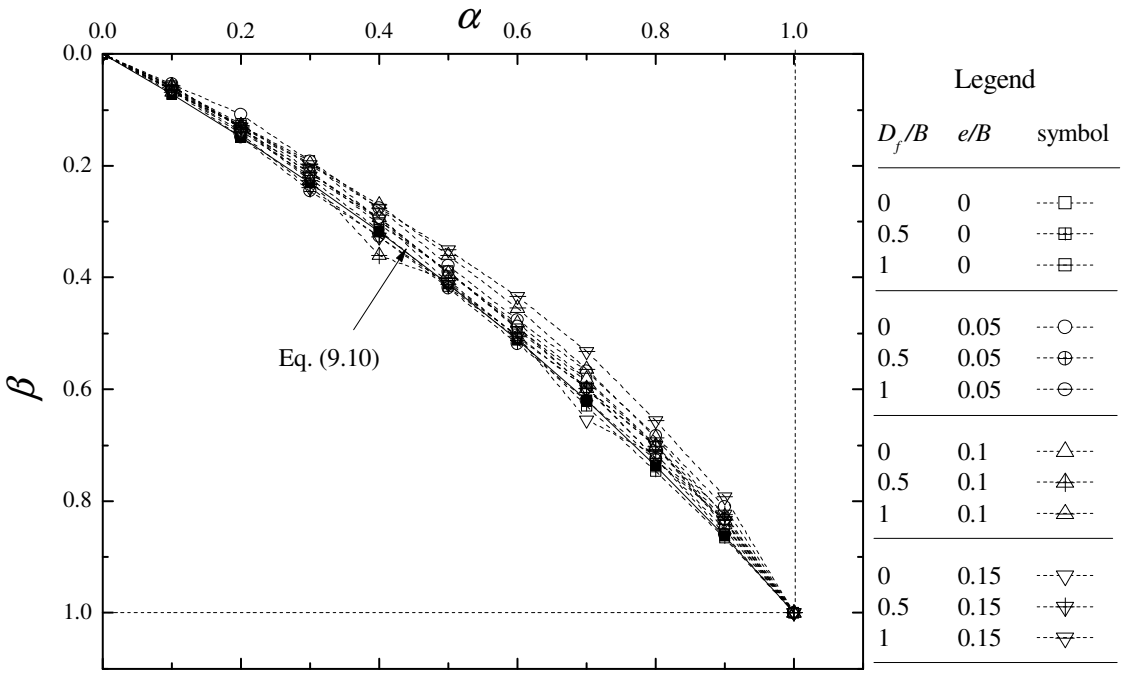

(b)

Figure 9.3: Plot of α vs. β curves obtained from laboratory tests along with Eq. (9.10) for (a) dense sand, (b) medium dense sand

9.5 Ultimate load under eccentric loading

Figure 9.4 shows a shallow strip foundation of width B located at a depth D_f on a granular soil having an unit weight γ and angle of friction ϕ. The foundation is subjected to a load of Q_u per unit length with an eccentricity e. Table 9.1 gives the variation of the ultimate average load per unit area of the foundation $\left[\frac{Q_u}{B}=q_{u(D_f/B,e/B)}\right]$ along with the average settlement along the center line $\left[\left(\frac{s_u}{B}\right)_{(D_f/B,e/B)}\right]$ at ultimate load which is based on the model tests [as per Figure 9.4] as discussed in Chapter 4.

It is also observed in Chapter 4 that for a given sand (i.e. relative density of compaction D_r and friction angle (ϕ) at a given embedment ratio D_f/B,

$$q_{u(D_f/B,e/B)} \approx q_{u(D_f/B,e/B=0)}\left[1-2\left(\frac{e}{B}\right)\right] \tag{9.11}$$

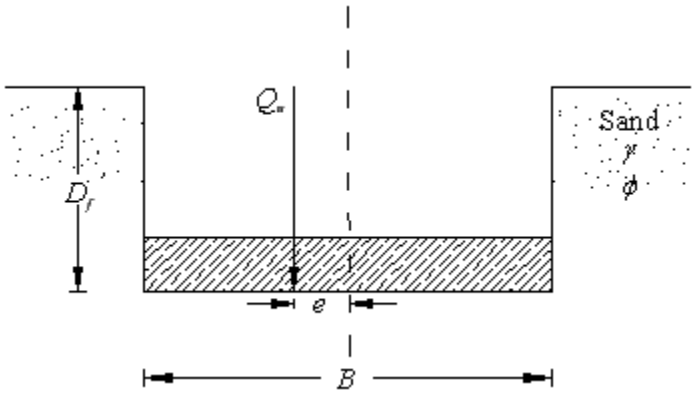

Figure 9.4: Eccentrically loaded embedded strip footing

Table 9.3. Ultimate load per unit area and corresponding average settlement based on the eccentrically loaded embedded tests. [Note: width of foundation B = 100 mm; relative density D_r for dense and medium dense sands are 69% and 51% respectively.]

Sand type (1)	$\frac{D_f}{B}$ (2)	$\frac{e}{B}$ (3)	$q_{u(D_f/B,e/B)}$ (kN/m^2) (4)	$\left(\frac{s_u}{B}\right)_{(D_f/B,e/B)}$ (5)	RF (Experimental) (6)	RF [Eq. (9.6)] (7)	Deviation—$\frac{\text{Col. 6} - \text{Col. 7}}{\text{Col. 6}}$ (%) (8)
Dense	0	0	166.77	**8.5**	1.0	1.0	**0.0**
	0.5	0	264.87	11.2	1.318	1.30	1.34
	1	0	353.16	13.90	1.635	1.60	2.16
(Unit weight = 14.36 kN/m^3)	0	0.05	133.42	6.96	0.819	0.893	-9.0
	0.5	0.05	226.61	10	1.176	1.160	1.38
	1	0.05	313.92	12.50	1.471	1.428	2.90
	0	0.1	109.87	6.00	0.706	0.785	-11.21
	0.5	0.1	195.22	8.4	0.988	1.021	-3.26
	1	0.1	278.60	11.10	1.306	1.256	3.82
	0	0.15	86.33	4.70	0.553	0.678	-22.53
	0.5	0.15	164.81	6.6	0.776	0.881	-13.43
	1	0.15	245.25	10.90	1.282	1.084	15.47
Medium	0	0	101.04	**8.4**	1.0	1.0	**0.0**

Table 9.3 (Continued)

Sand type (1)	$\frac{D_f}{B}$ (2)	$\frac{e}{B}$ (3)	$q_{u(D_f/B,e/B)}$ (kN/m^2) (4)	$\left(\frac{s_u}{B}\right)_{(D_f/B,e/B)}$ (5)	RF (Experimental) (6)	RF [Eq. (9.6)] (7)	Deviation—$\frac{\text{Col. 6} - \text{Col. 7}}{\text{Col. 6}}$ (%) (8)
dense (Unit weight = 13.97 kN/m^3)	0.5	0	143.23	9.9	1.179	1.3	-10.30
	1	0	208.95	13.4	1.595	1.600	-0.30
	0	0.05	84.37	7.4	0.881	0.893	-1.31
	0.5	0.05	123.61	8.4	1.000	1.160	-16.03
	1	0.05	193.26	12.3	1.464	1.428	2.48
	0	0.1	68.67	5.6	0.667	0.785	-17.75
	0.5	0.1	103.99	7.7	0.917	1.021	-11.33
	1	0.1	175.60	11.7	1.393	1.256	9.83
	0	0.15	54.94	4.4	0.524	0.678	-29.34
	0.5	0.15	87.31	6.7	0.798	0.881	-10.42
	1	0.15	156.96	10.6	1.262	1.084	14.10

9.6 Suggested procedure for estimation of average settlement at allowable load

Based on the present test results, following is a step by step procedure to estimate the average settlement at allowable average load per unit area.

1. For a given D_f/B with e/B=0, estimate the magnitude of $q_{u(D_f/B,e/B=0)}$ for the procedure described by Vesic (1973)

2. Estimate $q_{(D_f/B,e/B)}$ using Eq. (9.11).

3. Estimate $\left(\frac{s_u}{B}\right)_{(D_f/B=0,e/B=0)}$ using Eq. (9.1).

4. With a known factor of safety F_s determine

$$q_{(D_f/B,e/B)} = \frac{q_{u(D_f/B,e/B)}}{F_s}$$

5. Determine α from Eq. (9.7).

6. Using Eq. (9.10) obtain β

7. Estimate $\left(\frac{s}{B}\right)_{(D_f/B, e/B)}$ via Eqs. (9.1), (9.4), (9.6), and (9.8) as

$$\begin{aligned}\left(\frac{s}{B}\right)_{(D_f/B,e/B)}(\%) &= \beta\left(\frac{s_u}{B}\right)_{(D_f/B,e/B)}(\%) \\ &\approx \beta\left(\frac{s_u}{B}\right)_{(D_f/B=0,e/B=0)}(\%)\left[1+0.6\left(\frac{D_f}{B}\right)\right]\left[1-2.15\left(\frac{e}{B}\right)\right]\end{aligned} \tag{9.12}$$

The magnitude of $\left(\frac{s_u}{B}\right)_{(D_f/B=0,e/B=0)}$ can be obtained from Eq. (9.1).

9.7 Conclusions

Laboratory model tests have been conducted to determine the ultimate settlement on eccentrically embedded strip footings on sand bed. Based on the analysis of the test results, the following conclusions are drawn.

- An empirical equation is developed from DeBeer's chart (1967) to estimate ultimate settlement of surface footing.
- Based on the results from model tests conducted, the above equation is extended to predict the ultimate settlement of eccentrically embedded footings.
- The load-settlement curve for eccentrically embedded footing on sand can be developed if the load intensity and settlement corresponding to ultimate level are known.
- The average settlement calculated by using Eq. (9.12) should be treated as an approximate first estimation.

10. CONCLUSIONS AND SCOPE FOR FUTURE RESEARCH WORK

10.1 Conclusions

The results of a large number of laboratory model tests conducted to determine the ultimate bearing capacity of a strip footing supported by sand and subjected to an eccentrically inclined load with an embedment ratio varying from zero to one have been reported. The line of load application is inclined towards or away from the center line of the footing. Tests have been conducted on dense and medium dense sand. The load eccentricity ratio e/B has been varied from 0 to 0.15, and the load inclination α is varied from 0^0 to 20° (i.e. $\alpha/\phi \approx 0$ to 0.5). The results obtained from the model tests conducted in the laboratory have been analysed both by regression analysis and artificial neural network. The following are the general conclusions obtained from the analysis.

- For $\alpha = 0$ and $0 \leq D_f/B \leq 1$,

$$RF = 1 - 2\left(\frac{e}{B}\right)$$

This is common to *reinforced* and *partially compensated* cases.

- For $e/B = 0$, $0 \leq D_f/B \leq 1$ and $\alpha > 0$, the reduction factor

$$RF = \left(1 - \frac{\alpha}{\phi}\right)^{2-(D_f/B)}$$

This is common to *reinforced* and *partially compensated* cases.

- For *partially compensated* case (i.e. line of load application is *towards* the center line of the footing)

  The reduction factor (*RF*) for ultimate bearing capacity is given by:

$$RF = \left[1 - 2\left(\frac{e}{B}\right)\right]\left(1 - \frac{\alpha}{\phi}\right)^{2-(D_f/B)}$$

- For *reinforced* case (line of load application is *away* from the center line of the footing)

  The reduction factor (*RF*) for ultimate bearing capacity is given by:

$$RF = \left[1 - 2\left(\frac{e}{B}\right)\right]\left(1 - \frac{\alpha}{\phi}\right)^{1.5-0.7(D_f/B)}$$

- For given values of D_f/B and e/B, the magnitude of (q_u–reinforced)/(q_u–partially compensated) increases with the load inclination α.
- For similar values of α and e/B, the above ratio shows a tendency to decrease with the increase in embedment ratio (D_f/B).
- For a given value of D_f/B and α, the ratio (q_u–reinforced)/(q_u–partially compensated) increases with the increase in e/B.
- At ultimate load, the settlement ratio of s_u in the *reinforced* case to s_u in the *partially compensated* case can be approximated as follows

$$\frac{s_u - \text{reinforced}}{s_u - \text{partially compensated}} \approx \begin{cases} 1 \text{ at } \alpha = 5^\circ \\ \text{to} \\ 1.4 \text{ at } \alpha = 20^\circ \end{cases}$$

- A model equation developed based on the trained weights of the ANN for the *partially compensated* case predicts slightly better than the present developed empirical equation.
- Similarly, the predictability of ANN models for the *reinforced* case as discussed in Chapter 7 are found better than the developed empirical equation.
- The developed combined ANN model equation can be applied for both modes of load application to predict ultimate bearing capacity which is in good agreement with other methods.
- An empirical equation is developed from DeBeer's chart (1967) to estimate ultimate settlement of surface footing. Based on the results from model tests conducted, the above equation is further extended to predict the ultimate settlement of eccentrically embedded footings.
- A relationship between average load per unit area and average settlement is developed and thus a step-wise procedure is suggested for estimating average settlement at any allowable load of the eccentrically loaded shallow foundation.

10.2 Future research work

The present thesis pertains to the study on the bearing capacity and settlement of eccentrically inclined loaded strip footing on dry sand bed. Due to time constraint all other aspects related to shallow foundations could not be studied. The future research work should address the below mentioned points:

- Large scale study should be carried out to validate the present developed equations.

- Settlement, failure pattern and stress distribution of eccentrically inclined loaded footing can be experimentally studied.
- Numerical constitutive modeling of the present work can be done and compared with the present results.
- The present work can be extended to foundations on cohesive soil.
- The present work can be extended to reinforced soil condition.

REFERENCES

Alapn, I. (1964). “Estimating the settlements of foundations on sands.” *Civil Eng Public Works Rev,* 58(11), 1415–1418.

Balla, A. (1962). "Bearing capacity of foundations." *J. Soil Mech. and Found. Div.,* ASCE, 88(5), 13-34.

Beradi, R. (1992). “Fondazioni superficiali su terreni sabbiosi, parametrie di progetto.” *PhD Dis.*, University of Genoa, Genoa, Italy.

Berardi, R., and Lancellotta, R. (1991). “Stiffnes of granular soils from filed performance.” *Goetechnique,* 41(1), 149–157.

Biarez, J., Burel, M. and Wack, B. 1961. “Contribution à l’étude de la force portante des fondations.” *Proc. of 5th Intl. Conf. Soil Mech. Found. Eng.,* Paris, France, 1: 603.

Bolt, A. (1982). "Bearing capacity of a homogeneous subsoil under rigid footing foundation loaded with inclined and eccentric force." *In~ynieria Morska,* 3(2), 108-110.

Briaud, J.L. and Jeanjean, P. (1994). “Load settlement curve method for spread footings on sand.” *Proc. of Settlement ’94*, Vertical and Horizontal Deformations of Foundations and Embankments, ASCE, 2, 1774-1804.

Burland, J.B., and Burbidge, M.C. (1985). “Settlement of foundations on sand and gravel.” *Proc*, *Inst. Civil Eng.,* Part 1, 78, 1325–1381.

Cerato, A. B. (2005). “Scale effects of shallow foundation bearing capacity on granular material”, *PhD Dis.*, University of Massachusetts Amherst, Amherst, US.

Cichy, W., Dembicki, E., Odrobinski, W., Tejchman, A., and Zadroga, B. (1978). *Bearing capacity of subsoil under shallow foundations: study and model tests.* Scientific Books of Gdansk Technical University, Civil Engineering 22, 1-214.

D' Appolonia, D.J., D' Appolonia, E, Brisette, R.F. (1968). "Settlements of spread footings on sand." *J. Soil Mech. Found. Div.,* ASCE, 94(3), 735–760.

Das, S.K., and Basudhar, P.K. (2006). "Undrained lateral load capacity of piles in clay using artificial neural network." *Comp. and Geotech.*, 33(8), 454–459.

DeBeer, E.E., Martens, A. (1957). "A method of computation of an upper limit for the influence of heterogeneity of sand layers in the settlements of bridges." *Proc. of 4th ICSMFE*, London, U.K., I, 275–282.

DeBeer, E.E. (1965). "Bearing capacity and settlement of shallow foundations on sand." *Proceedings*, Symposium on Bearing Capacity and Settlement of Foundations, Duke University, 15-33.

DeBeer, E.E. (1967). "Proefondervindelijke bijdrage tot de studie van het gransdraagvermogen van zand onder funderingen op staal, Bepaling von der vormfactor s_b." *Annales des Travaux Publics de Belgique,* 6, 481-506.

DeBeer, E.E. (1970). "Experimental determination of the shape factors and the bearing capacity factors of sand." *Geotechnique*. 20(4), 387-411.

Dubrova, G.A. (1973). "Interaction of Soils and Structures." *Rechnoy Transport*, Moscow.

Feda, J. (1961). "Research on bearing capacity of loose soil." *Proc. 5th Int. Conf. Soil Mech and Found. Eng.*, Paris, 1, 635-642.

Garson, G.D. (1991). “Interpreting neural-network connection weights.” *Artif. Intell. Exp.,* 6(7), 47–51.

Goh, A.T.C. (1994). “Seismic liquefaction potential assessed by neural network.” *J. Geotech. Eng.*, ASCE, 120(90), 1467-1480.

Goh, A.T.C., Kulhawy, F.H., and Chua, C.G. (2005). “Bayesian neural network analysis of undrained side resistance of drilled shafts.” *J. Geotech. and Geoenv. Eng.,* ASCE, 131(1), 84-93.

Guyon, I., and Elisseeff, A. (2003). “An Introduction to variable and feature selection.” *J. Mach. Learn. Res.*, 3, 1157-1182.

Hansen, J.B. (1970). “A revised and extended formula for bearing capacity.” *Bull. No. 28*, Danish Geotechnical Institute, Copenhagen.

Hartikainen, J., and Zadroga, B. (1994). "Bearing capacity of footings and strip foundations: comparison of model test results with EUROCODE 7." *Proc., of 13th ICSMFE,* New Delhi, India, 2, 457-460.

Hjiaj, M., Lyamin, A.V., Sloan, S.W. (2004). “Bearing capacity of a cohesive-frictional soil under non-eccentric inclined loading.” *Comp. and Geotech.*, 31, 491–516.

Hjiaj, M., Lyamin, A.V. and Sloan, S.W. (2005). “Numerical limit analysis solutions for the bearing capacity factor N_γ.” *Int. J. of Soils and Struc.* 43, 1681.

Ingra, T.S., and Baecher, G.B. (1983). “Uncertainty in bearing capacity of sands.” *J. Geotech. Eng.,* ASCE, 109(7), 899-914.

IS 1888: (1982) Method of Load Test on Soils.

IS 6403: (1981) Code of Practice for Determination of Bearing Capacity of Shallow Foundations.

IS 8009: (1976-Part I) Code of Practice for Determination of Settlements of Foundations-Shallow Foundations Subjected to Symmetrical Static Vertical loads

Jaksa, M.B., Maier, H.R. and Shahin, M.A. (2008). "Future challenges for artificial neural network modelling in geotechnical engineering." *Proc. of 12th Int. Conf. IACMAG,* Goa, India, 1710-1719.

Janbu, N. (1957). "Earth pressures and bearing capacity calculations by generalized procedure of slices." *Proc. of 4th Int. Conf. on Soil Mech, and Found. Eng*., London, 2, 207-211.

Jeyapalan, J.K., Boehm, R. (1986). "Procedures for predicting settlements in sands." *Proc. settlement of shallow foundations on cohesionless soils: design and performance, Geotech. Spe. Public. No*. 5, ASCE, 1–22, Seattle, Wash., 7302–1043.

Krizek, R.J. (1965). "Approximation for Terzaghi's bearing capacity." *J. Soil Mech. Found. Div.*, ASCE, 91(2), 146.

Leonards, G.A. and Frost, J.D. (1988). "Settlement of shallow foundations on granular soils." *J. Geotech. Eng.*, ASCE, 114(7), 791-809.

Loukidis, D., Chakraborty, T. and Salgado, R. (2008). "Bearing capacity of strip footings on purely frictional soil under eccentric and inclined loads." *Can. Geotech. J.*, 45(6), 768-787.

Lundgren, H., and K. Mortensen. (1953). "Determination by the theory of plasticity of the bearing capacity of continuous footings on sand." *Proc. of 3rd Intl. Conf. Mech. Found. Eng.*, Zurich, Switzerland, 1: 409.

Meyerhof, G.G. (1951). "The ultimate bearing capacity of foundations." *Geotechnique*, 2, 301.

Meyerhof, G.G. (1953). “The bearing capacity of foundations under eccentric and inclined loads.” *Proc.*, *3rd Int. Conf. on Soil Mech. and Found. Eng.*, 1, 440-445.

Meyerhof, G.G. (1963). “Some recent research on the bearing capacity of foundations.” *Canadian Geotechnical Journal*, 1(1): 16-26.

Meyerhof, G.G. (1965). “Shallow foundations.” *J. Soil Mech. Found. Div.,* ASCE, 91(SM2), 21-31.

Meyerhof, G.G., and Koumoto, T. (1987). “Inclination factors for bearing capacity of shallow footings.” *J. of Geotech. Eng.,* ASCE*,* 113(9), 1013-1018.

Michalowski, R.L. (1997). “An estimate of the influence of soil weight on bearing capacity using limit analysis.” *Soils and Foundations.* 37(4), 57-64.

Michalowski, R.L., and You, L. (1998). “Effective width rule in calculations of bearing capacity of shallow footings.” *Comp. and Geotech.*, 23, 237-253.

Milovic, D. M. (1965). "Comparison between the calculated and experimental values of the ultimate bearing capacity." *Proc., 6th ICSMFE, Montreal 1965,* 2, 142-144.

Mosallanezhad, M., Hataf, N., and Ghahramani, A. (2008). “Bearing capacity of square footings on reinforced layered soil.” *J. of Geotech. and Geolog. Eng.,* 26, 299-312.

Muhs, H. (1963). “Über die zulässige Belastung nichtbindiger Böden, Berichte aus der Bauforschung, Heft 32, Flachgründungen, Grundbruch und Setzungen, Berlin, S. 103-121.

Muhs, H., and Weiss, K. (1972). "Der Einfluss von Neigung und Ausmittigkeitder Last auf die Grenztragfahigkeit flach genrundeter Einzelfundamente." DEGEBO Mitteilungen, Heft 34, Welhelm Ernst and Sohn, Berlin, Germany.

Muhs, H., and Weiss, K. (1973). "Inclined load tests on shallow strip footing." *Proc., 8th Int. Conf. on Soil Mech. and Found. Eng.*, Moscow, 1.3.

Nova, R. and Montrasio, L. (1991). "Settlement of shallow foundations on sand." *Geotechnique*, 41(2), 243-256.

Olden, J. D. (2000). "An artificial neural network approach for studying phytoplankton succession." *Hydrobiologia,* 436, 131-143.

Olden, J.D., Joy, M.K., and Death, R.G. (2004). "An accurate comparison of methods for quantifying variable importance in artificial neural networks using simulated data." *Eco. Model.,* 178(3), 389-397.

Ozesmi, S.L., and Ozesmi, U. (1999). "An artificial neural network approach to spatial modeling with inter specific interactions." *Eco. Model.,* 116, 15-31.

Papadopoulos, B.P. (1992). "Settlements of shallow foundations on cohesionless soils." *J. Geotech. Eng.,* ASCE, 118(3), 377-393.

Park, H. II. (2011). "Study for Application of Artificial Neural Networks in Geotechnical Problems." *Book chapter in Artificial Neural Networks - Application*, 303-336.

Perloff, W.H., and Barron, W. (1976). *Soil Mechanics: Principles and Applications.* Ronald Press, New York.

Poulos, H.G., Carter, J.P. and Small, J. C. (2001). "Foundations and retaining structures— research and practice." in *Proc. of 15th Intl. Conf. Soil Mech. Found. Eng.*, Istanbul, Turkey, 4, A. A. Balkema, Rotterdam, 2527.

Prakash, S. and Saran, S. (1971). "Bearing capacity of eccentrically loaded footings." *J. Soil Mech. and Found. Div.*, ASCE, 97(1), 95-117.

Prandtl, L. (1921). "Uber die eindringungs-festigkeit plastisher baustoffe und die festigkeit von schneiden." *Z. Ang. Math. Mech.*, 1(1), 15.

Purkayastha, R.D., Char, R.A.N., (1977). "Stability analysis for eccentrically loaded footings." *J. Geotech. Eng. Div.,* ASCE, 103(6), 647–651.

Reissner, H. (1924). "Zum erddruckproblem." *Proc. of 1st Int. Cong. of Appl. Mech.*, 295-311.

Saran, S. and Agarwal, R.K. (1991). "Bearing capacity of eccentrically obliquely loaded foundation." *J. Geotech. Eng.*, ASCE, 117(11), 1669-1690.

Salgado, R., Lyamin, A.V., Sloan, S.W. and Yu, H.S. (2004). Two- and three-dimensional bearing capacity of foundations in clay. *Geotechnique.* 54(5), 297-306.

Salgado, R. (2008). *The engineering of foundations,* New York, McGraw-Hill.

Sastry, V.V.R.N., Meyerhof, G.G. (1987). "Inclination factors for strip footings." *Journal of Geotechnical Engineering*, ASCE, 113(5), 524-527.

Schmertmann, J.H. (1970). "Static cone to compute static settlement over sand." *J. Soil Mech. Found. Div.,* ASCE, 96(3), 1011-1043.

Schmertmann, J.H., Hartman, J.P., and Brown, P.R. (1978). "Improved strain influence factor diagrams." *J. Geotech. Eng. Div.,* ASCE, 104(8), 1131-1135.

Schultze, E., and Sherif, G. (1973). "Prediction of settlements from evaluated settlement observations for sand." *Proc. of 8th Int. Conf. on Soil Mech. and Found. Eng.,* 1(3), 225–230.

Shahin, M.A., Maier, H.R., and Jaksa, M.B. (2002). "Predicting settlement of shallow foundations using neural network." *J. Geotech. and Geoenv. Eng.*, ASCE, 128(9), 785-793.

Shahin, M.A., Jaksa, M.B. and Maier, H.R., (2008). "State of the art of artificial neural networks in geotechnical engineering." *Elect. J. of Geotech. Eng.*, 08.

Shiraishi, S. (1990). "Variation in bearing capacity factors of dense sand assessed by model loading tests." *Soils and Found.,* 30(1), 17-26.

Spangler, M.G. and Handy, R.L. (1982). *Soil Engineering,* 4th edition, Harper and Row, New York.

Tan, C.K., and Duncan, J.M. (1991). "Settlement of footings on sands: accuracy and reliability." *Proc., Geotech. Eng. Congress 1991*, Colorado, 1, 446-455.

Terzaghi, K. (1943). *Theoretical Soil Mechanics*, Wiley, New York.

Terzaghi, K., and Peck, R.B. (1948). *Soil mechanics in engineering practice,* 1st Edition, John Wiley & Sons, New York.

Trautmann, C.H. and Kulhawy, F.H. (1988). "Uplift load-displacement behavior of spread foundations." *J. of Geotech. Eng.*, ASCE, 114(2), 168-183.

Vesic, A.S. (1973). "Analysis of ultimate loads of shallow foundations." *J. of Soil Mech. and Found. Div.*, ASCE, 99(1), 45-73.

Vesic, A.S. (1975). Bearing capacity of Shallow foundations. *In* Geotechnical Engineering Handbook. Edited by Braja M. Das, Chapter 3, J. Ross Publishing, Inc., U.S.A.

Wahls, H.E. (1981). "Tolerable settlement of buildings." *J. Geotech. Eng. Div.,* ASCE, 107(11), 1489-1504.

Wilby, R.L., Abrahart, R.J., and Dawson, C.W. (2003). "Detection of conceptual model rainfall-runoff processes inside an artificial neural network." *Hydro. Sci.*, 48(2), 163-181.

Zadroga, B. (1975). "Bearing capacity of inclined subsoil under a foundation loaded with eccentric and inclined forces: Part 1--method review and own model tests." *Archive of Hydroengrg.,* 22(3/4), 333-336.

APPENDIX A

Table A.1. Comparative value of Present analysis results with other approaches

e/B	D_f/B	α/ϕ	LA	Expt. q_u (kN/m^2)	RF_{expt}	RF_{Emp}	RF_{ANN}	$RF_{M(1963)}$	$RF_{S\ \&\ A(1991)}$	$RF_{L(2008)}$	$RF_{ANN\ (C)}$
Line of load application is *towards* the center line of the footing											
0	0	0.000	0.000	166.77	1.000	1.000	0.983	1.000		1.000	0.998
0.05	0	0.000	0.000	133.42	0.800	0.900	0.811	0.810		0.817	0.823
0.1	0	0.000	0.000	109.87	0.659	0.800	0.668	0.640		0.652	0.653
0.15	0	0.000	0.000	86.33	0.518	0.700	0.552	0.490		0.506	0.541
0	0	0.123	0.000	128.51	0.771	0.770	0.781	0.773		0.766	0.767
0.05	0	0.123	-1.000	103.01	0.618	0.693	0.636	0.626		0.677	0.616
0.1	0	0.123	-1.000	86.33	0.518	0.616	0.520	0.495		0.554	0.522
0.15	0	0.123	-1.000	65.73	0.394	0.539	0.429	0.379		0.431	0.434

e/B	D_f/B	α/ϕ	*LA*	Expt. q_u (kN/m^2)	RF_{expt}	RF_{Emp}	RF_{ANN}	$RF_{M(1963)}$	$RF_{S\ \&\ A(1991)}$	$RF_{L(2008)}$	$RF_{ANN\ (C)}$
0	0	0.245	0.000	96.14	0.576	0.570	0.587	0.579		0.563	0.582
0.05	0	0.245	-1.000	76.52	0.459	0.513	0.473	0.469		0.503	0.481
0.1	0	0.245	-1.000	62.78	0.376	0.456	0.385	0.370		0.418	0.393
0.15	0	0.245	-1.000	51.99	0.312	0.399	0.317	0.284		0.326	0.319
0	0	0.368	0.000	66.71	0.400	0.400	0.416	0.414		0.388	0.422
0.05	0	0.368	-1.000	53.96	0.324	0.360	0.332	0.335		0.343	0.343
0.1	0	0.368	-1.000	44.15	0.265	0.320	0.270	0.265		0.283	0.274
0.15	0	0.368	-1.000	35.12	0.211	0.280	0.222	0.203		0.217	0.219
0	0	0.490	0.000	43.16	0.259	0.260	0.283	0.277		0.238	0.280
0.05	0	0.490	-1.000	34.83	0.209	0.234	0.224	0.224		0.205	0.221
0.1	0	0.490	-1.000	29.43	0.176	0.208	0.181	0.177		0.164	0.180

e/B	D_f/B	α/ϕ	LA	Expt. q_u (kN/m^2)	RF_{expt}	RF_{Emp}	RF_{ANN}	$RF_{M(1963)}$	$RF_{S\ \&\ A(1991)}$	$RF_{L(2008)}$	$RF_{ANN\ (C)}$
0.15	0	0.490	-1.000	23.54	0.141	0.182	0.149	0.136		0.119	0.148
0	0.5	0.000	0.000	264.87	1.000	1.000	1.005	1.000			0.993
0.05	0.5	0.000	0.000	226.61	0.856	0.900	0.854	0.855			0.863
0.1	0.5	0.000	0.000	195.22	0.737	0.800	0.730	0.721			0.733
0.15	0.5	0.000	0.000	164.81	0.622	0.700	0.632	0.597			0.620
0	0.5	0.123	0.000	223.67	0.844	0.822	0.855	0.821			0.841
0.05	0.5	0.123	-1.000	193.26	0.730	0.740	0.722	0.705			0.718
0.1	0.5	0.123	-1.000	165.79	0.626	0.658	0.615	0.597			0.635
0.15	0.5	0.123	-1.000	140.28	0.530	0.575	0.529	0.497			0.549
0	0.5	0.245	0.000	186.39	0.704	0.656	0.718	0.667			0.698
0.05	0.5	0.245	-1.000	160.88	0.607	0.590	0.604	0.575			0.612

e/B	D_f/B	α/ϕ	*LA*	Expt. q_u (kN/m^2)	RF_{expt}	RF_{Emp}	RF_{ANN}	$RF_{M(1963)}$	$RF_{S\ \&\ A(1991)}$	$RF_{L(2008)}$	$RF_{ANN\ (C)}$
0.1	0.5	0.245	-1.000	137.34	0.519	0.525	0.513	0.489			0.526
0.15	0.5	0.245	-1.000	116.74	0.441	0.459	0.438	0.410			0.448
0	0.5	0.368	0.000	151.07	0.570	0.503	0.584	0.535			0.551
0.05	0.5	0.368	-1.000	129.49	0.489	0.453	0.491	0.464			0.496
0.1	0.5	0.368	-1.000	111.83	0.422	0.402	0.416	0.397			0.420
0.15	0.5	0.368	-1.000	94.18	0.356	0.352	0.353	0.335			0.357
0	0.5	0.490	0.000	115.76	0.437	0.364	0.455	0.422			0.420
0.05	0.5	0.490	-1.000	98.10	0.370	0.328	0.382	0.369			0.383
0.1	0.5	0.490	-1.000	85.35	0.322	0.291	0.323	0.318			0.322
0.15	0.5	0.490	-1.000	72.59	0.274	0.255	0.274	0.271			0.273
0	1	0.000	0.000	353.16	1.000	1.000	1.030	1.000			0.992

e/B	D_f/B	α/ϕ	LA	Expt. q_u (kN/m^2)	RF_{expt}	RF_{Emp}	RF_{ANN}	$RF_{M(1963)}$	$RF_{S\ \&\ A(1991)}$	$RF_{L(2008)}$	$RF_{ANN\ (C)}$
0.05	1	0.000	0.000	313.92	0.889	0.900	0.906	0.878			0.920
0.1	1	0.000	0.000	278.60	0.789	0.800	0.808	0.763			0.816
0.15	1	0.000	0.000	245.25	0.694	0.700	0.735	0.656			0.703
0	1	0.123	0.000	313.92	0.889	0.877	0.892	0.842			0.910
0.05	1	0.123	-1.000	277.62	0.786	0.790	0.787	0.742			0.787
0.1	1	0.123	-1.000	241.33	0.683	0.702	0.705	0.648			0.716
0.15	1	0.123	-1.000	215.82	0.611	0.614	0.642	0.559			0.634
0	1	0.245	0.000	264.87	0.750	0.755	0.769	0.705			0.794
0.05	1	0.245	-1.000	239.36	0.678	0.679	0.678	0.625			0.699
0.1	1	0.245	-1.000	212.88	0.603	0.604	0.607	0.548			0.615
0.15	1	0.245	-1.000	188.35	0.533	0.528	0.548	0.475			0.533

e/B	D_f/B	α/ϕ	*LA*	Expt. q_u (kN/m^2)	RF_{expt}	RF_{Emp}	RF_{ANN}	$RF_{M(1963)}$	$RF_{S\ \&\ A(1991)}$	$RF_{L(2008)}$	$RF_{ANN\ (C)}$
0	1	0.368	0.000	225.63	0.639	0.632	0.658	0.587			0.654
0.05	1	0.368	-1.000	206.01	0.583	0.569	0.579	0.522			0.595
0.1	1	0.368	-1.000	179.52	0.508	0.506	0.513	0.461			0.514
0.15	1	0.368	-1.000	155.98	0.442	0.443	0.456	0.402			0.445
0	1	0.490	0.000	183.45	0.519	0.510	0.561	0.485			0.526
0.05	1	0.490	-1.000	166.77	0.472	0.459	0.489	0.434			0.493
0.1	1	0.490	-1.000	143.23	0.406	0.408	0.427	0.385			0.427
0.15	1	0.490	-1.000	126.55	0.358	0.357	0.372	0.338			0.375
0	0	0.000	0.000	101.04	1.000	1.000	0.983	1.000	1.000	1.000	0.998
0.05	0	0.000	0.000	84.37	0.835	0.900	0.811	0.810		0.817	0.823
0.1	0	0.000	0.000	68.67	0.680	0.800	0.668	0.640	0.537	0.652	0.653

e/B	D_f/B	α/ϕ	*LA*	Expt. q_u (kN/m^2)	RF_{expt}	RF_{Emp}	RF_{ANN}	$RF_{M(1963)}$	$RF_{S\ \&\ A(1991)}$	$RF_{L(2008)}$	$RF_{ANN\ (C)}$
0.15	0	0.000	0.000	54.94	0.544	0.700	0.552	0.490		0.506	0.541
0	0	0.133	0.000	79.46	0.786	0.751	0.765	0.754		0.766	0.750
0.05	0	0.133	-1.000	63.77	0.631	0.676	0.622	0.611		0.677	0.605
0.1	0	0.133	-1.000	52.97	0.524	0.601	0.508	0.483		0.554	0.512
0.15	0	0.133	-1.000	42.18	0.417	0.526	0.419	0.369		0.431	0.424
0	0	0.267	0.000	55.92	0.553	0.538	0.554	0.546	0.439	0.563	0.552
0.05	0	0.267	-1.000	47.09	0.466	0.484	0.445	0.442		0.503	0.456
0.1	0	0.267	-1.000	38.46	0.381	0.430	0.362	0.349	0.331	0.418	0.370
0.15	0	0.267	-1.000	31.39	0.311	0.376	0.298	0.268		0.326	0.299
0	0	0.400	0.000	38.26	0.379	0.360	0.377	0.373		0.388	0.383
0.05	0	0.400	-1.000	32.37	0.320	0.324	0.301	0.302		0.343	0.309

e/B	D_f/B	α/ϕ	*LA*	Expt. q_u (kN/m^2)	RF_{expt}	RF_{Emp}	RF_{ANN}	$RF_{M(1963)}$	$RF_{S\ \&\ A(1991)}$	$RF_{L(2008)}$	$RF_{ANN\ (C)}$
0.1	0	0.400	-1.000	26.98	0.267	0.288	0.244	0.239		0.283	0.247
0.15	0	0.400	-1.000	20.60	0.204	0.252	0.200	0.183		0.217	0.198
0	0	0.533	0.000	24.03	0.238	0.218	0.244	0.232	0.364	0.238	0.236
0.05	0	0.533	-1.000	19.62	0.194	0.196	0.193	0.188		0.205	0.184
0.1	0	0.533	-1.000	16.68	0.165	0.174	0.156	0.148	0.183	0.164	0.154
0.15	0	0.533	-1.000	13.34	0.132	0.152	0.128	0.114		0.119	0.129
0	0.5	0.000	0.000	143.23	1.000	1.000	1.005	1.000	1.000		0.993
0.05	0.5	0.000	0.000	123.61	0.863	0.900	0.854	0.858			0.863
0.1	0.5	0.000	0.000	103.99	0.726	0.800	0.730	0.727	0.598		0.733
0.15	0.5	0.000	0.000	87.31	0.610	0.700	0.632	0.605			0.620
0	0.5	0.133	0.000	120.66	0.842	0.807	0.843	0.816			0.830

e/B	D_f/B	α/ϕ	LA	Expt. q_u (kN/m^2)	RF_{expt}	RF_{Emp}	RF_{ANN}	$RF_{M(1963)}$	$RF_{S\ \&\ A(1991)}$	$RF_{L(2008)}$	$RF_{ANN\ (C)}$
0.05	0.5	0.133	-1.000	103.99	0.726	0.726	0.712	0.704			0.710
0.1	0.5	0.133	-1.000	90.25	0.630	0.645	0.606	0.599			0.626
0.15	0.5	0.133	-1.000	72.59	0.507	0.565	0.521	0.501			0.541
0	0.5	0.267	0.000	98.10	0.685	0.628	0.694	0.659	0.516		0.671
0.05	0.5	0.267	-1.000	84.86	0.592	0.565	0.584	0.571			0.591
0.1	0.5	0.267	-1.000	72.59	0.507	0.502	0.495	0.489	0.384		0.506
0.15	0.5	0.267	-1.000	60.82	0.425	0.440	0.423	0.412			0.431
0	0.5	0.400	0.000	79.46	0.555	0.465	0.550	0.525			0.516
0.05	0.5	0.400	-1.000	67.89	0.474	0.418	0.462	0.458			0.466
0.1	0.5	0.400	-1.000	56.90	0.397	0.372	0.391	0.395			0.393
0.15	0.5	0.400	-1.000	48.07	0.336	0.325	0.332	0.336			0.335

e/B	D_f/B	α/ϕ	*LA*	Expt. q_u (kN/m^2)	RF_{expt}	RF_{Emp}	RF_{ANN}	$RF_{M(1963)}$	$RF_{S\ \&\ A(1991)}$	$RF_{L(2008)}$	$RF_{ANN\ (C)}$
0	0.5	0.533	0.000	58.27	0.407	0.319	0.412	0.413	0.382		0.376
0.05	0.5	0.533	-1.000	50.03	0.349	0.287	0.345	0.363			0.344
0.1	0.5	0.533	-1.000	43.16	0.301	0.255	0.292	0.316	0.221		0.290
0.15	0.5	0.533	-1.000	36.30	0.253	0.223	0.247	0.272			0.245
0	1	0.000	0.000	208.95	1.000	1.000	1.030	1.000	1.000		0.992
0.05	1	0.000	0.000	193.26	0.925	0.900	0.906	0.881			0.920
0.1	1	0.000	0.000	175.60	0.840	0.800	0.808	0.769	0.629		0.816
0.15	1	0.000	0.000	156.96	0.751	0.700	0.735	0.663			0.703
0	1	0.133	0.000	186.39	0.892	0.867	0.882	0.840			0.902
0.05	1	0.133	-1.000	168.73	0.808	0.780	0.777	0.743			0.780
0.1	1	0.133	-1.000	153.04	0.732	0.693	0.697	0.652			0.708

e/B	D_f/B	α/ϕ	*LA*	Expt. q_u (kN/m^2)	RF_{expt}	RF_{Emp}	RF_{ANN}	$RF_{M(1963)}$	$RF_{S\ \&\ A(1991)}$	$RF_{L(2008)}$	$RF_{ANN\ (C)}$
0.15	1	0.133	-1.000	137.34	0.657	0.607	0.635	0.564			0.625
0	1	0.267	0.000	160.88	0.770	0.733	0.748	0.702	0.556		0.770
0.05	1	0.267	-1.000	144.21	0.690	0.660	0.660	0.625			0.681
0.1	1	0.267	-1.000	129.49	0.620	0.587	0.590	0.550	0.411		0.597
0.15	1	0.267	-1.000	112.82	0.540	0.513	0.532	0.479			0.516
0	1	0.400	0.000	133.42	0.638	0.600	0.632	0.584			0.619
0.05	1	0.400	-1.000	118.70	0.568	0.540	0.554	0.522			0.567
0.1	1	0.400	-1.000	106.93	0.512	0.480	0.489	0.463			0.489
0.15	1	0.400	-1.000	94.18	0.451	0.420	0.433	0.406			0.425
0	1	0.533	0.000	98.10	0.469	0.467	0.529	0.483	0.391		0.485
0.05	1	0.533	-1.000	92.21	0.441	0.420	0.459	0.435			0.460

e/B	D_f/B	α/ϕ	*LA*	Expt. q_u (kN/m^2)	RF_{expt}	RF_{Emp}	RF_{ANN}	$RF_{M(1963)}$	$RF_{S\ \&\ A(1991)}$	$RF_{L(2008)}$	$RF_{ANN\ (C)}$
0.1	1	0.533	-1.000	84.37	0.404	0.373	0.399	0.388	0.241		0.400
0.15	1	0.533	-1.000	75.54	0.362	0.327	0.345	0.342			0.354
Line of load application is *away* from the center line of the footing											
0	0	0.000	0.000	166.77	1.000	1.000	0.993			1.000	0.998
0.05	0	0.123	1.000	113.80	0.682	0.740	0.697			0.748	0.764
0.1	0	0.123	1.000	107.91	0.647	0.658	0.627			0.643	0.634
0.15	0	0.123	1.000	92.21	0.553	0.575	0.558			0.517	0.542
0.05	0	0.245	1.000	88.29	0.529	0.590	0.549			0.575	0.559
0.1	0	0.245	1.000	85.35	0.512	0.525	0.524			0.533	0.513
0.15	0	0.245	1.000	81.42	0.488	0.459	0.479			0.456	0.467
0.05	0	0.368	1.000	68.67	0.412	0.453	0.435			0.406	0.433

e/B	D_f/B	α/ϕ	*LA*	Expt. q_u (kN/m^2)	RF_{expt}	RF_{Emp}	RF_{ANN}	$RF_{M(1963)}$	$RF_{S\ \&\ A(1991)}$	$RF_{L(2008)}$	$RF_{ANN\ (C)}$
0.1	0	0.368	1.000	66.71	0.400	0.402	0.390			0.393	0.426
0.15	0	0.368	1.000	64.75	0.388	0.352	0.398			0.352	0.389
0.05	0	0.490	1.000	53.96	0.324	0.328	0.338			0.256	0.337
0.1	0	0.490	1.000	51.99	0.312	0.291	0.311			0.255	0.320
0.15	0	0.490	1.000	49.05	0.294	0.255	0.301			0.237	0.306
0	0.5	0.000	0.000	264.87	1.000	1.000	1.000				0.993
0.05	0.5	0.123	1.000	196.20	0.741	0.774	0.736				0.779
0.1	0.5	0.123	1.000	173.64	0.656	0.688	0.656				0.669
0.15	0.5	0.123	1.000	152.06	0.574	0.602	0.585				0.589
0.05	0.5	0.245	1.000	166.77	0.630	0.651	0.629				0.636
0.1	0.5	0.245	1.000	151.07	0.570	0.579	0.556				0.573

e/B	D_f/B	α/ϕ	LA	Expt. q_u (kN/m^2)	RF_{expt}	RF_{Emp}	RF_{ANN}	$RF_{M(1963)}$	$RF_{S\ \&\ A(1991)}$	$RF_{L(2008)}$	$RF_{ANN\ (C)}$
0.15	0.5	0.245	1.000	132.44	0.500	0.507	0.487				0.514
0.05	0.5	0.368	1.000	137.34	0.519	0.531	0.527				0.531
0.1	0.5	0.368	1.000	129.49	0.489	0.472	0.462				0.496
0.15	0.5	0.368	1.000	112.82	0.426	0.413	0.411				0.443
0.05	0.5	0.490	1.000	113.80	0.430	0.415	0.439				0.429
0.1	0.5	0.490	1.000	105.95	0.400	0.369	0.395				0.413
0.15	0.5	0.490	1.000	95.16	0.359	0.323	0.364				0.371
0	1	0.000	0.000	353.16	1.000	1.000	1.003				0.992
0.05	1	0.123	1.000	284.49	0.806	0.811	0.811				0.825
0.1	1	0.123	1.000	251.14	0.711	0.721	0.734				0.736
0.15	1	0.123	1.000	228.57	0.647	0.630	0.681				0.653

e/B	D_f/B	α/ϕ	*LA*	Expt. q_u (kN/m^2)	RF_{expt}	RF_{Emp}	RF_{ANN}	$RF_{M(1963)}$	$RF_{S\ \&\ A(1991)}$	$RF_{L(2008)}$	$RF_{ANN\ (C)}$
0.05	1	0.245	1.000	249.17	0.706	0.719	0.717				0.715
0.1	1	0.245	1.000	225.63	0.639	0.639	0.656				0.637
0.15	1	0.245	1.000	203.07	0.575	0.559	0.586				0.566
0.05	1	0.368	1.000	217.78	0.617	0.624	0.628				0.613
0.1	1	0.368	1.000	193.26	0.547	0.554	0.556				0.552
0.15	1	0.368	1.000	171.68	0.486	0.485	0.487				0.489
0.05	1	0.490	1.000	179.52	0.508	0.525	0.528				0.519
0.1	1	0.490	1.000	156.96	0.444	0.467	0.463				0.477
0.15	1	0.490	1.000	143.23	0.406	0.408	0.411				0.415
0	0	0.000	0.000	101.04	1.000	1.000	0.993			1.000	0.998
0.05	0	0.133	1.000	71.61	0.709	0.726	0.682			0.748	0.746

e/B	D_f/B	α/ϕ	*LA*	Expt. q_u (kN/m^2)	RF_{expt}	RF_{Emp}	RF_{ANN}	$RF_{M(1963)}$	$RF_{S\ \&\ A(1991)}$	$RF_{L(2008)}$	$RF_{ANN\ (C)}$
0.1	0	0.133	1.000	62.78	0.621	0.645	0.618			0.643	0.620
0.15	0	0.133	1.000	52.97	0.524	0.565	0.551			0.517	0.535
0.05	0	0.267	1.000	56.90	0.563	0.565	0.530			0.575	0.532
0.1	0	0.267	1.000	51.99	0.515	0.502	0.502			0.533	0.498
0.15	0	0.267	1.000	49.05	0.485	0.440	0.466			0.456	0.454
0.05	0	0.400	1.000	42.58	0.421	0.418	0.404			0.406	0.406
0.1	0	0.400	1.000	41.20	0.408	0.372	0.362			0.393	0.400
0.15	0	0.400	1.000	38.65	0.383	0.325	0.371			0.352	0.368
0.05	0	0.533	1.000	31.39	0.311	0.287	0.320			0.256	0.306
0.1	0	0.533	1.000	30.41	0.301	0.255	0.299			0.255	0.280
0.15	0	0.533	1.000	29.43	0.291	0.223	0.288			0.237	0.276

e/B	D_f/B	α/ϕ	*LA*	Expt. q_u (kN/m^2)	RF_{expt}	RF_{Emp}	RF_{ANN}	$RF_{M(1963)}$	$RF_{S\ \&\ A(1991)}$	$RF_{L(2008)}$	$RF_{ANN\ (C)}$
0	0.5	0.000	0.000	143.23	1.000	1.000	1.000				0.993
0.05	0.5	0.133	1.000	105.95	0.740	0.763	0.726				0.764
0.1	0.5	0.133	1.000	94.18	0.658	0.679	0.648				0.659
0.15	0.5	0.133	1.000	77.50	0.541	0.594	0.577				0.582
0.05	0.5	0.267	1.000	88.29	0.616	0.630	0.611				0.617
0.1	0.5	0.267	1.000	77.50	0.541	0.560	0.538				0.558
0.15	0.5	0.267	1.000	67.69	0.473	0.490	0.471				0.501
0.05	0.5	0.400	1.000	73.58	0.514	0.500	0.502				0.504
0.1	0.5	0.400	1.000	63.77	0.445	0.445	0.442				0.476
0.15	0.5	0.400	1.000	56.90	0.397	0.389	0.396				0.424
0.05	0.5	0.533	1.000	58.86	0.411	0.375	0.411				0.394

e/B	D_f/B	α/ϕ	*LA*	Expt. q_u (kN/m^2)	RF_{expt}	RF_{Emp}	RF_{ANN}	$RF_{M(1963)}$	$RF_{S\ \&\ A(1991)}$	$RF_{L(2008)}$	$RF_{ANN\ (C)}$
0.1	0.5	0.533	1.000	53.96	0.377	0.333	0.378				0.379
0.15	0.5	0.533	1.000	48.07	0.336	0.291	0.353				0.348
0	1	0.000	0.000	208.95	1.000	1.000	1.003				0.992
0.05	1	0.133	1.000	170.69	0.817	0.803	0.800				0.815
0.1	1	0.133	1.000	156.96	0.751	0.713	0.729				0.728
0.15	1	0.133	1.000	144.21	0.690	0.624	0.674				0.645
0.05	1	0.267	1.000	148.13	0.709	0.702	0.703				0.697
0.1	1	0.267	1.000	135.38	0.648	0.624	0.639				0.620
0.15	1	0.267	1.000	120.66	0.577	0.546	0.567				0.552
0.05	1	0.400	1.000	124.59	0.596	0.598	0.602				0.588
0.1	1	0.400	1.000	114.78	0.549	0.532	0.530				0.532

e/B	D_f/B	α/ϕ	LA	Expt. q_u (kN/m^2)	RF_{expt}	RF_{Emp}	RF_{ANN}	$RF_{M(1963)}$	$RF_{S\ \&\ A(1991)}$	$RF_{L(2008)}$	$RF_{ANN\ (C)}$
0.15	1	0.400	1.000	103.01	0.493	0.465	0.464				0.470
0.05	1	0.533	1.000	99.08	0.474	0.489	0.494				0.486
0.1	1	0.533	1.000	92.21	0.441	0.435	0.436				0.449
0.15	1	0.533	1.000	86.33	0.413	0.380	0.392				0.391

Note:

RF_{expt}: Reduction Factor values corresponding to present experimental results

RF_{Emp}: Reduction Factor values by using developed empirical equations in Chapter 4 and 5

RF_{ANN}: Reduction Factor values by using developed ANN model equations in Chapter 6 and 7

$RF_{M(1963)}$: Reduction Factor values corresponding to Meyerhof (1963)

$RF_{S\ \&\ A(1991)}$: Reduction Factor values corresponding to Saran and Agarwal (1991)

$RF_{L(2008)}$: Reduction Factor values corresponding to Louikidis et al. (2008) for both clockwise and anti-clockwise load inclination

$RF_{ANN\ (C))}$: Reduction Factor values by using present combined ANN model equation

PUBLISHED PAPERS

International Journals

1. C R Patra, **R N Behera**, N Sivakugan, B M Das (2012). "Ultimate bearing capacity of shallow strip foundation under eccentrically inclined load: part I", *International Journal of Geotechnical Engineering*, 6(3), 343-352.
2. C R Patra, **R N Behera**, N Sivakugan, B M Das (2012). "Ultimate bearing capacity of shallow strip foundation under eccentrically inclined load: part II", *International Journal of Geotechnical Engineering*, 6(4), 507-514.
3. **R N Behera**, C R Patra, N Sivakugan, B M Das (2013). "Prediction of Ultimate Bearing Capacity of Eccentrically Inclined Loaded Strip Footing by ANN", *International Journal of Geotechnical Engineering*, 7(1), 36-44.
4. **R N Behera**, C R Patra, N Sivakugan, B M Das (2013). "Prediction of Ultimate Bearing Capacity of Eccentrically Inclined Loaded Strip Footing by ANN in Reinforced Condition", *International Journal of Geotechnical Engineering*, 7(2), 165-172.
5. C R Patra, **R N Behera**, N Sivakugan, B M Das (2013). "Estimation of average settlement of shallow strip foundation on granular soil under eccentric loading", *International Journal of Geotechnical Engineering*, 7(2), 218-222.